SEISMIC BEHAVIOUR OF STEEL FRAMES WITH SEMI-RIGID CONNECTIONS

A thesis submitted for the degree of Doctor of Philosophy
in the Faculty of Engineering of the University of London

by

Fakhreddin Ahmadi Danesh Ashtiani BSc, MSc

Civil Engineering Department

Imperial College of Science, Technology and Medicine

University of London

August 1996

To my beloved wife

ABSTRACT

In this thesis, experimental and analytical studies are performed to investigate the seismic behaviour of semi-rigid steel frames.

Five two-storey steel frames tested under cyclic and pseudo-dynamic loading are described. The set up, instrumentation and details of members and connections are presented. A full description of the experimental results is given. The test results are used to verify an analytical model proposed for the moment-rotation curve of top and seat angle with double web angles connection.

The seismic response of semi-rigid frames is investigated through non-linear dynamic analyses including the proposed connection representation. A parametric study, conducted to examine the effect of flexibility of the connection on the overall behaviour of structures, is undertaken. The design of partial strength semi-rigid steel frames is discussed with respect to the provisions of the structural Eurocodes.

Finally, dynamic analysis is employed in the evaluation of seismic design behaviour factors for semi-rigid frames. It is concluded that the partial strength semi-rigid steel frames is a viable alternative to welded moment-resisting steel frames where problems of brittle fracture have been recently identified. Criteria for the design of connection, connecting members and frame with bolted connections are given, based on the experimental and analytical work.

ACKNOWLEDGEMENT

I would like to express my heartfelt appreciation to my supervisor Professor Amr Elnashai whose support and encouragement has been gratefully received. His valuable advice and guidance throughout my studies have been fundamental to the completion of this work.

Funding for the test programme was kindly provided by the UK Engineering and Physical Sciences Research Council (EPSRC).

The financial support of Iranian Government during these years is gratefully acknowledged.

I would like to thank Dr. Brian Broderick for his valuable advice on the experimental work and for many useful suggestions and discussions. Thanks are also to Dr. Ahmed Elghazouli who was of great help in giving valuable guidance on testing procedures.

The expert technical support of the staff of the structures laboratories at Imperial College is gratefully acknowledged, especially, but not exclusively, that of Messrs Tony Boxall and Alan Roberts.

I thank all the researchers in the ESEE and structures sections, especially that of J. Enrique Martinez-Rueda and Mark Manzocchi for providing a pleasant working environment.

Finally, greatest thanks go to my wife, whose care and patient understanding during this time have provided the greatest support of all.

TABLE OF CONTENTS

		Page
ABSTRACT		3
ACKNOWLEDGEMENTS		4
TABLE OF CONTENTS		5
NOTATION		10
1	**INTRODUCTION**	14
1.1	Seismic design	14
1.2	Seismic design of steel structure	15
1.2.1	Material behaviour	16
1.2.2	Member behaviour	16
1.2.3	Behaviour and design of frames	18
1.3	Beam-to-column connections	19
1.3.1	Classification of connections	20
1.3.2	Semi-rigid connections	21
1.4	Objectives and scope	22
2	**REVIEW OF RESEARCH ON SEMI-RIGID CONNECTIONS**	27
2.1	Introduction	27
2.2	Experimental behaviour of different types of semi-rigid connections	28
2.3	Modeling of connections	31
2.3.1	Global models	31
2.3.2	Component-based models	38
2.3.3	Finite element models	39
2.3.4	Remarks	39
2.4	Cyclic behaviour of semi-rigid connections	40
2.5	Seismic behaviour of semi-rigid steel frames	44

2.6 Commentary 50

3 DESIGN CODES 61

3.1 Classification of connections 61

3.1.1 Classification system in Eurocode 61

3.1.2 Classification system used by the American Institute of Steel Construction (AISC) 62

3.1.3 Classification system by researchers 63

3.2 Moment-rotation relationship in EC3 66

3.2.1 Determination of the moment resistance of connections 66

3.2.2 Calculation of rotational stiffness 67

3.2.3 Comparison of moment-rotation curves with experimental data 68

3.3 Seismic design philosophy for semi-rigid steel frames 70

3.3.1 Dissipative and non-dissipative structures 70

3.3.2 Limit state requirements 71

3.3.3 Behaviour factor 72

3.3.4 Collapse mechanism 74

3.4 Commentary 75

4 EXPERIMENTAL INVESTIGATIONS 81

4.1 Introduction 81

4.2 Test-rig 81

4.3 Description of the models 83

4.3.1 Specimen details 83

4.3.2 Material properties 85

4.4 Electro-hydraulic servo control 85

4.5 Instrumentation 86

4.6 Experimental measurement 88

4.7 Loading regime 88

4.7.1 Gravity load 88

4.7.2 Cyclic load 88
4.7.3 Pseudo-dynamic tests 89
4.8 Definition of the response parameters 94
4.8.1 Yield criteria 94
4.8.2 Ultimate criteria 94
4.8.3 Ductility 95
4.8.4 Plastic hinge length 96
4.8.5 Behaviour factor 96
4.9 Experimental Results 98
4.9.1 Cyclic loading tests 99
4.9.1.1 Model CR1 99
4.9.1.2 Model CS1 99
4.9.1.3 Model CS2 100
4.9.1.4 Model CS3 102
4.9.2 Pseudo-dynamic tests 103
4.10 Discussion of the Results 105
4.10.1 Plastic hinge length 105
4.10.2 Point of contra-flexure in column 105
4.10.3 Panel zone deformation 106
4.10.4 Ductility 107
4.10.5 Behaviour factors 108
4.10.6 Initial stiffness of the connections 109
4.10.7 First and second storey stiffness 110
4.10.8 Fundamental period 111
4.11 Commentary 111

5 ANALYSIS OF SEMI-RIGID STEEL FRAMES 144
5.1 The Non-linear Dynamic Analysis Programe "ADAPTIC" 144
5.2 The Elasto-plastic Cubic Element 145
5.3 Material Model 146
5.4 Modeling of Connections 147

5.4.1 Proposed bilinear moment-rotation curve 147
5.4.1.1 Theory and assumptions 147
5.4.1.2 Calculation of yield moment 149
5.4.1.3 Yield rotation 151
5.4.1.4 Evaluation of the elastic and post elastic stiffness 151
5.4.1.5 Maximum rotation of the connection 152
5.4.2 Verification of proposed bilinear model 152
5.5 Comparison with Experimental Results 155
5.5.1 Monotonic tests 155
5.5.2 Cyclic tests 156
5.5.3 Dynamic tests 158
5.6 Remarks 159

6 ANALYTICAL PARAMETRIC STUDY 173
6.1 Introduction 173
6.2 The Design of Semi-rigid Steel Frames 174
6.2.1 Design of beam and column sections 174
6.2.2 Effective length of column 175
6.2.3 Panel Zone 176
6.2.4 Beam-column connection 177
6.2.5 Bolts design 178
6.3 Limit State Criteria 178
6.3.1 Yield state 179
6.3.2 Ultimate state 179
6.3.2.1 Storey failure criteria 179
6.3.2.2 Local failure criteria 180
6.4 Selection and Scaling of Earthquake Ground Motion 184
6.4.1 Selection of Records 184
6.4.2 Scaling of the selected records 187
6.5 Design and Modeling of Frames 189
6.5.1 Design of frames 189

6.5.2 Modeling of frames 191
6.6 Results of Dynamic Analysis 191
6.6.1 Two-storey frames 192
6.6.2 Four storey frames 199
6.6.3 Six storey frames 205
6.7 Discussion and Design Implications 209
6.7.1 Capacity design for semi-rigid steel frames 209
6.7.2 Frame configurations 210
6.7.3 Over-strength for semi-rigid frames 212
6.7.4 Behaviour factors 212
6.7.5 Rotation ductility 217
6.8 Concluding remarks 217

7 CLOSURE 234
7.1 Summary and Conclusion 234
7.2 Future Research 238

REFERENCES 239

APPENDIX A: Strain Gauge Results 251

APPENDIX B: Frame Member Dimensions 258

APPENDIX C: Calculation of Moment Capacity and Rotational Stiffness 265

Notation

Symbols

a_u	peak ground acceleration causing collapse
a (t)	acceleration vector
a_y	peak ground acceleration causing the attainment of the yield limit
C	viscous damping matrix
C_i	curve-fitting constants
D	width of nuts across the flat sides for bolt fasteners
D_k	constant parameters for the linear function
d_b	depth of beam
d_{max}	the maximum relative displacement reached during the whole test
E	Modulus of Elasticity
E_{st}	strain-hardening modulus
$F_{1,2}$	lateral force of first or second storey, respectively
F_{pt}	plastic shear force in the vertical leg of the angle
F_o	plastic bending moment without coupling
F(t)	external force vector
F_{max}	the greatest load level of the whole test
F_u	the load level corresponding to displacement d_{max}
I_b	moment of inertia of the beam
$K_{1,2}$	first or second storey stiffness, respectively
$K_{e,con}$	initial stiffness of the connection
L_p	the length of plastic hinge in the member
L_b	span of the beam
l_t	length of the top angle
M	mass matrix
M_o	plastic bending moment without coupling
M_{ut}	moment capacity of the top angle
M_{us}	moment capacity of the seat angle

M_{yc}	yield moment of the connection
M_u	ultimate moment capacity
M_{pb}	plastic moment of the beam
M_{con}	moment of the connection
M_{pt}	plastic moment of the top angle
$M_{j,Rd}$	design moment resistance of connection
$M_{j,Sd}$	design moment of connection
m	M/M_u
$\overline{m}$	M_{con}/M_{pb}
n	shape parameter of M-θ curve
q	behaviour factor
r	the bolt-row number
R	normalised critical stress ($R= \sigma_{cr}/\sigma_y$)
R (t)	structural restoring force vector
R_d (T)	the ordinate of the normalised inelastic design response spectrum
R_{kf}	strain-hardening stiffness
R_o	the maximum normalised spectra value
R_{ki}	initial connection stiffness
$R_{\theta\,col}$	rotation capacity of the column
$R_{\theta con}$	rotation capacity of the connection
S_j	rotational stiffness of the connection
$S_{j,ini}$	initial rotational stiffness of the connection
$S_{j,h}$	rotational stiffness of the connection in post-elastic case
SI	spectrum intensity
S_v	velocity spectrum
S_a	acceleration spectrum
T	natural period of the structure
t_t	thickness of the top angle
t_s	thickness of the seat angle

t_f	thickness of the flange
t_w	thickness of the web
$v(t)$	velocity vector
V_y	base shear at yield
V_u	base shear at failure model
z	lever arm
α	σ_o/σ_y
α_u	load multiplier at the attainment of the ultimate limit state
α_y	load multiplier at the attainment of the yield limit state
α_f	slenderness parameter of the flange
α_w	slenderness parameter of the web
$\delta_{1,2}$	first or second storey displacement
ε_y	yield strain
ε_p	plastic strain
Δ_{sy}	interstorey drift at yield
Δ_{su}	interstorey drift at ultimate state
$\Delta_{i\,(design)}$	design value of interstorey drift
Δt	time step
λ_e	yield multiplier acceleration
λ_m	multiplier of the acceleration at ultimate state
λ_p	plastic yielding factor
λ_{p1}	first plastic hinge coefficient
μ_θ	rotation capacity
$\mu_{\Delta s}$	global ductility
$\mu_{\theta\,col}$	rotation ductility of the column
$\mu_{\theta\,con}$	rotation ductility of the connection
θ	rotation of the connection

θ_k	starting rotations of the linear components
θ_o	reference plastic rotation, M_u/R_{ki}
θ_p	plastic rotation of the connection
θ_y	yield rotation of the connection
θ_u	rotation at ultimate state
$\bar{\theta}$	θ_{con}/θ_p
σ_o	axial stress
σ_y	yield stress
σ_{cr}	critical stress
σ_{yf}	yield stress of the flange
σ_{yw}	yield stress of the web

CHAPTER 1

1 INTRODUCTION

1.1 Seismic Design

It is accepted that a higher risk of damage exists under seismic design forces than under other variable loads, such as live or wind loads. For example, modern building codes specify the design earthquake forces that correspond to a return period of 100 to 500 years for ordinary structures, such as office buildings. The corresponding design forces are generally too high to be resisted within the elastic range of the material response. It is common to design for a strength which is a fraction, perhaps as low as 15% of that corresponding to the elastic response. Therefore, the structures are expected to survive an earthquake by large inelastic deformations and energy dissipation due to damage.

It has been demonstrated that seismic design to lateral force levels specified in codes was inadequate to ensure that the structure is not subjected to higher forces in the event of an earthquake. However, provided that the structural strength could be maintained without excessive degradation as inelastic deformations develop, the structure could survive earthquakes and may be repaired economically.

As a consequence of this observation, which indicated that excessive strength is not necessary in seismic design, the inelastic structural response has become an essential part of structural design for earthquake forces. Therefore, design codes permit some elements of the structure to response well into the inelastic range and demonstrate ductility.

Generally, high global ductility is associated with careful choice of the locations of plastic hinges, where inelastic deformations may occur. In addition, to ensure the ductility of dissipative elements, it is necessary that the other parts of the structure

remain in the elastic range. Both of these concepts are the basis of the capacity design philosophy.

Procedures for the application of capacity design to ductile structures have been developed primarily in New Zealand over the last 20 years. With some modifications, the philosophy has also been adopted in modern codes, such as Eurocode 8.

In the capacity design of structures for earthquake resistance, distinct elements of the primary lateral force resisting system are selected and suitably designed so that they have the capability to dissipate energy during strong ground motion. Plastic hinges are located in the critical regions of these members. They are detailed for inelastic flexural action and prevented from failing in shear. Other elements are designed to provide sufficient strength, i.e. greater than the maximum strength in plastic hinge regions. This is achieved as described below.

The location of plastic hinges is clearly defined and designed to have flexural strength as close as possible to the required ultimate strength. To achieve the target ductility used in the design of the structure, these regions must be detailed carefully. To prevent undesirable modes of inelastic deformation that occur as a result of shear or instability within members containing plastic hinges, the strengths of these modes should exceed the capacity of the plastic hinges when over-strength factors are applied. The non-dissipative elements should remain elastic during severe earthquake forces. For this purpose, these regions are designed to resist forces in the elastic range and are prohibited from undergoing significant inelastic deformation.

The above is a statement describing strict capacity design. Variations exist, whereby limited inelastic deformations in locations other than the pre-selected dissipative zone is allowed, for economy.

1.2 Seismic Design of Steel Structure

When steel frame structures are subjected to earthquake ground motions, beams are designed to enter into the inelastic range first. The plastic hinges are located in these

elements to dissipate energy and permit the structure to survive earthquake forces through adequate ductility. During this procedure, the frame connections have to sustain forces developed in connected members by providing sufficient strength.

Moreover, according to conventional capacity design the key elements mentioned above are used to develop a carefully chosen ductile failure mode for attainment of the full capacity of the structural system. The other elements are designed to resist forces consistent with the ultimate capacity of the key elements. In the following sections, the material properties that influence ductility are presented.

1.2.1 Material Behaviour

According to EC3 and EC8 for plastic and seismic design it is recommended that the steel properties satisfy the following requirements:

1. The ratio between ultimate tensile strength f_u and the yield strength f_y has to satisfy the condition $f_u/f_y > 1.2$.
2. In order to guarantee an adequate deformation capacity, the ratio between the ultimate strain ε_u and the yield strain ε_y, can not be less than 20.

Increase in material yield strength causes some reduction in attainable ductility and energy absorption capacity Recent investigations (Kuwamura and Kato, 1989; Elnashai and Chryssanthopoulos,1991) have confirmed that random variability in yield stress has an adverse effect on the failure mode control. Furthermore, the deformation capacity decreases substantially with an increase in the yield strength (Kato, 1990). Therefore, it is important to set a limit on the ratio $f_{y\ actual}/f_{y\ design}$. This is, however, not implemented in current codes for steel structures yet.

1.2.2 Member Behaviour

In order to design cross-sections capable of providing sufficient rotational capacity, local buckling has to be controlled. In particular the occurrence of local buckling in the

elastic range has to be avoided. Therefore, geometrical properties of the cross-sections have to guarantee the occurrence of buckling only well into the plastic range and after the realisation of the design ductility.

A very important concept in designing steel structures, which has been introduced for the first time in EC3, is represented by the sub-division of the structural sections into four different behavioural classes (Figure 1.1). Sections belonging to the first class are characterised by the capability to develop a plastic hinge with high rotation capacity, hence they are defined as "plastic". The second class of sections are able to attain their maximum plastic flexural strength, but because they have limited deformation capacity due to local effects they are referred to as "compact". Structural sections fall in the third class when the bending moment leading to first yielding can be attained but, due to local buckling, plastic redistribution is not possible. These are called "semi-compact". Finally, the sections belonging to the fourth class (slender sections) are not able to develop their total elastic flexural resistance due to the premature occurrence of local buckling of the parts of the sections under compression and failure occurs in the elastic range. The parameter governing the above behaviour and defining the class of structural sections is the width-to-thickness ratio (b/t) of the compressed parts. The b/t limit values are given in EC3.

Local ductility of members vary with values of axial loads, the slenderness of the elements and the steel grades. Studies carried out by Azevedo and Calado (1992) indicated that the local ductility decreases very rapidly with an increase in the axial load. As would be expected, high slenderness values cause reduction in the ductility of the members. In addition, the steel grade has a slight influence on the ductility of the members and commonly-used higher steel grades tend to be less ductile.

For the development of the full plastic moment capacity of the members such as columns, it is necessary to have a limitation on width-to-thickness ratios for the web and flanges. Also, the ratio of axial load to the yield capacity must be limited.

Members behaving mainly in flexure, such as beams, have a plastic moment capacity given by the product of the plastic section modulus Z_p and the material yield stress f_y. In limit design of the structures, it is postulated that plastic hinges have a sufficient rotation capacity. Therefore, it is clear that the cross section of a member has to satisfy precise geometrical requirements in order to allow plastic deformations so that the collapse mechanism of the structure is reached, without losing its load carrying capacity.

1.2.3 Behaviour and Design of Frames

The total deformation of steel frames is the sum of the member and connection deformations. For accurate assessment of frame deformations, the following should be taken into account :

- Flexural and shear deformation of beams and beam-columns.
- Deformation of the beam-column connection including shear effects in panel zone.
- Strain-hardening and effect of residual stresses.
- Second order (P-δ) effect on overturning moment.
- In certain cases, soil flexibility.

Clearly, simplifying assumptions are warranted in cases where some of the above effects may be neglected and appropriate allowances made. In moment resisting frames, the elements are designed such that the development of the first plastic hinge occurs in the beam and not in the column. The only exception to this requirement is at the base of the ground floor columns, where plastic hinges may form without jeopardising the stability of the structure.

Connection design is of great significance for earthquake resistance of steel structures. Premature failure of connections will prevent the structure from developing its full ductile capacity and will undermine failure mode control. The concept of conventional capacity design requires that connections should sustain loads consistent with the

ultimate strength of the other frame members, as well as deform in a manner consistent with the assumptions used in structural analysis. The role of connection is further discussed in section 1.3.

Simplified calculation of the deformation of frames can be performed by either plastic limit analysis procedures or by superposition of beam, column and connection deformation. Neglecting strain-hardening and use of elastic-perfectly plastic moment-curvature relations will lead to a conservative estimate of the overall strength and deformations.

It is observed that when the steel frame is prevented from premature local and overall buckling, as well as connection failure and shear failure in the panel zone, it is a very effective seismic resistance system. This is due to its favourable mass-to-stiffness ratio, inherent ductility and sustainable energy absorption capacity.

1.3 Beam-to-Column Connections

In normal analysis and design of steel frames, beam-to-column connections are assumed to behave either as pinned or as fully rigid. Experimental work and research indicate that pinned joints have some ability to resist rotational deformations and exhibit some rigidity. Also, it has been shown that fully-welded connections have finite flexibility.

The primary distortion of a steel beam-to-column connection is the rotational deformation θ caused by the in-plane bending moment M (Figure 1.2). This connection deformation has an effect on frame stability since additional drift will occur as a result of the decrease in stiffness of the members to which the connections are attached. An increase in frame drift will intensify the P-δ effect and hence the overall stability of the frame will be affected. Thus, the non-linear characteristics of the beam-to-column connection play a very important role in frame stability.

1.3.1 Classification of Connections

In preliminary design, it is useful to estimate what influence the connection will have on the behaviour of the structure without having to perform a non-linear analysis. In the case of elastic design, the classification by rigidity leads to three main categories:

i. Nominally pinned connections, which are assumed to transfer the shear and eventually the normal force from the beam to the column. They must be capable of rotating without developing significant moments which might adversely affect the stability of the column.
ii. Rigid connections, which transmit all end reaction forces and whose deformation is sufficiently small, so that any influence on the moment distribution in the structure or on its overall deformation may be neglected.
iii. Semi-rigid connections, which are designed to provide a predictable degree of interaction between members and are based on the design moment-rotation characteristics of the joints.

The first two categories are traditional. Nominally pinned connections are widely used when lateral stiffness of structure is guaranteed by appropriate bracing systems. In the case of moment resisting frames rigid connections often lead to excessive construction costs. The intermediate stiffness category has been introduced to fill the gap between pinned and rigid connections and it is now accepted in modern codes (e.g. EC3).

From the comparison of moment versus rotation curves shown in Figure1.3, it is observed that different non-linear behaviour ranges from the quasi-perfectly rigid (fully welded, extended end plates) to the flexible (double web angle). The intermediate range corresponds to the class of semi-rigidity. Some common types are: top and bottom flange splices, flush end plate, top and seat angles with double web angles, flange angles and extended end plate.

For use in plastic design, the connections may be divided into two categories (Figure 1.4). Full strength connections should have a design resistance at least equal to the strength of one of the connected members (case A). A plastic hinge will be formed in

the adjacent member but not in the connection. If the rotation capacity is limited (case B), an extra reserve of strength would be required to account for possible over-strength effects in the member.

Partial strength connections should have a design resistance less than the strength of one of the connected members (case C). A plastic hinge is formed in the connection, hence sufficient rotation capacity is required (case D). It follows that case C is unsuitable, because its rotation capacity could be exceeded under design loads. According to the state of codification in the field of seismic resistant structures, only full strength connections are now allowed and an over-strength of 1.2 is suggested in the ECCS Recommendations for fillet welds and bolted connections.

1.3.2 Semi-Rigid Connections

The results obtained from previous investigations clearly indicated that the semi-rigid connection is feasible and indeed more economical than the rigidly-connected frame. They also show that the optimum seismic design solution is not necessarily a rigidly connected frame.

An analytical study by Rosales (1991), for example, showed that semi-rigid frames have the advantage of a longer period, hence attract lower inertial loads. This may offset the effect of the increased flexibility, hence resulting in a most satisfactory earthquake-resistant design solution, even in areas of high seismicity.

Experimental work performed by Elnashai and Elghazouli (1994) indicated that semi-rigid frames do exhibit a ductile and stable hysteretic behaviour. Although both the stiffness and capacity of semi-rigid frames are lower than similar rigid frames under monotonic and cyclic loading, the response under earthquake loading largely depends on the dynamic characteristics of the frames and the frequency content of the input motion. In many cases, the response of semi-rigidly connected frames may be superior to rigid frames, provided that stable hysteretic behaviour is ensured. Furthermore, comparative experiments conduced by Astaneh and his co-workers (1989), indicated

that the rigid frame is not always the optimum solution, and that semi-rigid designs may perform adequately under simulated earthquake loading.

Kuwamura and Suzuki (1992) indicated that any welded connections, whatever level of workmanship is employed, eventually suffer fatigue fracture. In the 1985 Mexico earthquake, there were some welded beam-to-column connections that failed. Many modern steel buildings that suffered from local failures during the 1994 Northridge earthquake confirmed that the dominant failure mode is by local failure in welded beam-to-column connections (Bertero et al., 1994). Additional reasons for use of semi-rigid-connections in earthquake resistance are discussed in the following.

The inherent inelastic behaviour of the connecting parts prevents high stress points in the connected members themselves, thus allowing more slender cross sections and the elimination of stiffeners. In addition, it reduces high stress concentration complications in ductility-based design. Also preliminary research indicates that the energy absorption of inelastic connections during earthquake motion actually controls excessive lateral drifts within reason. Moreover, the use of plastic design in steel represents a higher order of optimisation in its process of developing failure mode mechanisms. Most semi-rigid frames reach their useful limit at a serviceability limit (excessive deformation) rather than a strength limit (frame collapse). This implies a retrofit benefit of using flexible connections in steel frames in the event of an earthquake.

On a philosophical level it is apparent that neither pinned nor rigid connections are actually obtained in real structures. Even approximate estimates of frame flexibility are closer to the real situation than the assumed ideals of nil or full restraint in the connections.

1.4 Objectives and Scope

Several major codes e.g. AISC, BS5950, permit partial restraint to be utilised but give little guidance on how this should be done. There is a great deal of data on the performance of different types of connection in the literature, but none of them show

the effect of axial loads on the behaviour of semi-rigid steel frames under cyclic and dynamic loads.

Based on studies cited in previous sections and other evidence emerging from the literature, it is clearly very important to undertake studies on semi-rigid frames subjected to earthquake loading. This may lead to significant economies, rendering steel frames a very attractive solution to seismic design problems.

Moreover, many frames in Europe are currently designed with semi-rigid connections. It is therefore urgent to develop techniques for assessing their inherent seismic resistance in anticipation of the full implementation of the new Eurocode 8 for seismic design.

The aim of this study is, therefore, to provide information on the performance of semi-rigid steel frames under cyclic and dynamic loading in the presence of axial load. For this purpose, five two-story steel frames, have been tested under cyclic and dynamic loads. These comprise one rigid and four semi-rigid structures, the latter with different connection strengths.

As a result of this investigation, conclusions are reached regarding the effect of flexibility of the connection on increasing the inter-storey drifts of the steel frames. In addition, the hysteretic behaviour of semi-rigid connections is studied in detail and compared with analytical predictions.

The pseudo-dynamic testing method is used in this programme. This is because it allows dynamic experiments to be executed practically at a static rate, whilst accounting for inertial and damping contributions. It is then possible to monitor in detail the frame deformations that are associated with internal frame forces. These deformations give important information about the stiffness characteristics of a moment resisting steel frame.

To compare experimental results with analysis, the advanced non-linear dynamic analysis program "ADAPTIC" is used. The efficiency of the proposed bilinear model

for predicting the moment-rotation relationship of the semi-rigid connections is proved by comparing the analytical predictions with experimental results.

Design recommendations for semi-rigid steel frames in seismic zones are presented and a modified capacity design method for this type of structure is described hereafter. An analytical parametric study is undertaken to investigate the dynamic behaviour of several semi-rigid steel frames. In this study, the lateral interstorey drifts, base shears and the behaviour factors that develop in semi-rigid and rigid frames subjected to the same ground motions of different records are evaluated. Also, the ultimate capacity of semi-rigidly connected steel frames is compared with that of rigid frames.

Finally, general conclusions from the present study are given alongside recommendations for further research.

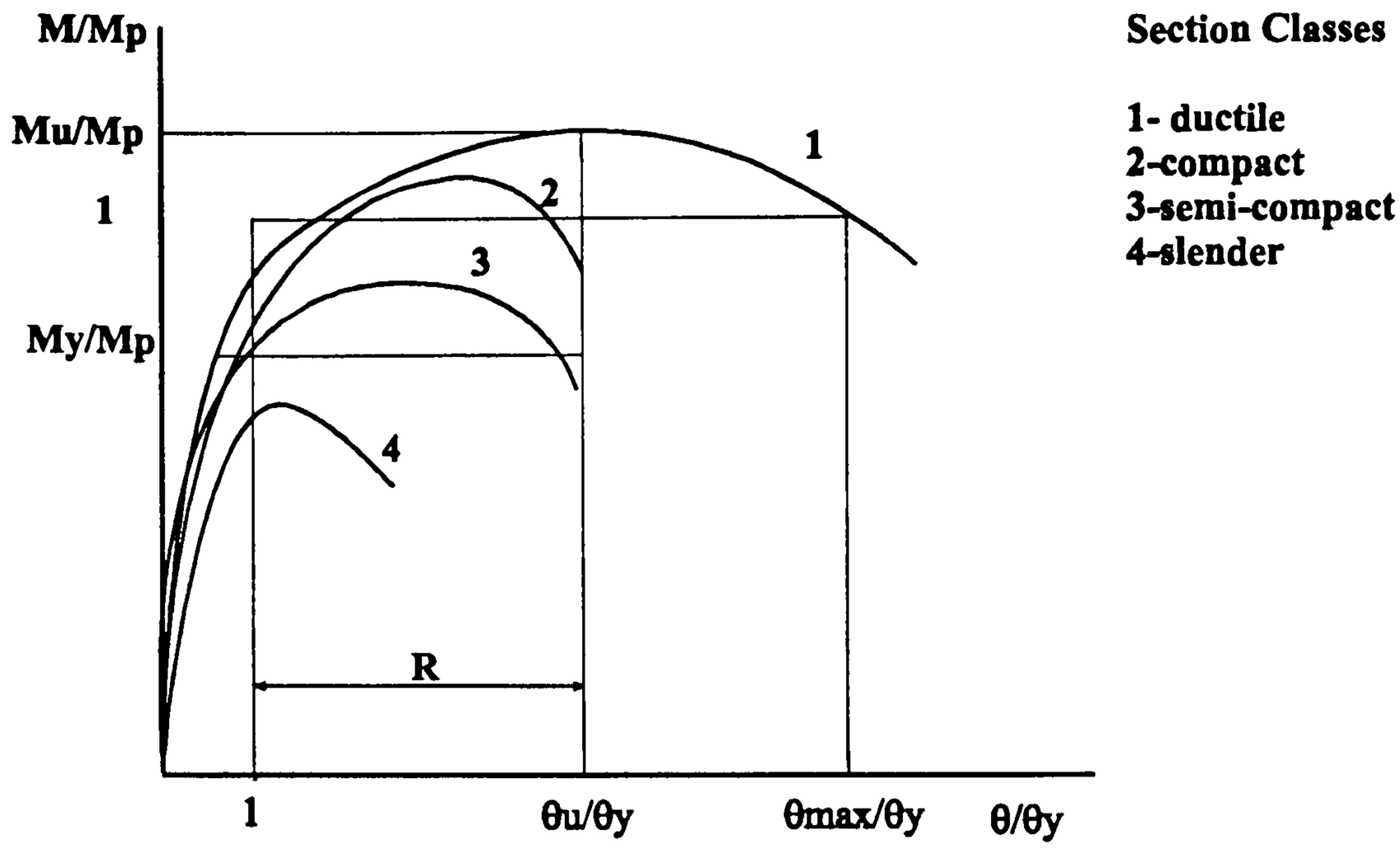

Figure 1.1 Cross-section behavioural classes

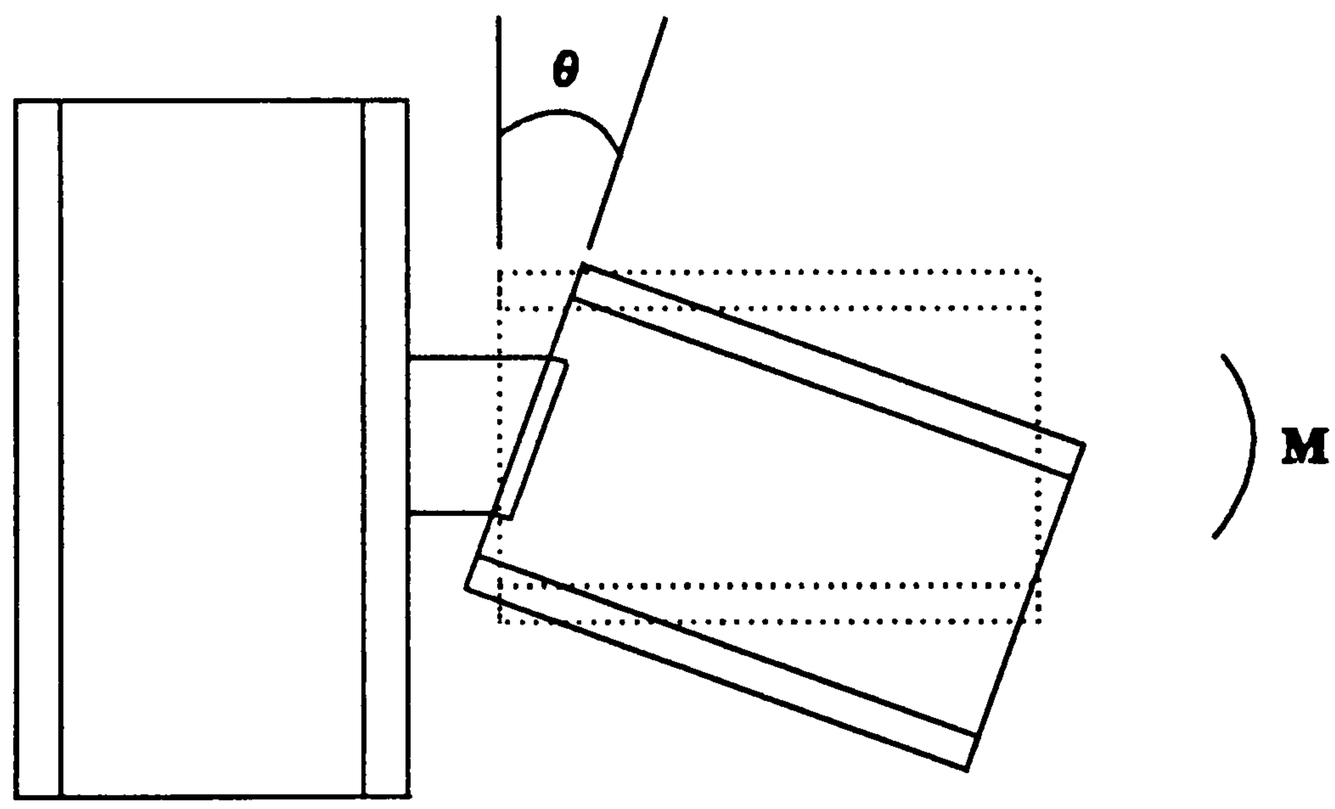

Figure 1.2 Rotational deformation of a connection

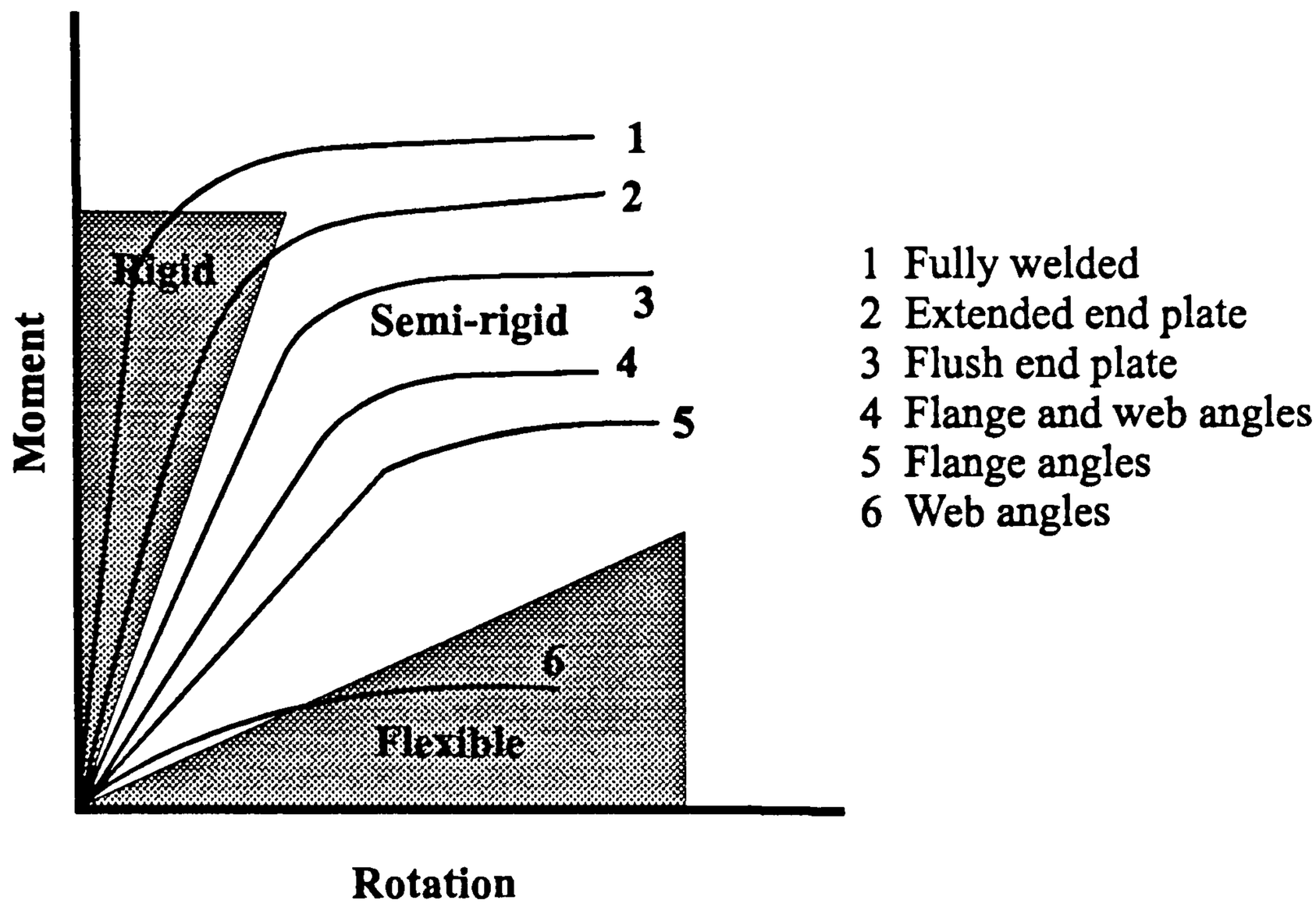

Figure 1.3 Moment-rotation relationship for commonly used connections

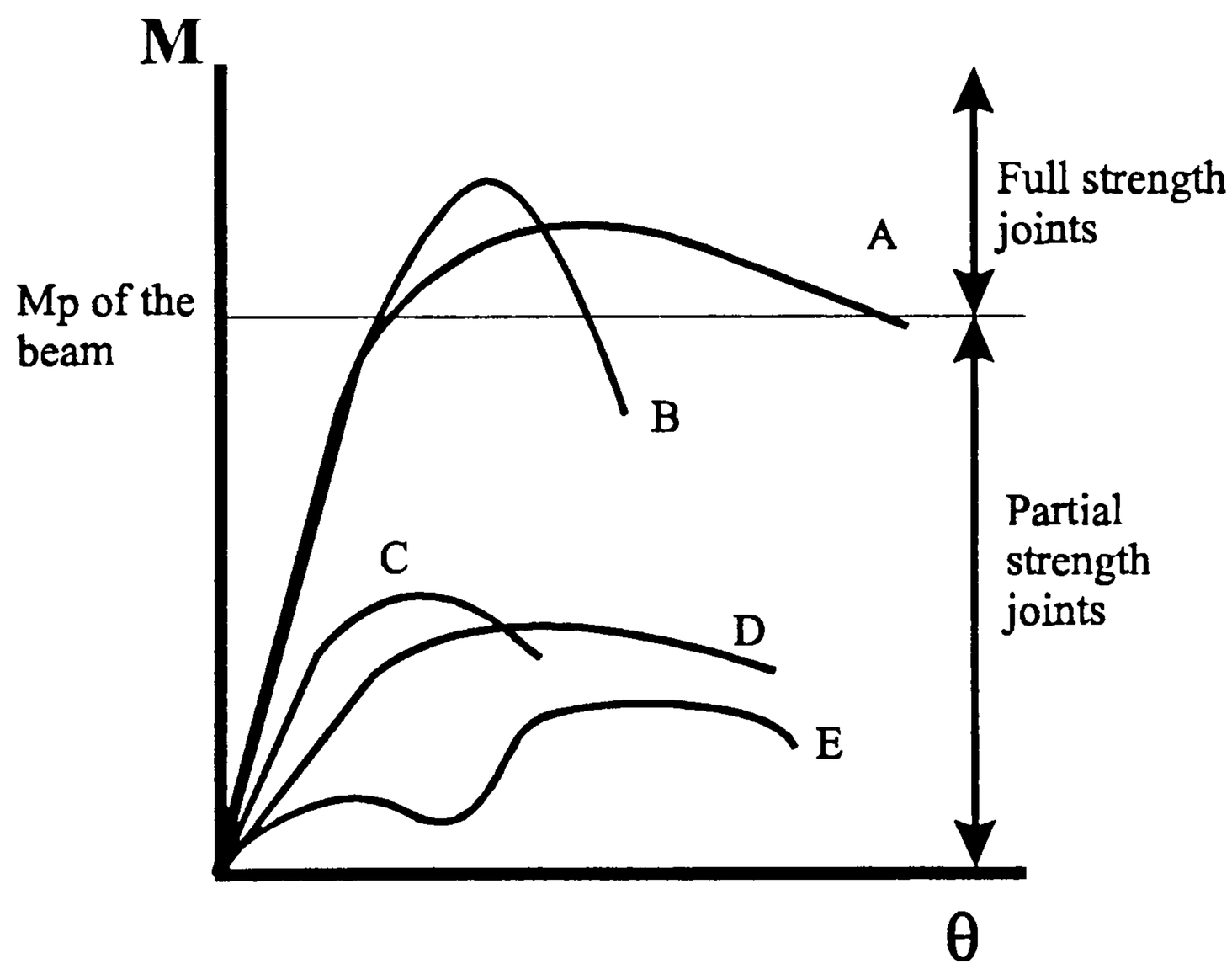

Figure 1.4 Moment-rotation curves of beam-to-column connections

CHAPTER 2

2 REVIEW OF RESEARCH ON SEMI-RIGID CONNECTIONS

2.1 Introduction

In the analysis and design of steel frame structures, it is assumed that the connections are either fully rigid or ideally pinned. A fully rigid connection implies that there is no relative rotation of the connection and hence the beam's end moments are transferred completely to the column. On the other hand, in a pinned connection, it is assumed that there is no restraint to the rotation of the connection and hence the moment of the connection is taken as zero. It is recognised, however, that the actual beam-to-column connection lies somewhere between these two extremes, i.e. real connections are neither fully rigid or ideally pinned. Such connections are described as semi-rigid.

To understand the behaviour of steel frames with semi-rigid connections, examination of the moment-rotation relationship of the beam-column connection must be undertaken. Indeed, several recent publications (described below) have highlighted the fact that connection rigidity does influence the overall behaviour of steel structures.

The primary aim of this chapter is to review the experimental and analytical work which was carried out on semi-rigid connections. It is emphasised that the review is not exhaustive; publications are selected on the basis of their relevance to the programme of research discussed herein. First, the experimental moment-rotation curves of the most common types of connection are presented and the key parameters influencing such behaviour are identified. Second, the different analytical models for predicting the moment-rotation relationship of the connection are discussed and compared with the experimental moment-rotation curves. Finally, the behaviour of steel frames with semi-rigid connections subjected to cyclic and dynamic forces is reviewed.

2.2 Experimental Behaviour of Different Types of Semi-Rigid Connections

The behaviour of semi-rigid connections subjected to monotonic loads have been an area of much experimental work in recent years. In the following sections, the results of some of this work is examined and discussed.

a- Single web angle: A single-web angle connection consists of an angle either welded or bolted to both the column and the beam web. An example of this type of connection is shown in Figure 2.1(a). The only known tests on this type of connection were apparently carried out by Lipson (1968, 1977) and Lipson and Antonio, (1980). Moreover, their published results only provided M-θ data. Lipson's ten M-θ curves show that for a given connection, by increasing the number of bolts (i.e. by effectively decreasing the distance between the lines of the bolts), the moment capacity of the connection is increased. However, with less than six bolts, it was indicated that the connection functions virtually as pinned. It is interesting to point out that increasing the number of bolts to eight or more produced an initial stiffness in the connection. However, this stiffness was largely independent of the exact number of bolts.

b- Web side plate: A typical web side plate connection is shown in Figure 2.1(b). The plate is usually welded to the column and bolted to the beam web. Work carried out by Hormby et al. (1984) and Richard et al. (1980, 1982) was primarily aimed at developing a method for predicting the M-θ behaviour for this type of connection. Using non-linear finite element analysis, coupled with empirically determined bolt load-deformation characteristics, the importance of the fastening to the beam was highlighted. From the above results, it may be concluded that bolts with no mechanical tightening produce connections with virtually no rotational stiffness or moment capacity. However, by fully torquing the bolts, sufficient friction is produced between the surfaces thereby generating stiffness and strength in the connection.

c- *Double web angle:* This type of connection consist of two angles bolted to both the column and the beam web as illustrated in Figure 2.1(a). Elimination of any slippage in the connection particularly for joints using a small number of bolts, appears to be of extreme importance in this type of connection. Davison et al., (1987) showed that moment capacities generally lie between 5% and 15% of the beam strength.

d- *top and seat angle:* This connection type is shown in Figure 2.1(c). It may be regarded as genuinely semi-rigid as it possesses a smooth non-linear M-θ curve. The restraint provided by this type of connection is approximately 50% of the moment capacity of the beam (Maxwell et al., 1981).

e- *Header plate:* This type of connection consists of an end plate whose depth is approximately 40 to 80% of the full depth of the beam. The plate is usually welded to the beam web and bolted to the column as shown in Figure 2.1(d). Figures.2.2 and 2.3 show the moment-rotation relationship for this type of connection as provided by Sommer (1969). These Figures indicate that the key parameters for stiffness and moment resistance are plate thickness, plate depth and the horizontal distance between lines of the bolts.

f- *Flush end plate:* Figure 2.1(e) shows an example of the flush end plate connection. The end plate in this type of connection is welded to the flange and web of the beam and generally bolted to the column. A number of tests have been carried out on this type of connection which serves to provide a systematic assessment of the influence of key parameters on stiffness and moment capacity. For example, The results from the experimental work completed by Ostrander (1970) indicate that increases in end-plate thickness lead to progressively higher rotational stiffness and moment capacity of the joint. It was also pointed out that by placing the top bolts as close to the beam flange as possible and minimising the gauge, the connection stiffness could be enhanced. Figure 2.4 shows that the moment capacity is influenced chiefly by the end-plate thickness and column web stiffening. In certain cases moments as high as M_y or even M_p of the connected beam can be attained.

g- *Extended end plate:* The extended end plate connection is illustrated in Figure 2.1(f). In general, this connection is welded to the beam and bolted to the column. Many tests have been carried out on this type of connection and a wide range of experimental data is provided in the literature. Hence, as a result of the large number of variables present, a useful comparison between the results of the different test series is difficult. Figures 2.5 and 2.6 show the effect of key parameters on the stiffness and strength of this type of connection as indicated by Ioannides (1978). From these results, coupled with experimental work carried out by Johnson et al. (1981), it can be seen that the increase in end plate thickness, bolt preload, column flange thickness and full-depth column web doubler plates can be effective in enhancing the performance of the connection. It should be noted that its configuration is preferred when the connection is subjected to moment reversal such as during severe earthquake loading.

h- *Combined double web with top and seat angles:* This type of connection consists of a combination of top, seat and web angles bolted to the beam flanges and web as well as to the column. This connection is illustrated in Figure 2.1(g).Tests carried out by Altman et al. (1982), showed that both initial stiffness and moment capacity are strongly influenced by the physical properties of the two types of angle. They also pointed out that factors which improved the performance of the connection included increased thickness and reduced gauge for the top and seat angles.

From an experimental investigation conducted by Azizinamini et al. (1985), it was observed that the geometric parameters which had the most significant effect on the initial stiffness and moment-rotation performance of the connection were the depth of the beam section into which the connections framed, the thickness of the flange angles and the gauge of the leg of the flange angle attached to the column (Figures 2.7 and 2.8). It was further concluded that variations in the length of the flange angles, coupled with the length and thickness of the web angles, have a less pronounced effect on the response of the connection as compared with other factors mentioned above.

Other types of connection are seldom used in steel frame structures. Furthermore, there is insufficient data from the tests to adequately identify the performance of these types of connection.

2.3 Modelling of Connections

Since the 1930s, analytical methods for modelling moment-rotation curves of semi-rigid connections have been developed in conjunction with experimental studies. There are several models proposed in the literature to represent the moment-rotation behaviour of various types of connections. The available analytical models may be classified, in increasing order of detail, into global, component-based and finite element models as described in subsequent sections.

2.3.1 Global Models

Modelling of the connection response may be achieved through the determination of key parameters (e.g. initial stiffness, ultimate moment etc.) and the fitting of a skeleton curve through the points. The key parameters can be obtained from experimental tests or through simple analysis by considering the response of one more components which are regarded to be the main source of flexibility and strength in the connection. In this section the most important models that were proposed by researchers are given and discussed.

a- Linear models: There are three types of linear models. The simple linear model utilises the initial stiffness K_i to represent the connection behaviour for its entire range of loading (Batho et al., 1931, 1934, 1936; Baker, 1934; Monforton and Wu, 1963; Lightfoot and Lemessurier, 1974). The second type, or bilinear model, has a shallower second slope at a certain transition moment M_T (Melchers and Kaur, 1982; Romstad and Subramanian, 1970; Lionberger, 1967; Lionberger and Weaver, 1969; Lui and Chen, 1983). In the third type, piecewise-linear model, the non-linear M-θ curve is approximated by a series of straight-line segments (Razzag, 1983; Vinnakoto, 1982). Although these linear models are easy to use, the abrupt changes

in stiffness at the transition points make them somewhat unrealistic. The three linear models are shown in Figure 2.9.

b- Polynomial model: Frye and Morris (1975) proposed an odd-power polynomial to represent the M-θ response which is given by:

$$\theta = C_1 (KM)^1 + C_2 (KM)^3 + C_3 (KM)^5 \qquad (2.1)$$

where

K = standardisation parameter

C_i = curve-fitting constants

The disadvantage of this model is that the connection stiffness as obtained from the first derivative of this equation, could be either discontinuous or even negative, neither of which is acceptable

Figure 2.10 shows a comparison between the M-θ relationship of a double web angle connection tested by Rathbun (1936) and the analytical result determined from the above equation. The differences between the experimental and analytical results of the moment-rotation curves for the various types of connection are summarised in Table 2.1.

Table 2.1

Comparison of analytical and experimental moment-rotation relationship

Types of connection	Rotation (rad)	Moment (kgm)		Differences
		Experiment	Polynomial Equation	%
double web angle	0.024	240.9	186.2	-22 %
top and seat angles	0.027	4471.2	4933.9	+10 %
header plate	0.054	9952.8	13518.8	+36 %
flush end plate.	0.052	6249.8	3666.1	-42 %
extended end plate	0.04	15263.7	13336	-13 %

The Table indicates that significant differences exist between the analytical and experimental results. This therefore leads to the conclusion that Equation (2.1) is unable to predict the moment-rotation curve for a variety of connections.

c- *Cubic B-spline model:* A cubic polynomial is used to fit segments of a curve. Between any two adjoining segments, the continuity of the first and second derivatives of each portion of the curve is enforced. To ensure a good curve-fitting process with test data, a large number of response points are needed.

d- *Power model*: A two-parameter power model (Batho and Lash, 1936; Krishnamurthy et al., 1979) has the simple form

$$\theta = a\,M^{b} \tag{2.2}$$

where a and b are two curve-fitting parameters with the conditions that a > 0 and b > 1.

Colson and Louveau (1983) introduced a three-parameter power function, as given below:

$$\theta = \frac{|M|}{K_i}\,\frac{1}{1-\left[M/M_u\right]^{n}} \tag{2.3}$$

where

K_i = initial connection stiffness

M_u = ultimate moment capacity

n = shape parameter of M-θ curve

Kishi and Chen (1987) proposed a similar power model given by,

$$\theta = \frac{M}{K_i\left[1-\left(M/M_u\right)^{n}\right]^{\frac{1}{n}}} \tag{2.4}$$

$$\theta = \frac{M}{K_i\left[1-\left(M/M_u\right)^n\right]^{\frac{1}{n}}} \tag{2.4}$$

where the definitions of parameters K_i, M_u and n are the same as those given in Equation 2.3. However, this model may not be suitable for test curves which do not have a plateau at the end of the M-θ relationship.

Ang and Morris (1984) used a Ramberg-Osgood (1943) function in a power form:

$$\frac{\theta}{\theta_o} = \left|\frac{KM}{(KM)_o}\right|\left[1+\left(\left|\frac{KM}{(KM)_o}\right|\right)^{n-1}\right] \tag{2.5}$$

where θ_o, $(KM)_o$ and n are variable parameters and K is the standardisation constant which is dependent on the connection type and geometry.

Comparison between the results calculated from the power model equation and the tests indicated that the initial stiffness is predicted very well. However, beyond the point of yielding, the moment-rotation equation does not correlate with the test results. The reason for this is that the model does not include the effect of strain hardening.

e- Exponential model: Chen and Lui (1985) proposed the following multi- parameter exponential model:

$$M = \sum_{j=1} C_j\left[1-\exp\left(\frac{|\theta|}{2j\alpha}\right)\right] + M_0 + R_{kf}|\theta| \tag{2.6}$$

where

M_o = starting value of the connection moment

R_{kf} = strain-hardening stiffness

α = scaling factor

C_j = curve-fitting constants

Kishi and Chen (1986a,1986b) refined the above model to accommodate the linear components that represent the M-θ curves accurately and to include the strain-hardening behaviour. The result is given as:

$$M=\sum_{j=1}^{m} C_j\left[1-\exp\left(\frac{|\theta|}{2j\alpha}\right)\right]+M_0+\sum_{k=1}^{n} D_k\left(\theta-\theta_k\right)H\left[\theta-\theta_k\right] \qquad (2.7)$$

where

D_k = constant parameters for the linear function

θ_k = starting rotations of the linear components

$H[\theta]$ = 1 $\theta > 0$

$H[\theta]$ = 0 $\theta < 0$

C_j, D_k = curve-fitting constants

Table 2.2

Comparison of analytical and experimental moment-rotation relationship

Types of Connection	Rotation (rad)	Moment (kgm)		Differences (%)
		Experiment	Modified Exponential Eq.	
double web angle	0.029	240.9	240.5	-0.02 %
top and seat angles	0.027	4471.2	4470.3	-0.02 %
header plate	0.054	9952.8	9949.4	-0.03 %
flush end plate	0.052	6249.8	6240.4	-0.15 %
extended end plate	0.040	15263.7	15270.8	+0.04 %

The advantage of the model (Equation 2.7) are as follows:

- The strain-hardening effect is included.
- The formulation are very simple and straightforward.
- It can apply to connection loading and unloading for the full range of relative rotation in second-order structural analysis with secant connection stiffness.

As shown in Figure 2.11 and Table 2.2, there is very good agreement between the results provided by the modified exponential equation and those obtained from experiments carried out by Ioannides (1978). In all the cases studied, the differences between the analytical and experimental results are less than 1%. It is therefore concluded that the modified exponential equation is capable of predicting within acceptable limit the moment-rotation curves for a range of experimental data.

f- Three Parameter Connection Model: A three parameter connection model is proposed by Kishi et al. (1991) for the analysis of semi-rigid frames. The selection of this connection model is guided by its simplicity for representing the basic behaviour of typical beam-to-column connections and for easy implementation in second-order analysis programs. The generalised equation of the power model has the form:

$$m = \frac{\theta}{\left(1+\theta^{n}\right)^{\frac{1}{n}}} \quad \text{for } \theta > 0 \text{ and } m > 0 \tag{2.8}$$

or equivalently,

$$\theta = \frac{m}{\left(1-m^{n}\right)^{\frac{1}{n}}} \quad \text{for } \theta > 0 \text{ and } m > 0 \tag{2.9}$$

The parameters in the above equations are defined as :

m = M / M_u,

M = connection moment,

M_u = ultimate moment capacity of the connection,

n = shape parameter,

θ = θ_r / θ_o,

θ_r = relative rotation between beam and column,

θ_o = reference plastic rotation, M_u / R_{ki},

R_{ki} = initial connection stiffness.

The parameters for these connection models are normally obtained by calibration with the experimental data. To demonstrate the accuracy of this model, the results of this approach are compared with the test results and are given in Table 2.3.

In Figure 2.12, the experimental results for top and seat angles with double web angles connection (Azizinamini et al., 1985) are compared to the results obtained from three of the proposed global models that are described above. As shown in Figure 2.12 and Table 2.3, the results calculated from the three parameter power models are in good agreement with the test results.

Table 2.3

Comparison of analytical and experimental moment-rotation relationship

Types of Connection	Rotation (radian)	Moment (kgm)		Differences (%)
		Experiment	Three parameter. Eq.	
double web angles	0.029	240.9	232	-3 %
top and seat angles	0.039	4341.2	3896.3	-10 %
header plate	0.054	9952.8	11213.1	+13 %

As noted earlier, this model is relatively easy to implement in a non-linear structural analysis program. The values both for initial stiffness and ultimate moment are accurate. But similar to other models, the calculation of these values is not obtained directly from analysis and limited to the range of calibration data.

As result of this investigation, it is concluded that the linear models are simple and easy to use but they are not very accurate. The polynomial model can fit the test results but the occurrence of negative stiffness is unacceptable. The cubic B-spline curve is adequate but it requires a large amount of data to represent the curve accurately. The power and exponential models are suitable for predicting the moment-rotation curves but, for good correlation with the test curves, it is necessary to have a large number of curve-fitting parameters. In addition, it is impossible to calculate the initial stiffness and ultimate moment of the connection for all of the above models directly from analysis.

2.3.2 Component-Based Models

In an effort to overcome the lack of theoretical background of the global models component-based approaches have adopted a technique which is based on the analytical modelling of individual sources of flexibility and strength (i.e. angles, bolts, shear panel, etc.) assembling the contributions made by the various components, it is envisaged that the overall connection response will be determined.

A component-based model for double web angle connections was developed by Wales and Rossow (1983). In their approach the connection is represented by two rigid bars linked by an independent non-linear spring which simulates the small segments of the double web angles. The parameters defining the trilinear load-deformation relationships for the spring are determined from an analysis of the double web angles, when these are subjected to simple tension or compression. The angle and column flange flexural deformations, as well as the bolt elongation, are accounted for under tension while the column web is assumed to contribute under compression. This model is also capable of representing the coupling effects between bending moment and axial force applied to the connection.

A similar approach was used by Kennedy and Hafez (1984) to describe the behaviour of the header plate connection (partially welded end-plate).

Recently, a component-based model was developed by Madas and Elnashai (1992) to account for the detailed behaviour of different types of welded and bolted beam-to-column connections. An idealisation of the model is shown in Figure 2.13, where points A and B represent the end of the beam and the centroid of the column, respectively. The non-linear spring sets, C and D, simulate the deformable connecting elements while the panel zone deformation is represented by the non-linear spring E.

The non-linear behaviour of spring sets C and D is idealised by a cyclic trilinear load-deformation relationship. The model also accounts for the effect of bolt slippage in the connection and non-linear behaviour of the shear panel Zone. Coupling between the component relationships is determined according to equilibrium and compatibility

requirements. The accuracy of this model is validated elsewhere (Madas and Elnashai, 1992).

2.3.3 Finite Element Models

Representation of the connection behaviour by finite elements can provide useful information on the deformational behaviour of connection components and at the same time, provides some insight into their complex interaction. In order to predict the moment-rotation curve accurately, the use of non-linear finite elements is essential.

An earlier study carried out by Bose et al. (1972), used finite elements to examine the behaviour of fully-welded beam-column connections. In their study, they assumed that the critical connection component was the column web which was subjected to moment and shear forces.

Patel and Chen (1984) investigated the behaviour of connections where the beam was either fully or partially-welded (only at the beam flanges) to the unstiffened column. Atamiaz and Frey (1988) performed 3-D finite element analyses on fully-welded connections using shell elements. Both studies compared satisfactorily to experimental results. Although the finite element technique represents an accurate tool for welded connections there is still room for refinements in the modelling of the welded parts of the connections.

For bolted-connections, the work of Richard et al. (1980) on single web-plate connections is based on the development of an inelastic finite element model for the simulation of the bolt action. Beaulieu and Picard (1988), in order to represent the bolt slippage effects, proposed a bar system for use in the finite element analysis.

2.3.4 Remarks

In conclusion, for global models, the prediction of connection response obtained through the determination of key parameters (e.g. initial stiffness, moment capacity, etc.) and the fitting of a skeleton curve through experimental data points, can represent

closely virtually any shape of M-θ curve. They suffer, however, from the disadvantage that they cannot be extended outside the range of calibration data. Additionally, they are unable to predict the different behaviour due to possible change of failure mode when connections with different geometrical and material properties are considered. The loading and unloading behaviour is also determined by the same rules applied to the monotonic case. Nevertheless, these models are useful for design purposes as well as for implementation in frame analysis programs.

On the other hand, the component-based models predict the M-θ connection response without the need to restrain it to predetermined response patterns, as in the case of other models. The accuracy of this method is increased as the number of components taken into account increases. The method is also capable of predicting the variation in failure modes due to changes in the connection geometry and material properties as well as loading conditions.

Prediction of the connection behaviour by finite element analysis can provide accurate results when welded connections are considered. It can provide acceptable solutions for bolted connections, but not to the same level of accuracy as for welded connections, due to modelling complexities. Modelling of connections, using finite elements, can represent an accurate simulation of the behaviour of such connections when compared with experimental results. From the point of view of frame analysis, this method is costly and time consuming in comparison with the other techniques discussed above.

2.4 Cyclic Behaviour of Semi-rigid Connections

During the past years, several tests have been conducted to study the monotonic response of the semi-rigid connections that were mentioned in the previous section. However, only a few cyclic and dynamic tests have been performed in order to obtain a better understanding of their behaviour under earthquake-type loading. In this section, some test and analytical results are presented and discussed.

A series of cyclic tests were conducted by Ballio et al. (1986) on flange plates connections, flange and web cleated connections, extended end plate connections and welded connections. In this study, the influence of column web stiffeners on the connection behaviour and the large bolt slippage, which significantly affect the shape of the experimental loops, have been discussed.

The results of this experimental work concentrated on the cyclic behaviour of full scale beam-to-column joints. The details of two types of connection, A and D, are shown in Figures 2.14 and 2.15.

As illustrated in Figure 2.14, type A is obtained by means of three plates welded to the column. Two of the plates are bolted to the beam flanges by 2x4 bolts and the third plate is fixed to the web by three bolts. Specimen A2 is formed from the basic A1 by introducing a diagonal stiffener in the central panel or column web. In specimen A3, reinforcing plates are added to the beam flanges as internal cover plates; both the variations of A2 and A3 are introduced in the A4 connection. The type D connection (Figure 2.15), is fully welded. The connection D2 is obtained from D1 by the addition of a double web splice plate.

The results of these two types of connection are given in Table 2.4. The additional stiffness in the panel zone in type A2 and A4 reduces the energy dissipated and increases the strength. When the maximum force of models A2 and A4 are compared to the forces at the failure mode (i.e. shear failure), F_u, it is seen that the shear failure of the bolts in A2 and A4 results in a brittle collapse behaviour. As a result of this behaviour, these two models have failed without dissipating energy.

Comparison between the values of strength of the two types of connection A1 and A3, and their cumulative energy indicated that the increase in thickness of the beam flanges produces an increase in energy dissipated and strength. As shown in Table 2.4, this increase of thickness does not increase the energy and strength for type A4 when compared to A2. This is because of the brittle behaviour of type A4 failing in bolt shear at 50 mm displacement.

Table 2.4

Cyclic response of all models tested by Ballio et al.(1986)

Specimens	d_{max} (mm)	F_{max} (kN)	F_u (kN)	Dissipated energy (kNm)
A1	100	173.9	151.9	440.12
A2	60	225.4	225.4	92.88
A3	100	178.9	132.3	501.66
A4	50	222.9	222.9	84.67
D1	90	166.6	147	324.45
D2	80	210.7	120	269.13

The stiffening of the column panel in D2 produces a decrease in energy absorption and an increase of load level reached when compared with D1. Comparison of the energy dissipated values for the two types of connection, semi-rigid connection (A1) and fully-welded connection (D1), indicated that flexibility of the bolted connection and also the effect of bolt slippage give an increase of energy dissipated in this type of connection.

In conclusion, the amount of energy absorption decreases with an increase of connection stiffness (comparison between A1 and A2) and increases with an increase of the local strength of the structural sub-elements (comparison between A1 and A3).

Bernuzzi et al. (1991) have tested top and seat angle (TSC) and flush end plate (FPC) connections under cyclic loading, observing the influence of the loading history and of the connection details. In particular, special attention was paid to evaluating the effects of bolt slippage which appears to increase (to a large extent) the joint flexibility. In this experimental investigation, the specimen consisted of a beam stub which was attached, by means of the connection, to a counter-beam having negligible deformation. A horizontal force was applied at the free end of the beam stub. The test arrangement was designed in order to simulate the condition of the beam-to-column connection with negligible column deformability thereby focusing the attention on the connection behaviour.

To examine the effect of the different loading histories, four different procedures of cyclic loads were imposed on the specimens. The main characteristics of the loading histories can be summarised as follows:

Proc. A : Three cycle for each even multiplier of yield displacement

Proc. B : One cycle for each integer multiplier of yield displacement

Proc. C : Two cycle for each integer multiplier of yield displacement

Proc. D : One cycle for each even multiplier of yield displacement

The results of the tests, in terms of initial stiffness $S_{j,\,init}$, the maximum moment M_{max} and the corresponding rotation θ_{max} are summarised in Table 2.5. As indicated in this Table, no significant effect of the type of cyclic loading history has been detected.

Table 2.5

Cyclic responses of the models was tested by Bernuzzi et al.(1991)

Test	$S_{j,\,init}$ (kNm/mrad)	M_{max} (kNm)	θ_{max} (radian)
Proc. A	24.2	70.6	74.2
Proc. B	23.7	72.0	69.0
Proc.C	21.0	67.1	67.1
Proc. D	29.1	70.6	68.7

The effect of bolt slippage on the behaviour of the structure was also examined in this investigation. It was observed that the maximum net rotation that can be evaluated by excluding the rotation due to slippage from the total rotation is approximately one third. It was also observed that the rotation due to slippage increases as the connection is subjected to more than one constant amplitude deformation cycle.

From this investigation, it was concluded that a large portion of the connection flexibility is due to bolt slip and that this phenomenon may become dominant if the connection is subjected to large cyclic loading thereby notably influencing the overall structural response.

2.5 Seismic Behaviour of Semi-rigid Steel Frames

A comparison of the seismic behaviour of rigid and semi-rigid steel moment frames indicates that the seismic forces generated in a semi-rigid frames are sometimes less than the comparable rigid frames.

The decrease in the forces and some increases in the displacements of semi-rigid frames are attributed to the elongation of the period of the structure, increase in damping and a decrease in the stiffness at an early stage of response.

Some experimental and analytical work were recently conducted by researchers to examine the seismic behaviour of semi-rigid frames. A brief review of these studies and their results are summarised below.

The hysteretical behaviour of bolted end-plate connections in terms of moment-rotation dependencies has been experimentally determined by Sedlacek and Ballio (1984). The tests demonstrated that the q-values are greater (by approximately 20%) than those for rigid connections (Table 2.6). This increase in behaviour factor causes a decrease in design forces. The effect of higher flexibility in decreasing response forces and increasing displacements has been confirmed.

Table 2.6

Calculated behaviour factors for models tested by Sedlacek et al.(1984)

Specimens	Yield Acceleration	Maximum Acceleration	Behaviour Factor
Semi-Rigid	0.09 g	0.33 g	3.7
Rigid	0.11 g	0.35 g	3.2

Two rigid frames with fully-welded connection and three semi-rigid frames with top and seat angles and double web angle connections were tested by Elnashai and Elghazouli (1994). The displacement response histories for both first and second floors from the two pseudo-dynamic tests for rigid and semi-rigid connection frames are given in Table 2.7. As shown in this Table, the semi-rigid response displacements are lower than the fully-welded case.

Table 2.7

Comparison of responses for rigid and semi-rigid frames (Elnashai et al., 1994)

Frame Type	1st Floor Displacement (mm)	2nd Floor Displacement (mm)
Rigid	70	120
Semi-Rigid	40	85

In this investigation, an analytical study was conducted with the aim of highlighting the effect of different connection types on the overall response of the frame. Four different types of connection (fully-welded to flexible connection) were considered in this study. It was observed that the height of the point of contra-flexure increases with increased flexibility of the connection. It was also found that the length of the plastic hinge in the first storey column increases with an increase in the flexibility of the connection.

To investigate the dynamic response of semi-rigid frames an analytical study was carried out by Rosales (1991). In this work the frame were modelled as two dimensional structures. Two storeys four bays and five storeys two bays frames were considered. The selected connections and the corresponding frames were referred to as semi-rigid medium stiffness. Two additional variants were studying by increasing and decreasing the reference stiffness and strength. All of the frames were subjected to two records (the E-W component recorded at San Ysisdro school, Gilory and the 350° component recorded at Emeryville).

The results from this investigation indicated that exception made of the case of very low stiffness connections, the performance of the 2x4 frame with rigid and semi-rigid connections was adequate. In all cases the maximum plastic rotations at the column bases were less than 25% of the admissible values and the maximum rotations in the connections were closer to their rotation capacity. The drifts in both storeys were less than 2%, which can be considered to be acceptable from the ultimate limit state point of view.

In the case of 5x2 frame, a fourth storey sway mechanism was developed in the rigid frame under strong ground motion. This is the cause for the large drifts (2.3%) in this level, that was the largest in all the storeys for all the frames. Except for the frame with high stiffness connections, for all the other semi-rigid frames the drifts are very similar and lower than.1.5%. For the most flexible frames the inelastic action at the columns is almost absent, even at the column base. This behaviour was attributed to the frequency content of the records used. It was observed that the selection of the more expensive rigid connection is not the optimum choice under any criteria and the use of flexible connections does not necessarily imply larger deformations under earthquake excitation.

Dubina et al. (1995) have studied the influence of the M-θ model of semi-rigid connections on the stability and seismic behaviour of steel structures. The structures analysed and tested were the four calibration frames recommended by the ECCS (1992). Full details of these structures are given in the reference mentioned above and summarised in Table 2.8.

Table 2.8

Frame Dimensions were analysed by Dubina et al.(1995)

Type of Frame	Storey	Bay	Height of Storey	Length of Bay
Frame-A	1	1	6.00 m	5.00 m
Frame-B	1	2	12.00 m	12.00 m
Frame-C	3	1	4.00 m	5.00 m
Frame-D	2	3	4.00 m	5.00 m

The multipliers λ_p (plastic yielding factor) and λ_{pl} (load factor) for the first plastic hinge moment were computed for each structure with different values of initial rotational stiffness, k_o, for the bilinear model of the M-θ curve. The values of λ_p and λ_{pl} are given in Table 2.9.

Table 2.9

Multiplier Factors for different rotational stiffnesses (Dubina et al., 1995)

	Frame A		Frame B		Frame C		Frame D	
Stiffness	λ_p	λ_{p1}	λ_p	λ_{p1}	λ_p	λ_{p1}	λ_p	λ_{p1}
k_{sec}	2.037	1.924	2.758	1.778	1.545	1.254	1.464	1.259
$k_i / 2$	2.036	1.833	2.757	1.585	1.542	1.135	1.461	1.034
k_i	2.039	1.736	2.756	1.385	1.553	1.017	1.452	0.778

It is observed that λ_p is weakly influenced by different values of stiffness because it depends primarily on the ultimate moment, M_u. However, λ_{p1}, the first plastic hinge coefficient is influenced by different values of stiffness for each type of structure.

From this investigation, it is concluded that the first plastic hinge coefficient, λ_{p1}, is influenced by the different initial rotational stiffness of the bilinear moment-rotation curve of the connection. In contrast, the plastic yielding factor, λ_p is not. This would imply that by using different initial rotational stiffness in the connection the load factor, λ_p remains the same while the load factor, λ_{p1} changes. Hence, by using different initial stiffnesses, a different behaviour factor is obtained for the structure.

The effect of the initial stiffness k_o of the bilinear curve on the first three eigenperiods of the structure was also examined in this studies. It was observed that only the first period is affected by the different values of initial rotational stiffness, whilst the second and the third eigenperiods remained almost constant.

In addition, a comparison between the time-history responses of the semi-rigid frames with the rigid frames were presented in this study. For this purpose, four structures were subjected to the time-history record of the 4 March 1977 Bucharest earthquake (NS component).

The values for the accelerogram multiplier λ_m and λ_c (λ_m is the multiplier of the accelerogram for which the elasto-plastic curve of the displacement intersects the

elastic curve and λ_e is the yield multiplier accelerogram), maximum displacements and the behaviour factor q are given in Table 2.10.

Table 2.10

Calculated behaviour factors for the frames were analysed by Dubina et al.(1995)

Frames	Type of Connection	λ_e	λ_m	Yield disp.(mm)	Max. displ. (mm)	q factor
Frame-A	Semi-Rigid	0.15	0.40	86	143	4.65
Frame-A	Rigid	0.13	0.26	82	139	3.40
Frame-B	Semi-Rigid	0.60	1.40	235	509	4.20
Frame-B	Rigid	0.89	1.30	387	460	3.10
Frame-C	Semi-Rigid	0.04	0.50	68	381	3.80
Frame-C	Rigid	0.12	0.66	89	447	2.40
Frame-D	Semi-Rigid	0.03	0.27	25	133	9.00
Frame-D	Rigid	0.06	0.20	44	122	3.50

Table 2.10 demonstrates that the values of the behaviour factors in structures with semi-rigid connections are greater than those for rigid structures. This implies that structures with semi-rigid connections attract lower seismic forces. However, the horizontal displacements of the structures with semi-rigid connections are greater than those of the rigid frames but the difference is not greater than 35%.

Astaneh and Nader (1991) have investigated the behaviour of a one storey single bay steel structure with rigid, semi-rigid and flexible connections subjected to a variety of base excitations using the shaking table. They also developed a first proposal for a recommended design procedure for design of semi-rigid frames (Nader and Astaneh, 1992). According to this procedure, it is suggested that the design of the connections should be such that yielding occurs only in the plate elements, (i.e. angles, splices and end plates) while the connectors (i.e. bolts and welds) should remain in the elastic range.

The seismic response of a four, seven and ten-storey semi-rigid steel frames that were designed according to this procedure, have been studied in this report. These frames were subjected to three different time-history earthquake ground motions. Full details of these buildings and the ground motions are given elsewhere (Nader et al., 1992).

Table 2.11

Frame dimensions and type of connection (Astaneh et al., 1992)

Frames	Height of Storey	Number of Bays	Length of Bay	Type of Connection
4-storey	14 ft.	4	30 ft.	Top and Bottom Angle with Tee-Connection
7-storey	12 ft.	2	30 ft.	Top and Bottom Angles with Double Web Angles
10-storey	12ft	3	30 ft.	Extended End plate Connection

Table 2.11 shows the geometric parameters of the frames while the interstorey drifts, the maximum rotation of the connections and members at ultimate state are given in Table 2.12.

Table 2.12

Time history responses of the frames of Astaneh et al.(1992)

Frames	Interstorey Drift	Max. Rotation of Connection	Max. Rotation of Members	Total Rotation	Rotation Capacity
4-Storey	0.017	0.009	0.003	0.012	0.035
7-Storey	0.019	0.005	0.012	0.017	0.025
10-Storey	0.018	0.008	0.007	0.015	0.030

As indicated in Table 2.12, in the four storey frame, the maximum rotation in the connection is 0.009 radians and in the connected member it is less than 0.003 radians. The total rotation is approximately 0.012 radians.

BRL. LAHOR. DEPT.

From the values of rotation in all members and connections it is seen that the damage is spread throughout the building and is primarily concentrated in the connections. However, some inelasticity is observed in the first floor beams and the third floor columns. This implies that the yielding in the connections and the undergoing of inelastic deformation in the noted members prevent any damage to other members of the structures. In addition, the interstorey drift in this building (approximately 0.017) is not very large and it is only slightly larger than the allowable limit state of 0.015.

In the seven storey frame, the damage is also spread throughout the building and concentrated in the connections. The maximum plastic rotation is 0.005 radians except for one record where the plastic rotation reached 0.012 radians in the connected beam. However, as indicated in Table 2.12, the total rotation is less than the rotation capacity of the connections

In the ten storey frame, none of the columns suffered inelastic deformations whereas the beams were subjected to a rotation of up to 0.007 radians. Once again, the damage was distributed over the entire building and was mostly concentrated in the connections.

From these results, it was concluded that the interstorey drift is not a severe problem for semi-rigid frames. It was also noted that if the connections were designed so that yielding occurred only in the plate elements and the brittle parts remained in the elastic range, the greatest damage to the building in the event of a major earthquake would be concentrated in the connections.

2.6 Commentary

Based on the results of the experimental and analytical investigations that were presented in this chapter, it is clear that semi-rigid frames demonstrate a ductile and stable hysteretic behaviour when subjected to cyclic and earthquake loading. The overall behaviour of such structures were mainly affected by the flexibility of the connections. It was shown that when the structures were designed such that yielding occurred in the connections, high stress concentration in the connected members are prevented. In addition, some of the results demonstrated that the behaviour factor for

semi-rigid steel frames were greater than for similar rigid frames which meant that semi-rigid frames attracted lower seismic forces in the inelastic response domain.

As mentioned previously, all rigid structures suffer from the soft storey mechanism with plastic hinges occurring in columns and beams. For frames with semi-rigid connections the yield mechanism was always global with plastic hinges occurring at connections or at the ends of the beams and finally at the columns base.

Few tests have been carried out on this type of structure, hence there is insufficient information to formulate a complete design for semi-rigid frames under earthquake loading. There is still an urgent requirement to investigate further the seismic behaviour of this type of structure. Such an approach should be focus on the effect of strength, stiffness and ductility of the connection on the overall behaviour of the frames and also on the seismic characteristics of the structures.

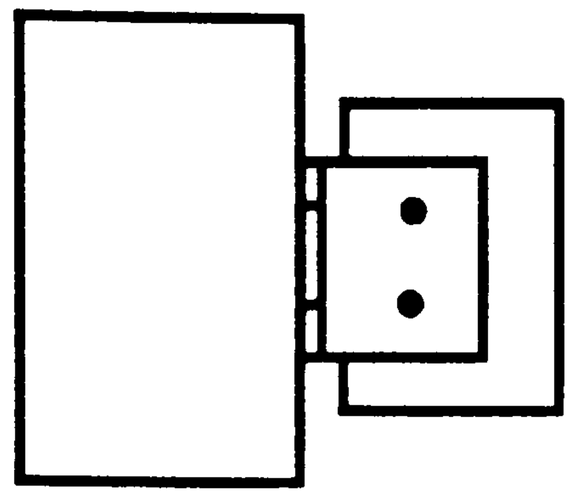

a) Single or double web angle

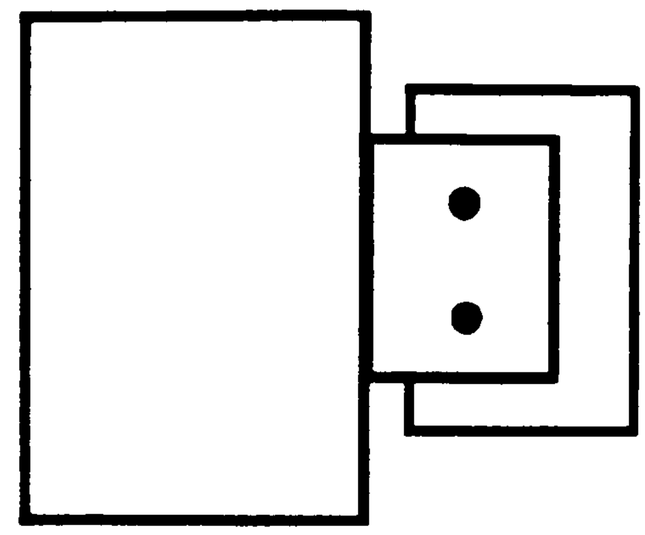

b) Web side angle

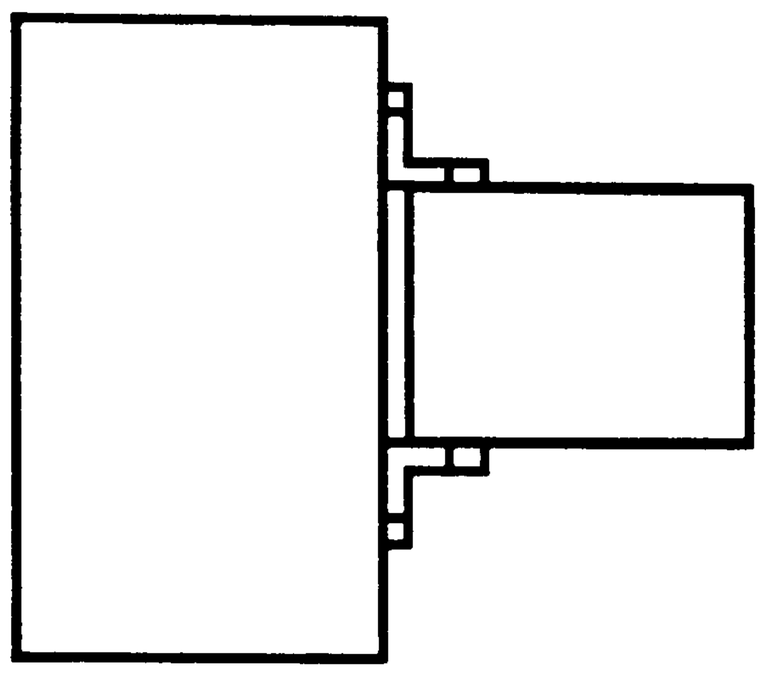

c) Top and seat angle

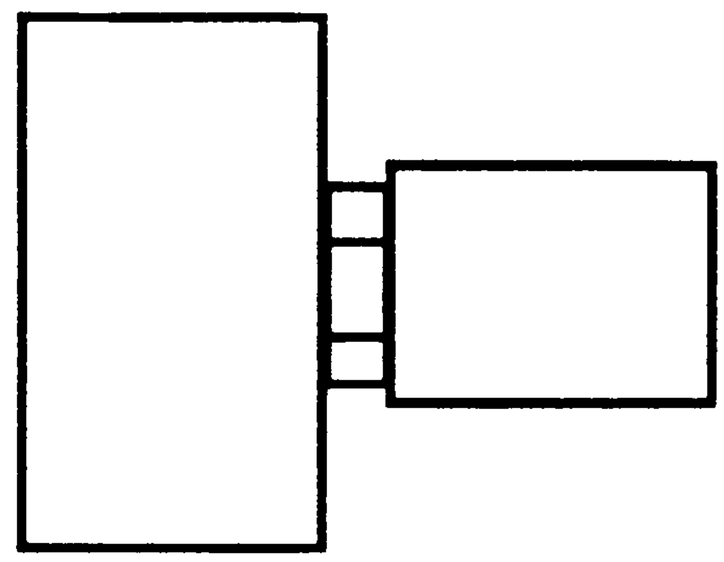

d) Header plate

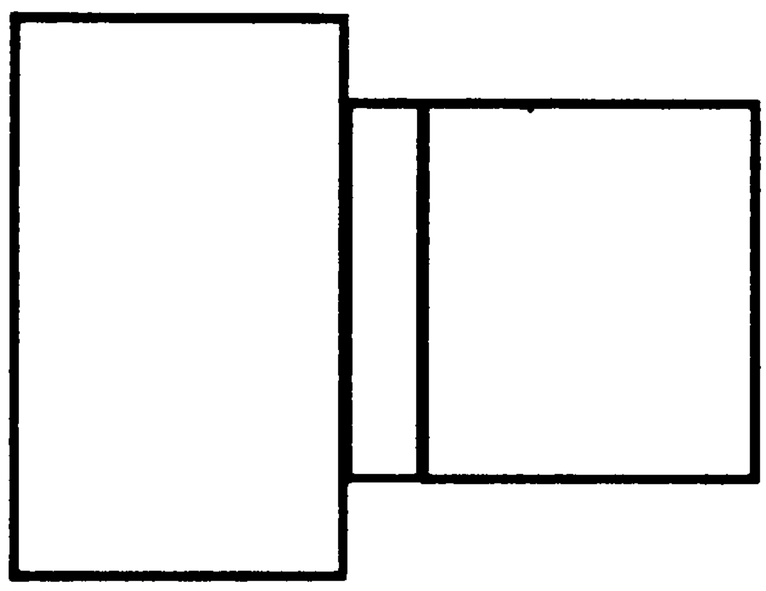

e) Flush end plate

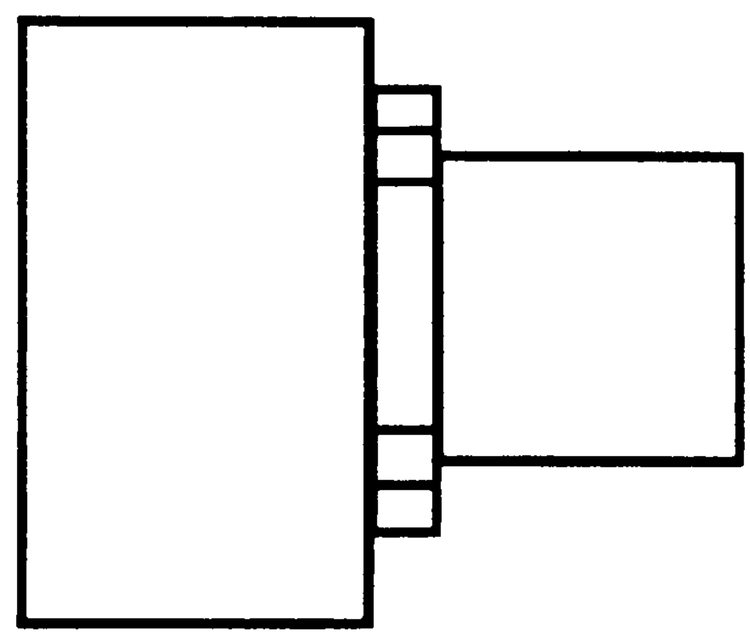

f) Extended end plate

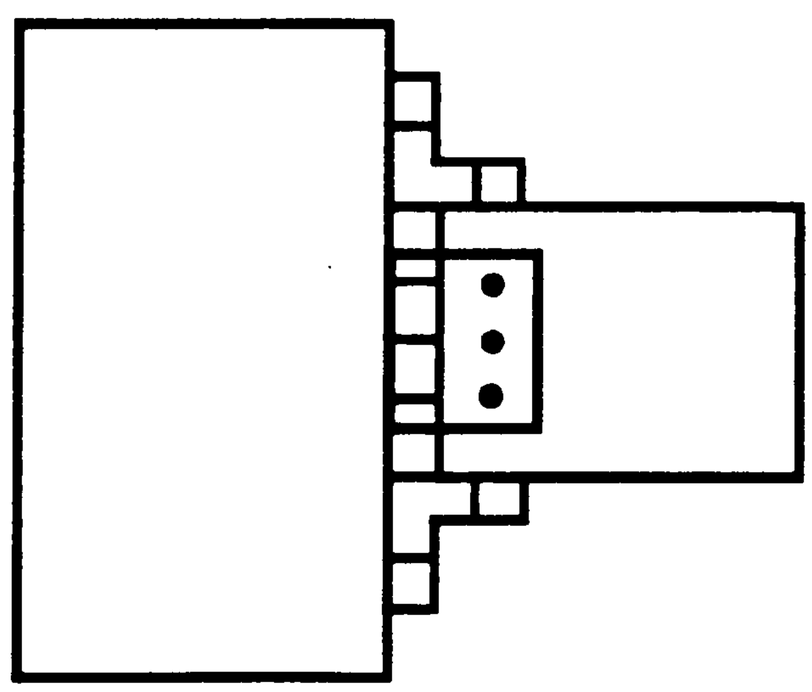

g) Top and seat with double web angles

Figure 2.1 Typical beam-to-column connections

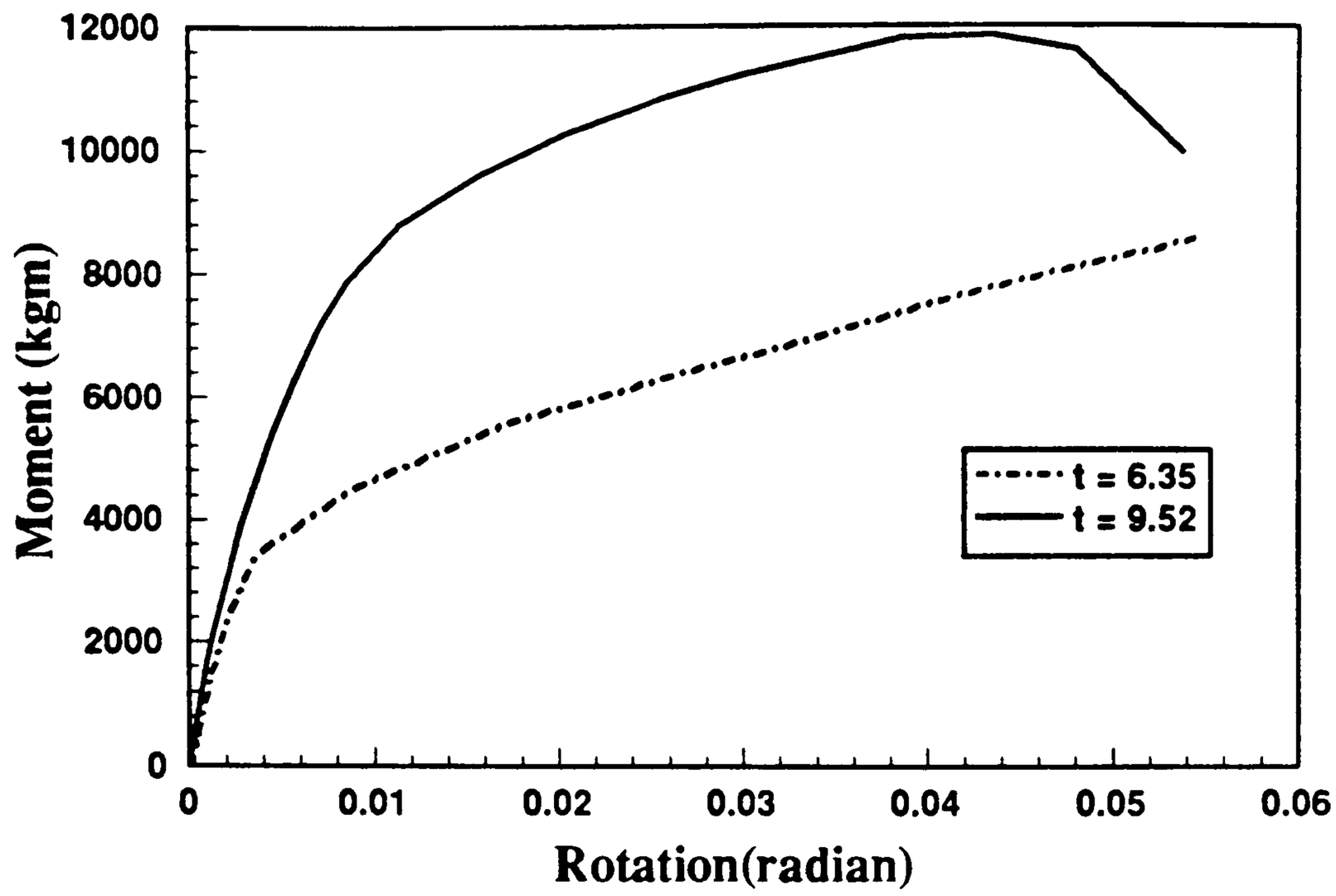

Figure 2.2 Experimental moment-rotation relationship of header plate connection with different thickness plate (Sommer, 1969)

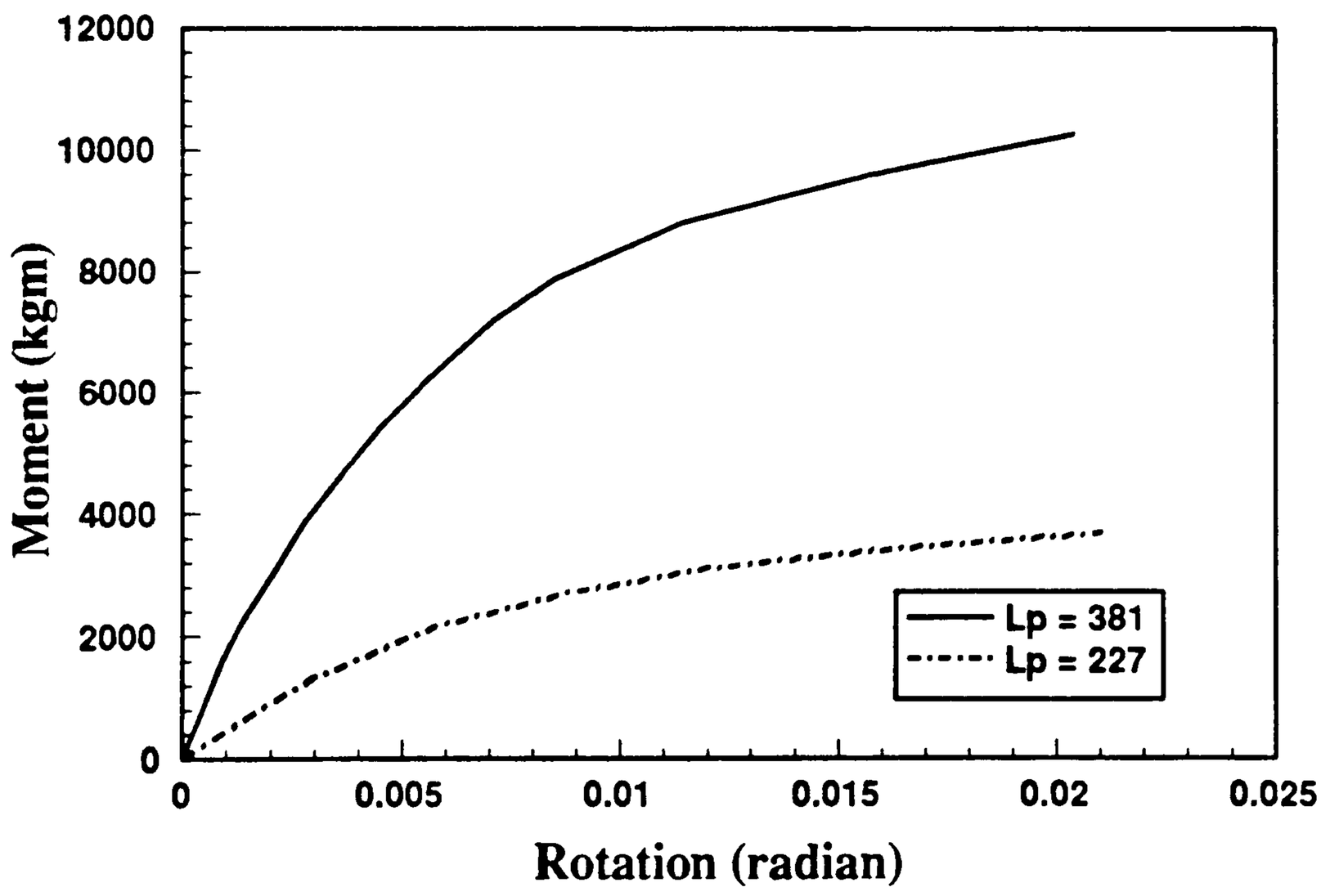

Figure 2.3 Moment-rotation relationship of header plate connection with different depth of plates (Sommer, 1969)

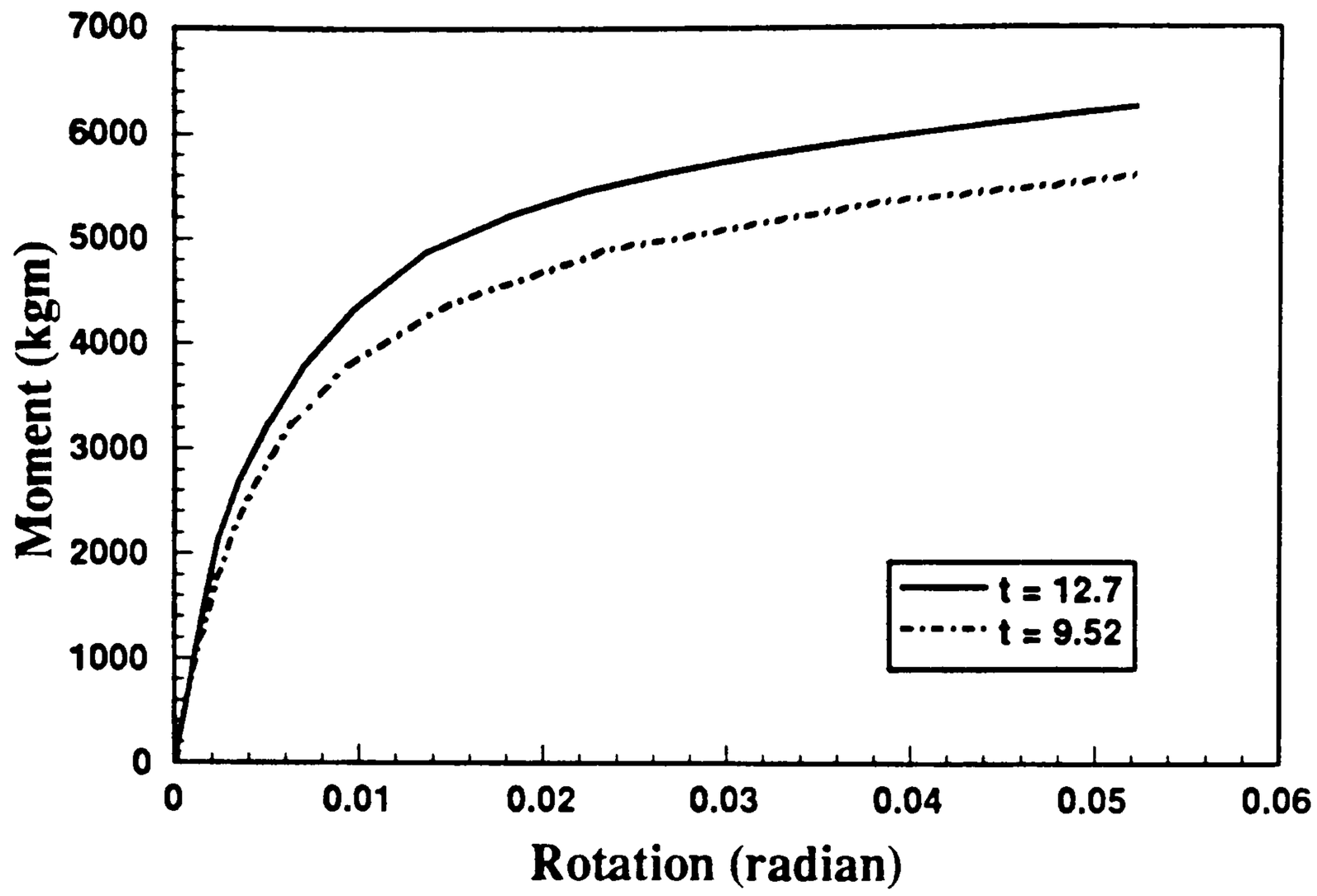

Figure 2.4 Experimental moment-rotation relationship of flush end plate connection with different thickness plate (Ostrander, 1970)

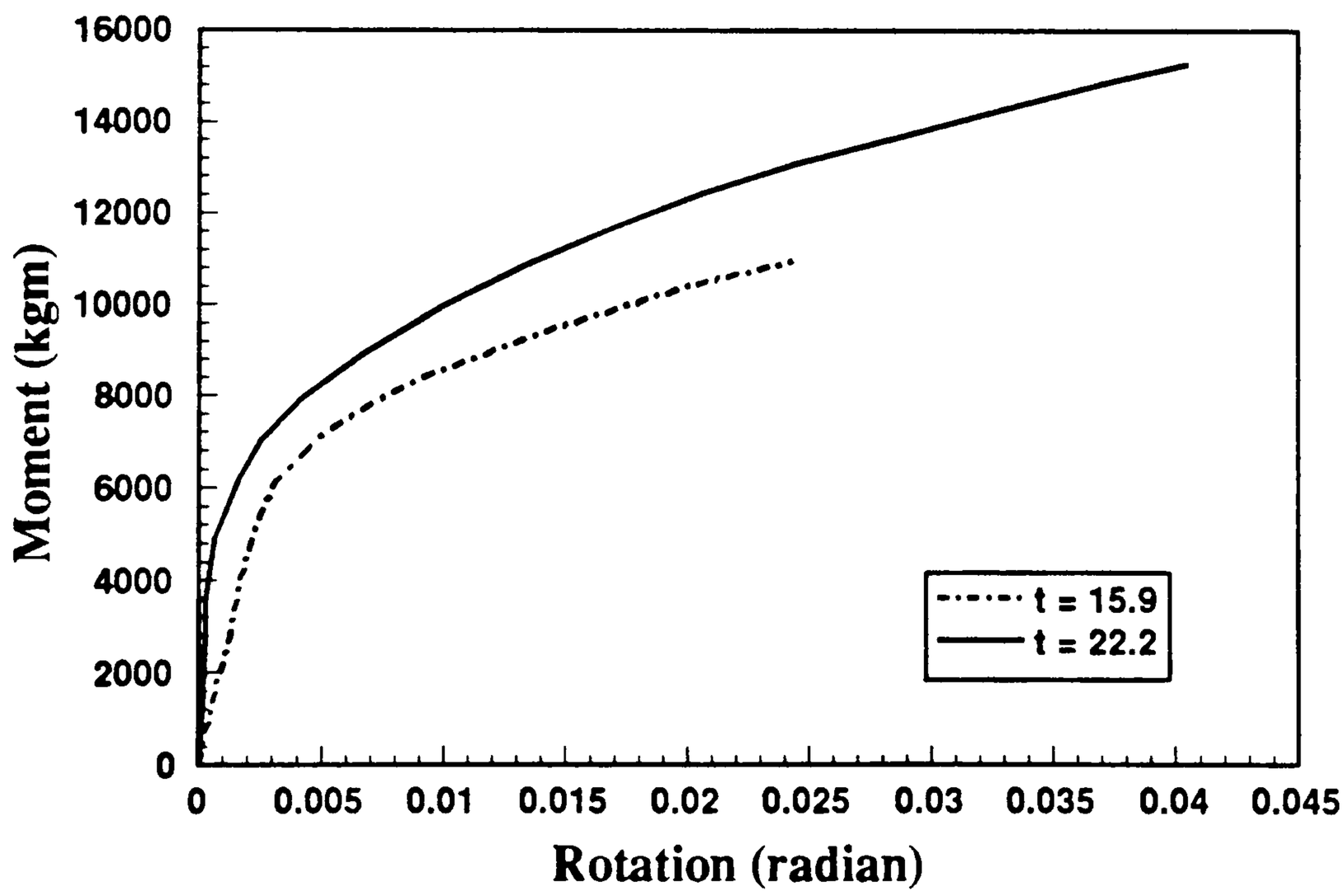

Figure 2.5 Moment-rotation relationship of extended end plate connection with different thickness plate (Ioannides, 1978)

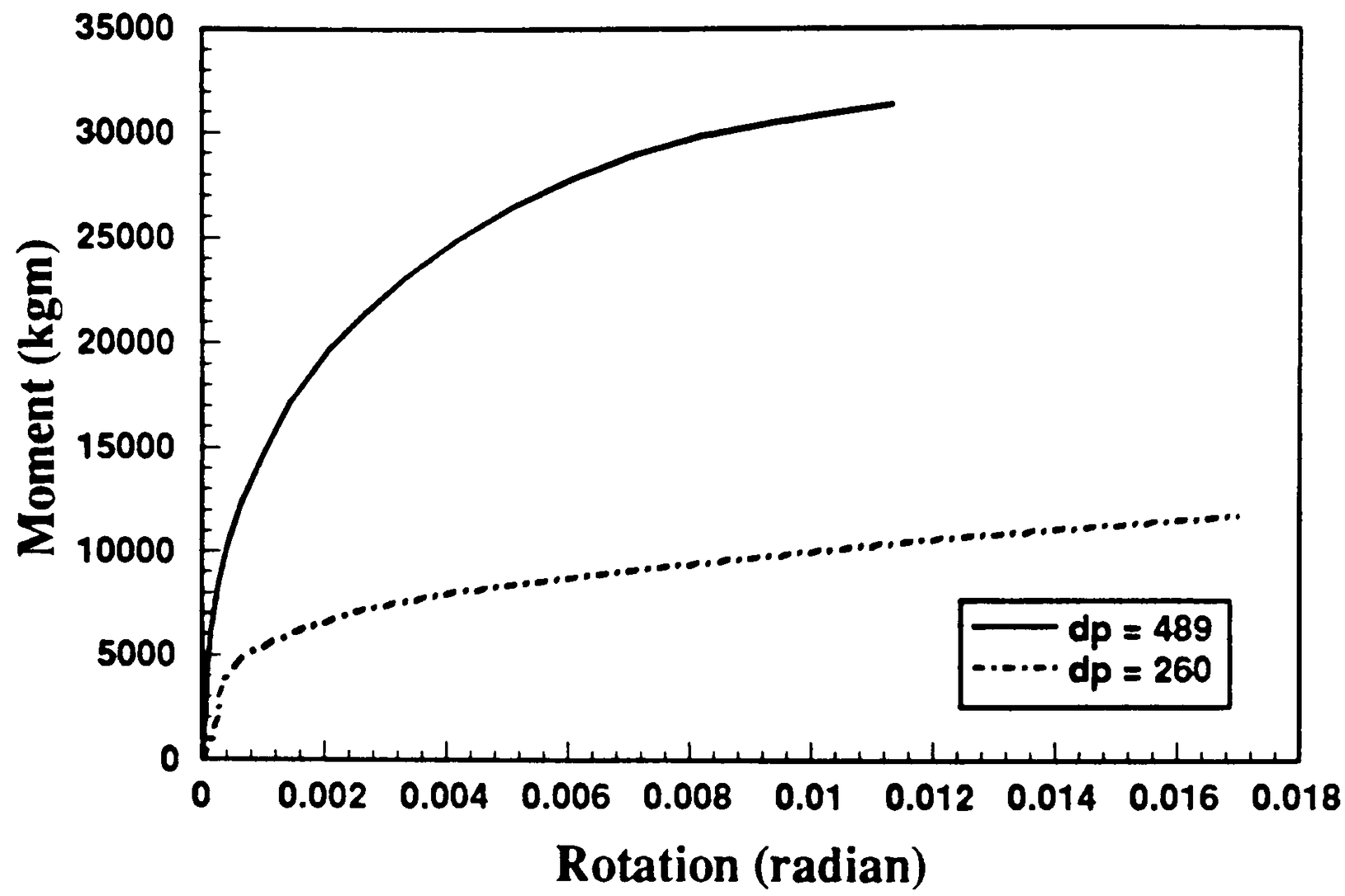

Figure 2.6 Experimental moment-rotation relationship of extended end plate connection with different depth-plate (Ioannides, 1978)

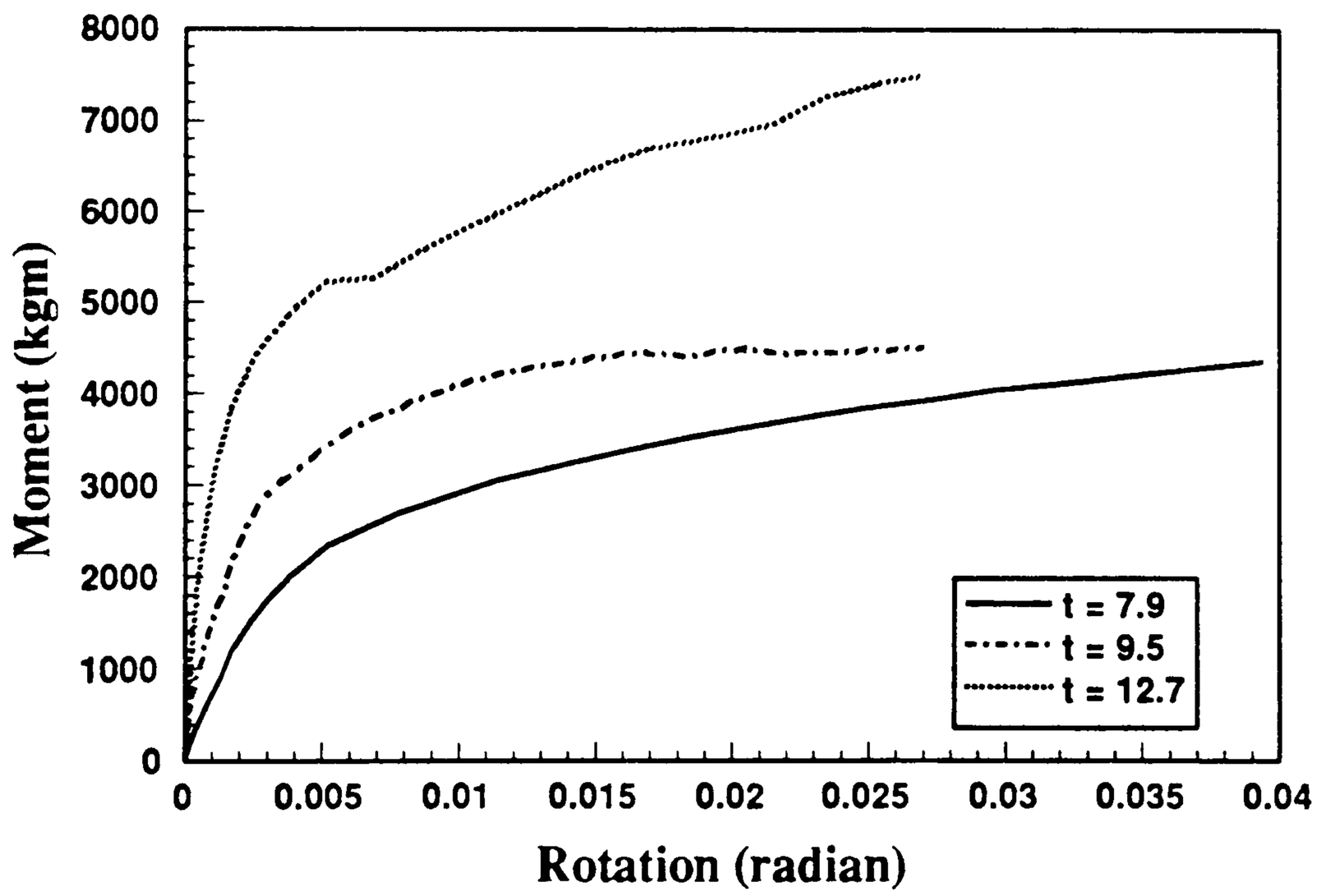

Figure 2.7 Moment-rotation of top and seat with double web angles connection with different thickness of angles (Azizinamini et al., 1985)

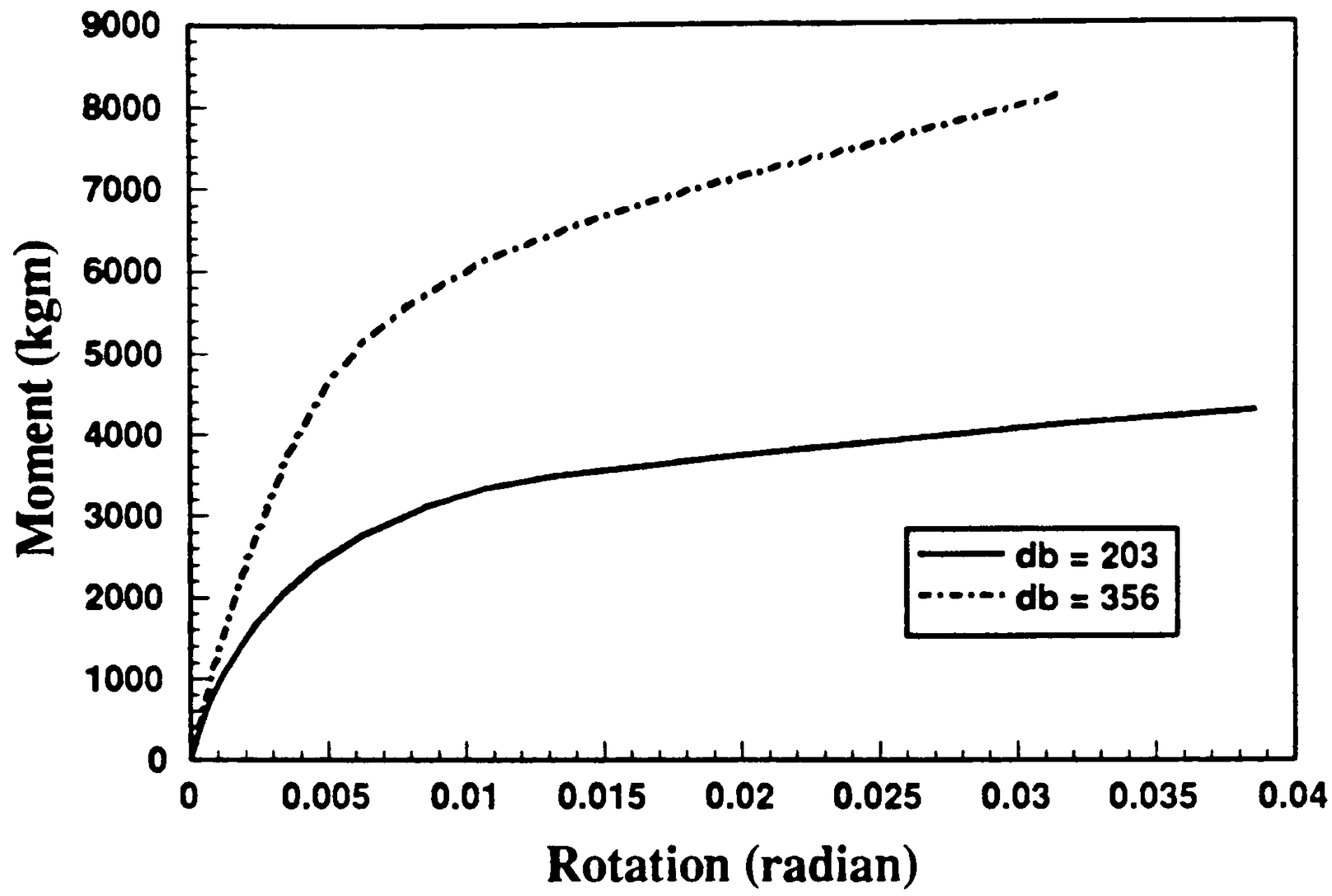

Figure 2.8 Experimental moment-rotation of top and seat with double web angles connection with different depth of the beam (Azizinamini et al., 1985)

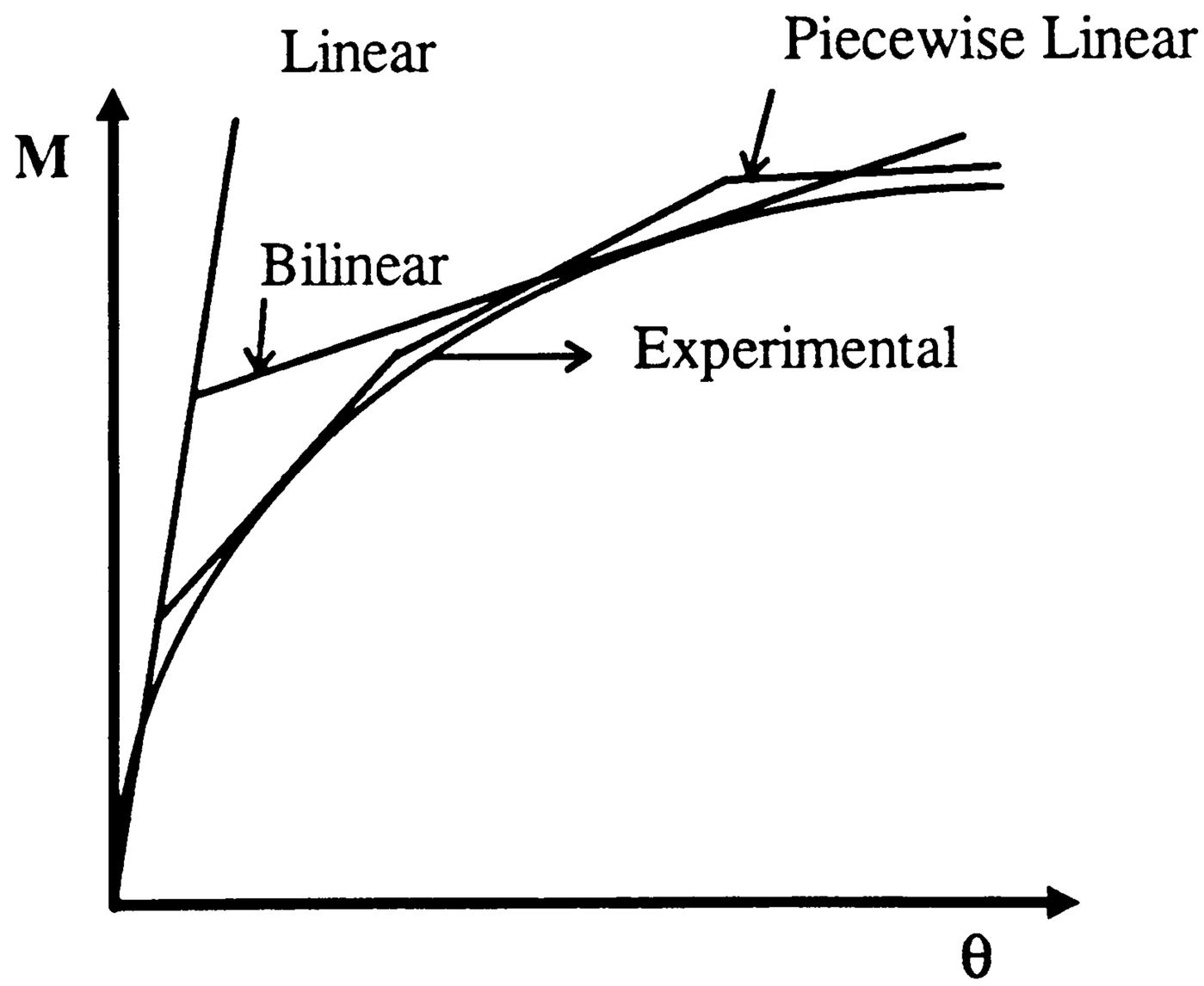

Figure 2.9 Linear M-θ models

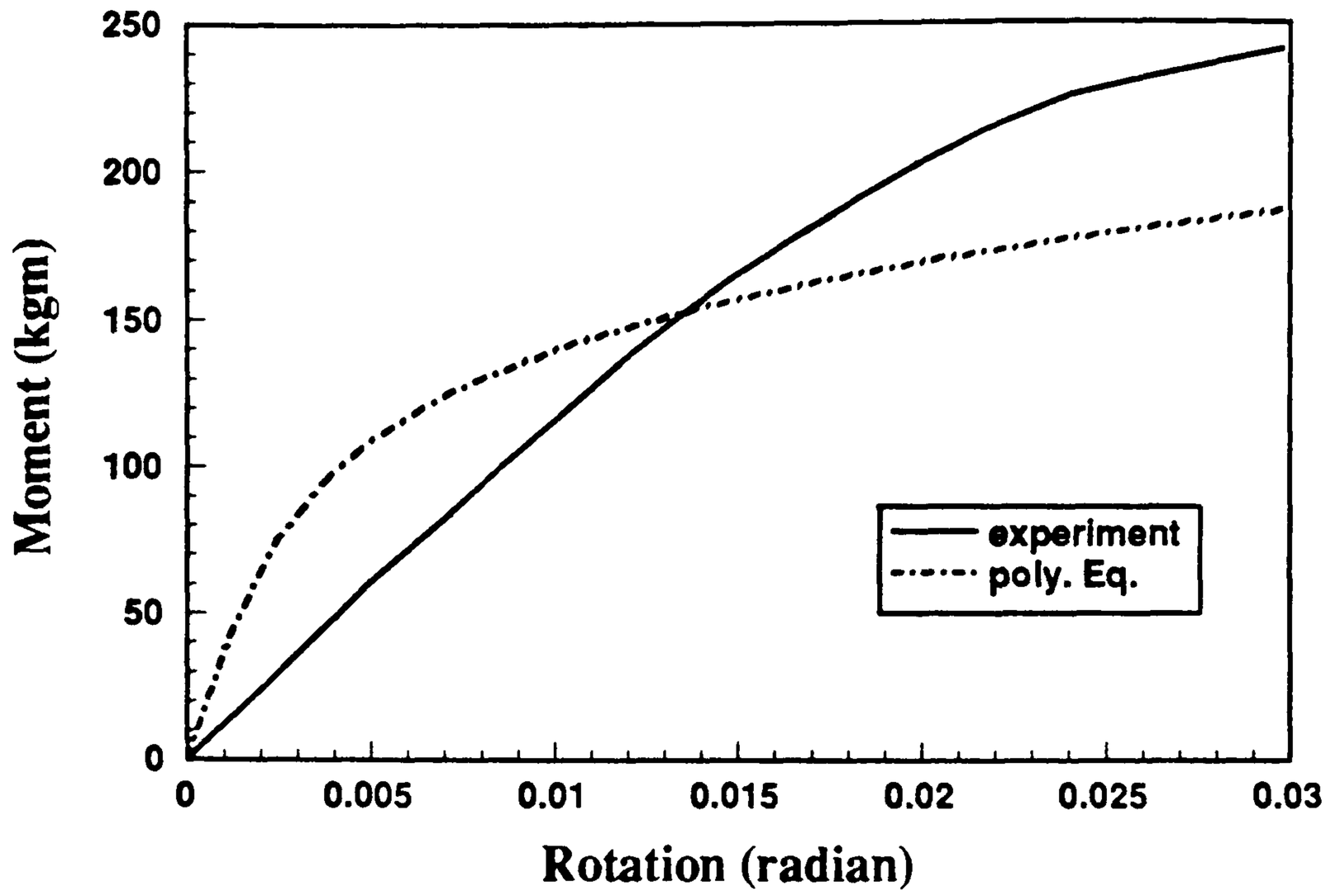

Figure 2.10 Comparison of experimental moment-rotation curve of double web angle connection (Rathbun, 1936) with analysis

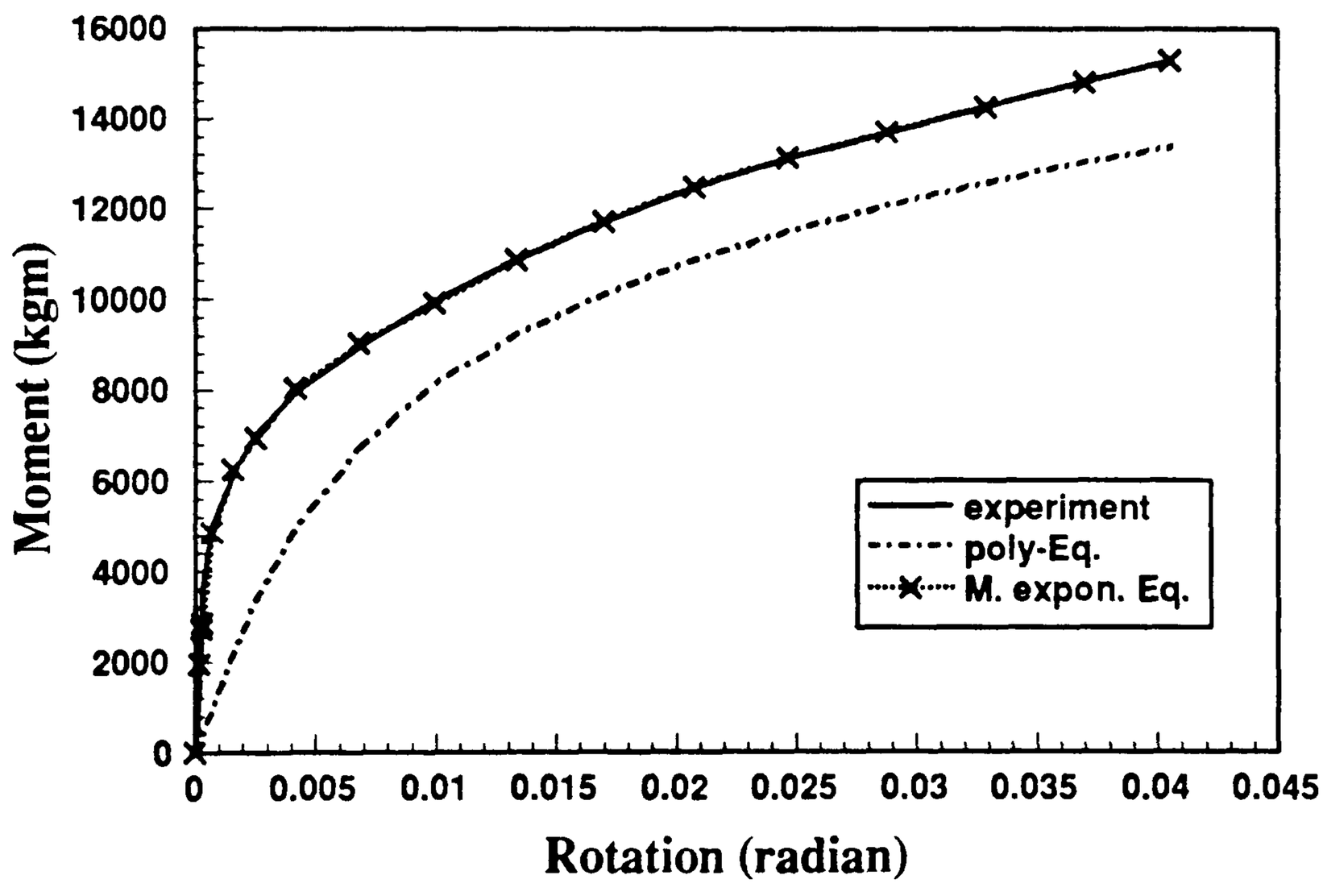

Figure 2.11 Comparison of experimental moment-rotation curve of extended end plate connection (Ioannides, 1978) with analysis using different equations

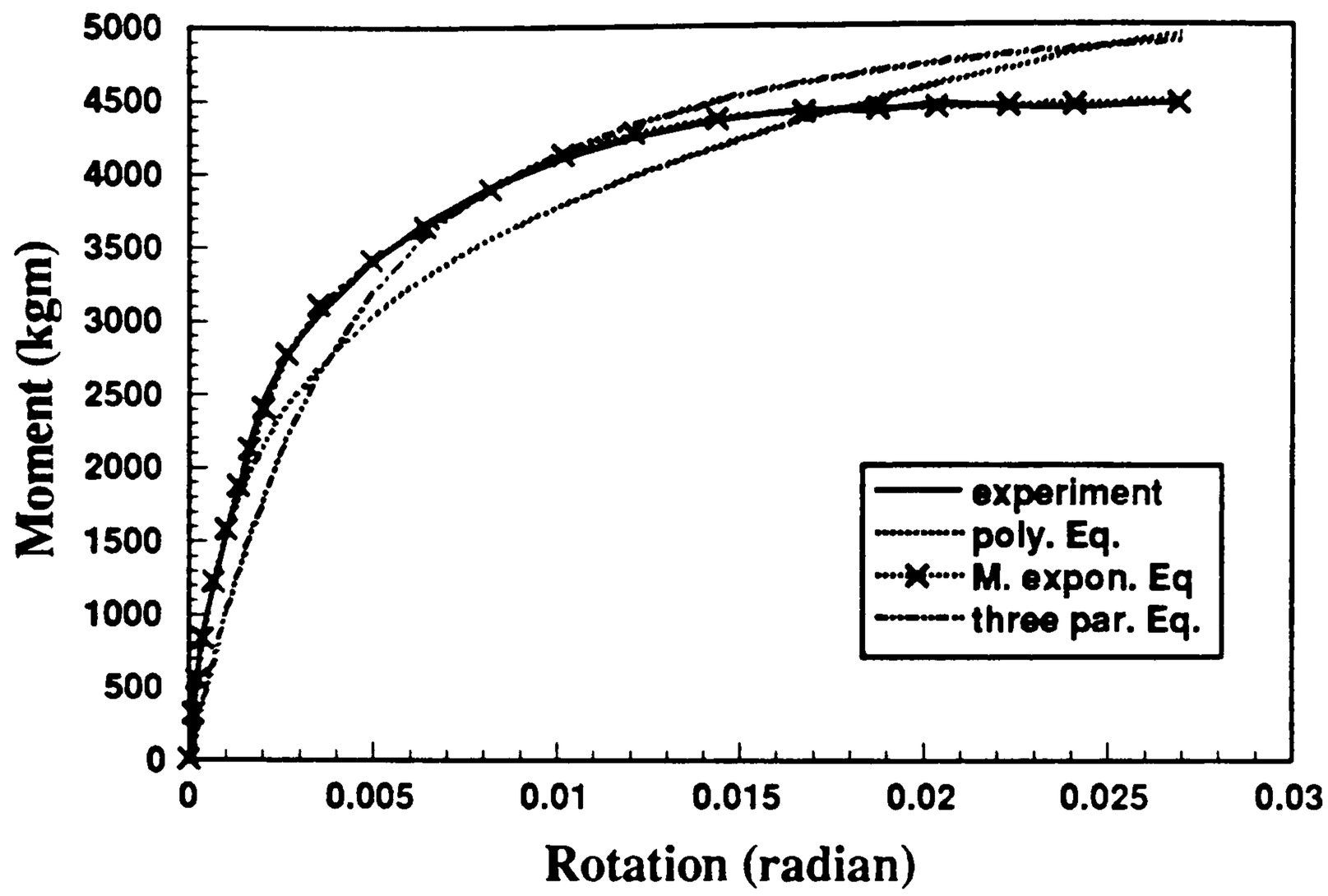

Figure 2.12 Comparison of experimental moment-rotation curve of top and seat with double web angles connection (Azizinamini et al., 1985) with analysis

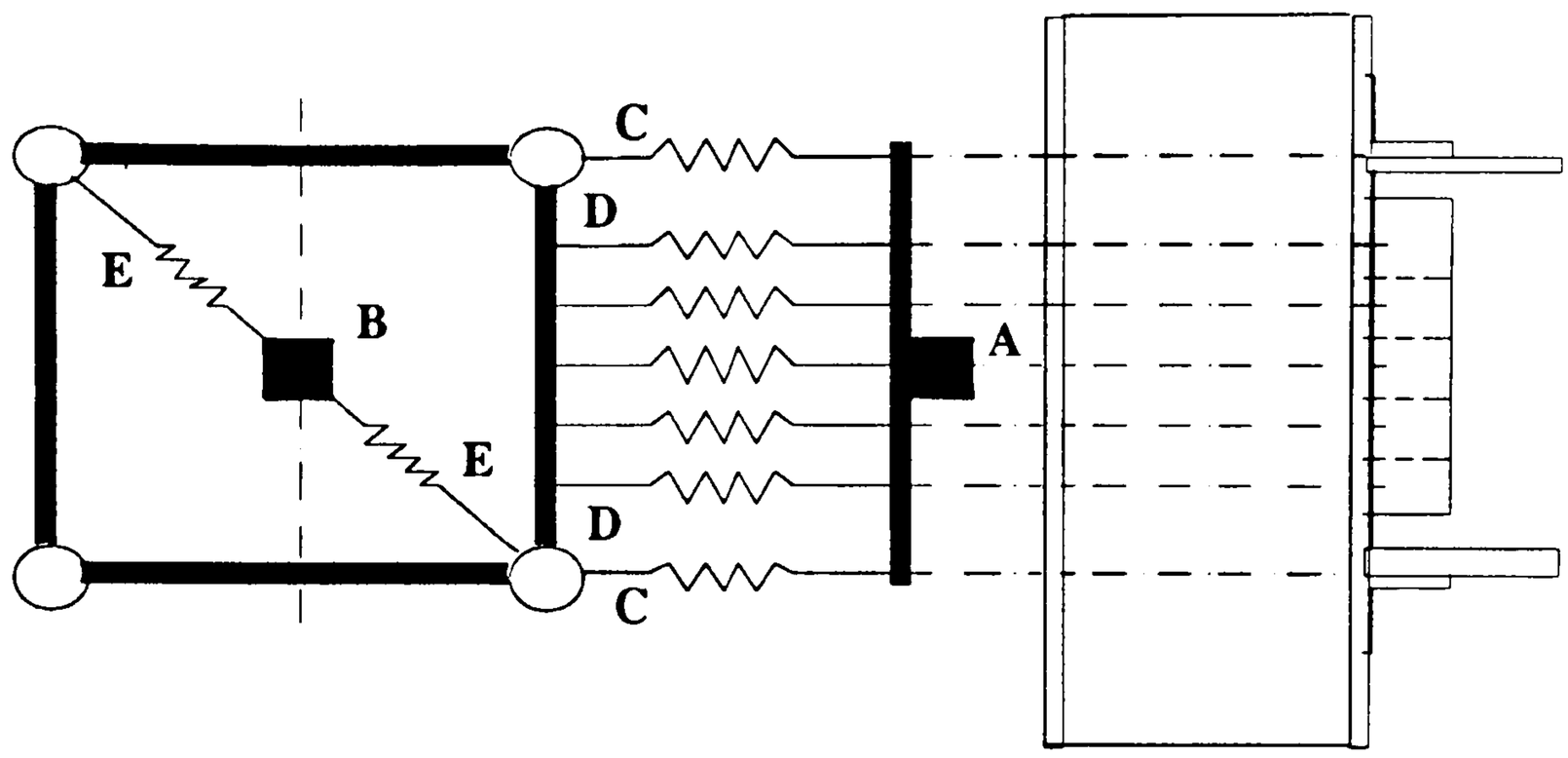

a) Undeformed mechanical analogue

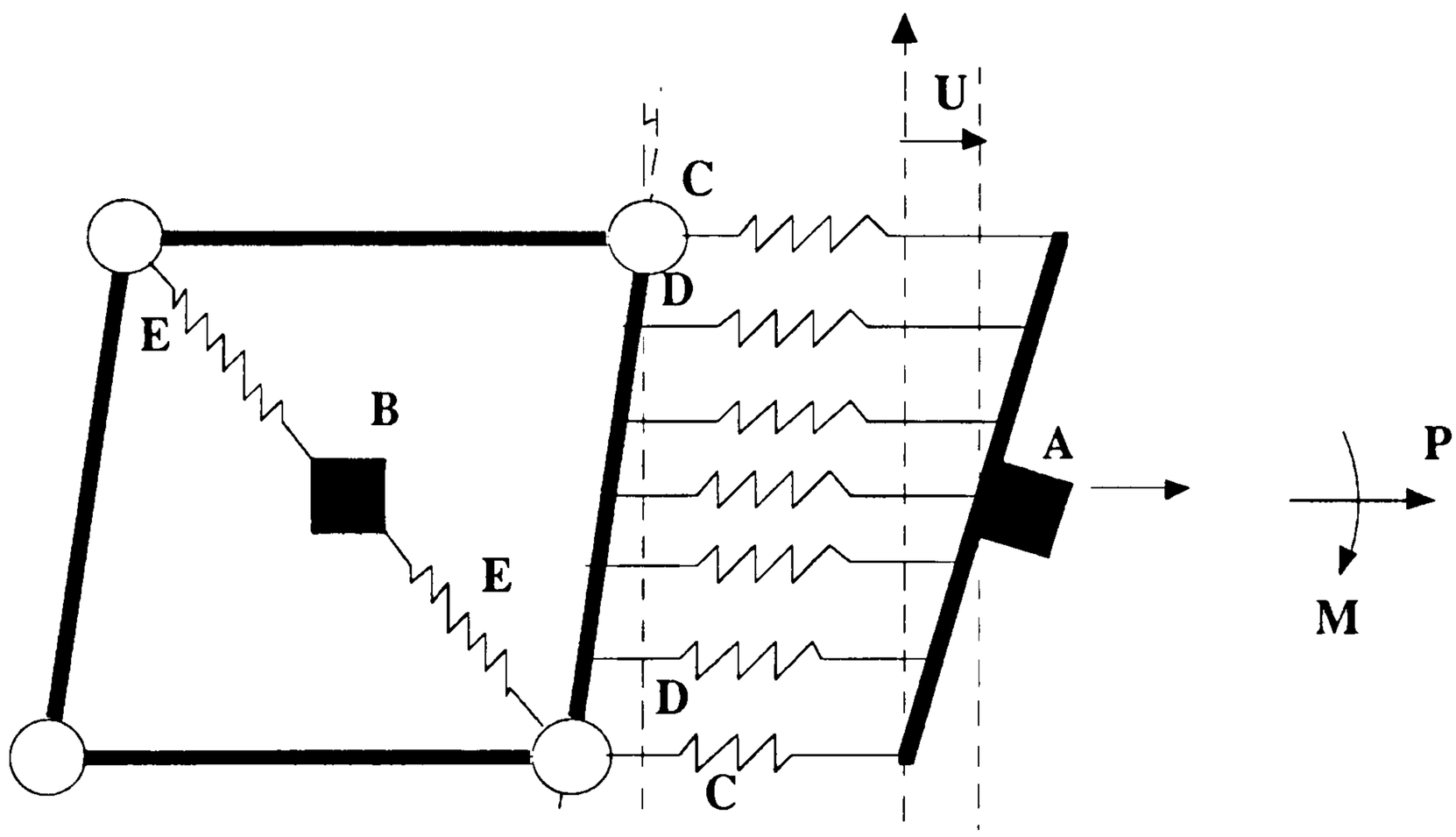

b) Deformed mechanical analogue

Figure 2.13 Idealisation of beam-column connection

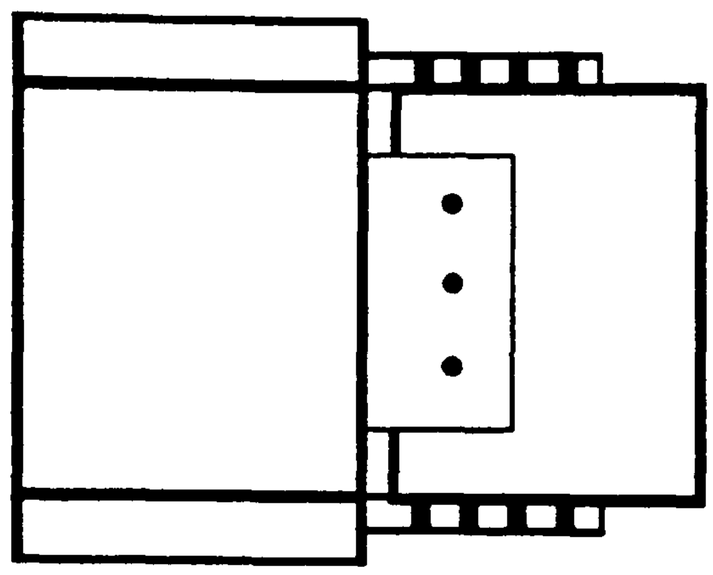

Type A1

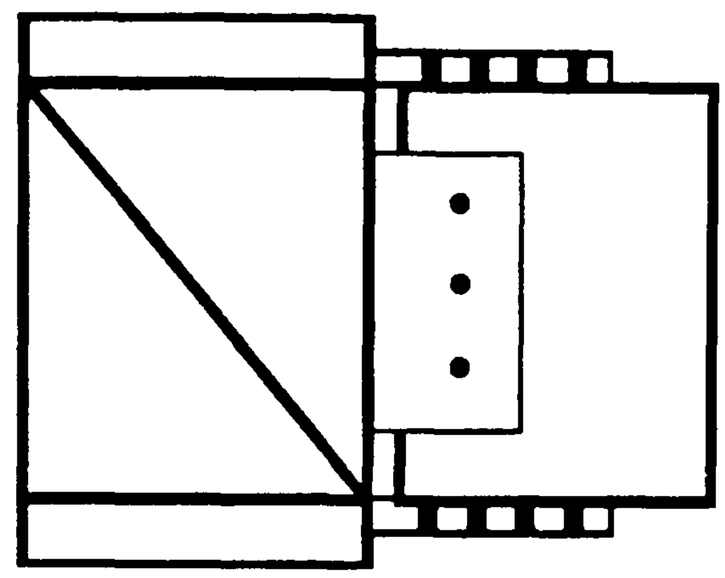

Type A2

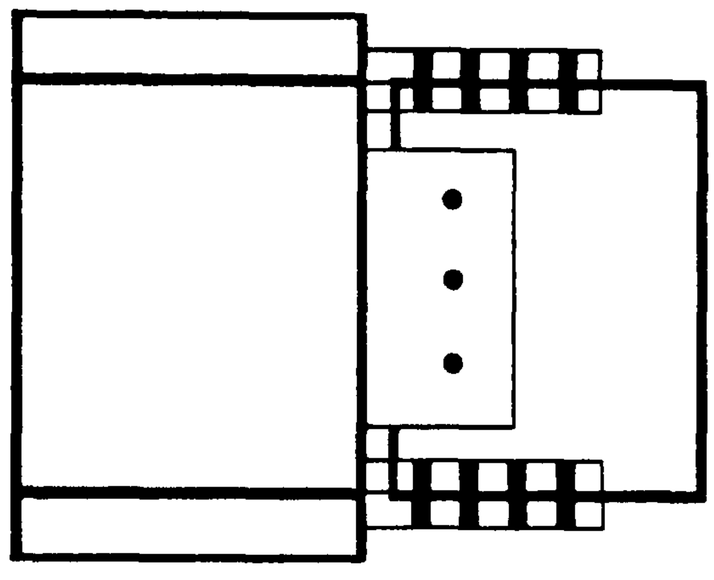

Type A3

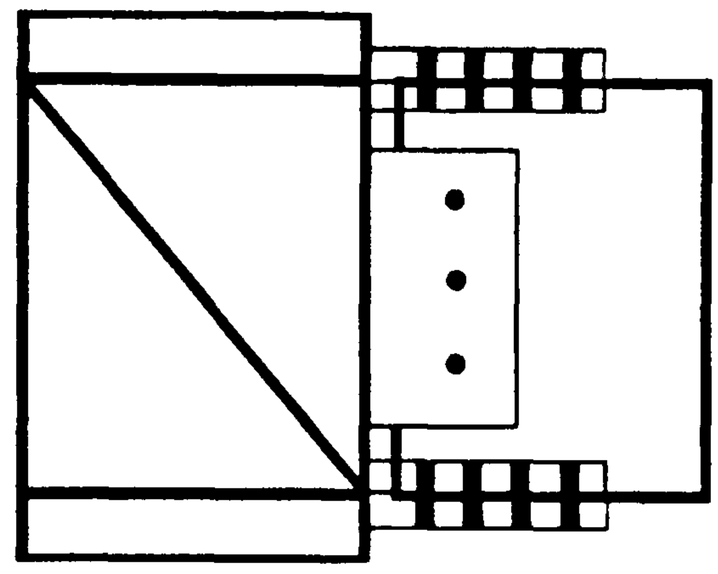

Type A4

Figure 2.14 Details of types A connection

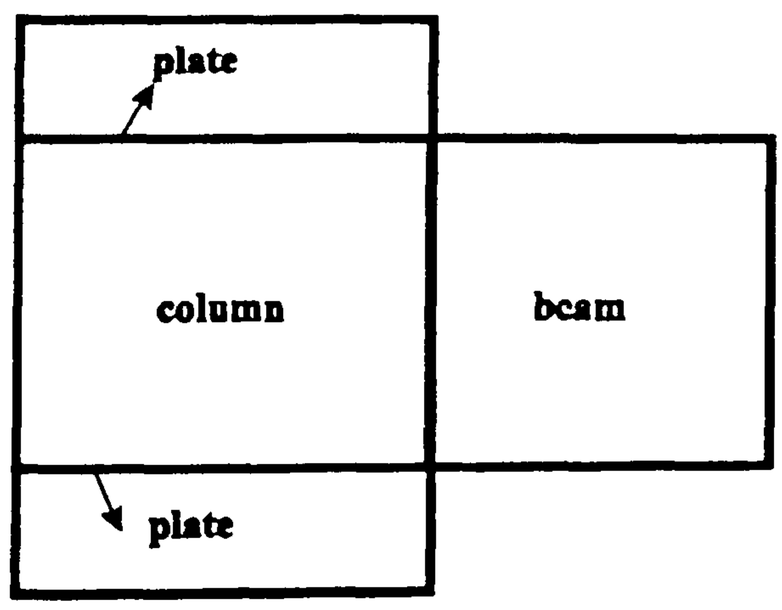

Type D1

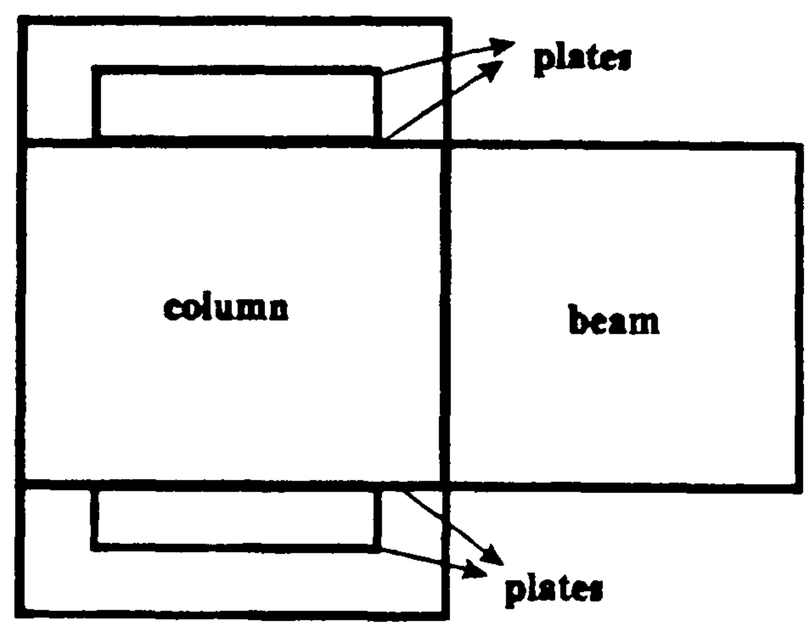

Type D2

Figure 2.15 Details of types D connection

CHAPTER 3

3 DESIGN CODES

Although semi-rigid connections have been used in practice for several years, many of the design regulations did not provide explicit recommendations for their design, but assumed that connections exhibited either pinned or rigid behaviour. However, in recent years, criteria for the design of frames with semi-rigid connections have begun to appear in some design codes. Indeed, the structural Eurocode for steel (EC3) and the American Institute of Steel Construction (AISC) are representatives of this trend. However, little or no guidance is given on the design of frames with semi-rigid connections themselves.

In this chapter, a brief review of the classification of steel connections that are detailed in the codes are presented. The moment-rotation relationship of the connections which have been evaluated according to Annex J of EC3 are compared with the experimental moment-rotation curves. The chapter concludes with an examination of the definitions and recommendations of EC8 for the seismic design of steel structures.

3.1 Classification of Connections

3.1.1 Classification System in Eurocode 3

According to EC3, a connection is defined as a part of a building frame which transfers the internal forces, from one member to another in the form of bending moments, shear and normal forces.

The structural properties of a connection are its moment of resistance, stiffness and rotational capacity. Depending on its design moment resistance, a connection may be regarded as full strength or partial strength. If the transfer of the moment between the connected members is not constrained by the moment resistance of the connection then plastic hinges will not be formed in the connection which is then defined as full

strength. In this case, the moment of resistance of the connection should be greater than the plastic moment of the connected beam.

On the other hand, when the transfer of the moment between connected members is constrained by the resistance of the connection then there is the possibility that plastic hinges will be formed in the connection. In this instance, the connection is defined as partial strength. According to this definition, a connection may be considered as partial strength if its moment of resistance is greater than 25% of the plastic moment of the connected beam.

Based on the initial stiffness, the connection may be regarded as either nominally pinned, rigid or semi-rigid. In pinned connections, the rotational continuity between the connected members is low and hence significant moments cannot develop in the connection. However, if the rotational continuity between the connected members is high and the deformation of the connection is such that the distribution of the internal forces is insignificant, then this signifies a rigid connection. A connection which fulfils neither the pinned nor the rigid criteria is considered to be semi-rigid.

The boundary between rigid and semi-rigid is shown in Figure 3.1 and is based on the assumption that the deformations of rigid connections should not reduce the resistance of the structure by more than 5%.

3.1.2 Classification System in American Institute of Steel Construction (AISC)

With Regard to the behaviour of beam-column connections, the AISC specification classifies such structures into three categories: Type 1, Type 2 and Type 3.

Type 1 construction assumes that the connections are very stiff and hence no angular distortion occurs between the beam and column centrelines, i.e. rigid behaviour is assumed. In this case, these are designed as moment connections.

Type 2 construction assumes that the connections are sufficiently flexible under gravity loads to undergo relative rotations between members so as to approach a pinned

condition. They should be sufficiently stiff to transfer wind moments. Generally, frames designed using the type 2 approach may result in under-designed columns (in particular, the exterior columns) and substantially over-designed beams.

In Type 3 construction the proportion of the moment which is transferred between beam and column depends on the rotational stiffness of the connection. This is determined by an analysis of the flexibly-connected frame system. However, no guidance is given on how to estimate the stiffness of such connections and as a result, the Type 3 approach has rarely been used.

3.1.3 Classification Systems by Researchers

Bjorhovde et al. (1990) proposed a classification system which make use of a reference beam length of '5d' to define the beam stiffness. The classification is based on the strength and stiffness of the connections with clearly defined boundary regions as shown in Figure 3.2. The three different regions in Figure 3.2 are,

(i) Rigid connection

In terms of strength : $\overline{m} > 0.7$ (3.1 a)

In terms of stiffness : $\overline{m} > 2.5\overline{\theta}$ (3.1 b)

(ii) Semi-rigid connection

In terms of strength : $0.7 > \overline{m} > 0.2$ (3.2 a)

In terms of stiffness : $2.5\overline{\theta} < \overline{m} < 0.5\overline{\theta}$ (3.2 b)

(iii) Flexible connection

In terms of strength : $\overline{m}<0.2$ (3.3 a)

In terms of stiffness : $\overline{m}<0.5\overline{\theta}$ (3.3 b)

where $\overline{m}$ and $\overline{\theta}$ are the normalised moment and rotation of the connection relative to the beam and are defined as:

$$\overline{m}=\frac{M_{con}}{M_{pb}} \tag{3.4}$$

$$\overline{\theta}=\frac{\theta_{con}}{\theta_p} \tag{3.5}$$

$$\theta_p=5\frac{M_{pb}\,d_b}{EI_b} \tag{3.6}$$

In addition, Bjorhovde et al.(1990) have proposed a simplified expression for calculating the rotation capacity of the connection based on calibrations with test data. This expression is given as :

$$\overline{m}=\frac{5.4-2\overline{\theta}}{3} \tag{3.7}$$

All parameters used in this system are consistent with those in EC3, except θ_p which is defined as $M_p/(EI_b/L_b)$ in EC3. It should be noted that according to the equation (3.7), the rotation capacity of the connection depends on the ratio of the ultimate moment capacity of the connection to the fully plastic moment of the beam and inversely proportional to the initial connection stiffness R_{ki}.

In comparing the two approaches, Bjorhovde et al. and EC3, it was concluded that EC3 was more appropriate for cases where the member details were known in advance. However, in the absence of such information (where prior knowledge of the member details was not available), Bjorhovde et al. approach was more applicable.

Astaneh (1989) proposed another approach for classifying connections. In the latter study a connection is defined as rigid if it is capable of developing a moment at the beam end which is greater than or equal to 90% of the fixed end moment and the end rotation is less than or equal to 10% of the rotation in a pin supported beam. On the other hand, a pinned connection is identified as that in which the moment of the connection is less than 20% of the fixed-end moment of the beam and the rotation is more than 80% of the end rotation in a pinned ended beam.

Moreover, according to Astaneh (1989), a semi-rigid connection is that with an intermediate value of stiffness. In addition, semi-rigid connections are divided into two categories, stiff semi-rigid and flexible semi-rigid. The former connections are capable of transferring significant levels of bending moment, shear, and axial loads. All other semi-rigid connections are considered to be flexible.

The reason for sub-dividing semi-rigid connections into the above categorises is that the available data indicates that the use of stiff semi-rigid connections in seismic regions can easily be justified. However, more research is needed to examine the behaviour of flexible semi-rigid connection in seismic zones.

According to the classification of connections as proposed by Astaneh (1989), the boundaries for rigid, semi-rigid and pinned connections are defined below and shown in Figure 3.3.

$m \geq 18$	rigid	(3.8.a)
$8 \leq m \leq 18$	stiff semi-rigid	(3.8.b)
$0.5 \leq m \leq 8$	flexible semi-rigid	(3.8.c)
$m \leq 0.5$	pinned	(3.8.d)

where m is the ratio of the elastic rotational stiffness of the connection to the elastic bending stiffness of the connected beam and is given in equation (3.9):

$$m = \frac{K_{e,con}}{(EI/L)_b} \tag{3.9}$$

A comparison between the three classification systems for connections is shown in Figure 3.4. As indicated in this Figure, the boundary between the rigid and semi-rigid regions in the system classified by Astaneh (1989) is only marginally different to the EC3 classification. Moreover, if the region of stiff semi-rigid is assumed to be rigid, this classification will be approximate to the EC3 recommendation. The boundary between the semi-rigid and pinned connections is also very similar in the two systems.

Current thinking is reflected in the recent American code AISC LRFD (1986) where only two types of construction are discussed, fully restrained and partially restrained, the latter being inclusive of semi-rigid and pinned connections.

3.2 Moment-Rotation Relationship in EC3

As mentioned in Chapter 2 of this thesis, on the basis of different joint models coupled with the use of experimental data, various theoretical relationships were proposed in order to represent the actual behaviour of semi-rigid connections. As a result of this experimental and analytical work, EC3 permits the use of semi-rigid connections subjected to static loading and gives in Annex J the design moment-rotation curve for the connection.

In this section, the method of calculating the moment resistance, initial stiffness and rotation of the connection, given in Annex J, are described and the proposed model for the moment-rotation curve for the connection is compared to the experimental result.

3.2.1 Determination of the Moment Resistance of Connections

The calculation of the moment of resistance of some types of connection are given only in Eurocode 3 (part 1.1, Annex J) whilst other codes do not offer any guidance in this respect. EC3 makes a number of assumptions in calculating the moment of resistance of the connections. For example, in welded and with end plates connections, the centre of compression is located at the mid-thickness of the beam flange in compression. However, the centre of compression to consider in the distribution of internal forces in

the top and seat angles connections is located at the mid-thickness of the leg of the seat angle in compression.

In designing for shear in connections with end plates, it is assumed that the part of the beam-web which is not subjected to longitudinal tension forces will transfer the shear forces. Also, that part of the beam-web which is subjected to tension forces may carry up to 50% of the design shear resistance of the beam-web without taking into account any force interaction.

In connections comprising top and seat angles, the design shear force may be transferred through the bolt-row connecting the angles in compression to the column flange. The bolt-row connecting the angle in tension to the column flange can transfer up to 30% of the design resistance of the bolts (in shear) without accounting for any force interaction.

By considering the above assumptions, the design moment of resistance of a bolted beam-to-column connection is determined from:

$$M_{rd} = \sum h_r F_{tr,Rd} \tag{3.10}$$

where

$F_{tr,Rd}$	=	the effective design tension resistance of bolt row 'r'
h_r	=	the distance from bolt-row 'r' to the centre of compression
r	=	the bolt-row number

Full details for determining the design tension resistance of the bolts are given in clause J.3.6.2 (Annex J) of EC3.

3.2.2 Calculation of Rotational Stiffness

According to Part 1.1 (Annex J) of EC3 the rotational stiffness of a connection is given by :

$$S_j = \frac{E z^3}{\mu \sum_i 1/k_i} \tag{3.11}$$

where

k_i	=	the stiffness coefficient representing component 'i'
z	=	the lever arm that is given in J.4.3 of Annex J
μ	=	the stiffness ratio $S_{j,ini}/S_j$
$S_{j,ini}$	=	the value of S_j when the moment $M_{j,Sd}$ is equal to $2/3\, M_{j,Rd}$
$M_{j,Sd}$	=	the design moment resistance

Generally the stiffness coefficient, k_i, for the basic component can be obtained from clause J.4.4 (Annex J). The stiffness ratio should be determined from:

$$\mu = \left(\frac{1.5 M_{j,Sd}}{M_{j,Rd}}\right)^{\psi} \tag{3.12}$$

in which

ψ = 2.7 for bolted end-plate connections

ψ = 3.1 for bolted angle cleats connections

3.2.3 Comparison of Moment-Rotation Curves with Experimental Data

As described in clause J.2.2 (Annex J) for semi-rigid connections, if the design bending moment $M_{j,Sd}$ does not exceed 2/3 $M_{j,Rd}$ then the initial rotational stiffness $S_{j,ini}$ may be used for global analysis. However, if the design moment exceeds 2/3 $M_{j,Rd}$, the rotational stiffness should be taken as $S_{j,ini}/\mu$, in which the stiffness coefficient $\mu = 2$ is given for extended end plate and top and seat angles connections. For further simplification, the value of rotational stiffness used for the elastic global analysis may be taken as $S_{j,ini}/\mu$ for all values of the design bending moment.

For elastic-plastic global analysis, in the case of semi-rigid connections, a simplified bi-linear model is given in a code in which the value of $\mu = 2$ is used in this bilinear model.

To validate this bilinear model with the test results, the moment-rotation curve for the top and seat angles tested by Maxwell et al. (1984) is compared with the bilinear model. The details of the tested connections are given in Table 3.1.

Table 3.1

Member and connection sizes of the test (Maxwell et al., 1984)

Universal Column	Universal Beam	Top and Seat Angles	Length of Angles	Diameter of Bolts
305x305x97	457x191x67	150x90x12	150 mm	20 mm

As mentioned above, the design moment-rotation relationship is built-up by combining the properties of the relevant components.

By calculating the stiffness coefficient of each component k_i and using Equations (3.10) and (3.11), the initial rotational stiffness $S_{j,ini}$ = 16.64 KNm/mrad and $M_{j,Rd}$ = 46.13 kNm are obtained. Figure 3.5 shows the comparison between the experimental moment-rotation curve with the bilinear model described in Annex J of EC3.

As shown in this Figure, the analytical moment-rotation curve of Annex J is at variance with the experiment. The lower initial stiffness in the bilinear model is due to bearing components which introduce very large deformations. If the bearing components were neglected, on the assumption of negligible effect in the elastic range, the predicted curve would provide an acceptable approximation of the actual behaviour for initial stiffness.

In addition, according to Annex J, the effect of strain hardening is not included in calculating the moment-rotation of the connection. Therefore, for more accurate results, the influence of strain hardening should be considered. To accomplish this objective, a linear variation in the moment M and rotation θ may be assumed with a slope equal to $S_{j,h} = 0.2\ S_{j,ini}$ based on experimental research.

From the above discussion, the formulation proposed by Annex J may be improved by implementing the following two modifications:

1- In calculating the initial stiffness, the terms accounting for bearing mechanisms, which arise in the inelastic range of behaviour should be neglected.
2- The influence of strain hardening on the behaviour of the moment-rotation curve of the connection should be taken into account.

The comparison between the modified bilinear model of Annex J and the experimental moment-rotation curve tested by Maxwell et al. (1981) is shown in Figure 3.6. As indicated in this Figure, both the initial stiffness and moment show good agreement compared with the values calculated using Annex J, after modifications.

3.3 Seismic Design Philosophy for Semi-Rigid Steel Frames

The use of semi-rigid connections in frames subjected to earthquake loads is subject to controversy. None of the design codes include provision for its use and, in zones of high seismicity the use of rigid full-strength connections is mandatory. Criteria for the determination of the connection capacity and stiffness, and the evaluation of the low-cyclic fatigue and rotation capacity under dynamic loads, are still pending. In this section, the general rules of EC8 are presented, with particular emphasis placed on their implications on semi-rigidly connected frames.

3.3.1 Dissipative and Non-dissipative Structures

According to the new generation of seismic codes, e.g. the ECCS (1993) and Eurocode 8, a distinction is made between dissipative and non-dissipative structures.

Non-dissipative structures must resist the most severe seismic event within the elastic range, whereas the dissipative structures are designed by allowing yielding to occur in predefined zones. During an earthquake these zones must dissipate energy by means of hysteretic ductile behaviour in the plastic range. The formation of appropriate dissipative mechanisms is related to the structural typology. Connections in such

dissipative zones must have sufficient over-strength to allow for yielding of the connected parts. For welded or bolted connections, the resistance R must be 1.2 times the resistance of the connected member, considering the upper value of its yield strength.

According to this assumption, only full strength connections can be used in steel structures when subjected to earthquake loading. However, there is evidence that partial strength semi-rigid connections possess sufficient plastic rotation and dissipates a large amount of energy when subjected to cyclic and dynamic loads. Such a connection, therefore, is capable of being used as a dissipative part of the structure. However, more experimental and analytical studies are needed to encourage the use of this type of connection in seismic areas and to provide practical design guidance.

3.3.2 Limit State Requirements

Field evidence following destructive earthquakes have indicated, with few notable exception, that steel structures suffer less damage compared to structures built in other construction materials. This is due to their inherent ductility and relative uniformity of characteristics. In case where significant damage has been inflicted on steel structures, it was mainly due to connection distress. And by-and-large, these connections were fully welded or hybrid (welded beam flanges with beam web shear tabs). This, in principle, points towards potential use of bolted connections to eliminate welding. In order to establish the fundamental requirements for bolted connection design in seismic conditions, the prevailing design philosophy is first examined.

Whereas this is not reflected explicity in the design process, three limit states are presumed to be considered in modern seismic codes, such as ECCS (1993) and EC8 (1994). These are serviceability, damage and collapse.

The serviceability limit state corresponds to minor frequent earthquake. The design objective is that structures together with non-structural components should suffer no damage and that discomfort to the inhabitants should be minimal. The first requirement (avoidance of damage) is satisfied by ensuring that the structure responds in the elastic

range. For the second requirement, (avoiding non-structural damage and inhabitants discomfort) it is necessary to provide sufficient stiffness to prevent significant deformations. The damage limit state allows some minor damage to non-structural components due to large local deformations in certain zones. The collapse limit state pertains to very infrequent severe earthquake ground motions in which both structural and non-structural damage are expected but the safety of the inhabitants must be guaranteed. Furthermore, The structure must be able to absorb and dissipate large amounts of energy.

In order to satisfy the above three conditions, semi-rigid steel frames should be capable of supplying the required stiffness strength and ductility. To satisfy the strength and stiffness requirements, the following recommendations would have to be considered in the serviceability and ultimate limit states.

For the serviceability limit state and to prevent yielding in the connection at this stage, the maximum rotations which the connections undergo should not exceed the yield rotation of these connections. In addition, most semi-rigid steel frames are prone to increases in interstorey drifts. Hence, controlling these drifts should be a key considerating in the design of this type of structure.

To ensure that a connection is ductile enough and has the capacity to provide the required rotations, the connection must be capable of developing adequate hinge rotations while sustaining its yield moment capacity.

3.3.3 Behaviour Factor

According to EC8, the ability of a structural system to resist seismic loads in the post-elastic range is allowed for by means of the behaviour factor (q-factor). This approach is used in the evaluation of the normalised design spectrum given by :

$$R_d(T) = \frac{R_o}{q} \qquad \text{for} \quad T < T_o \tag{3.13}$$

$$R_d(T) = \frac{R_o}{q(T/T_o)^k} \quad \text{for} \quad T > T_o \tag{3.14}$$

where

$R_d(T)$ = the ordinate of the normalised inelastic design response spectrum

R_o = the maximum normalised spectra value (assumed to be constant between T_1 and T_o)

q = the behaviour factor

K = the parameter which influences the shape of the response spectrum for a vibration period greater than T_o.

Design forces are inversely proportional to the value of q. For example, q=1 implies that the structure must remain elastic even during a very strong earthquake. This condition is therefore necessary for non-dissipative structures. For dissipative structures, q is always greater than 1 depending to the ductility and over-strength of the structure.

As a general definition, the behaviour factor is given by the ratio:

$$q = \frac{a_u}{a_y} \tag{3.15}$$

where

a_u = peak ground acceleration causing collapse of the structure

a_y = peak ground acceleration causing the attainment of the elastic limit of the structure.

According to this definition, the evaluation of the q-factor is performed by non-linear analysis. Many authors proposed approximate methods for determining the q-factor for design purposes but the corresponding results are often different and sometime contradictory.

In semi-rigid steel frame structures, the case may be that earthquake forces are lower that those for a comparable rigid frame. This is because the flexible connections result

in a longer vibration period when compared with the rigid connection. In addition, the results from experimental work indicate that the behaviour factor increases when semi-rigid connection are used due to added energy dissipation. However, there is no guidance in the codes as to how this behaviour factor can be evaluated from these parameters or how it should be used in the analysis of semi-rigid steel frames. It is, therefore, necessary not only to drive design expression for connections and members, but also to furnish equations for vibration periods and behaviour factors for semi-rigid frames.

3.3.4 Collapse Mechanism

The collapse mechanism plays a very important role in the seismic design of structures because it influences the available global ductility and the energy dissipation capacity. The condition that the collapse mechanism should be of a global type is rather severe. One of the main advantages of using semi-rigid partial strength connections is that it controls column and beam forces thus the likelihood load of local collapse mechanism is greatly reduced.

On the other hand, the large lateral deformation of the frame, due to the flexibility of the connection, causes an increase of rotational deformation in the columns. In addition, experimental results show that the effective length of the columns in semi-rigid steel frames increases when more flexible connections are used. As a result of these effects, the failure mode may be occurred locally in semi-rigid steel frames.

Sufficient local ductility is availed of by limiting the width-to-thickness ratio b/t in the compressed parts of the cross-sections. In non-dissipative zones (q=1) the b/t ratio should respect the limit given in the Eurocode 3. In dissipative zones of a structure (q>1), three ductility classes have been proposed, depending on the chosen values of the q-factor:

Class A	$4 < q < 6$
Class B	$2 < q < 4$
Class C	$q < 2$

Class A values are necessary where large rotation capacity in the plastic zones is required. They correspond to Class 1 (plastic sections) of EC3. Class B values must be reached where the plastic resistance should be attained. They correspond to Class 2 (compact sections) of EC3. Class C values are necessary where the resistance is limited by the yielding in extreme fibres of members. They are intermediate between class 2 and class 3 (compact and semi-compact sections) of EC3 (ECCS, 1993)

3.4 Commentary

In this chapter, different classification of connections that are provided in the codes are described. Two classification systems, as proposed by researchers, are compared to the EC3 classification. Among the various codes, only EC3 proposed a model for predicting the moment-rotation behaviour of extended end plate and top and seat angles connections. A proposal was made to improve the correlation between the EC3 approach and experimental results.

Although the codes permit the use of semi-rigid connections in structures, there is no guidance for their seismic design. Based on capacity design philosophy, and according to the definition of dissipative and non-dissipative parts in structures, the connections are assumed to be non-dissipative parts. However, in semi-rigid steel frames, the connection may be assumed to be dissipative or non-dissipative, depending on its capacity (full strength or partial strength).

Conventional capacity design of frames imposes that yielding should occur in beams with the connections and columns remaining largely elastic (with the exception of bases of ground floor column). The concept may be altered though, whilst achieving the same objective. If connections are allowed to yield first, this may provide a ceiling on beam and column action, rendering their design economical. Moreover, significant energy may be dissipated in a stable manner in the connections, thus increasing the behaviour factor q however, this is coupled with period elongation and, in general, an increase in lateral deformations. This in turn imposes high demand on non-structural components. It is the complexity and inter-dependence of the above effects that is the

basis for the urgent need for experimental and analytical studies on semi-rigid steel frames, with the objective of providing a viable alternative to full welding.

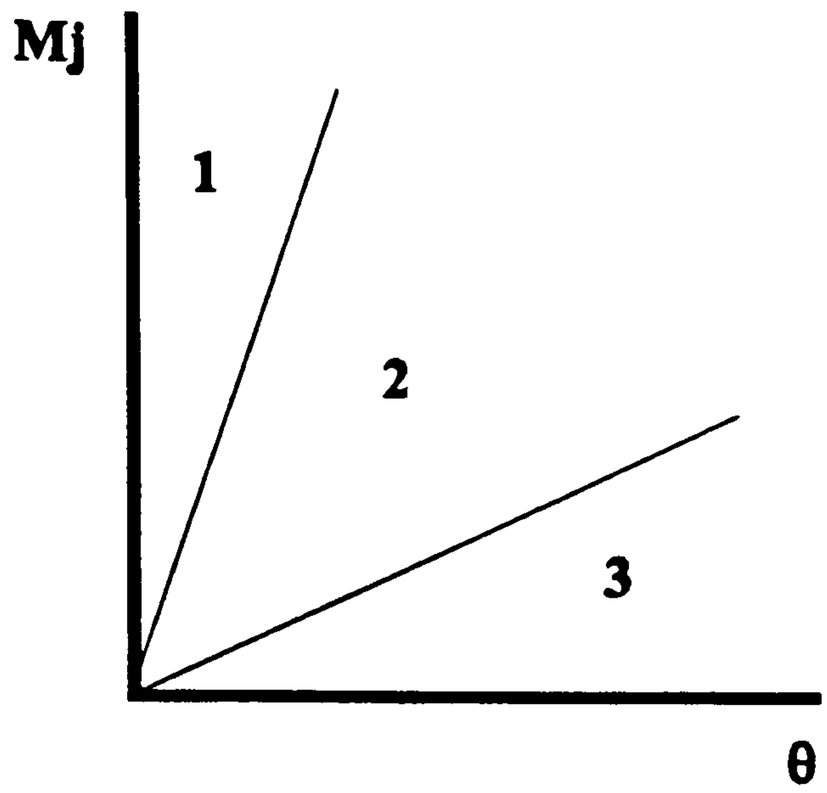

1 Rigid, if $S_{j,ini} \geq 8EI_b / L_b$

2 Semi-rigid

3 Nominally pinned, if $S_{j,ini} < 0.5EI_b / L_b$

a) Braced frames

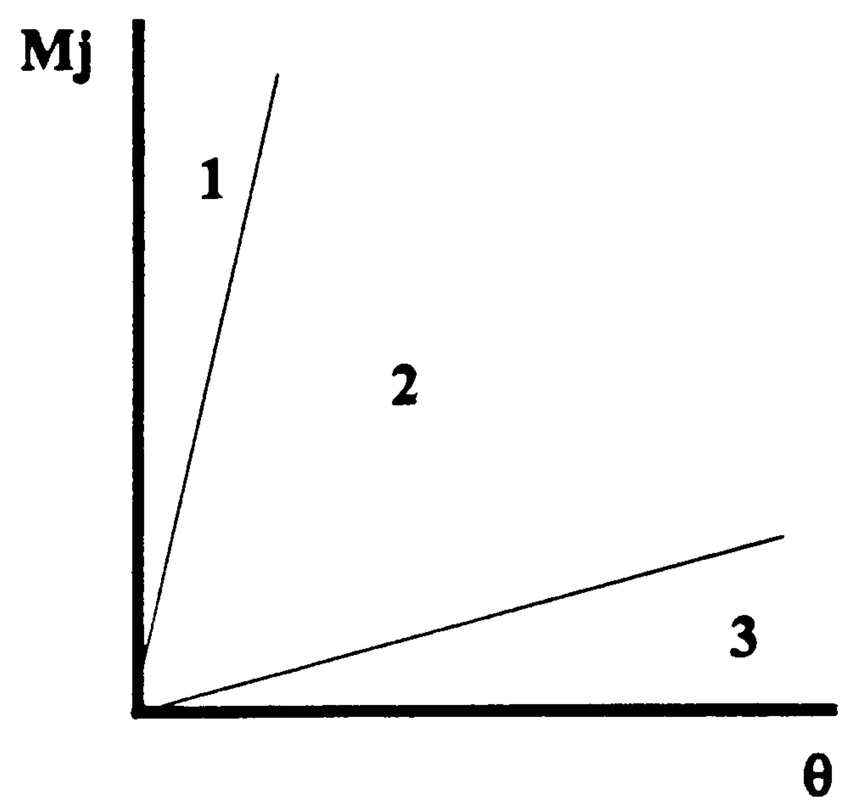

1 Rigid, if $S_{j,ini} > 25EI_b / L_b$

2 Semi-rigid

3 Nominally pinned, if $S_{j,ini} < 0.5EI_b / L_b$

b) Unbraced frames

Figure 3.1 Boundaries for stiffness classification

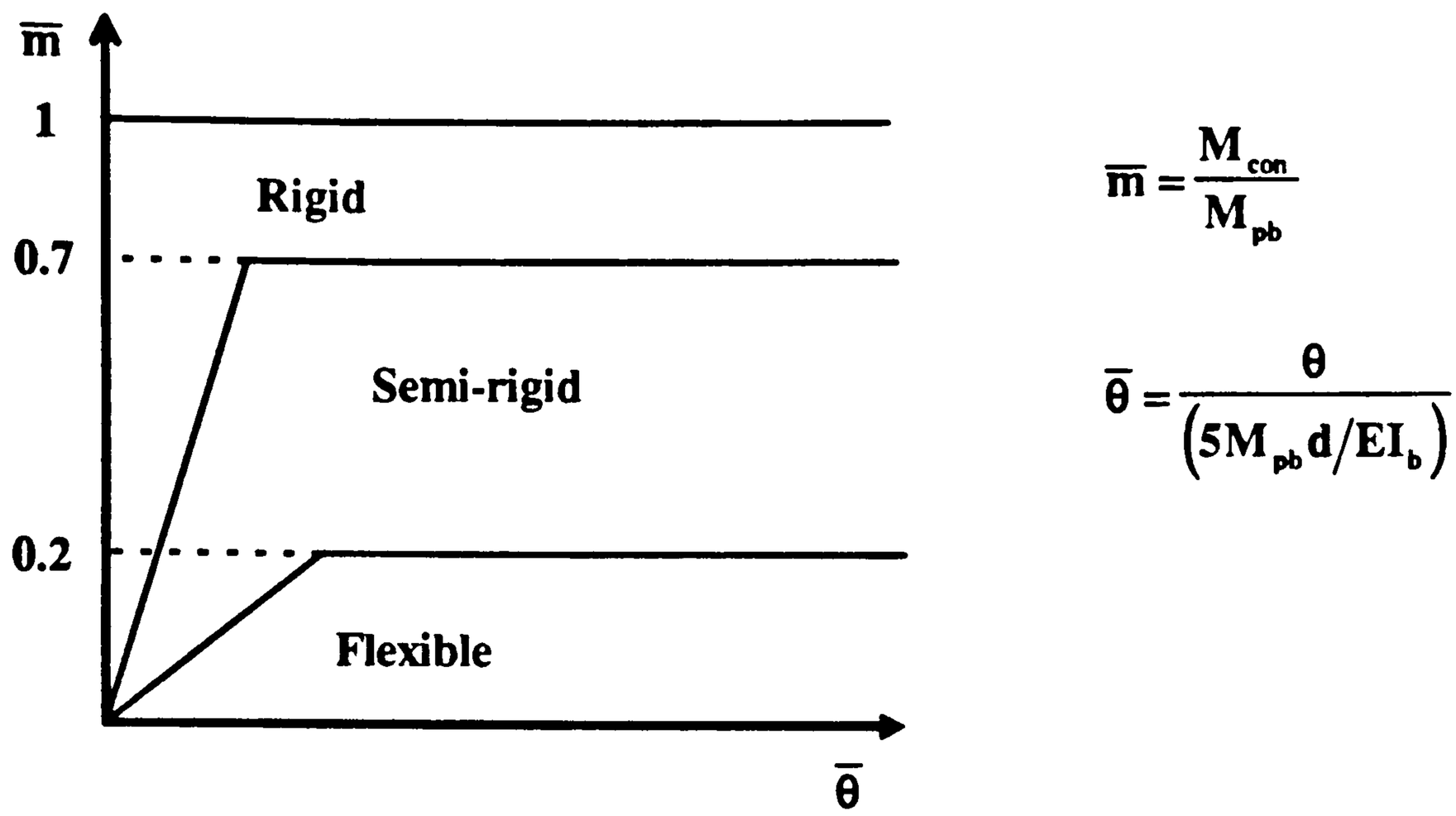

Figure 3.2 Classification of connection according to Bjorhovde et al.(1990)

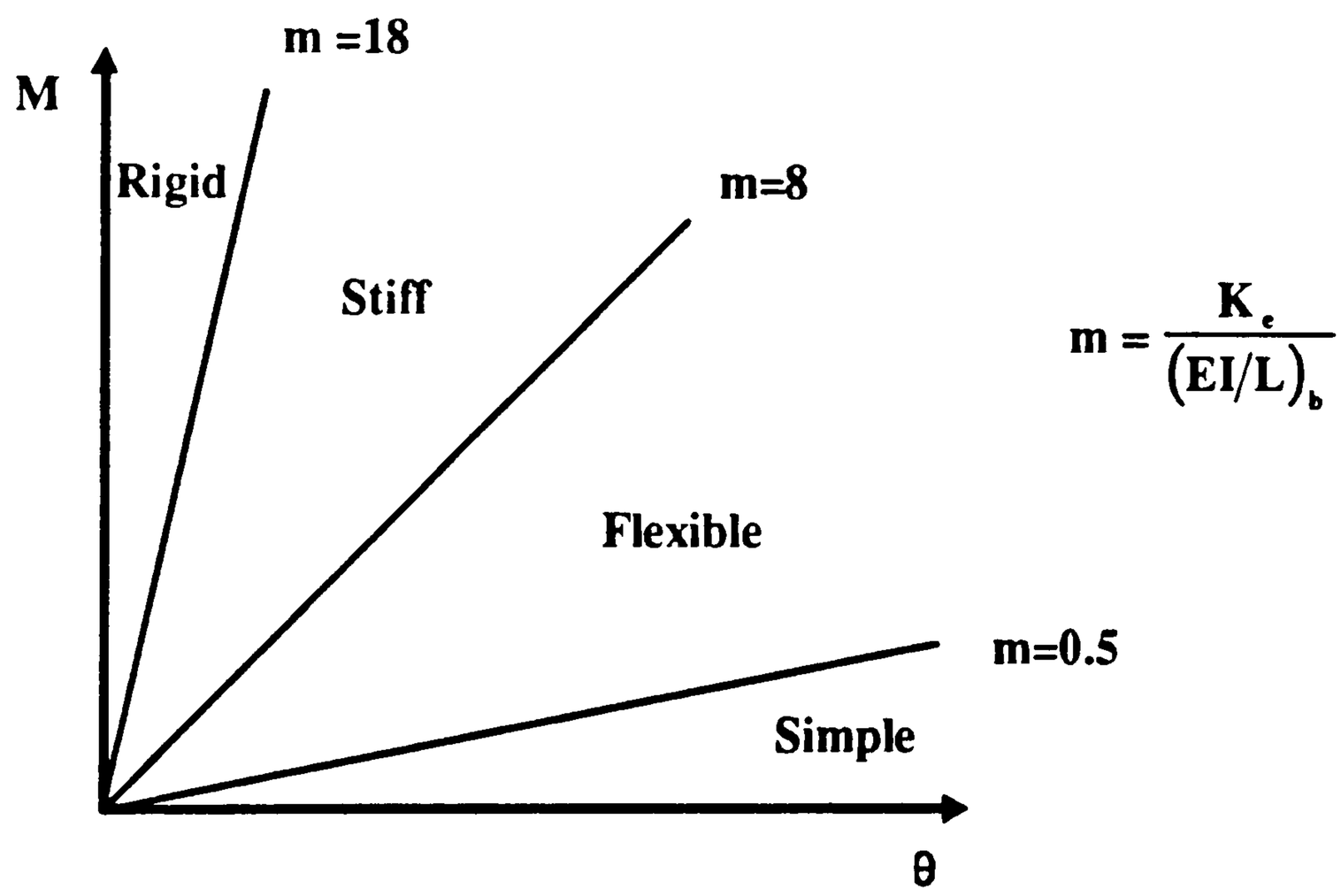

Figure 3.3 Classification of connection according to Astaneh et al.(1989)

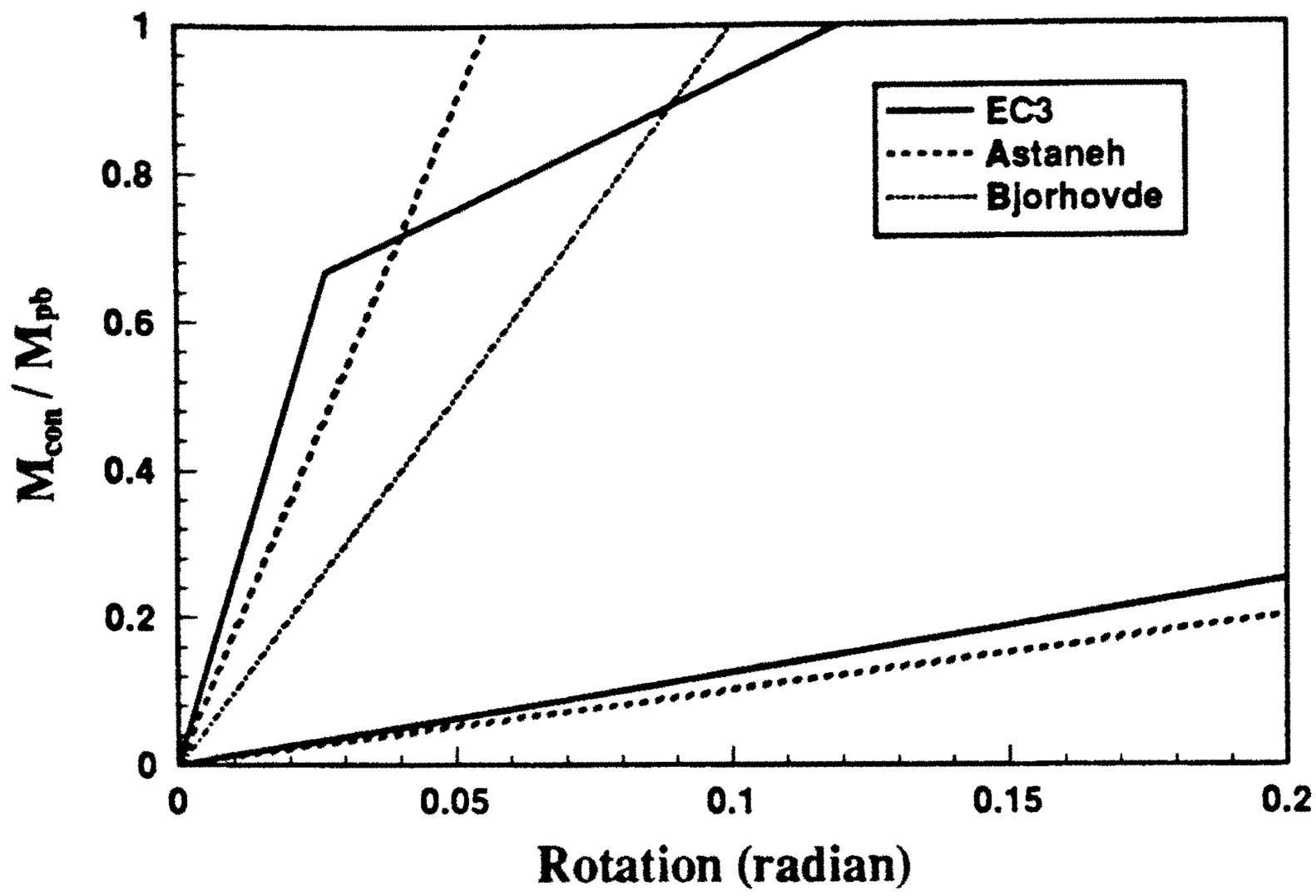

Figure 3.4 Comparison between different methods of classification of connection

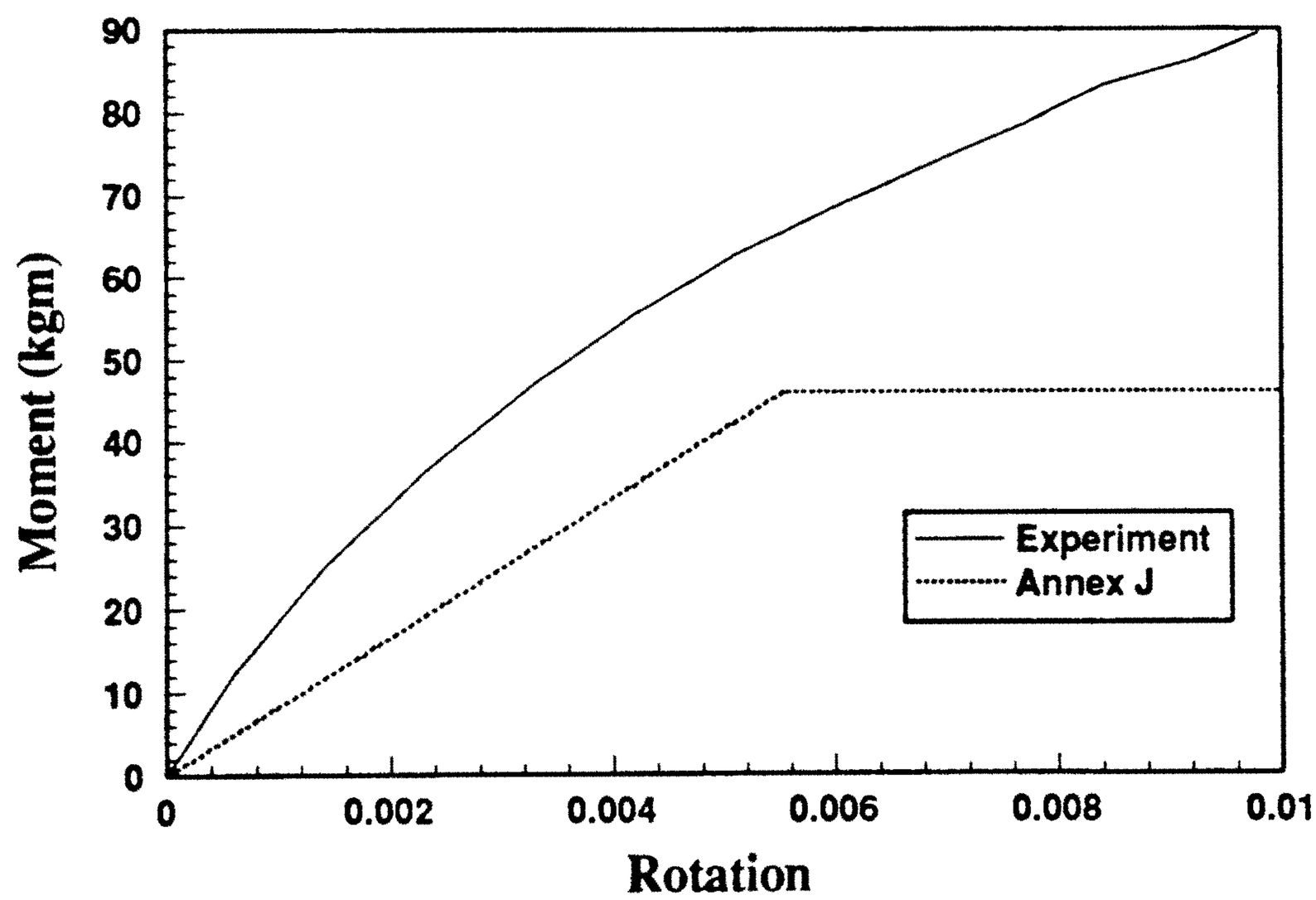

Figure 3.5 Comparison moment-rotation curve of top and seat angles tested Maxwell et al.(1984) with bilinear model of Annex J.

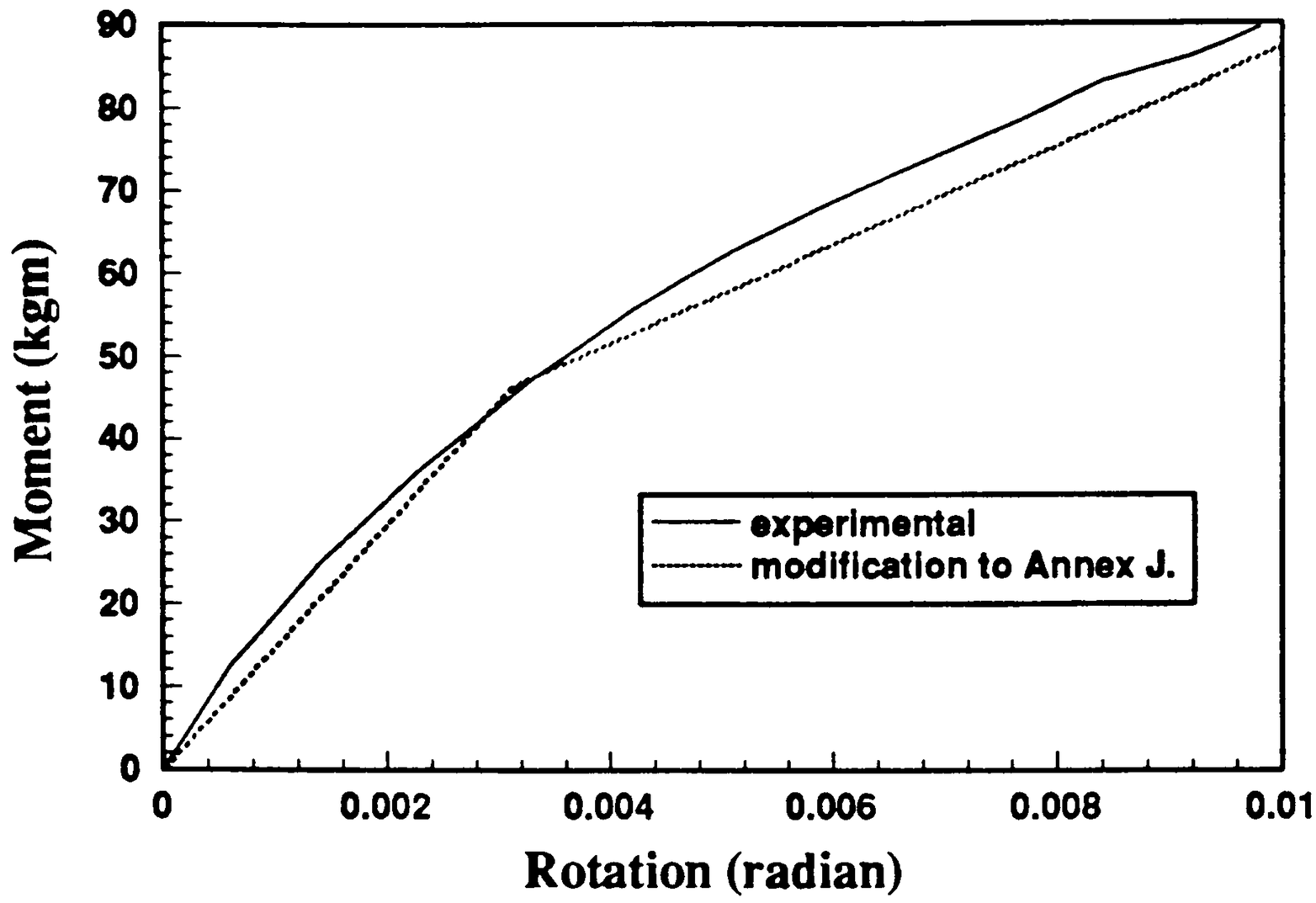

Figure 3.6 Comparison of experimental moment-rotation curve tested by Maxwell et el.(1984) with modified bilinear model of Annex J.

CHAPTER 4

4 EXPERIMENTAL INVESTIGATIONS

4.1 Introduction

The primary objective of this experimental work is to study the performance of semi-rigid steel frames under cyclic and dynamic loads. Accordingly, five two-storey steel frames, one rigid and four semi-rigid were designed and tested. In this chapter, the experimental procedure is described, the details of the specimens and materials are given and the results obtained from the tests are presented and discussed.

As shown in table 4.1, the specimen CR1 (rigid connection) was used to verify the behaviour of the two-storey steel frame with fully-welded connections subjected to constant axial and lateral cyclic loading. Three semi-rigid steel frames (specimens CS1, CS2 and CS3) were used to investigate the influence of the flexibility of the connection on the overall behaviour of the frame under cyclic loads. Finally, in order to examine the seismic behaviour of semi-rigid connections steel frames subjected to earthquake loading, specimen DS1 was tested using pseudo-dynamic technique.

4.2 Test-Rig

Figure 4.1 shows the details of the test-rig. The different parts of the assembly were adequately prestressed to form a self-reacting frame. An actuator which imposes displacements was connected to the end of the beam at the second floor level whilst another actuator operated in force control was fixed to the end of the beam at the first floor level. A third actuator with two hinges to allow for in-plane movement was installed at the top of the column to apply an axial load.

Plate 4.1 shows a general view of the testing set-up. To facilitate testing, the frame was placed horizontally. The end of the column was welded to a plate of dimension 400x300x30 mm and bolted to a fixed plate of dimension 665x460x70 mm using 8

bolts with 20 mm diameter. A second plate was bolted to a very short stiff beam with 4 bolts of 40 mm diameter. This stiff beam was fully welded to the base plate which was securely fixed to the laboratory strong floor using 8 bolts of 40 mm diameter, each tensioned to a load of 60 tonnes.

Table 4.1
Model reference and applied loading

Model reference	Connection	Testing technique
CR1	Rigid	Cyclic
CS1	Semi-rigid	Cyclic
CS2	Semi-rigid	Cyclic
CS3	Semi-rigid	Cyclic
DS1	Semi-rigid	Pseudo-dynamic

Displacements were applied to the end of beam at the second floor level using a double-acting hydraulic actuator. This actuator had a load capacity of +/- 100 kN and a maximum stroke of +/- 125 mm. The second actuator which controlled the force in the first floor, had a load capacity +/- 250 kN and a maximum stroke +/- 75 mm.

The backs of the two actuators were fixed to two plates with dimensions 710x460x70 mm each and these plates were connected to a very stiff short beam with 4 bolts of 40 mm diameter.

Two rectangular hollow sections, 250x250x10 mm, were provided with stiffening tubes at the location of the bolts to avoid local buckling at these points. The stiff beam which supported the actuators was fixed to the strong floor using 40 mm diameter high strength bolts tensioned to 60 tonnes each. The top of the column was welded to a plate of dimension 300x300x30 mm and bolted to another plate of the same dimension using 4 bolts of 20 mm diameter. The actuator, which was used to impose an axial load, had a capacity of 50 tonnes and was connected to the top of the column by

means of two swivel joints to allow it to rotate horizontally (Plate 4.2). The distance between the two swivel joints was 1685 mm.

The back of this actuator was fixed to a plate using 6 bolts of 40 mm diameter and then connected to a short stiff beam. This short beam was fixed to the strong floor via two thick plates attached to the beam with 4 bolts of 40 mm diameter (which were tensioned-up to a load of 60 tonnes each).

In the rigid model, the beams were fully welded to the column flange whilst in the semi-rigid case a bolted connection was used. In both models, the second end of the beams was welded to plates of dimensions 400x400x25 mm which were then connected by means of 4 bolts of 20 mm diameter (Plate 4.3). Two low friction Instron swivel joints were used to connect two actuators to the end of the beams such that horizontal and rotational movement were permitted but vertical movement was constrained.

4.3 Description of the Models

4.3.1 Specimen Details

Details of all the models are shown in Figures 4.2 to 4.4 and summarised in Table 4.2. All the frame members (beams and columns) were fabricated from Grade 43 steel. A typical stress-strain response is shown in Figure 4.5. The height of each storey was 2000 mm for the rigid frame and 1450 mm for semi-rigid frames. For specimen CR1, half of the beam span was 2000 mm whilst in the other specimens it was 1850 mm. The reason for considering only half of the frame in the testing procedure was to take advantage of symmetry.

The frames were designed according to the recommendations given in EC8. The design acceleration for determining the forces in the members was 0.3g. However, the limitation of the maximum horizontal force of the actuator (100 kN) and the maximum actuator displacement at the second floor (120 mm) were factors which had to be considered in the design for calculating the ultimate forces in these frames.

Table 4.2

Specimen Details

Model reference	Section Type	b_f x t_f	d_w x t_w
Rigid	UB254x102x22	101.6x6.8 mm	225x5.8 mm
	UC 203x203x46	203.2x11 mm	160.8x7.3 mm
Semi-rigid	UB 254x146x31	146.1x8.6 mm	218.9x6.1 mm
	UC 203x203x46	203.2x11 mm	160.8x7.3 mm

In the rigid steel frame, the flanges and the web of the beam were fully welded to the flange of the column. Top and seat angles with double web angles were used for the connections in the semi-rigid frames. To reduce the risk of shear failure of the panel zone, two stiffeners were welded to the flange and the web of the column. In all the models a constant axial load was applied at the top of the column by means of hydraulic jack.

Table 4.3

Connection Details of Semi-rigid Models

Model references	Top and seat angles		Double web angles	
	Size (mm)	Length (mm)	Size (mm)	Length (mm)
CS1	80x80x8	120	80x80x8	180
CS2	150x90x12	140	80x80x8	180
CS3	150x90x15	140	100x100x15	180
DS1	150x90x15	140	80x80x8	180

The details of the connections for each semi-rigid model are given in Table 4.3 and shown in Figure 4.6. The connections in these models were designed as partial strength semi-rigid connections with a moment capacity which varied between 30% and 70% of the plastic moment of the connected beams.

4.3.2 Material Properties

Coupon tests were conducted on the steel sections used. For the rolled sections, specimens from both the flange and web were tested. The yield and ultimate strength and the corresponding strain values are given in Table 4.4.

Table 4.4

Properties of Steel Sections

Model	Element	σ_y N/mm^2	σ_u N/mm^2	ε_y %	ε_u %
CR1	column flange	285.6	476.5	0.14	23.4
	beam flange	287.60	420	0.14	25.9
CS1	column flange	278.8	471.3	0.13	25.7
	beam flange	313.8	465.9	0.15	23.2
CS2 CS3 DS1	column flange	301	480	0.14	24
	beam flange	295	450	0.14	24
Angles	Top & seat angles	280	424	0.15	24.5
Angles	Web angles	280	467	0.14	25

In all cases, the values presented are the average of at least three tests. In the coupon tests, both stress-strain curves and load-displacement curves are plotted. The stress-strain curves were limited to a specific strain level whereas the load-displacement curve represented the full relationship up to fracture.

4.4 Electro-Hydraulic Servo Control

Control of the actuator was achieved by means of a servo-controller which compared the command signal voltage with the displacement transducer voltage output signal. The difference between these two values was converted into a current which was fed through a servo-valve causing the actuator to move by directing oil to either end of the actuator piston. The process was performed in a closed loop until the output

displacement signal reached the command signal. This signal was generated from the displacement feedback received from a linear variable displacement transducer (LVDT).

When the actuator was operated under force control, as was the case for the first floor device, the feed-back signal came from a load cell. In either case, the optimum controller loop gain settings were used to ensure the best performance of the equipment and to avoid any oscillatory approach to the command setting.

The servo-controller used in this test was an Instron series 2180 mini-controller fitted with two channels. Each channel controls one actuator and the latter is capable of either force or displacement control. The loop gain settings for each channel were optimised for either displacement or force control, whichever was relevant.

The selection of appropriate servo-valves is dependent on the actuator amplitude and operating frequency. For large stroke amplitudes and high operating frequencies, a greater capacity would be required. Based on these criteria, Moog series 72 servo-valves, with capacities of 96 and 230 litres per minute, were selected for the two horizontal actuators.

Whilst the LVDT was fixed permanently within the actuator, the load cell was independently selected and fitted to the end of the piston by means of a coupler.

4.5 Instrumentation

The actuator transducer measured the horizontal displacement whilst the load cell, mounted on the actuator piston, measured the restoring force. The transducer in the second actuator measured the displacement at the first floor. To determine the magnitude of the force at the first floor level, the output force from the second floor was continuously monitored. After adding the horizontal component of the axial load and scaling by 50%, this force was applied instantaneously as a command signal for the first floor actuator. The reason for adopting this approach is that in dynamic analysis of

the frame, the force in the first floor is half of the force in the second floor when only the first mode of vibration is of interest.

For specimen CR1, a "solatron" data logger (capable of scanning up to 1000 channels) was linked to the system. Strain gauges were attached to the flanges of the beams and column. As indicated in Figure 4.7 many of the gauges were located in the zones where plastic hinges were predicted. It was also deemed necessary to measure directly the section moments at locations which were likely to remain elastic. Accordingly, six such sections were chosen for instrumentation by strain gauges.

Measurement of the angular deformation at the beam-column connections is not straightforward. Six transducers were used to measure the angular deformation at two connections. As shown in Figure 4.8, one transducer was attached to the flange of the beam whilst a second device was fixed to the flange of the column. To measure the panel zone deformation, four transducers were mounted inside the panel zone as indicated in Figure 4.8. Two special rosette strain gauges were used in the centre of the panel zone to measure the strain in the three directions (i.e. horizontal, vertical and diagonal).

The data logger in the first test was neither accurate nor fast. In subsequent tests, it was replaced by a windows-based data acquisition program (recorder). The program was capable of updating the display once every second and optionally recorded values on disk. Measurement speed, using this system, varied between 40 and 400 readings/sec.

The position of the strain gauges on the flanges of the beam and column for all semi-rigid specimens are shown in Figure 4.9. Four transducers were used for measuring the angular deformation of connections as described for specimen CR1 and shown in Plate (4.4) and Figure 4.10. As illustrated in Plate (4.5), in order to measure panel zone deformation, two diagonal transducers were placed in the panel zone. Two strain gauges were also used in the centre of the panel zone to determine the strain in the diagonal direction in column web.

Fourteen strain gauges were used to measure the yield and ultimate stress in the top, seat and web angles in the connections. These strain gauges were located at those points where the angles experienced large deformations. Additional strain gauges were used to measure the shear stresses in the angles.

4.6 Experimental Measurement

To determine the restoring force at the second floor level, it is necessary to obtain the horizontal component of the force imposed by the axial load actuator at the top of the column. In each step, this force was then added to the restoring force (measured by the second actuator) to give the total restoring force at the second floor.

As mentioned previously, in order to measure the angular deformation of the connections, two transducers were connected on the flange of the column and the beam (Plate 4.4). The total angular deformation at the joint would be equal to the sum of two values of rotation in the column and the beam. These rotations were evaluated from the ratio of the displacements obtained from the transducer to the length of the member.

4.7 Loading Regime

4.7.1 Gravity Load

As described above, the model was designed such that the gravity load, applied at the top of the column, would remain constant throughout the test. The value of this load is 30 tonnes for specimen CR1 and 40 tonnes for the remaining specimens. These axial loads represent 24% and 29% of the squash load for the respective column sections.

4.7.2 Cyclic Load

For all cyclic tests, the increments of displacement were sufficiently small to ensure that at least four levels of displacement had been achieved prior to the yielding displacement. This procedure is the one proposed by the European Convention for

Constructional Steelwork (ECCS, 1986). The displacement cycles were used at amplitudes which were defined in terms of the yield displacement as follows :

- One cycle at each of +/- 0.125, 0.25, 0.5 and 0.75 of the yield displacement.
- Three cycles at each of +/- 1, 2 and 3 of the yield displacement.

The procedure also allows for the modification of the above regime and the number of cycles, depending on actual observations of the specimen during testing. Because of the absence of monotonic loading results, the test proceeded with the short regime. This is defined as the application of small amplitudes to ensure that four levels were applied prior to yield, followed by the remaining part of the complete testing procedure, as described above. The yield displacement adopted for the procedure was estimated by analysis.

4.7.3 Pseudo-dynamic Tests

Pseudo-dynamic testing is an on-line computer controlled technique which combines numerical analysis with physical measurements and whereby the dynamic behaviour of the structural system can be investigated. Researchers in Japan (Takanashi et al, 1980), the USA (Mahin and Shing, 1984; Mahin et al, 1989) and Europe (Elnashai, et al., 1990) have been utilising this technique for the past two decades. The theory and procedure for this testing technique and comparisons with the shaking table are described and discussed in the literature (Elghazouli, 1991). In this section, a brief review of this method (giving a summary of the theory, assumptions, description of the computer program and the sources of the errors) are presented below.

The basic assumption in the pseudo-dynamic test method is that the dynamic behaviour of the structure can be represented by a discrete-parameter model with a finite number of degrees of freedom. The equation of motion for this system can be expressed in terms of a set of second-order ordinary differential equations which, in matrix form, are:

$$M a(t) + C v(t) + R(t) = F(t) \tag{4.1}$$

where M and C are the mass and damping matrices, a(t) and v(t) are acceleration and velocity vectors, R(t) is the structural restoring force vector and F(t) is the external force vector applied to the system.

Equation 4.1 can be solved using a direct step-by-step integration method to obtain the displacement response to any arbitrary external forcing function. In the step-by-step integration, the duration T is divided into equal time intervals Δt. Therefore, an approximate solution of the equations of motion can be obtained by considering the equilibrium equation at times 0, Δt, 2 Δt, ..., n Δt.

In the central difference method, a parabolic variation of acceleration is assumed. The velocity and acceleration can be represented by the following difference equations:

$$v_n = \frac{d_{n+1} - d_{n-1}}{2\Delta t} \tag{4.2}$$

$$a_n = \frac{d_{n+1} - 2d_n + d_{n-1}}{\Delta t^2} \tag{4.3}$$

Where d, v, and a are the displacement, velocity and acceleration for each step, respectively. By substituting equations (4.2) and (4.3) into the equilibrium equation (4.1) displacement, velocity and acceleration for the n+1 step are :

$$d_{n+1} = d_n + \Delta t\, v_n + \frac{\Delta t^2}{2} a_n \tag{4.4}$$

$$a_{n+1} = \left[M + \frac{\Delta t}{2} C\right]^{-1} \left[F_{n+1} - R_{n+1} - C v_n - \frac{\Delta t}{2} C a_n\right] \tag{4.5}$$

$$v_{n+1} = v_n + \frac{\Delta t}{2}\left[a_n + a_{n+1}\right] \tag{4.6}$$

Using these equations, the step in the pseudo-dynamic algorithm can be summarised as:

i) Input an initial excitation: F_{n+1}

ii) Calculate the corresponding displacement response d_{n+1} from equation 4.4

iii) Impose the displacement d_{n+1} on the structure using actuators

iv) Wait for the actuator to stop and measure the restoring forces R_{n+1}

v) Compute the acceleration a_{n+1} and the velocity v_{n+1}, using equations (4.5) and (4.6)

vi) Set n=n+1

vii) Go to step 1.

It is important to note that the total time required for the test execution is much larger than the sum of the intervals Δt which corresponds to the actual duration of the earthquake motion. In practice, to impose the displacement increments at each step, it is necessary to sub-divide the time interval into two phases: a ramp period (T_1) and a hold period (T_2).

The ramp period should be large enough so that the hydraulic actuators can apply the loads on the structure with a speed sufficiently low so as to avoid instability in the testing system.

During the hold period (T_2), the restoring forces developed by the specimen are measured and fed back to the numerical algorithm for computing the response in the next step. This depends on the number of actuators used in the test.

It was observed that the numerical solutions became unstable when $\omega \Delta t$ exceeded a certain critical value, Δt_{cr}. It can be shown (Bathe, 1982) that this value for the central difference method is given as :

$$\Delta t_{cr} = \frac{T_n}{\pi} \tag{4.7}$$

where T_n is the smallest period of vibration of a system with n degrees of freedom. For non-linear systems, the time step should also be small enough to trace the inelastic response of the test structure over the range of displacement increments. Generally, a time step of $T_y/20$ would be sufficient, where y is the highest frequency mode of interest.

It should be noted that the stability and accuracy characteristics of the explicit schemes for linear systems are valid for non-linear systems. This is because a non-linear system can be modelled as a linear system in which the tangent stiffness is changing. By increasing the natural period of the system which is inversely proportional to the square root of the tangent stiffness, the time interval for non-linear system will be larger than for the linear system. This implies that the Δt selected for a linear system will be conservative if the system becomes non-linear.

A computer program was used for running the test. The flowchart for this pseudo-dynamic testing program is shown in Figure 4.11. The program begins by checking all the parameters (e.g. masses, viscous damping, number of channels, excitation record file name and time increment). The ramp period and hold period can be predefined by the user. A choice is available for updating the graphics and data storage within or outside the ramp generation.

In each step, the control loop commenced by reading the data from all the channels through the A/D converters and the force vectors are checked with the limit values that are defined for each actuator. Once the excitation vector at the current step is read, the control displacements for the following step are computed. The displacement ramps are then generated and sent to the D/A converters. The horizontal component of the

axial load in each step is added to the restoring force and the calculated value is used to determine the displacement increments.

The procedure can be interrupted at any step and the user has the choice of either terminating or resuming the test. The program also has a routine for unloading the test at the end of execution.

The experimental and analytical errors in the pseudo-dynamic testing method are discussed in detail in the literature (Shing and Mahin, 1983; Nakashima and Kato, 1988). Suffice it to say that there are three sources of experimental errors. These are the displacement control errors, the displacement measurement errors and the force measurement errors.

Inaccurate application of the displacement (from the controller-actuator closed-loop system), the flexibility of the specimen supports and the resolution limits of the A/D converters contribute to the displacement control errors in the test. On the other hand, the inaccurate measurement of the response displacement by the transducer, electrical noises and geometric effects introduce the displacement measurement errors. Force measurement errors are usually caused by high friction existing in the model, inaccurate measurement of the forces from the load cell or geometric effects.

As mentioned previously, the computed displacements were used in the numerical algorithm (instead of the measured ones) for calculating the displacements for subsequent steps. This approach avoided the cumulative growth of displacement feedback error throughout the test. However, the force feedback errors, which are the result of the force displacement and displacement control errors, are always included in the numerical computation.

Although the cumulative growth of the force feed-back errors is unavoidable, it has to be constrained to a minimum. As discussed above, the force feed-back errors depend largely on the magnitude of the displacement control errors at each step. Consequently, to reduce the force measurement errors, it was necessary to decrease the displacement control errors.

4.8 Definition of the Response Parameters

In order to process the results, all the relevant factors effecting the response parameters must be determined. Some of these factors are not uniquely defined in the literature. Moreover, a useful comparison of the results obtained from the experimental work with those from the analyses can only be achieved if uniform assessment criteria are imposed for these parameters.

4.8.1 Yield Criteria

There are various definitions for the yield displacement. Some of these are shown in Figure 4.12 where F_y is the yield force and δ_y is the corresponding yield displacement. These definitions are as follow:

a. The value corresponding to first yield in any fibre, or in other words the first deviation from linearity.

b. The maximum load reached. This applies well in buckling problems but may correspond to large deformation in flexure-dominated behaviour.

c. The value corresponding to a certain deformation which would have been obtained in a purely elastic behaviour. Figure 4.12(c) gives an example with twice the elastic deformation. This definition applies well to flexural behaviour of beams and connections but not to buckling problems.

d. The intersection of the two tangents shown in Figure 4.12(d). This definition can be used in most applications.

4.8.2 Ultimate Criteria

In order to assess the seismic performance of moment-resisting steel frames from the dynamic analyses a set of criteria, corresponding to the conditions at which structural failure occurs, are defined. The failure criteria may be either global (e.g. interstorey

drift and storey stability) or local (e.g. local buckling in the members). The definition of each criteria is in the Codes (EC3 and EC8).The ultimate response of the structure is related to this limit criteria whichever occurs first.

The failure criterion plays a very important role in seismic design of structures because it influences the value of the available global ductility and the energy dissipation capacity of the structure. Generally, if the structure fails according to a global mechanism, it will be capable of exhibiting sufficient ductility to withstand severe earthquakes. To avoid local failure (i.e. local buckling) in the structure, recommendations are provided in the codes. Further discussion of these criteria and the code recommendations are given in Chapter 6.

4.8.3 Ductility

The ability of a member or a system to sustain deformations beyond its yield point without significant loss of strength is usually referred to as ductility. The ratio of the ultimate response to the value at the yield point is used to calculate the ductility.

Displacement ductility in the present study is related to inter-story displacements in the structure whilst curvature ductility is associated with the member section rotation per unit length in the plastic hinge regions.

The flexural plastic behaviour of a steel structure depends on the amount of moment redistribution. The attainment of the predicted collapse load is related not only to the hinge position which reaches the full plastic moment but also to the inelastic rotation at other hinges. Hence, plastic hinges should exhibit some degree of ductility in addition to their strength requirement. The rotation ductility is a measure of this ductility and can be evaluated from the ratio of the plastic rotation at the collapse state to the yield rotation.

4.8.4 Plastic Hinge Length

The plastic hinge length occurring in the individual members are important in that they define the extent to which members should be detailed to ensure adequate resistance to local inelastic instability and the proportion of each member in which energy dissipation may occur.The plastic hinge length in a member is estimated from the ultimate and yield moments. The plastic hinge length is given by :

$$L_p = \left(1 - \frac{M_y}{M_u}\right)L \tag{4.8}$$

where L is the length of the column, M_y is the yield moment of the column and M_u is the ultimate moment.

4.8.5 Behaviour Factor

Structures are usually designed such that the earthquake input energy during severe ground motion is dissipated through inelastic deformation. In order to avoid collapse, the values of these plastic deformations have to be limited. The behaviour factor is employed to reduce the seismic design loads to a level which takes advantage of the energy dissipation capability of each structure while still ensuring that the imposed ductility demand do not exceed the available supply. The behaviour factor depends on the configuration and loading of the structural system, second order effects, plastic rotations of the members and their connections.

For a particular response period, the behaviour factor q as employed in EC8 is the ratio of the elastic acceleration spectrum (which is defined for the seismic hazard of a site) to the inelastic spectrum that is used in the derivation of the seismic design forces. Hence, the q factor is defined as:

$$q = \frac{(S_a)_d^{el}}{(S_a)_d^{in}} \tag{4.9}$$

where, $(S_a)_d$ is the design spectral acceleration and the superscripts 'el' and 'in' represent its elastic and inelastic values, respectively. In EC8, the maximum allowable behaviour factors are specified for steel frames. While these values reflect the ability of each type of frame to undergo stable oscillations in the inelastic range, they are also intended to represent lower bounds on the actual ductility supply of individual structures. Thus it should be expected that $q_{code} \leq q'$ where q' is the ultimate value which relates not the elastic and inelastic design spectra of equation (4.9) but the response spectra corresponding to the ground motion intensities which produce structural collapse and yield, i.e.,

$$q' = \frac{(S_a)_c^{el}}{(S_a)_y^{el}} \tag{4.10}$$

where the subscripts 'c' and 'y' denote collapse and yield, respectively.

In comparing equations (4.9) and (4.10) it is observed that the Eurocode 8 behaviour factors correspond to the case where collapse is imminent under the loading defined by the elastic design spectrum and yield is equally imminent with the condition of the inelastic design spectrum. For a given ground motion, however, the collapse intensity will be uniquely defined. In which case, by combining equations (4.9) and (4.10), it is possible to further define the behaviour factor of an individual structure as:

$$q'_D = \frac{(S_a)_c^{el}}{(S_a)_d^{in}} \tag{4.11}$$

The subscripts in equation 4.11 denotes that the behaviour factor has been determined using the design spectrum. While this definition has the advantage that it relates the intensity of loading at collapse to the design loads, it fails to include for the disparity between the ground acceleration at yield which will vary with ground motion, structural design and response period and that related to inelastic design spectrum. By

assuming a constant dynamic acceleration amplification, the ratios in equations (4.10) and (4.11) can be represented by the peak ground accelerations. Thus,

$$q' = \frac{a_{g\,(collapse)}}{a_{g\,(yield)}} \tag{4.12}$$

$$q'_D = \left(\frac{a_{g\,(collapse)}}{a_{g\,(design)}}\right) q \tag{4.13}$$

where $a_{g(collapse)}$ and $a_{g(design)}$ are the peak ground accelerations which produce collapse and yield in the structure.

According to EC8 and the ECCS recommendations for steel structures in seismic zones, the q factor value is given as a function of the ratio α_u/α_y. In this expression, α_y is the multiplier of horizontal seismic actions (keeping the other design loads constant) corresponding to the point where the structure reaches its elastic limit in one section. Similarly, α_u is the multiplier of horizontal seismic actions (keeping the other design loads constant) corresponding to the point where the structure reaches its maximum load bearing capacity at the collapse state.

4.9 Experimental Results

In this section, the experimental results of the cyclic and pseudo-dynamic tests are presented. For the cyclic tests, the peak load values in the two directions were not identical, hence the peak loads given are the average of the positive and negative values. In all the semi-rigid models high strength bolts (Grade 8.8) were used. To reduce bolt slippage in the connection, bolts were tightened to 75% of their maximum torque.

For all the tests, the displacement values are recorded in mm, loads are given in kN and strains are illustrated in microstrains. The response parameters of all models are given in this section and a brief discussion of the results, in particular those which are related

to the objective of this research, are included. A comparison of the experimental results with analysis and further discussion are given in Chapters 5 and 6.

4.9.1 Cyclic Loading Tests

4.9.1.1 Model CR1

As mentioned previously, this model was designed as a rigid frame with fully-welded connections. Constant axial load was imposed at the top of the column, whilst horizontal displacements were applied at one end of the second floor beam. The second storey force was measured and half of its value was applied at the first storey level. This, as mentioned earlier, represented the first mode response.

The loading regime imposed on this model and the relationship between the lateral restoring force in the second floor and the top floor displacement are shown in Figures 4.13 and 4.14. Following the initial elastic response, it was observed that the load-displacement response deviated noticeably from linearity at approximately 38 mm and subsequently yielding was detected at the base of the first floor column. At the yield point, the restoring force in the 2nd floor was measured at 42 kN. Because of the limitations in the test equipment, it was not possible to impose displacements greater than 120 mm. At 120 mm top frame displacement at the second floor the test was stopped. The peak load at this stage was measured at 59.8 kN.

4.9.1.2 Model CS1

This model was designed as a semi-rigid frame with top and seat angles with double web angle connections. The details of the connections are shown in Figure 4.5. The radial bolt clearance used was 1.0 mm and the prestressing torque was 0.43 kNm.

The displacement cycles which were applied to this model are shown in Figure 4.15. The frame yielded at the base of the column when it was subjected to a 30 mm displacement at the second floor level. At this point, the restoring force at the second

floor was measured at 30 kN and the yield moment at the base of the column in the first storey was estimated at 101.23 kN m.

Figure 4.16 shows the relationship between the lateral restoring force at the second floor level and the top floor displacement. The force versus displacement at the first floor level and the relationship between the base shear and the top floor displacement are given in Figures 4.17 and 4.18.

At a displacement of 45 mm at the top floor, a gap was observed between the flange of the column and the leg of the top angle. When the displacement was increased to 110 mm in the third cycle, the flange at the base of the column in the first floor started to buckle. Nonetheless, the force in the second floor continued to increase as the displacement in the top floor reached 118 mm. The maximum moment at the base of the column in the first storey was estimated at 167.5 kNm.

The beams at the first and second floor level showed no sign of yielding and the maximum moment developed in the beam was estimated at 35.63 kNm (which is equal to 30% of the plastic moment capacity). The moment at the base of the column in the first floor versus the top floor displacement and the moment-rotation of the connection in the first floor are shown in Figures 4.19 and 4.20, respectively.

As the maximum displacement approached 120 mm (which was the limit of the actuator stroke) the test was terminated. At this point, the maximum restoring force at the second floor level was 50.63 kN.

4.9.1.3 Model CS2

As shown in Figure 4.5, the sizes of the angles in the connections in this model were changed such that the moment capacity of the connections were approximately 50% of plastic moment of the beam.

The displacement cycles applied to this model are shown in Figure 4.21 and the relationship between the lateral force in the second floor and the top frame displacement is illustrated in Figure 4.22. The frame yielded at the base of the column

in the first storey when a 26 mm displacement was applied at the second floor level. At this point, the shear force at the second storey level was 40 kN and the yield moment at the base of the column was 101.7 kNm.

The value of three strain gauges attached to the top angle of the connection in the first floor indicated that the connection yielded when the imposed displacement at the second floor level reached 29 mm. At this stage, the moment in the beam was 39.70 kNm which is less than its plastic moment.

When the applied displacement at the top of the frame reached a value of approximately 105 mm, the compression flange at the base of the column in the first storey started to buckle. At 115 mm displacement, it was observed that both flanges of the column buckled completely. The values of strain in the web angles (as recorded by the gauges) were still below yield.

A maximum horizontal force of 65 kN was observed at the second floor level in this test. The force-displacement relationship at the first floor level and the base shear versus the top floor displacement are represented in Figures 4.23 and 4.24.

The maximum moments in the beam and column, calculated from the experimental results, were 60 kNm and 168 kNm, respectively. The moment at the base of the column versus the top floor displacement and the moment-rotation of the connection at the first floor level are shown in Figures 4.25 and 4.26.

By monitoring the data provided by the strain gauges that were located in several locations in the column and the beam members, it was observed that these elements (except at the base of the column in the first floor) did not yield. Instrumentation in the column panel zone shows that the values of strain in the web were below the yield value.

4.9.1.4 Model CS3

The connections in this frame were designed with a moment capacity of approximately 70% of the plastic moment of the beam. The details of the connection are shown in Figure 4.5.

The procedure for imposing axial and cyclic loads on the above frame was the same as in the previous tests. The displacement cycles imposed on this frame are shown in Figure 4.27. All the bolts were 20 mm diameter with a 1 mm radial bolt clearance and were tightened to 75% of the bolt maximum capacity.

Under the imposed loading, the model yielded at the base of the column. At this point, the top frame displacement was 24 mm which was lower than the yield displacement in the previous models. The reason for this is that the connections in this model are stiffer and stronger. The lateral force at the second floor level at this point was 42 kN and the moment in the column was 100 kNm. Figures 4.28 and 4.29 represent the force-displacement relationship at the first and second floor levels. The base shear versus the top floor displacement is shown in Figure 4.30.

The top angles in the connections yielded at a displacement of 49 mm at the top floor. Concurrently, the moment of the connection in the first floor was 52 kNm. Figure 4.31 shows the relationship between the moment in the connection and its rotation at the first floor level.

The maximum lateral force at the second floor was 72.5 kN. The corresponding top frame displacement was 100 mm. At a displacement amplitude of 95 mm in the second cycle of the last three cycles, the compression flange of the column in the first storey started to buckle. Thereafter, at a displacement of 110 mm in the opposite direction, both flanges of the column buckled (Plate 4.6). Similar to the CS1 and CS2 models, the beams and columns in this model did not show signs of yielding except at the base of the column in the first storey. The maximum moment at the end of the beam was 85 kNm and at the base of the column (at the first storey level) was 169 kNm. Figure 4.32

shows the relationship between the moment at the base of the column in the first storey and the top frame displacement.

The values of strain observed in the panel zones at the first and second floor levels and on the web angles in the connections show that these sections of the connection did not yield. It was also observed that changes in the size of the web angles in the connections had no influence on the moment capacity of the connection.

Table 4.5

Yield and ultimate values of parameters of different models

Model	yield displ. (mm)	yield shear (2nd floor) (kN)	max. shear (2nd floor) (kN)	yield mom (column) (kNm)	max. mom. Column (kNm)	max. mom. Beam (kNm)
CR1	38	42	59.8	101	119.2	68.2
CS1	30	30.03	50.63	101.2	167.5	35.63
CS2	26	40	65	101.7	168	60
CS3	24	42	72.5	100	169	85

The yield and ultimate capacity parameters of the rigid and semi-rigid models, obtained from experimental results, are indicated in Table 4.5. It should be noted that the results of the rigid frame in this Table are related to the CR1 model which is not the same size as the semi-rigid frames. The comparison of these parameters for the semi-rigid frames with the results of the rigid frame (with the same size as the semi-rigid frames) are given in Chapter 5.

4.9.2 Pseudo-Dynamic Tests

To verify the reliability and stability of the developed system, a number of pseudo-dynamic tests were conducted in the elastic range on model DS1. The El Centro S-E component acceleration time history record was used for these tests. In addition, in order to predict the analytical response the ADAPTIC computer program (Izzuddin and Elnashai, 1989) was used. This is described in detail in Chapter 5.

To select the correct time interval and the ramp and hold periods for the tests, the model was subjected to a 5% and 8% scaled El-Centro record. After running the test with different periods, it was identified that a time step of 2.5 seconds for the ramp and hold periods would be reliable for imposing the displacement and measuring the forces.

When the experimental displacement response of the second floor for the DS1 frame was compared with the analytical response, better agreement was found with the 8% scaled El-Centro acceleration record. The reason for this is that in the test, for the 5% scaled acceleration record, the value of the imposed displacement increment in each step was too small and outside the calibrated range of the actuator.

Finally, to justify the procedure of the pseudo-dynamic test, the model was subjected to a 15% scaled El-Centro acceleration record. The elastic response obtained from this pseudo-dynamic test is shown in Figure 4.33. To compare the analytical results with the tests, a value of 5% damping was used in the analysis. The reason is that in semi-rigid frames with bolted connections the value of damping are greater than the rigid frames. Hence, a value of 5% was deemed reasonable. Figure 4.34 illustrates the comparison between the experimental and the analytical results. As shown in these Figures, there was very good agreement between the numerical results and the pseudo-dynamic response.

The DS1 model was tested for the first 6 seconds of the El-Centro record and under an axial load of 29% of the squash load. A mass of 16 tonnes was assumed at the top of the column in each storey and a time step of 0.01 seconds was used. Based on a predictive analysis, the frame was subjected to a scaled 120% El-Centro acceleration record. The displacement response obtained in the test is shown in Figure 4.35 and the measured load history is illustrated in Figure 4.36.

The model yielded at the base of the column in the first floor after imposing 1.70 seconds of the record. The yield displacement at this point was 23 mm. After imposing 2 seconds of the record, the maximum displacement was observed to be 76 mm. The maximum base shear was 115 kN and this was observed after applying 2.4 seconds of the record.

The strain gauge readings at the top angle indicated that after applying 1.79 seconds of the record the connection yielded. At this point, the top frame displacement was 33 mm. As observed in the cyclic tests, the strain gauge values at several locations in the members, e.g. beams and columns, indicate that these parts of the structure did not yield. Moreover, the strain gauges attached to the web angles and the column web in the joints (i.e. inside the panel zone) did not reach their yield value.

Additional strain gauge results for all the models are given in Appendix A, where force versus strain for a number of strain gauges are presented. As mentioned earlier, the value of strain in the column members and in the beams is lower than the yield value. Yield was not also reached in the web angle.

4.10 Discussion of the Results

4.10.1 Plastic Hinge Length

Figure 4.37 depicts the plastic hinge length normalised by the column height for the specimen CR1. The results are plotted against the second floor displacement. As shown in this Figure, the maximum plastic hinge length for the CR1 model was 0.26 when a displacement of 120 mm was imposed at the top of the frame.

Figure 4.38 shows the plastic hinge length normalised by the column height, for three semi-rigid models. The results are also plotted against the second floor displacement. The maximum normalised length of the plastic hinge at the base of the column for these models is given in Table 4.6 and compared with those of the rigid frame with the same sizes and fully-welded connections. It is seen that the flexibility of the connection influences the length of the plastic hinge.

4.10.2 Point of Contra-Flexure in Column

Figures 4.39 and 4.40 show the migration of the point of contra-flexure within the first storey column. The distance from the base of the frame to the point of contra-flexure in the column, normalised by the height of the first storey and is shown versus the

displacement at the second floor level. The values of the height of the point of contra-flexure for each semi-rigid frame is depicted in Table 4.6.

Table 4.6

Experimental plastic hinge length and effective length of the column

Frame	Yield displacement	Plastic hinge length	Height of contra-flexure	Effective length
Rigid frame	18 mm	0.18	0.62	1.24
CS1	30 mm	0.195	0.85	1.7
CS2	26 mm	0.21	0.89	1.78
CS3	24 mm	0.26	1.01	2.02

As indicated in Figure 4.39, in the rigid frame (CR1 model) the height of the point of contra-flexure increased, with increasing displacement, up to 0.84 of the length of the column at the first floor level. In the semi-rigid frames this value at first lies outside of the column length and then decreases to a constant value in the range 0.8-1.0, depending on the strength of the connection.

Figure 4.40 shows that the height of the point of contra-flexure varies with the flexibility of the connection. This points towards the fact that the effective length of the column changes with the flexibility of the connection hence it may be related to the rotation ductility of the connection.

4.10.3 Panel Zone Deformation

The rotation of the panel zone versus the top frame displacement in the CS1 model is shown in Figure 4.41. The maximum rotation of the panel zone at the end of the test was 0.0032 radians and the deformation related to this value was 0.7 mm. This represents 0.58% of the maximum top storey displacement.

As mentioned previously, and shown in Figure 4.41, the panel zone did not yield. The maximum rotation of the panel zone measured in the cyclic and dynamic tests varied

from 0.0032 to 0.004. When these values are compared with the values of the maximum rotation of the connection obtained in these models, it is concluded that this deformation has no significant influence on the moment-rotation curve of the connection. This would suggest that the deformation of the non-yielding panel zone can be ignored.

4.10.4 Ductility

As mentioned in Section 4.8.3, to calculate the ductility response it is necessary to define the ultimate criteria for these frames. The maximum drift at the second storey level for the first test was 0.031 which was related to a top storey displacement of 117 mm. Therefore, the ultimate criterion for the CR1 model, will be defined by the 3% drift.

The yield and ultimate displacements for the CR1 rigid frame are 38 mm and 117 mm, respectively. The displacement ductility for this model is therefore 3.1. The yield and the ultimate rotations for the column, as obtained in the test, can be determined by integrating the areas under the corresponding curvatures at the yield and ultimate limit states. By calculating the yield and ultimate rotation, the rotation ductility for the column at the ground floor level for this model is 4.4.

The definition of the ultimate criteria for all semi-rigid models are related to the maximum drift at the second storey level and also to the buckling at the base of the column in the ground floor. As a result of this description, and by considering the minimum value of these two criteria, a top storey displacement of 80 mm was defined as the ultimate displacement for the CS1 model corresponding to 3% drift. The ultimate displacements for the CS2, CS3 and DS1 models are 82 mm, 81 mm and 76 mm, respectively. Table 4.7 gives the displacement ductility for all the semi-rigid models.

By considering the ultimate criteria identified for all the semi-rigid frames, the yield and ultimate rotation at the critical locations in the column (at the first storey level for each model) are determined and the calculated rotation ductility are given in Table 4.7. A

maximum rotation of 0.036 was observed in the column section at the onset of buckling.

Table 4.7

Seismic response parameters for all semi-rigid models

Models	yield displ.	Ultimate displ.	displ. ductility	yield rotation	ultimate rotation	rotation ductility
CS1	30 mm	80 mm	2.67	0.0064	0.028	4.37
CS2	26 mm	82 mm	3.15	0.0065	0.030	4.61
CS3	24 mm	81 mm	3.37	0.0063	0.030	4.76
DS1	23 mm	76 mm	3.30	0.0065	0.029	4.73

As shown in Table 4.7, the rotation of the column decreased when the flexibility of the connection increased. Consequently, it is concluded that flexible connections delay the onset of buckling in the column.

4.10.5 Behaviour Factors

According to the EC8 and ECCS recommendations for the design of steel structures in seismic zones, the q factor is given by:

$$q = 5\frac{\alpha_u}{\alpha_y} \tag{4.14}$$

Taking into account the values of the yield and ultimate forces obtained from the tests, and using equation (4.14), the q factor can be determined. The behaviour factors for all the models are given in Table 4.8.

Table 4.8
Calculated behaviour factor for all models

models	yield force	ultimate force	α_u/α_y	q- factor
CR1	65 kN	89	1.37	6.85
CS1	45 kN	70 kN	1.55	7.75
CS2	60 kN	94 kN	1.57	7.85
CS3	65 kN	104.5	1.60	8.00
DS1	65.5 kN	106	1.61	8.05

As indicated in Table 4.8, the ratio of the ultimate-to-yield base shear for the rigid frame is larger than the value of 1.2 which is the minimum value recommended in EC8. Moreover, it is clearly indicated in the Table that the behaviour factor for semi-rigid frames is comprehensively larger than for rigid frame.

4.10.6 Initial Stiffness of the Connections

The rotational stiffness of the connection is determined from the slope of the experimental moment-rotation curve. Figure 4.42 shows the monotonic moment-rotation curves for the three semi-rigid models.

Table 4.9 gives the initial stiffness for the connection for the semi-rigid models. The moment at the yield point and the rotation of the connections obtained from the tests are also given in Table 4.9.

Table 4.9
Experimental yield and ultimate rotation of the connections

Model	Stiffness (kN-m/rad)	Yield moment	Yield rotation	Ultimate rotation	Rotation ductility
CS1	3600	18.7 kNm	0.0049	0.027	5.51
CS2	7270	40.1 kNm	0.0051	0.024	4.71
CS3	10400	52 kNm	0.0053	0.022	4.15

It should be noted that these moments and rotations were evaluated from the readings of the strain gauges and transducers at the positions on the top and seat angles where yielding occurred. The maximum rotation of the connection at 3% drift (which defined the ultimate limit state for these frames), and the rotation ductility of the connection for each model are given in Table 4.9.

As indicated in Figure 4.42 and Table 4.9, changes to the thickness of the top and seat angles (which influence the moment capacity and rotational stiffness of the connection) do not influence the value of the rotation at the yield point.

4.10.7 First and Second Storey Stiffness

The stiffness at each storey level may be evaluated from the slope of the force-displacement curve which is obtained from the test. The values of the first and second storey stiffness for each semi-rigid model were calculated from the following equations:

$$K_1 = \frac{F_1 + F_2}{\delta_1} \tag{4.15}$$

$$K_2 = \frac{F_2}{\delta_2 - \delta_1} \tag{4.16}$$

where K_1 and K_2 are the first and second storey stiffness, F_1 and F_2 are the shear forces in the first and second storey and δ_1 and δ_2 are the first and second storey displacements.

The monotonic force-displacement for the first and second floor levels for the three models, as recorded in the cyclic tests, are shown in Figures 4.43 and 4.44. The values of the stiffnesses are evaluated from these monotonic force-displacements and given in Table 4.10.

4.10.8 Fundamental Period

In dynamic analysis, the evaluation of the natural period of vibration for a structure with two degrees of freedom is given as:

$$T = 2\pi \sqrt{\frac{2m}{(K_1 + 2K_2) - \sqrt{K_1^2 + 4K_2^2}}} \qquad (4.17)$$

where T is the natural period of vibration for the structure, m is the mass of each floor and K_1 and K_2 are the first and second storey stiffnesses, respectively. By calculating the storey stiffnesses from Equations 4.15 and 4.16, the natural period for each of the semi-rigid model is evaluated using Equation 4.17. Table 4.10 gives the values of the stiffnesses and the natural period of vibration for the three semi-rigid frames.

Table 4.10
Stiffness and natural period of semi-rigid frames

Models	K_1 (N/mm)	K_2 (N/mm)	T (second)
CS1	4600	2250	0.69
CS2	5300	3200	0.66
CS3	5800	3300	0.64

It is observed that with an increase in the flexibility of the connection, the natural period of the structure increases. Consequently, frames with more flexible connections attract less lateral forces when subjected to seismic forces.

4.11 Commentary

From the experimental results, it is concluded that the flexibility of the connections influences the overall behaviour of the frames. The static lateral deformation of the frames increases as the connection flexibility increases. The effective length of the column members increases with an increase in flexibility of the connections. Moreover, the frames with flexible connections attracts lower earthquake forces when compared with stiffer structures.

The seismic response parameters for the structures are also affected by changing the stiffness and strength of the connections. It is seen that the rotational ductility of the column members varied with the type of connection used in the structure. The behaviour factors for semi-rigidly connected frames were larger than their rigid counterparts, mainly due to the earlier attainment of the yield limit states.

From this investigation it was observed that the top and seat angles with double web angles connections possessed sufficient strength and ductility which enhanced its capability of dissipating energy when the structure was subjected to seismic forces. Hence, this type of connection can be used effectively in semi-rigid steel frames in seismic areas.

Plate 4.1 General view of testing assembly

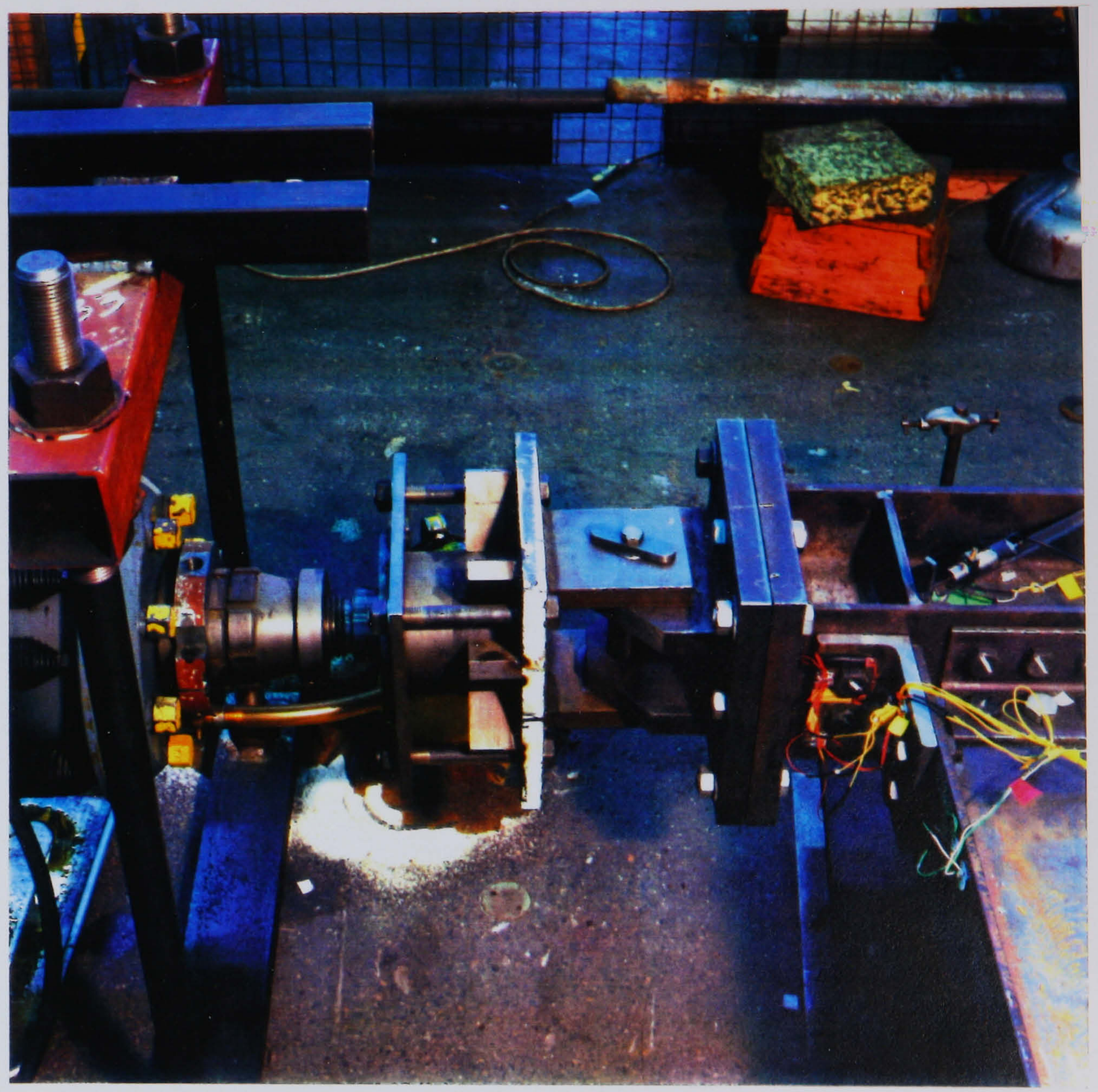

Plate 4.2 Details of actuator connected to the column

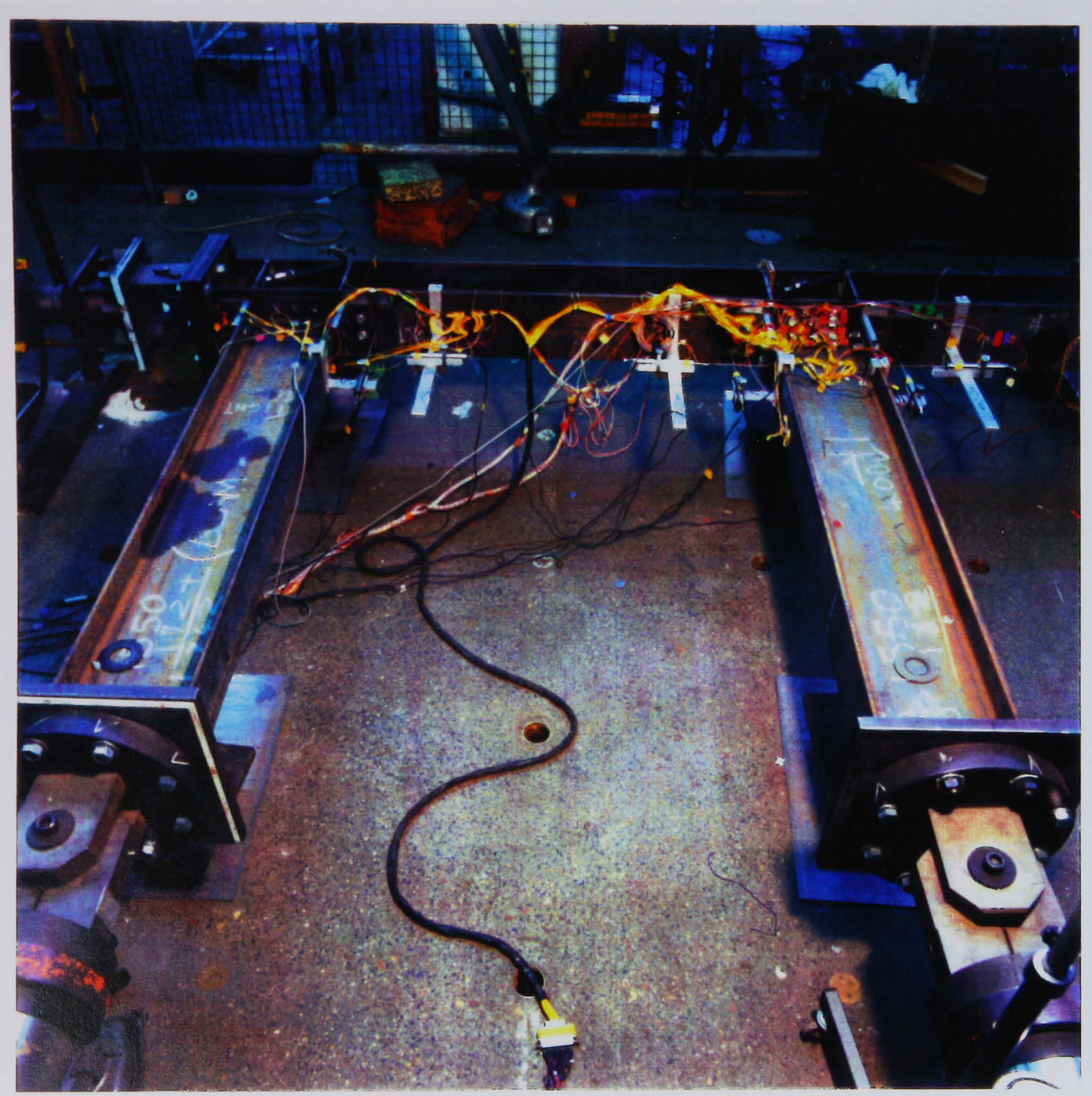

Plate 4.3 Details of actuators connected to the beams

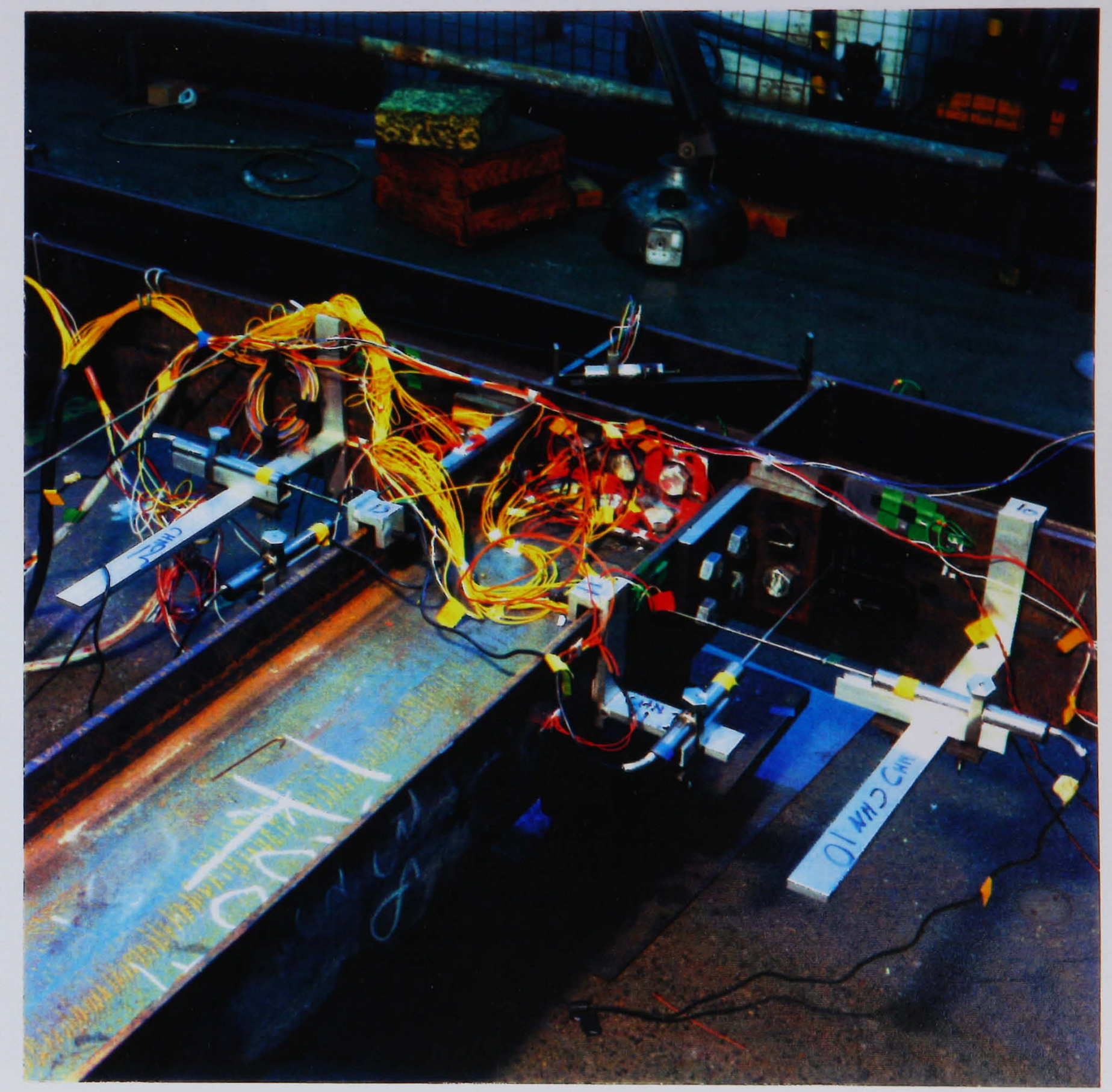

Plate 4.4 Transducers for measuring the angular deformation

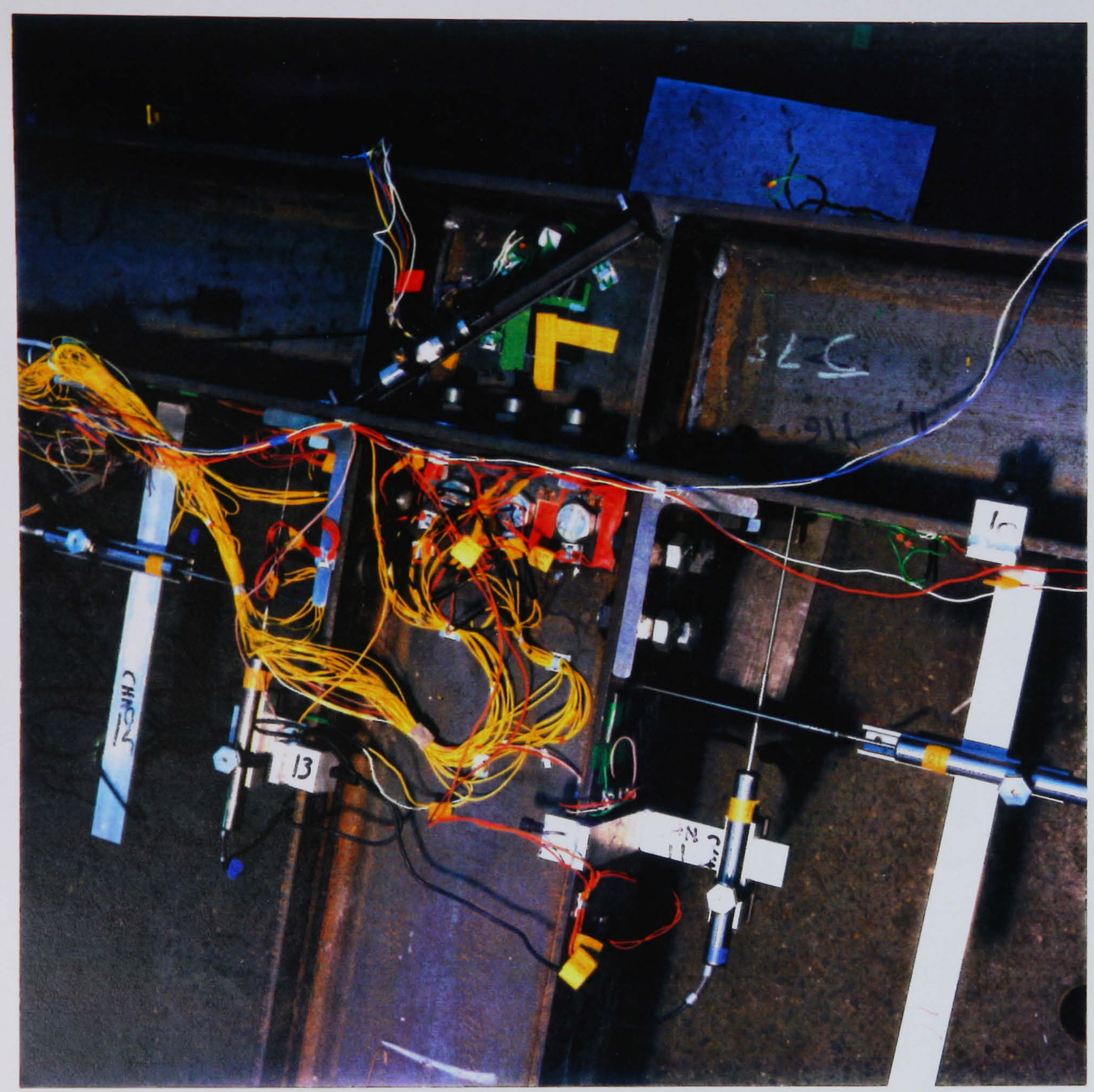

Plate 4.5 Transducers for panel zone deformation

Plate 4.6 Local buckling of compression flange

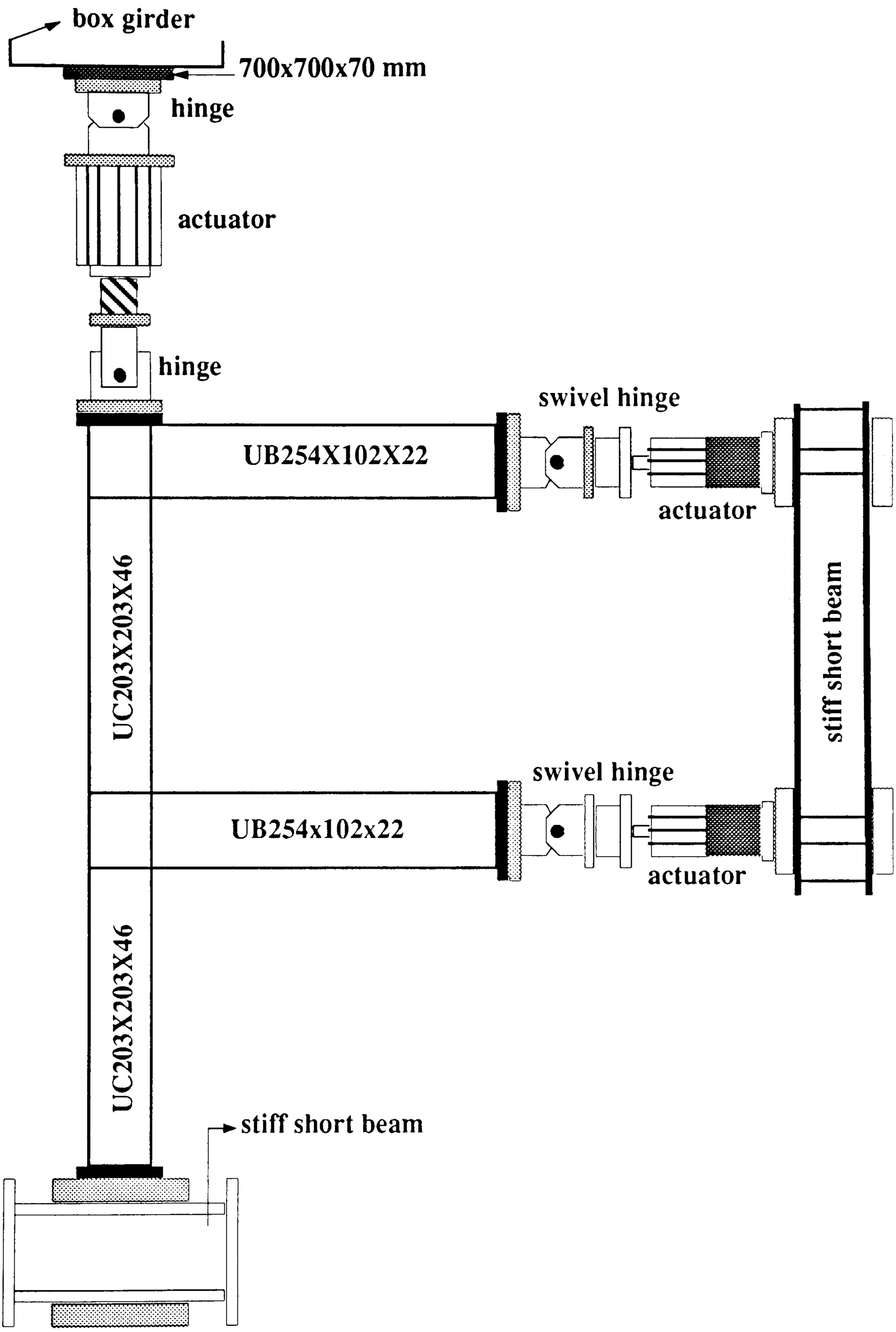

Figure 4.1 : Arrangement of specimen and actuators in test-rig

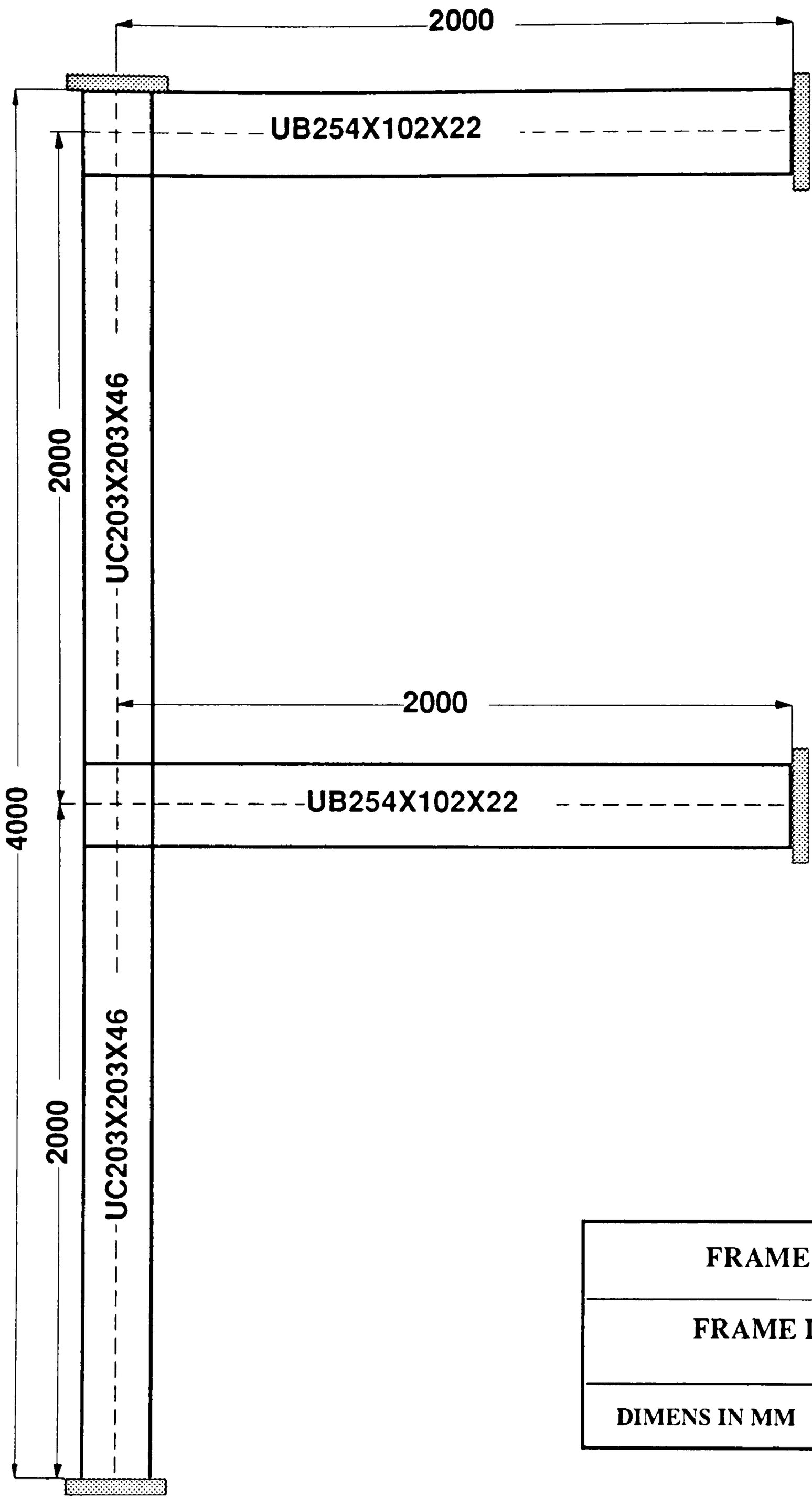

FRAME TEST	
FRAME LAYOUT	
DIMENS IN MM	SCALE 1:20

Figure 4.2

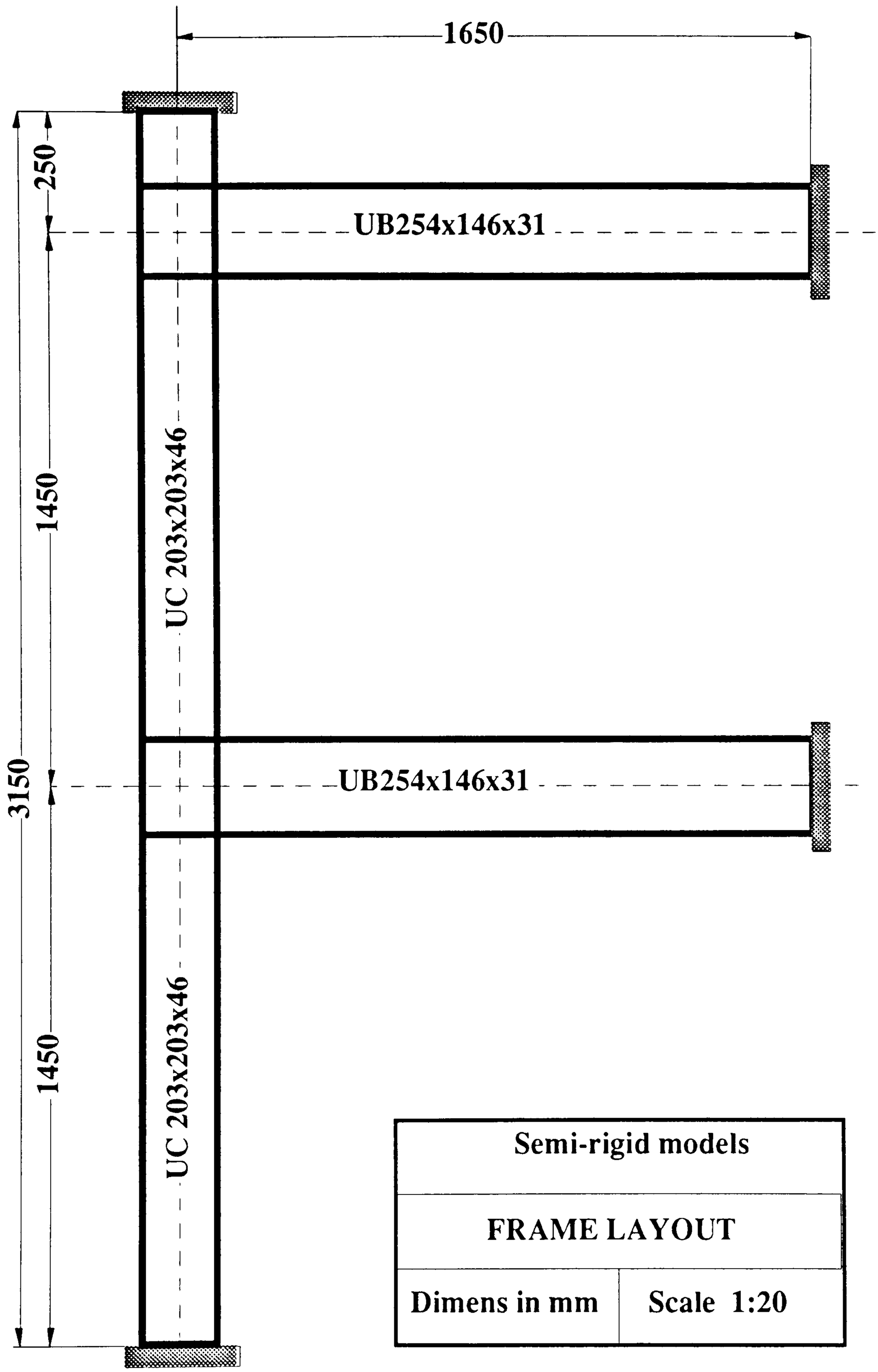
1650
250
UB254x146x31
1450
UC 203x203x46
3150
UB254x146x31
1450
UC 203x203x46
Semi-rigid models
FRAME LAYOUT
Dimens in mm
Scale 1:20

Figure 4.3

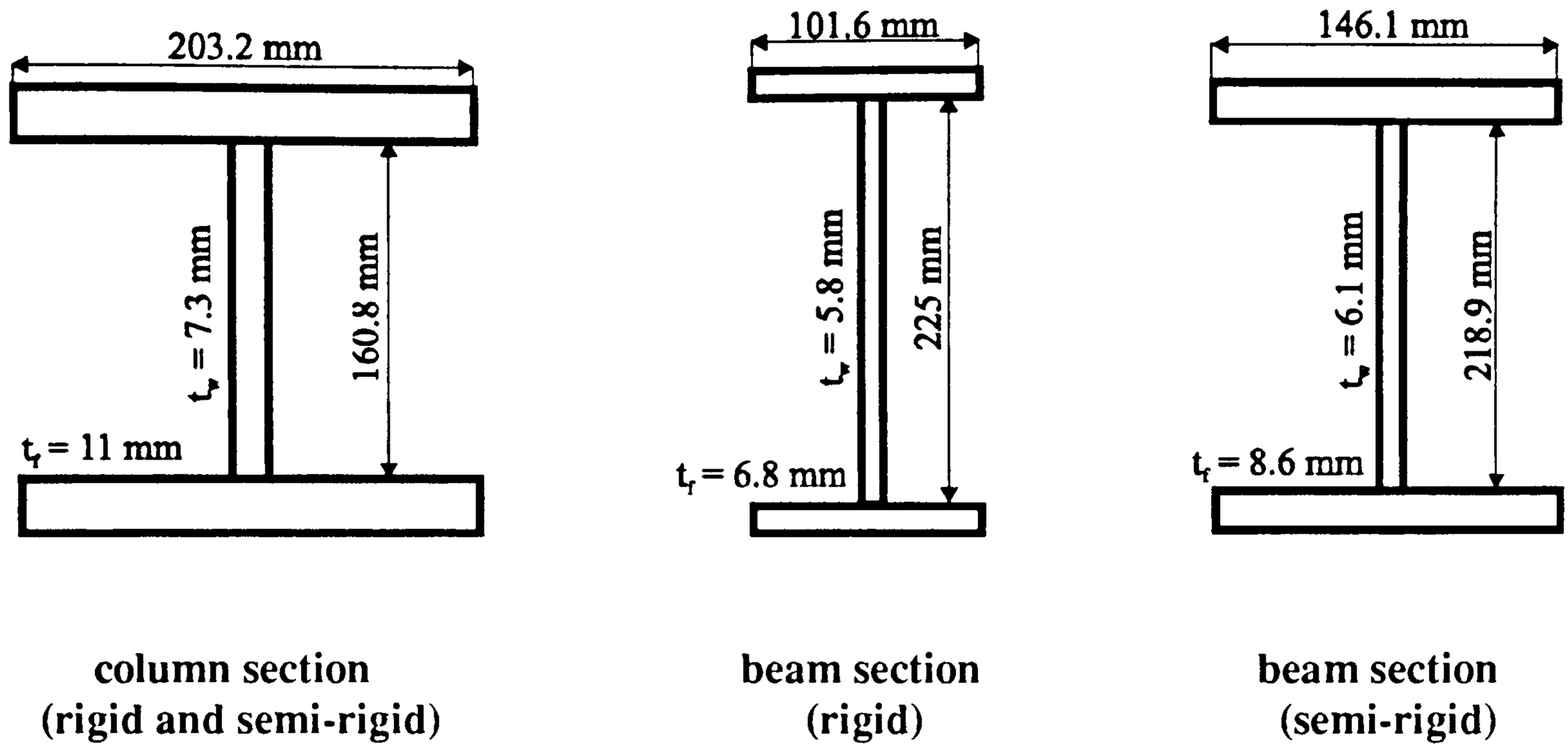

Figure 4.4 Column and beam sections for specimens

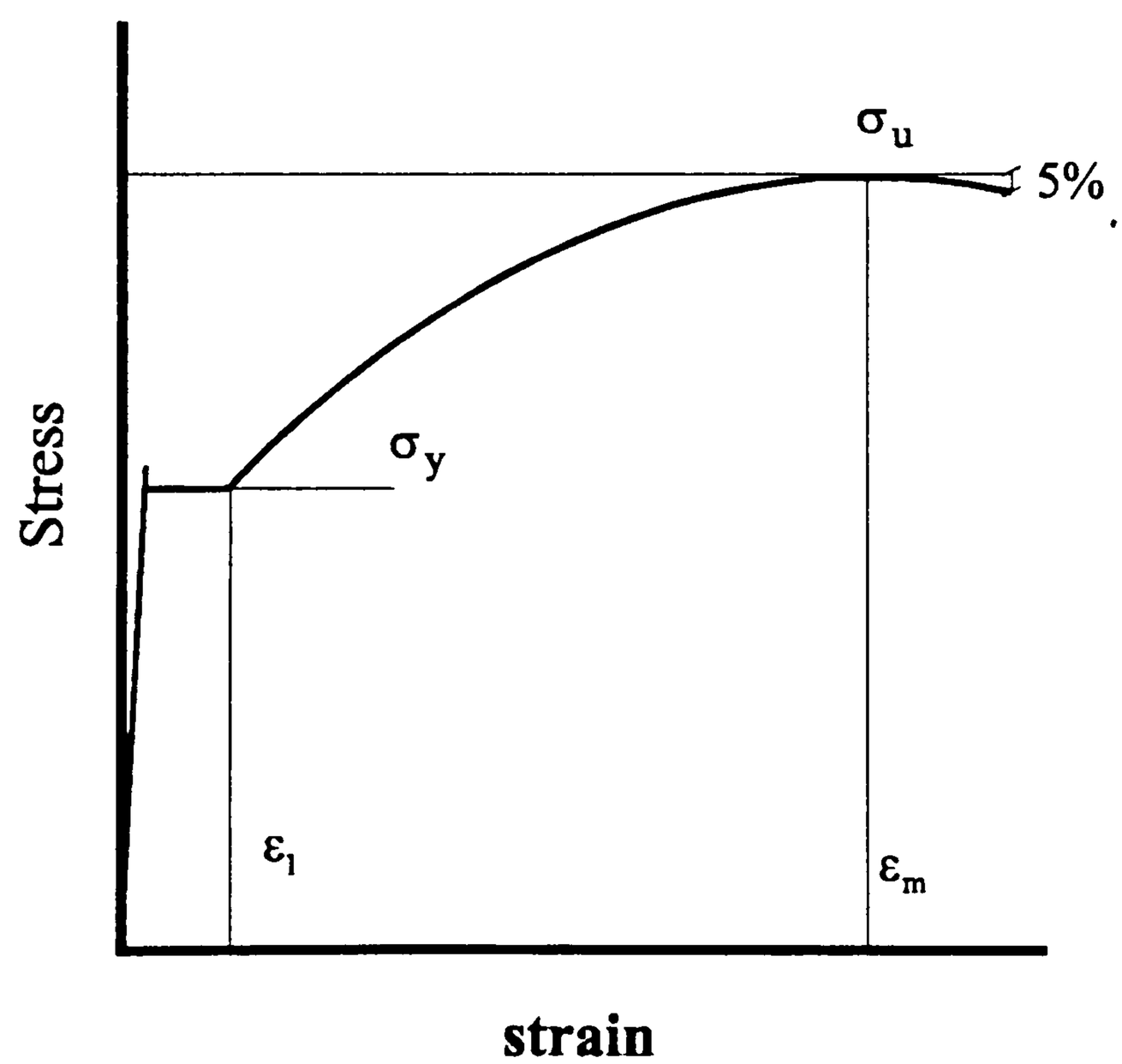

Figure 4.5 Typical stress-strain relationship

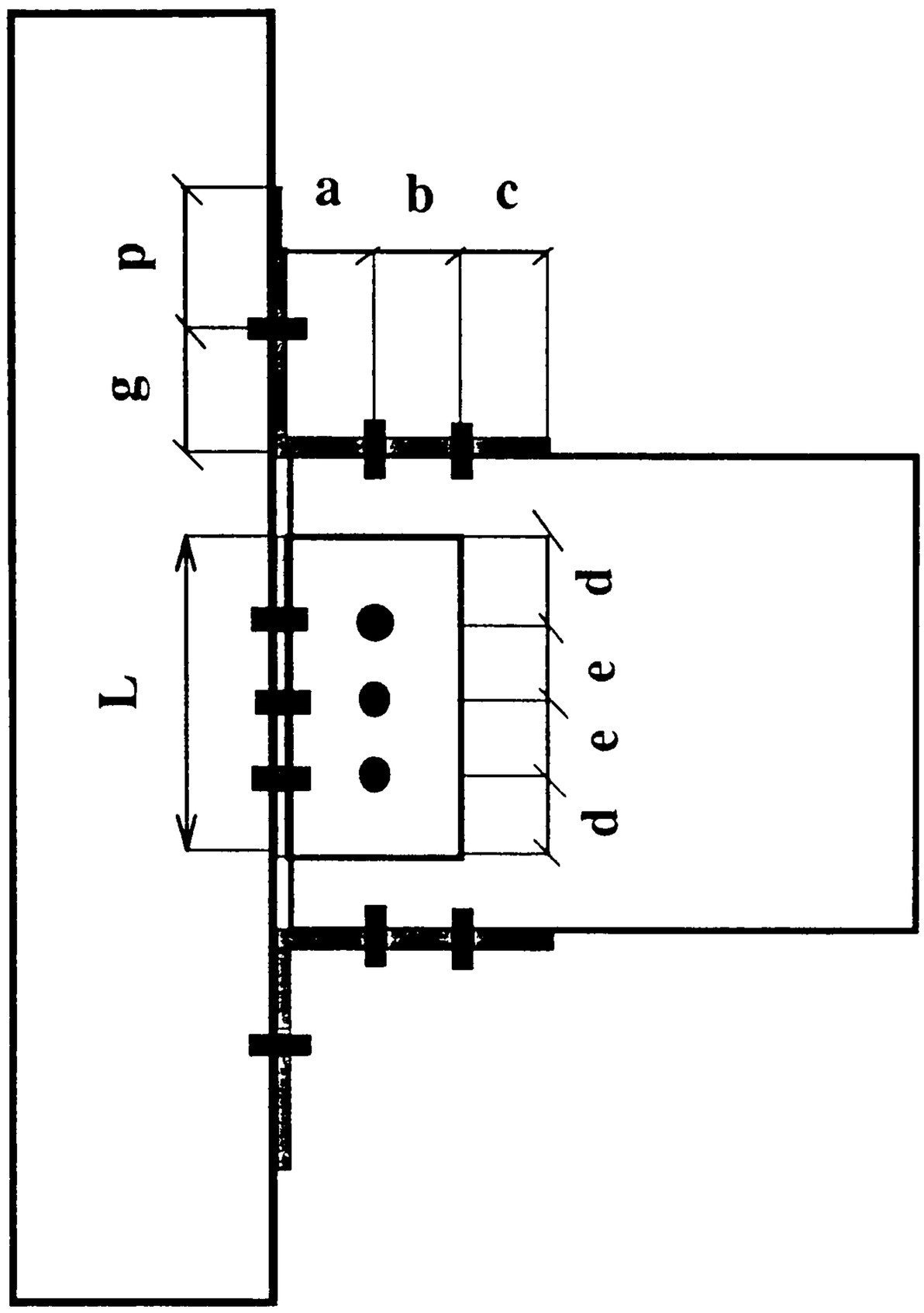

Model reference	a (mm)	b (mm)	c (mm)	d (mm)	e (mm)	p (mm)	g (mm)	L (mm)
CS1	37	-	35	35	55	35	45	180
CS2	41	60	37	35	55	37	53	180
CS3	38	60	37	40	50	37	53	180
DS1	38	60	37	35	55	37	53	180

Figure 4.6 Characteristics of connections for semi-rigid frames

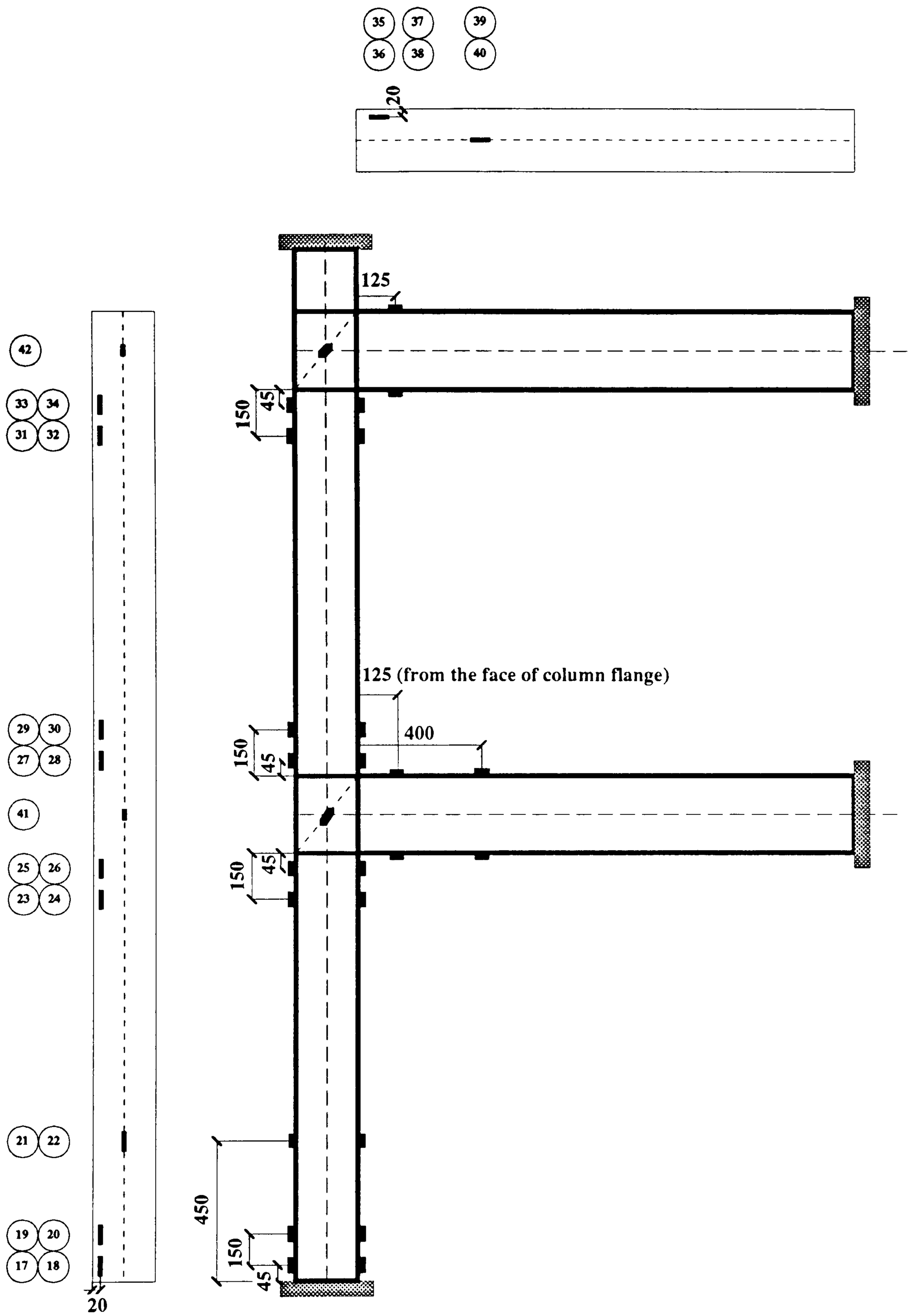

Figure 4.7 Strain gauge layout for specimen CR1

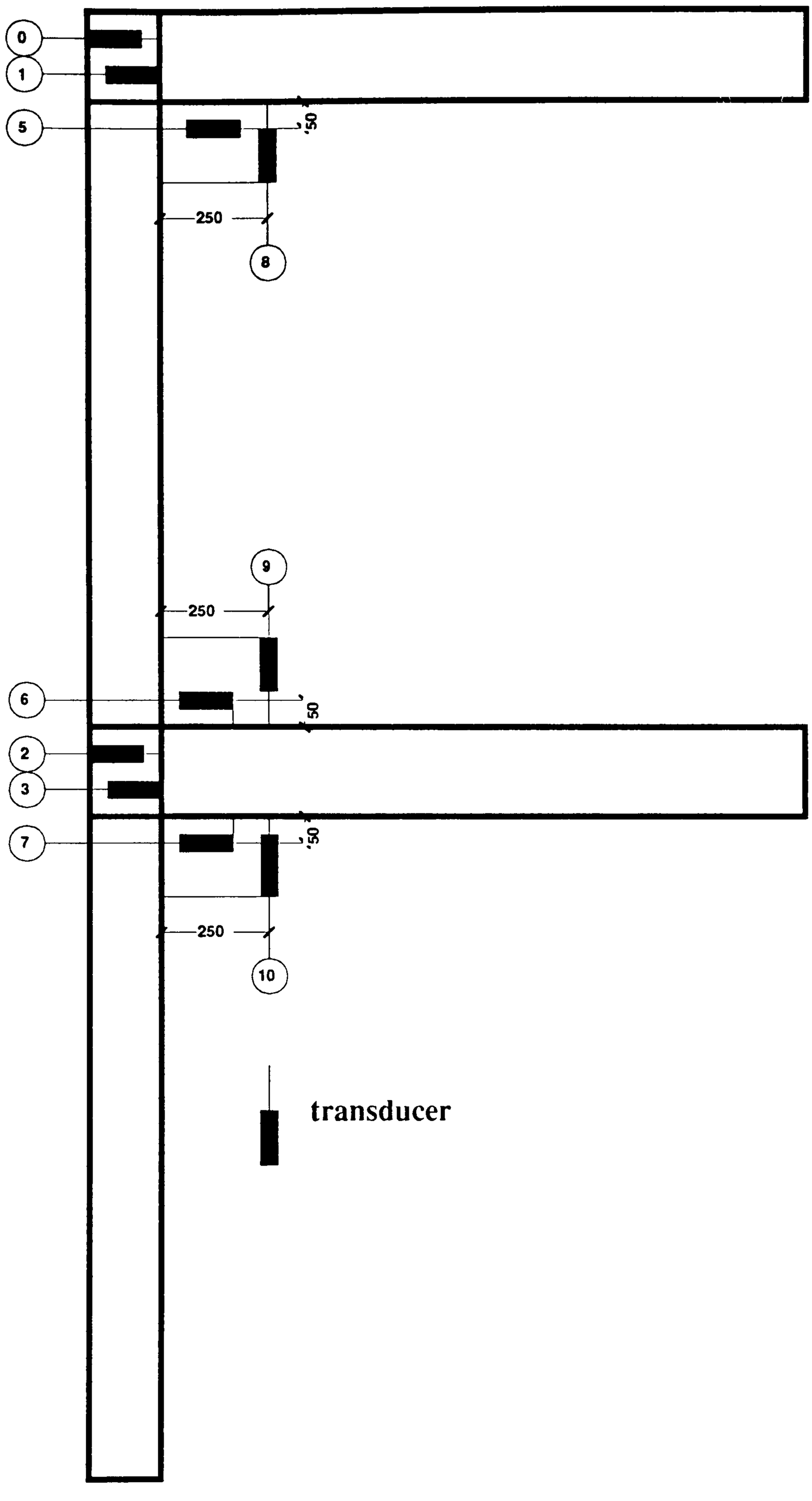

Figure 4.8 Transducer layout for model CR1

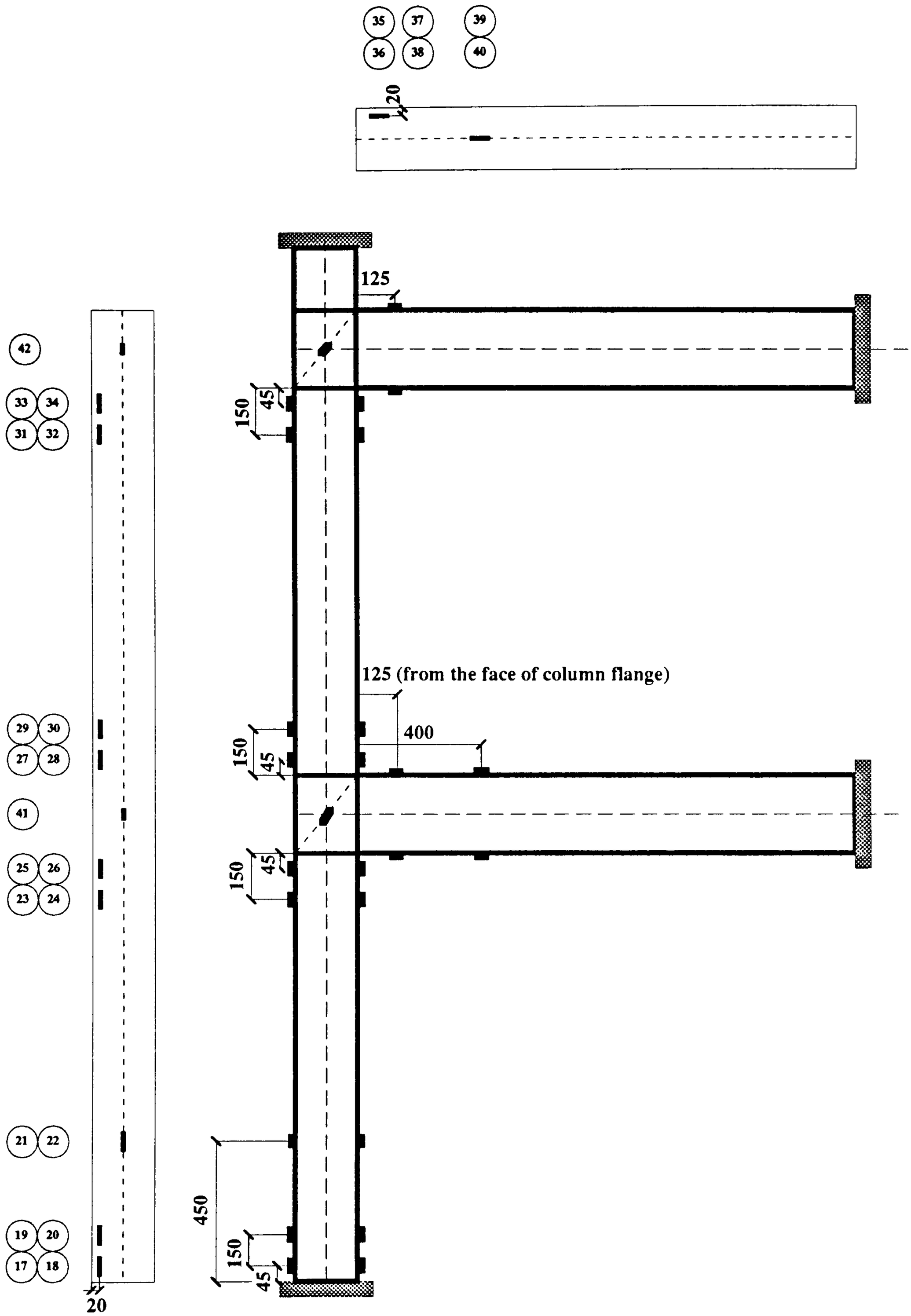

Figure 4.9 Strain gauge layout for semi-rigid models

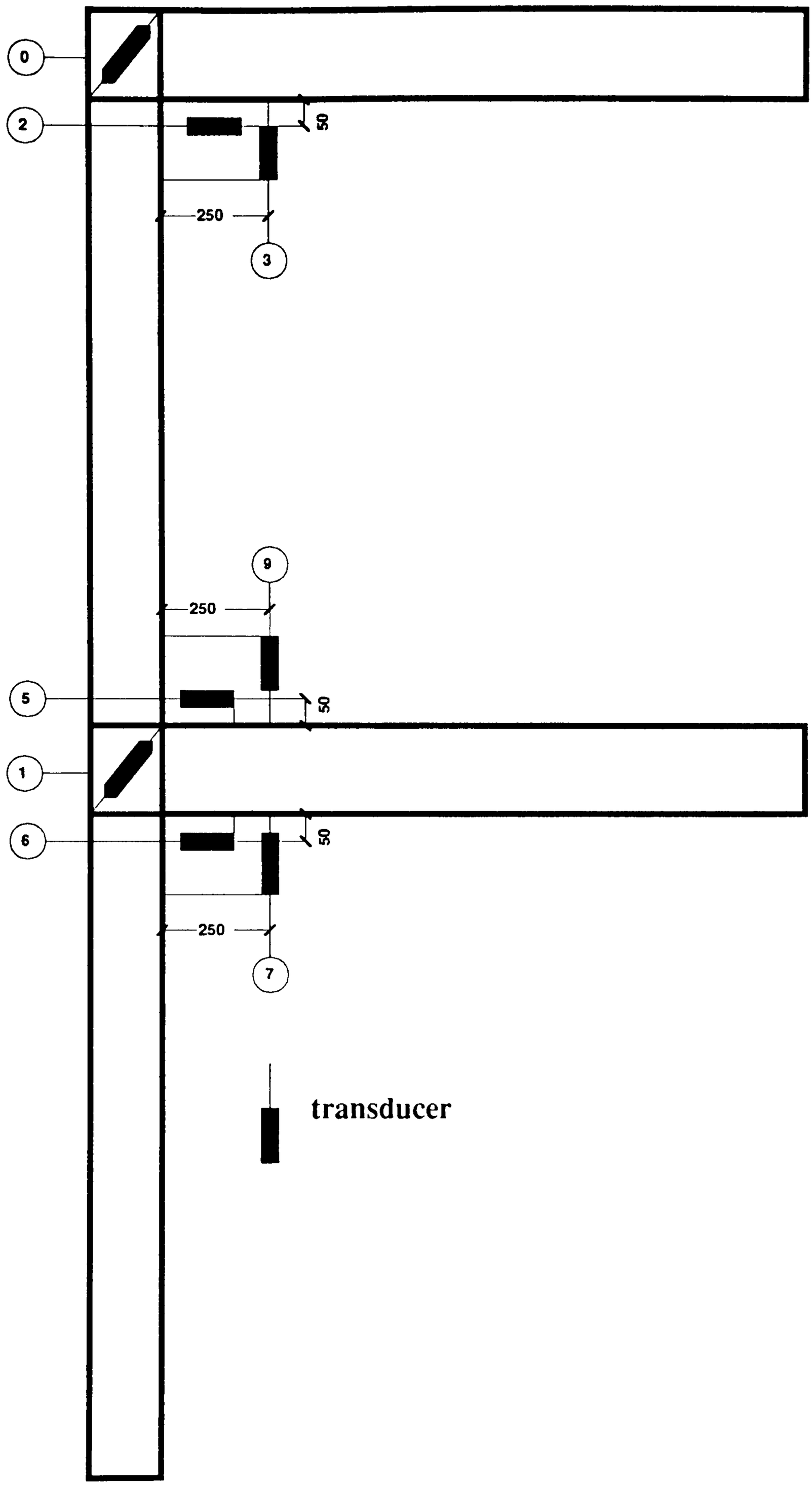

Figure 4.10 Transducer location for semi-rigid models

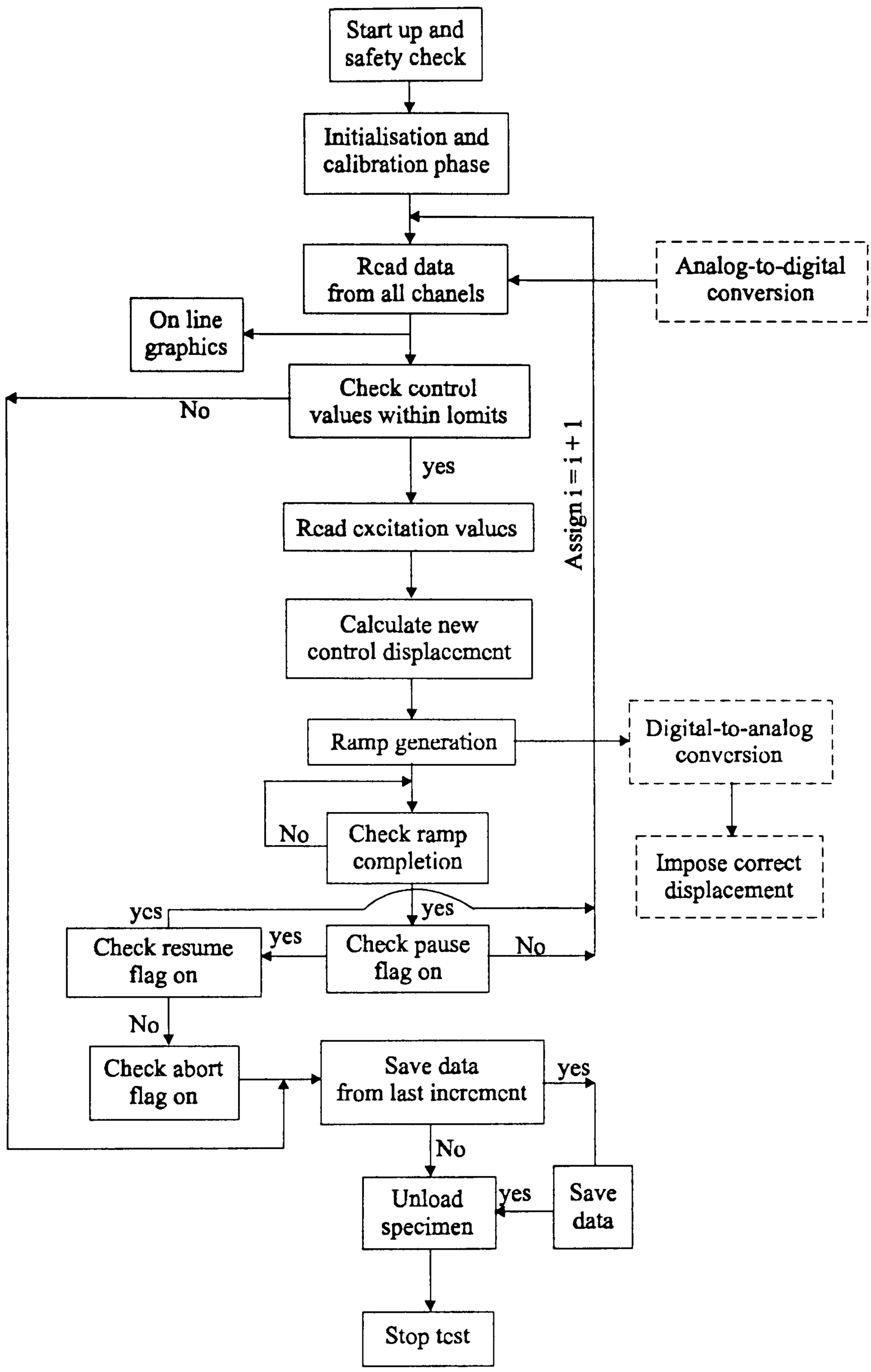

Figure 4.11 Software flow chart

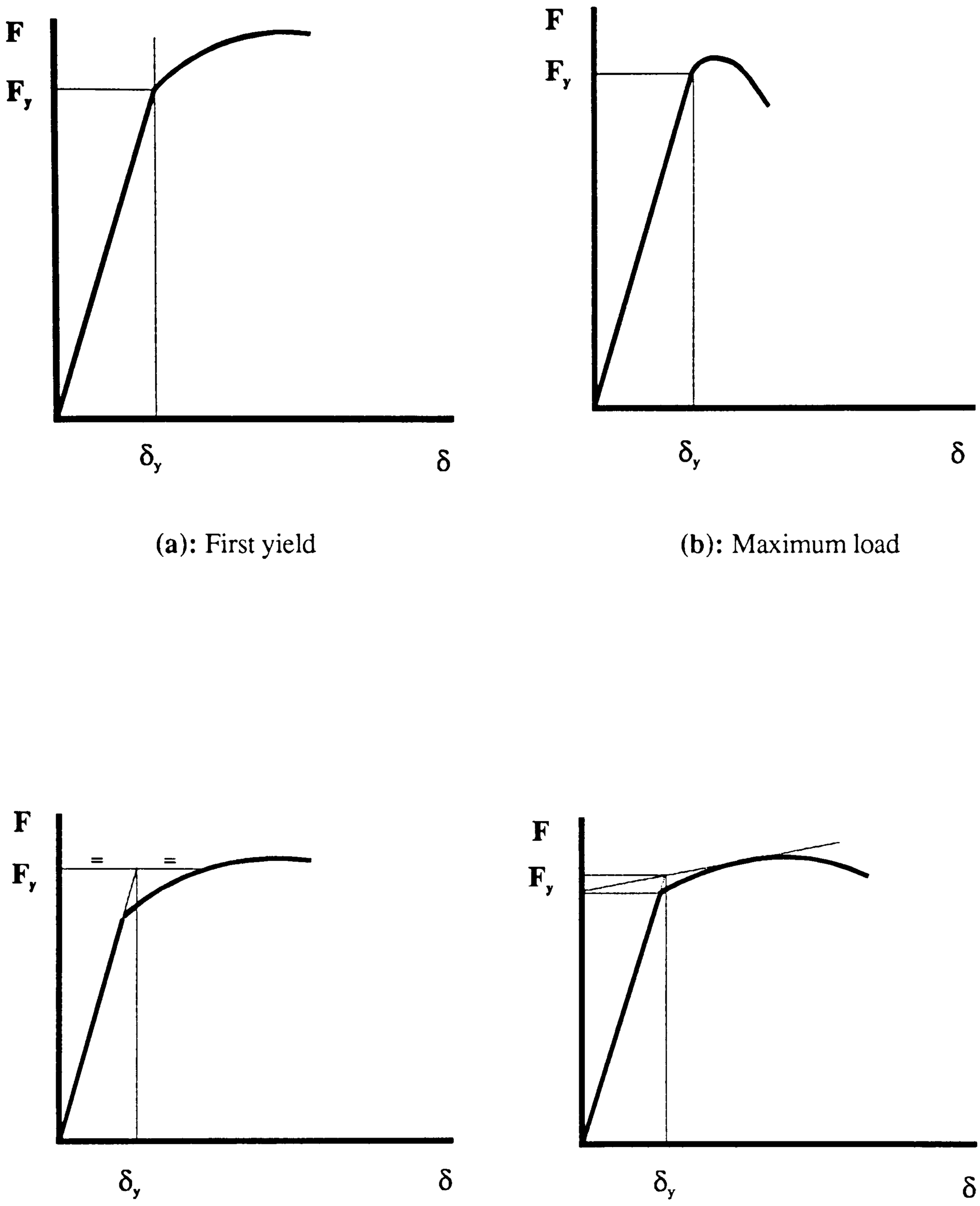

Figure 4.12 Definition of yield point

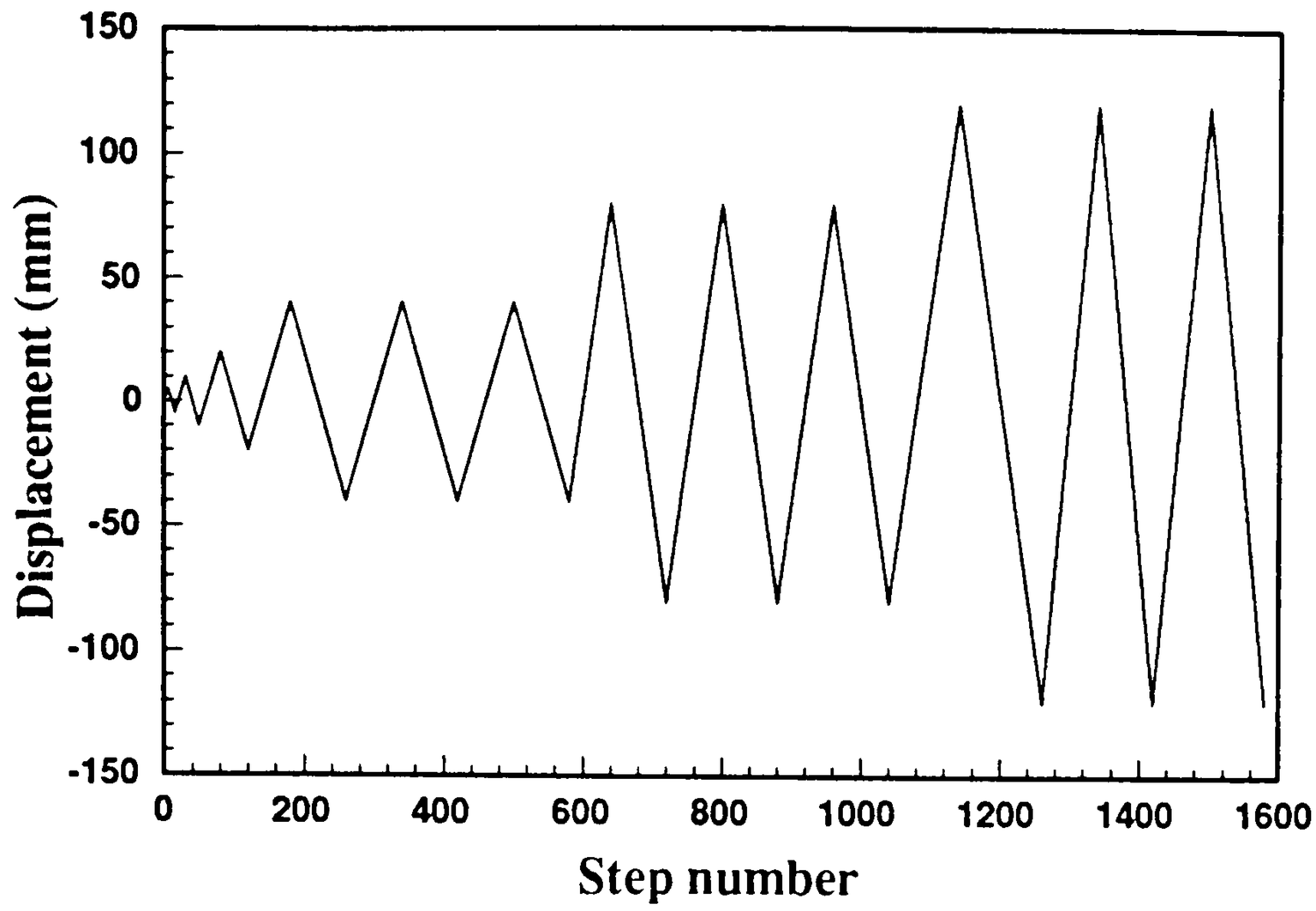

Figure 4.13 Loading history for model CR1

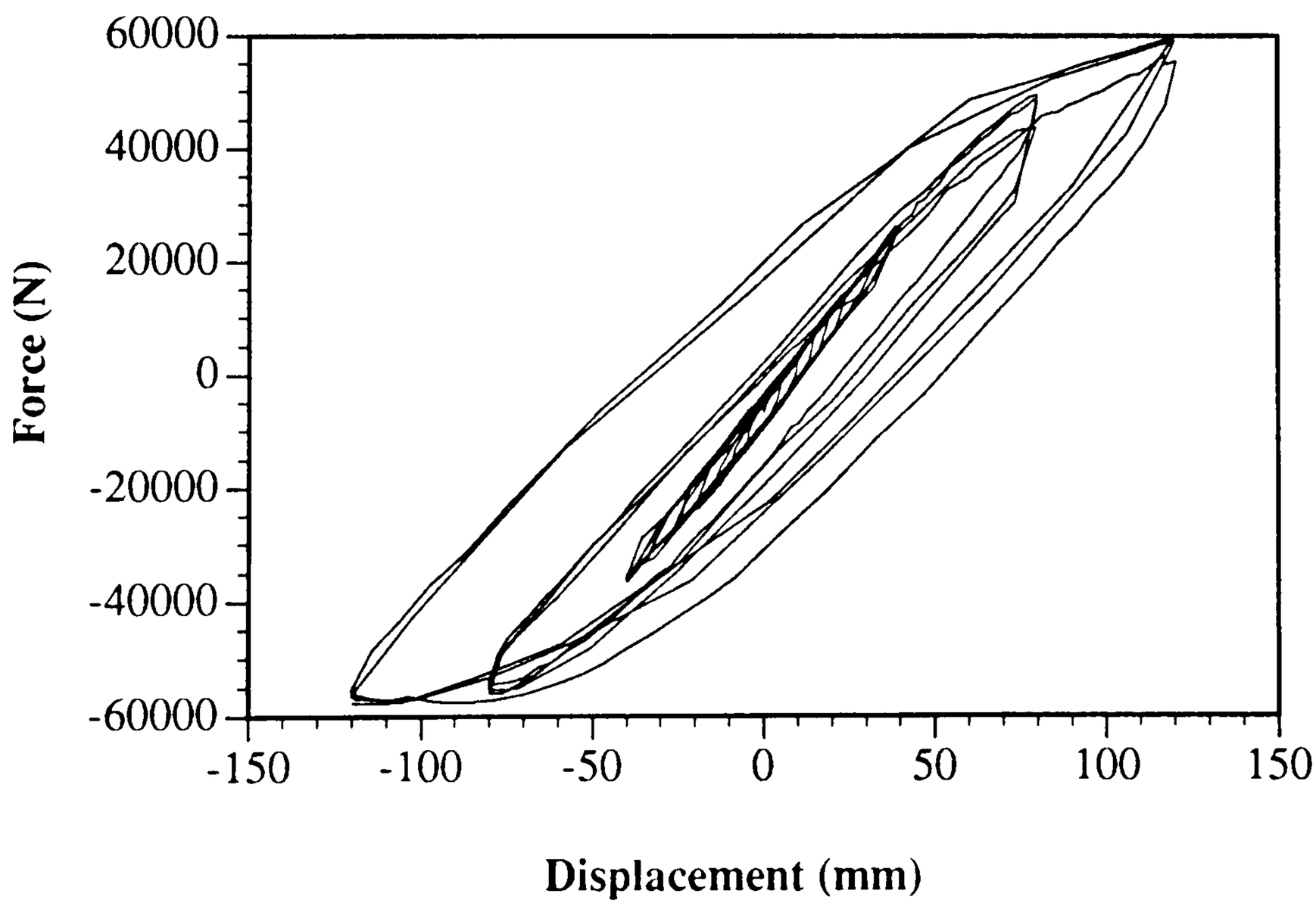

Figure 4.14 Experimental force-displacement relationship at the second floor of rigid frame (model CR1)

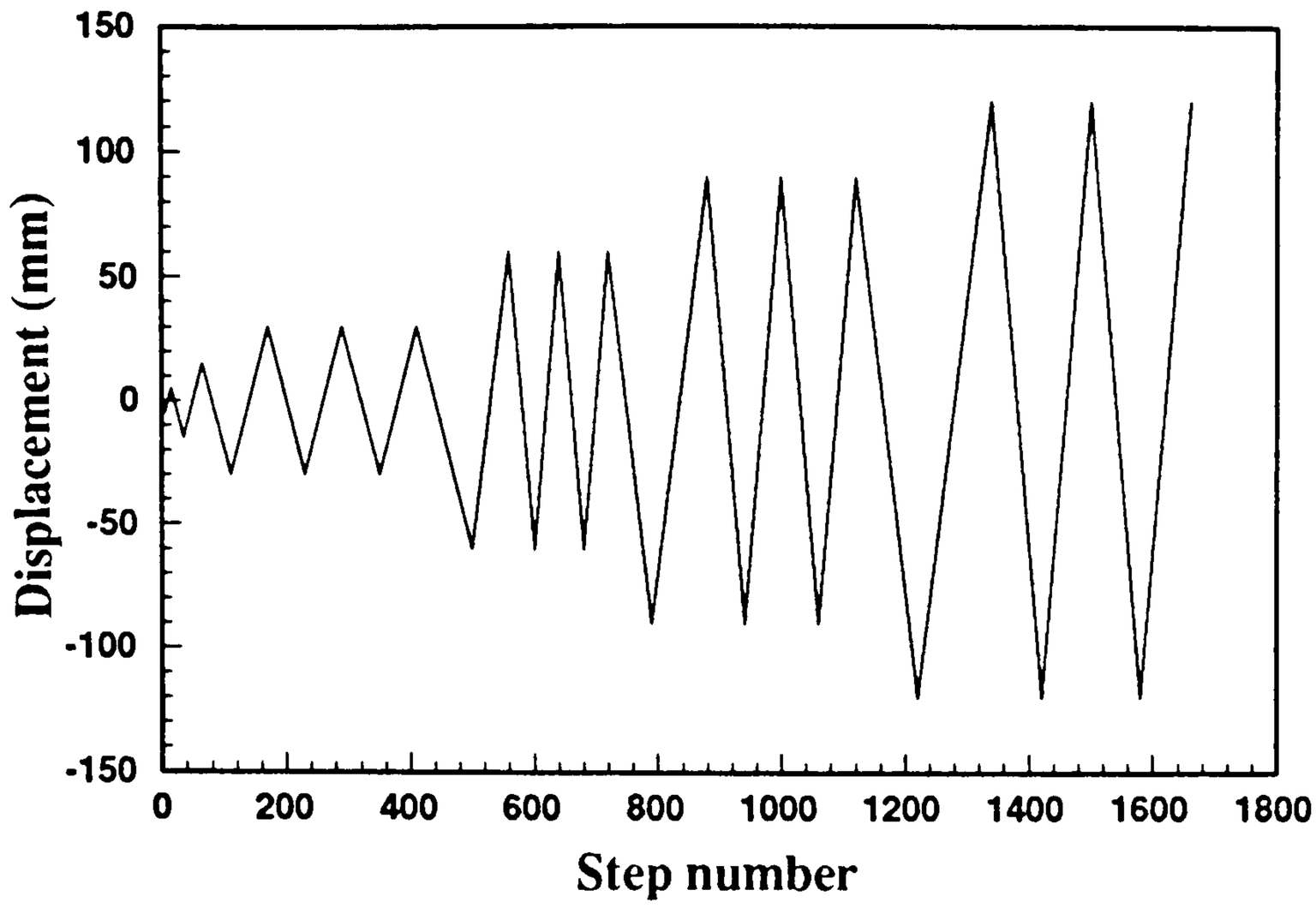

Figure 4.15 Loading history of model CS1

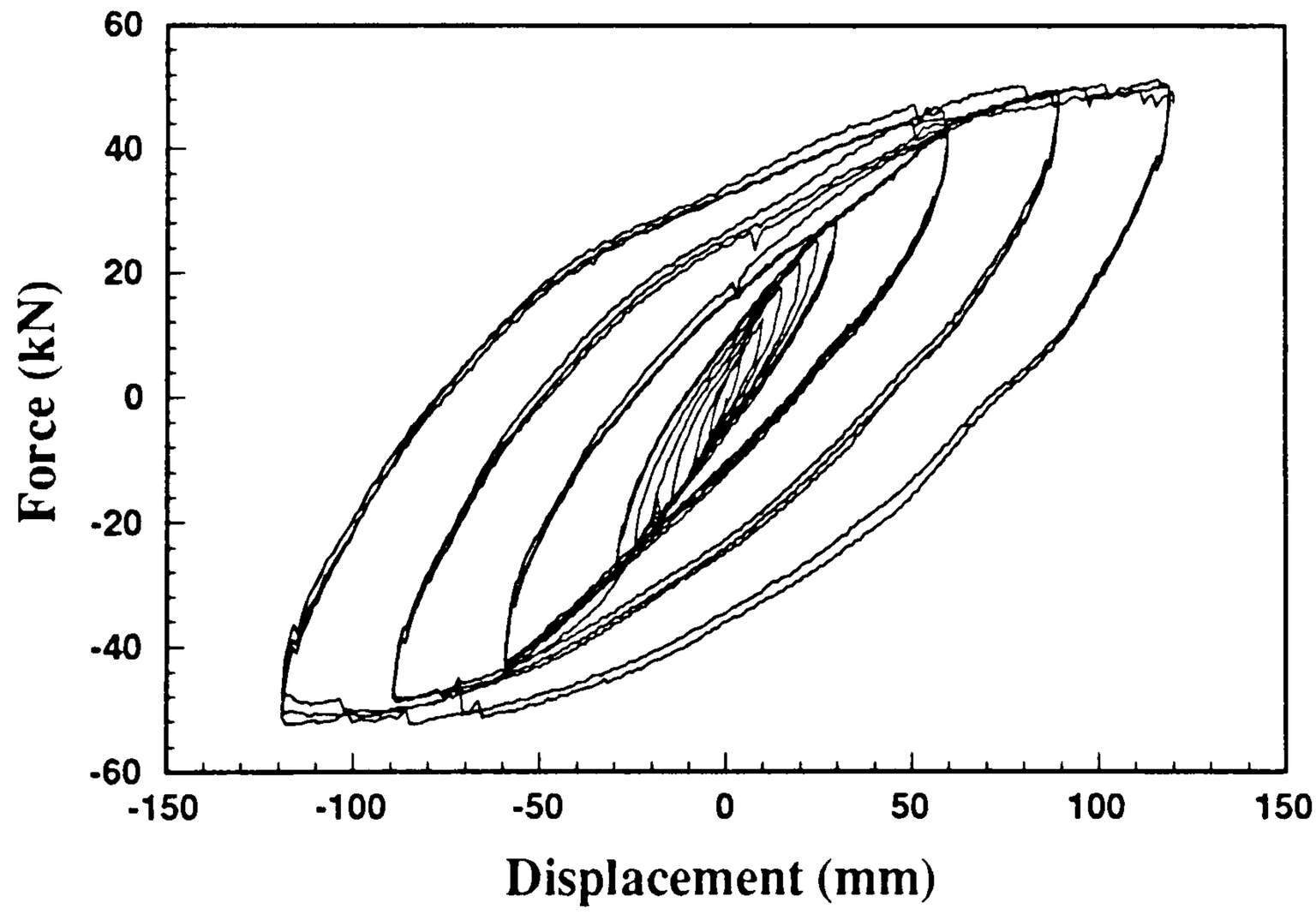

Figure 4.16 Experimental force-displacement at the second floor of model CS1

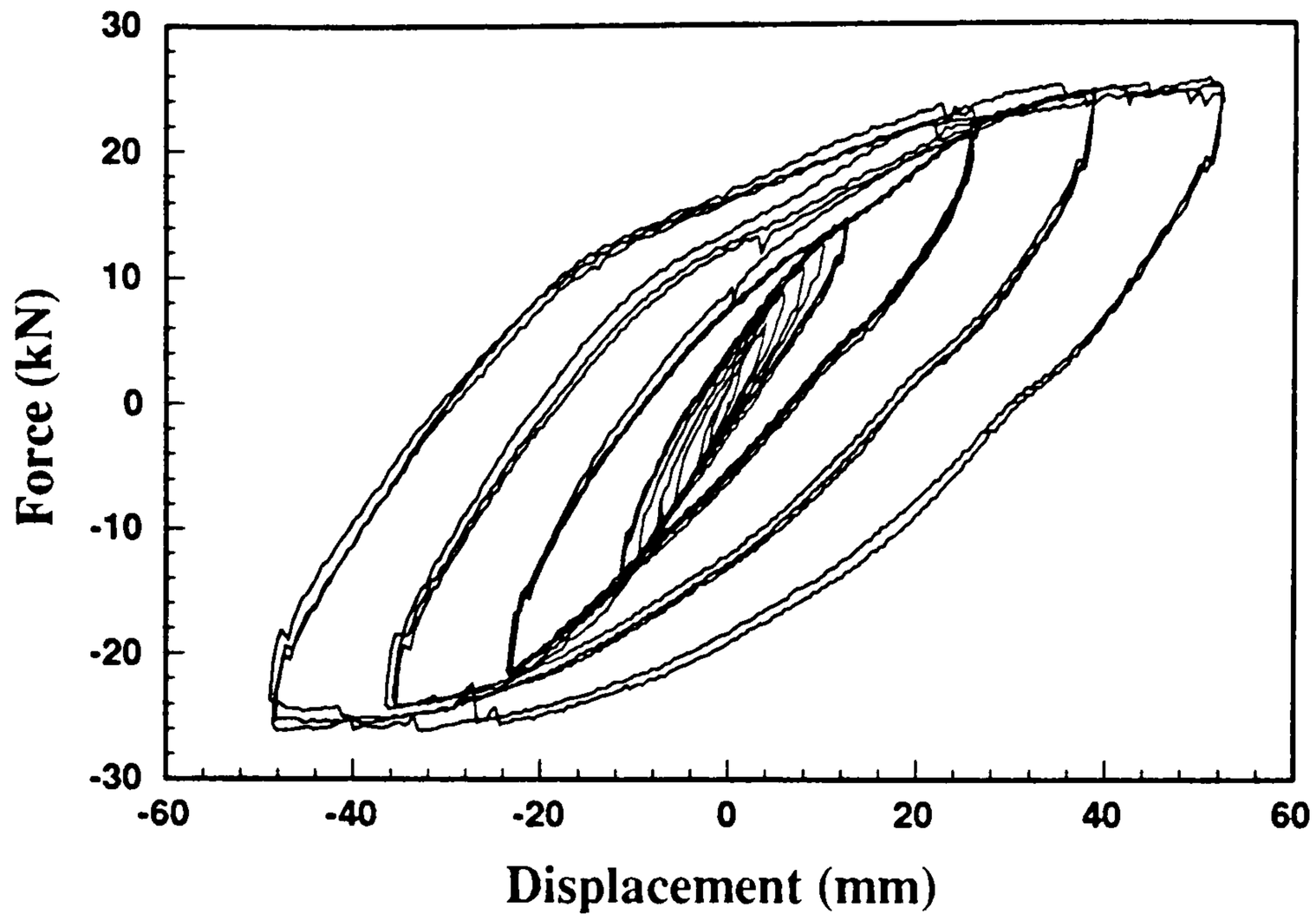

Figure 4.17 Experimental force-displacement at the first floor of model CS1

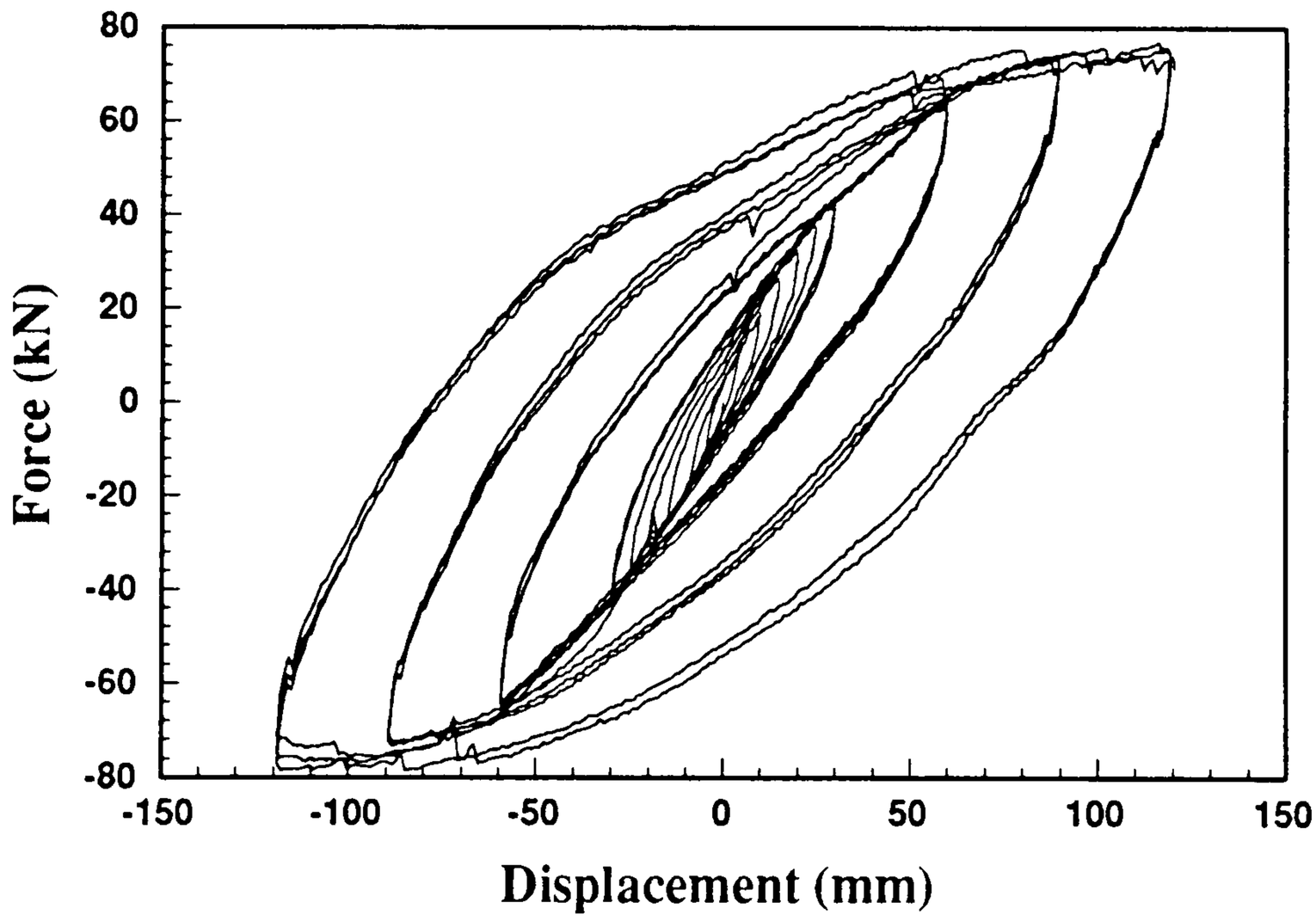

Figure 4.18 Experimental base shear versus top frame displacement (model CS1)

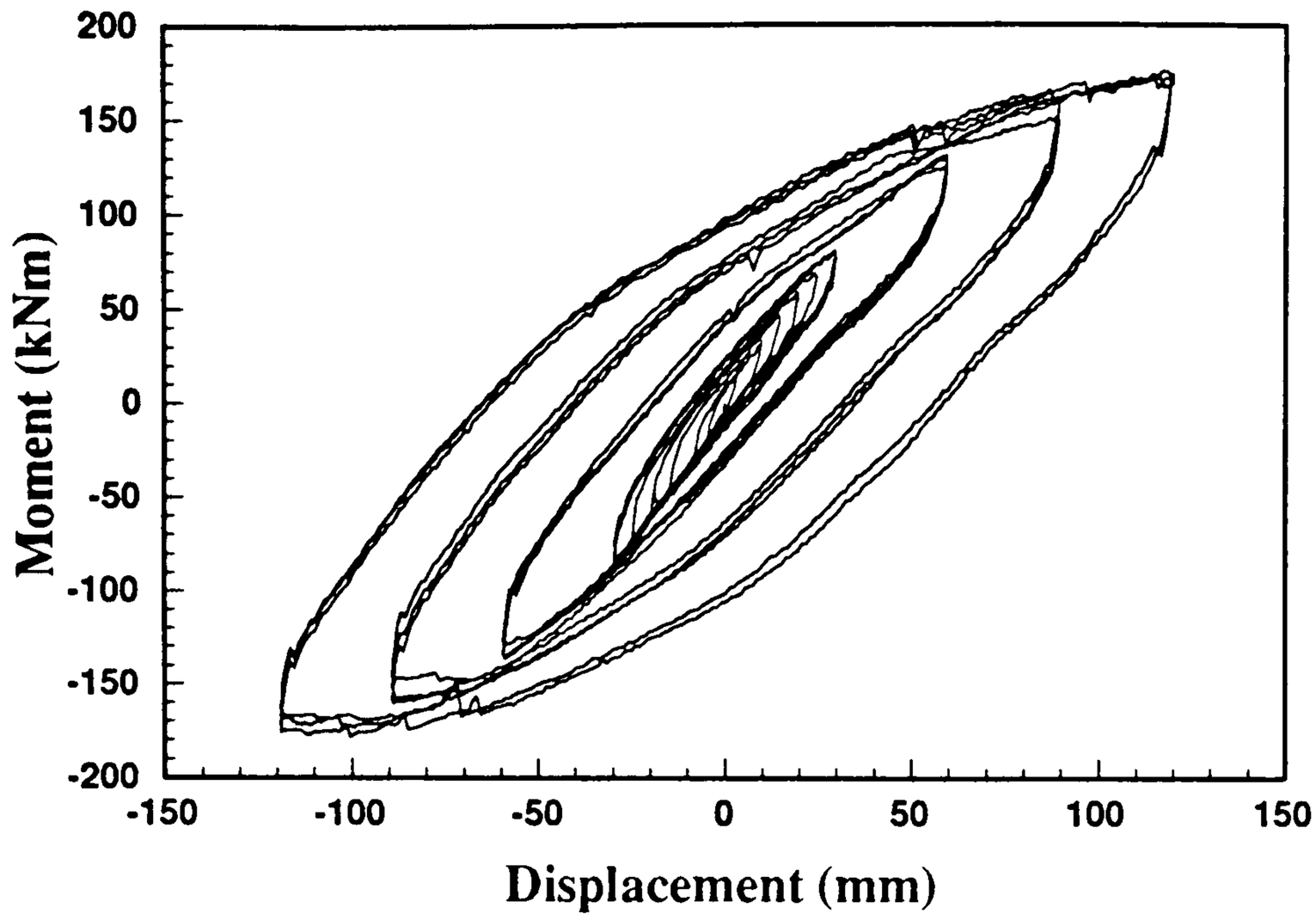

Figure 4.19 Experimental moment at the base of the column versus top frame displacement of model CS1

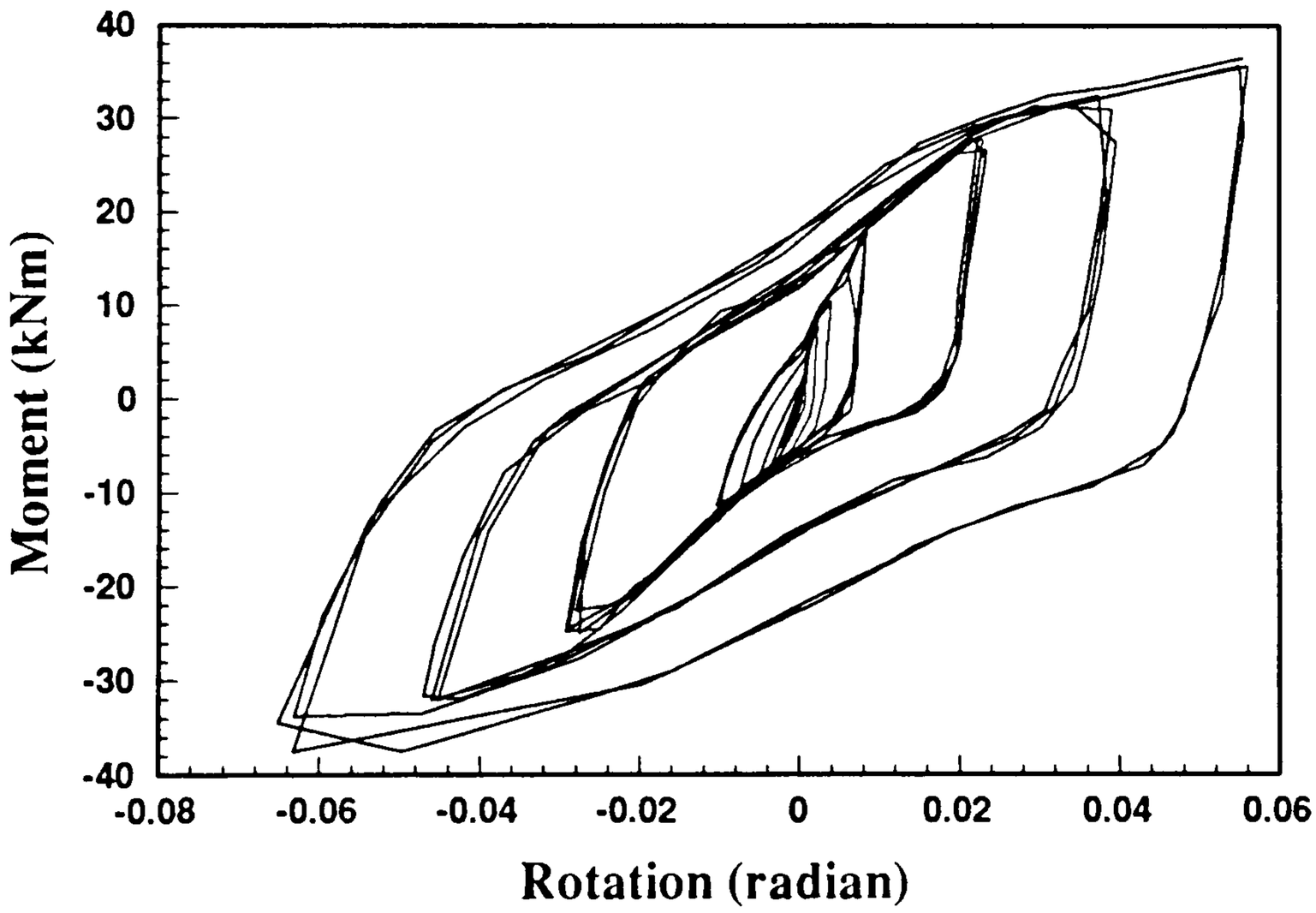

Figure 4.20 Experimental moment-rotation relationship of connection in the first floor for model CS1

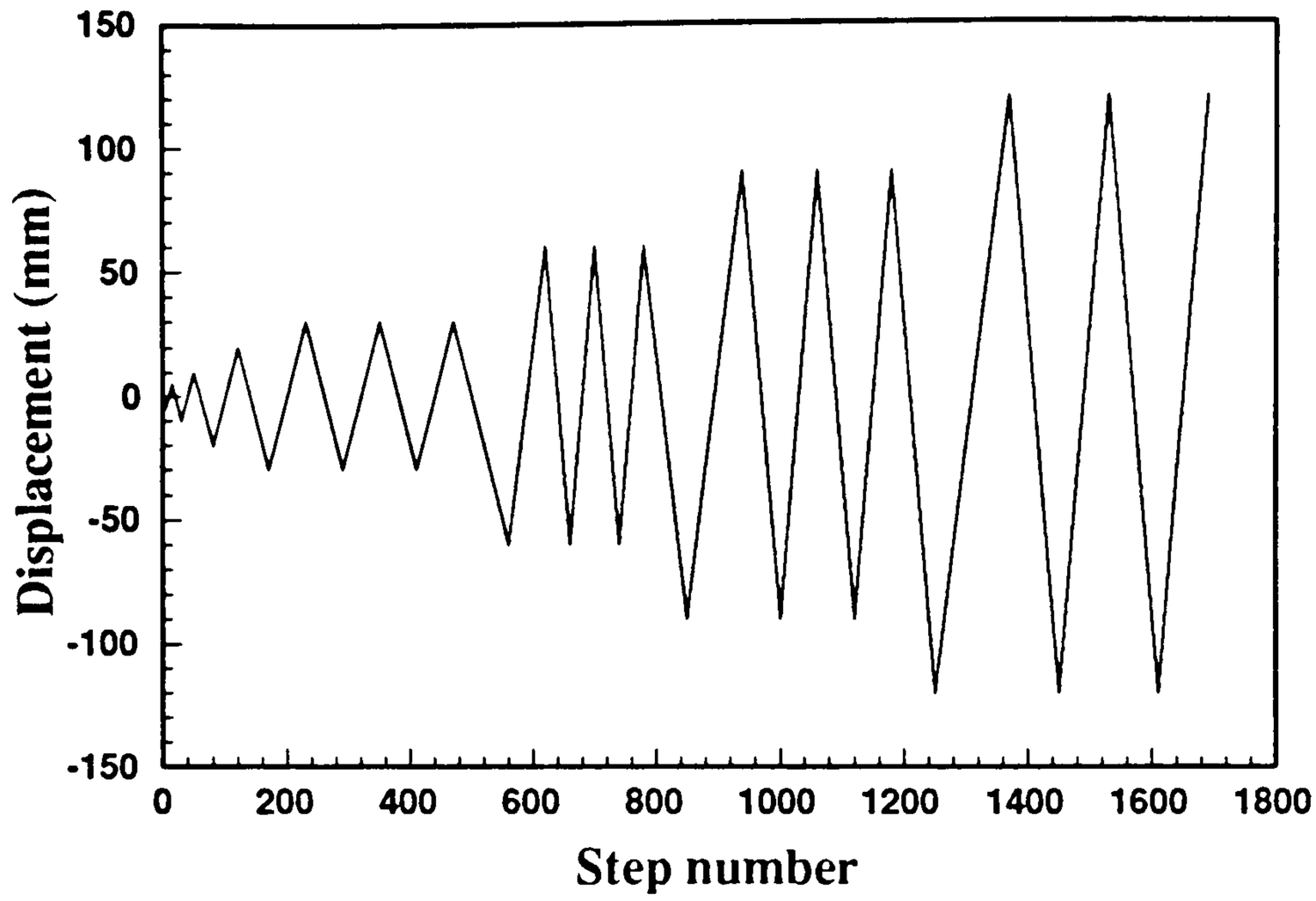

Figure 4.21 Loading history for model CS2

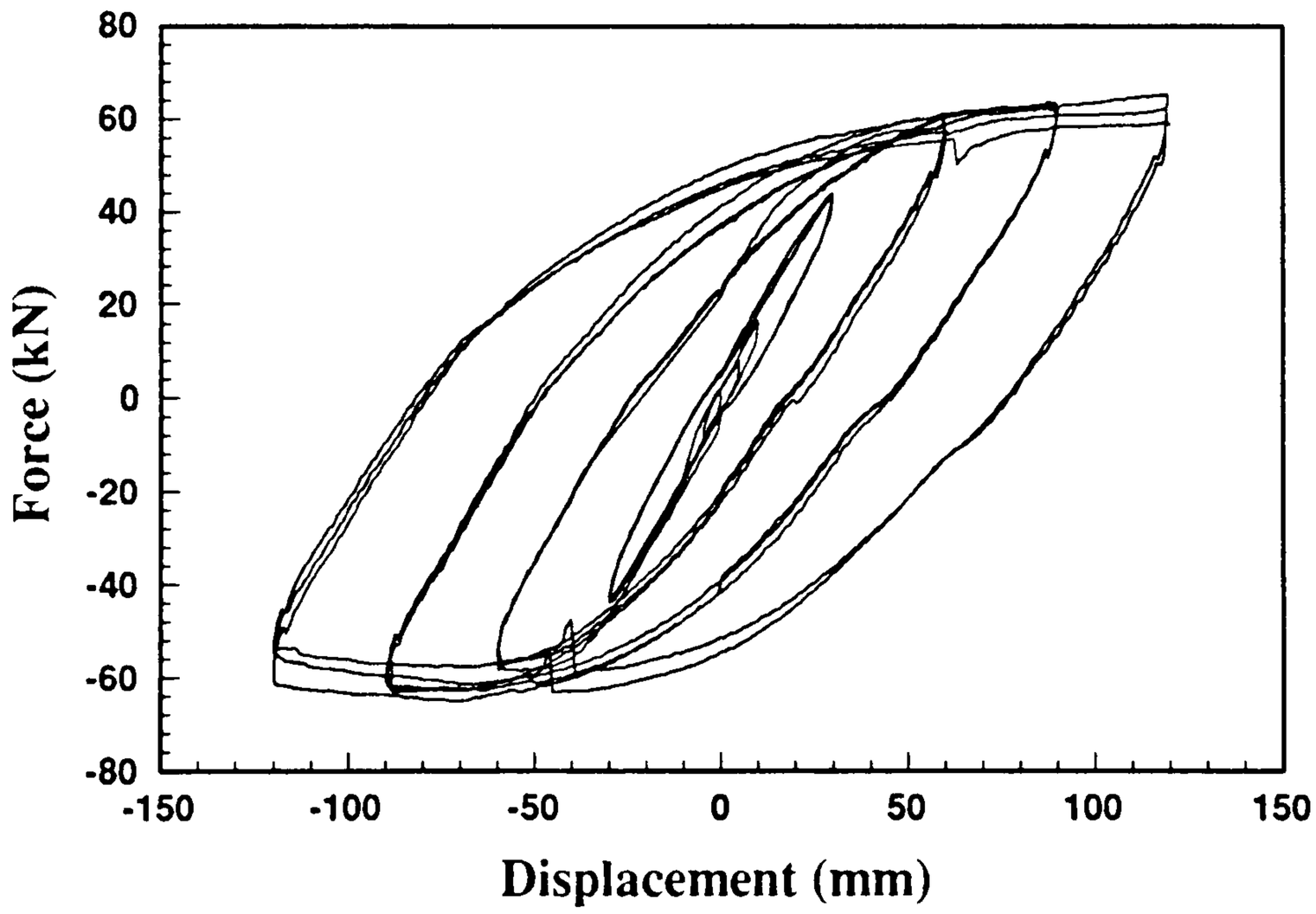

Figure 4.22 Experimental force-displacement at the second floor for model CS2

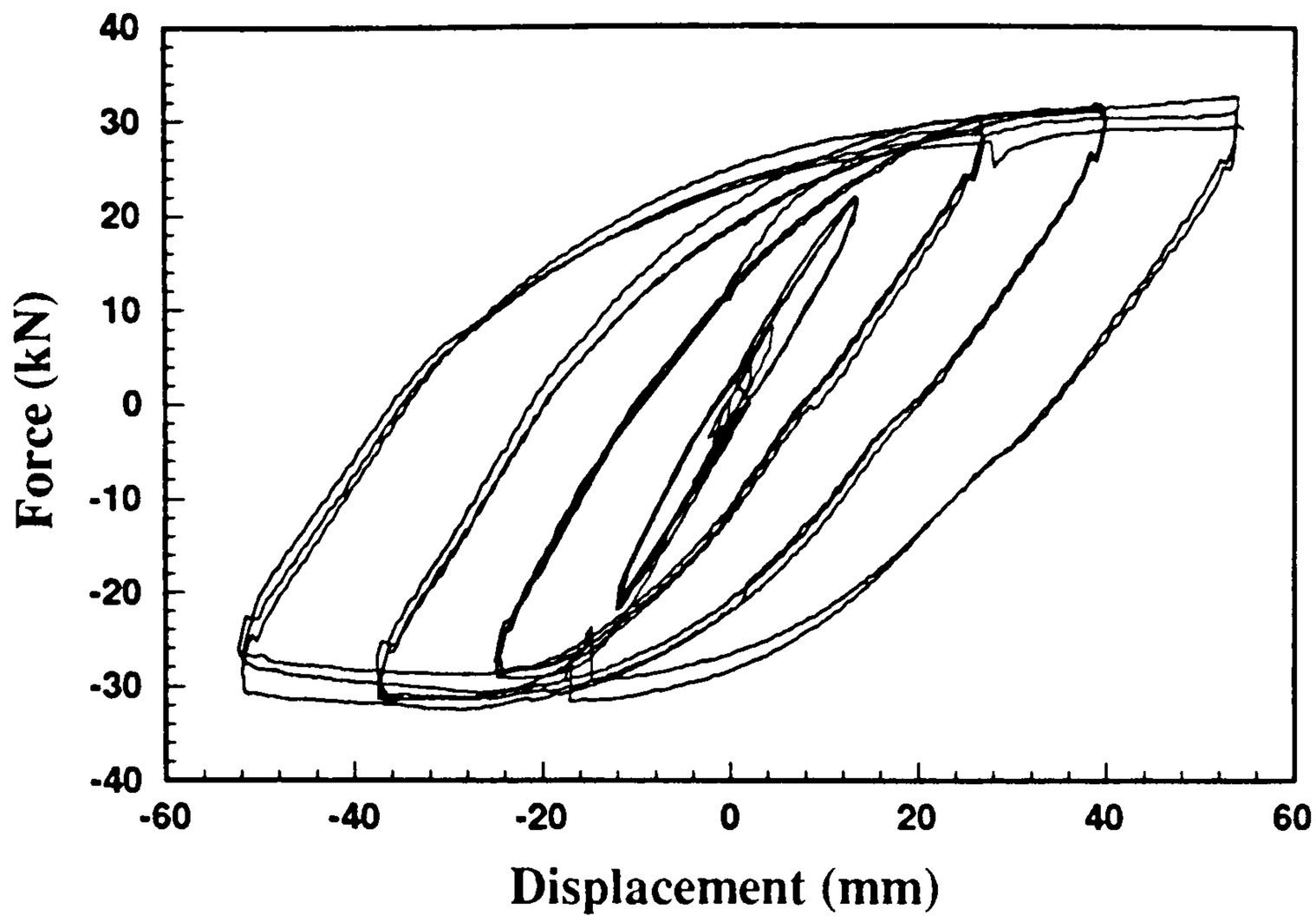

Figure 4.23 Experimental force-displacement at the first floor (model CS2)

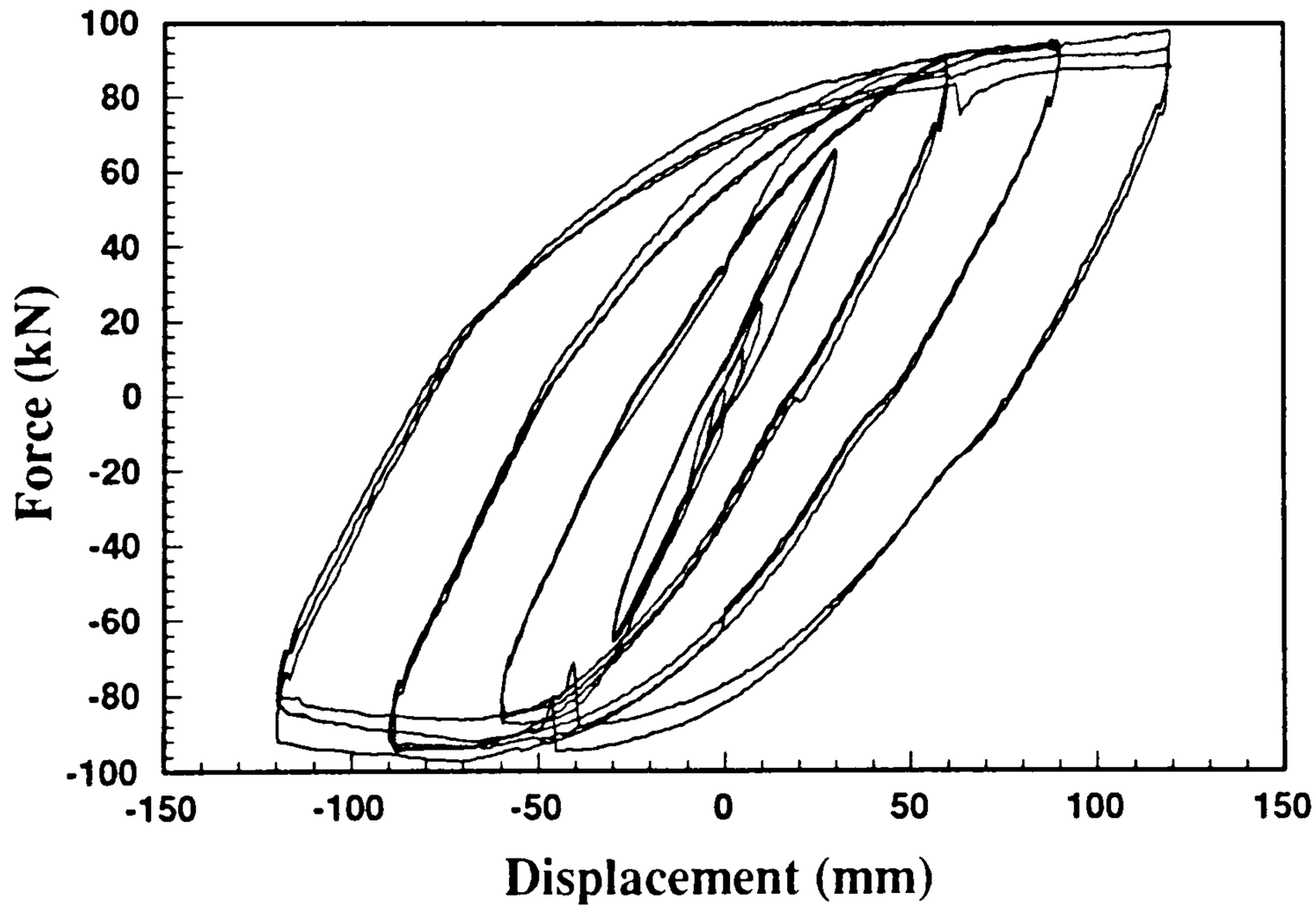

Figure 4.24 Experimental base shear versus top frame displacement (model CS2)

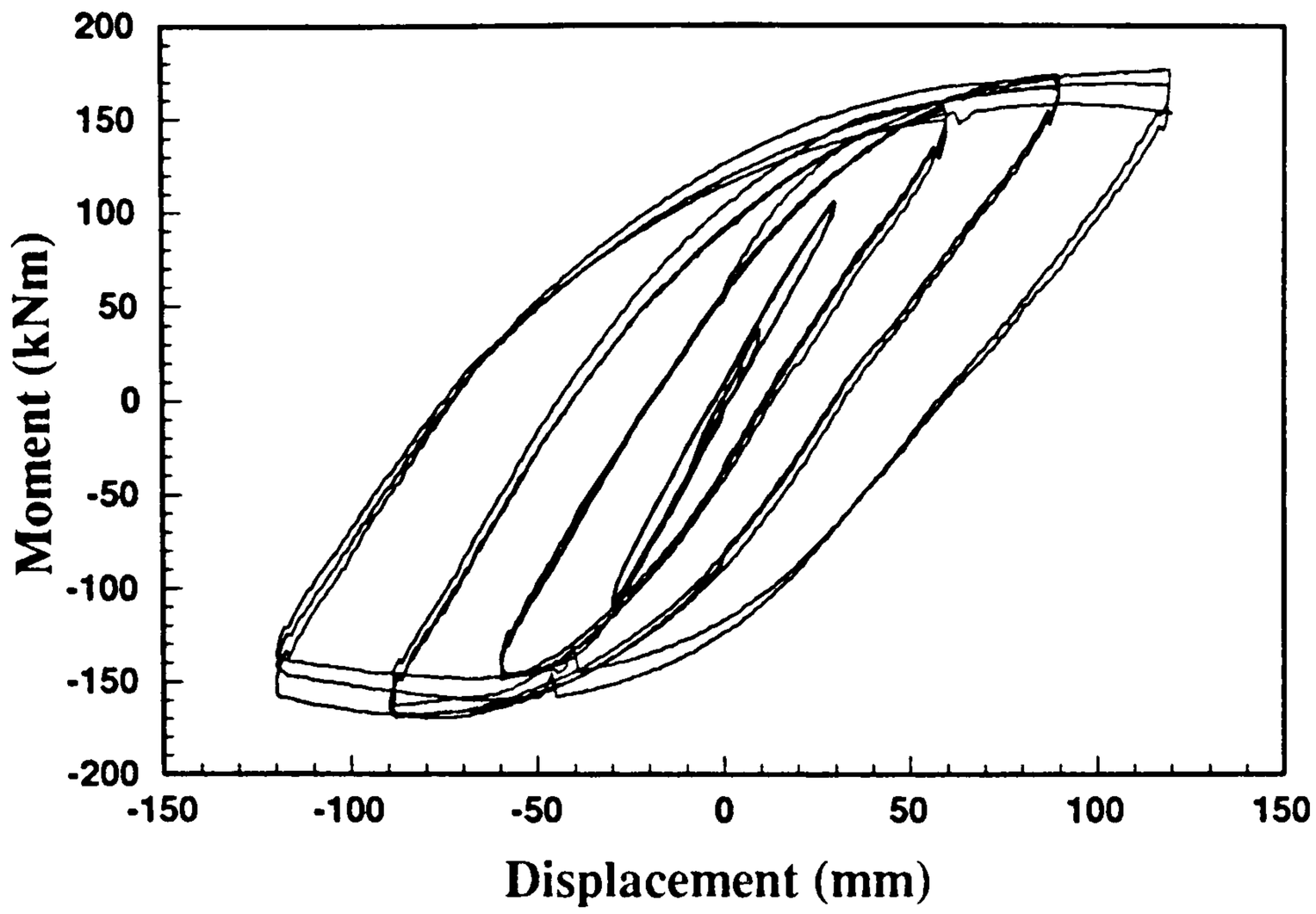

Figure 4.25 Experimental moment at the base of the column versus top frame displacement for model CS2

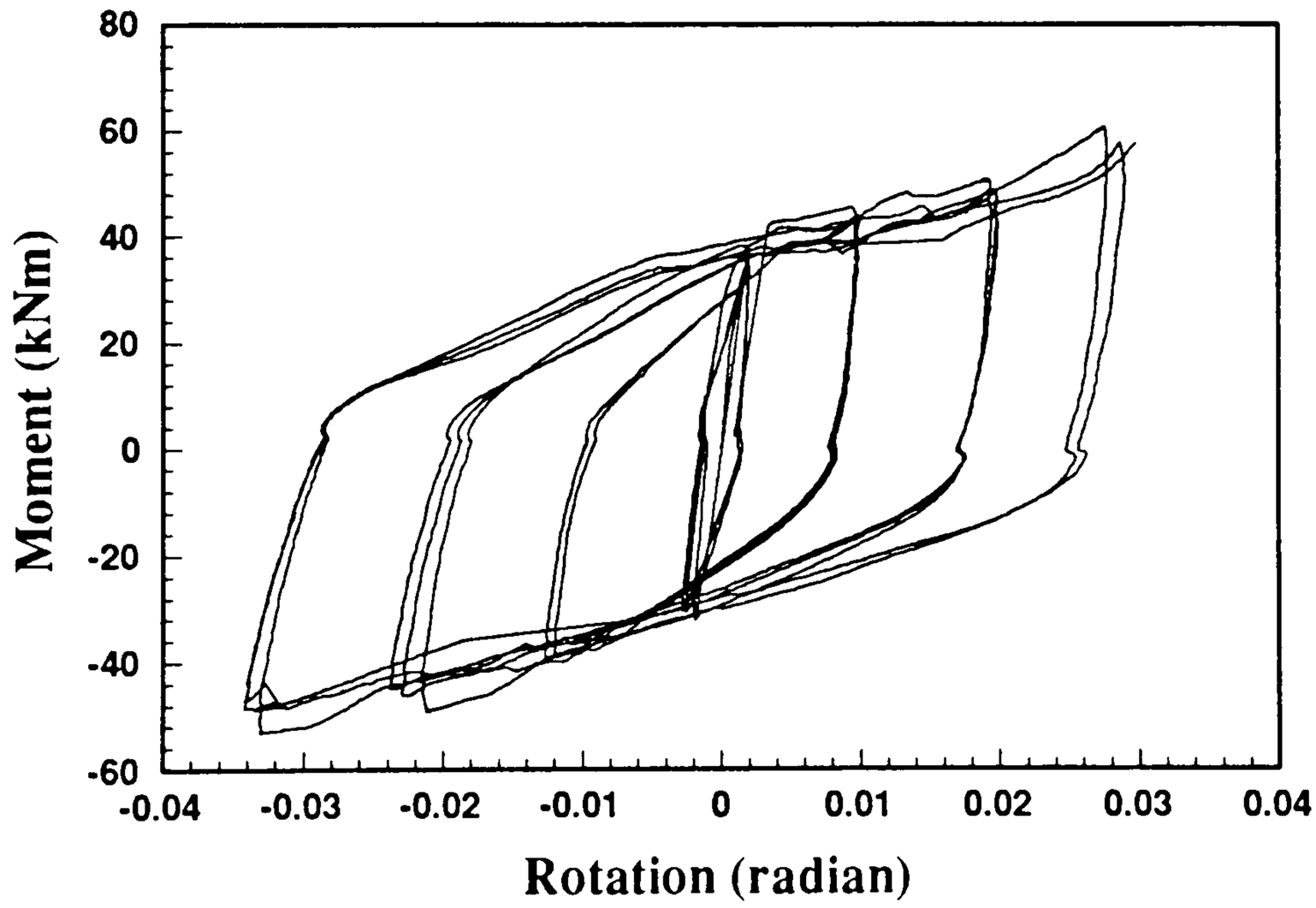

Figure 4.26 Experimental moment-rotation relationship of the connection in the first floor for model CS2

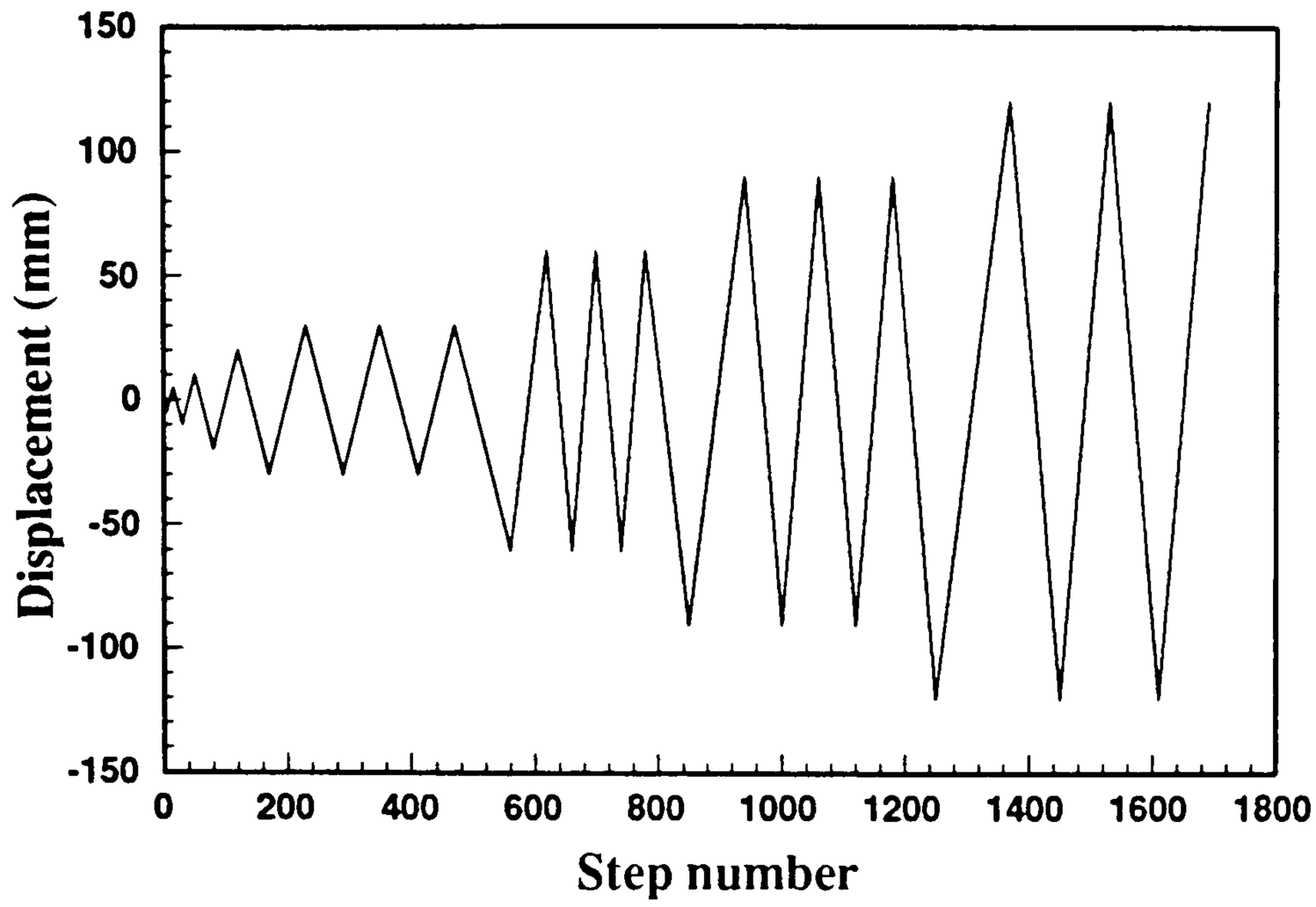

Figure 4.27 Loading history for model CS3

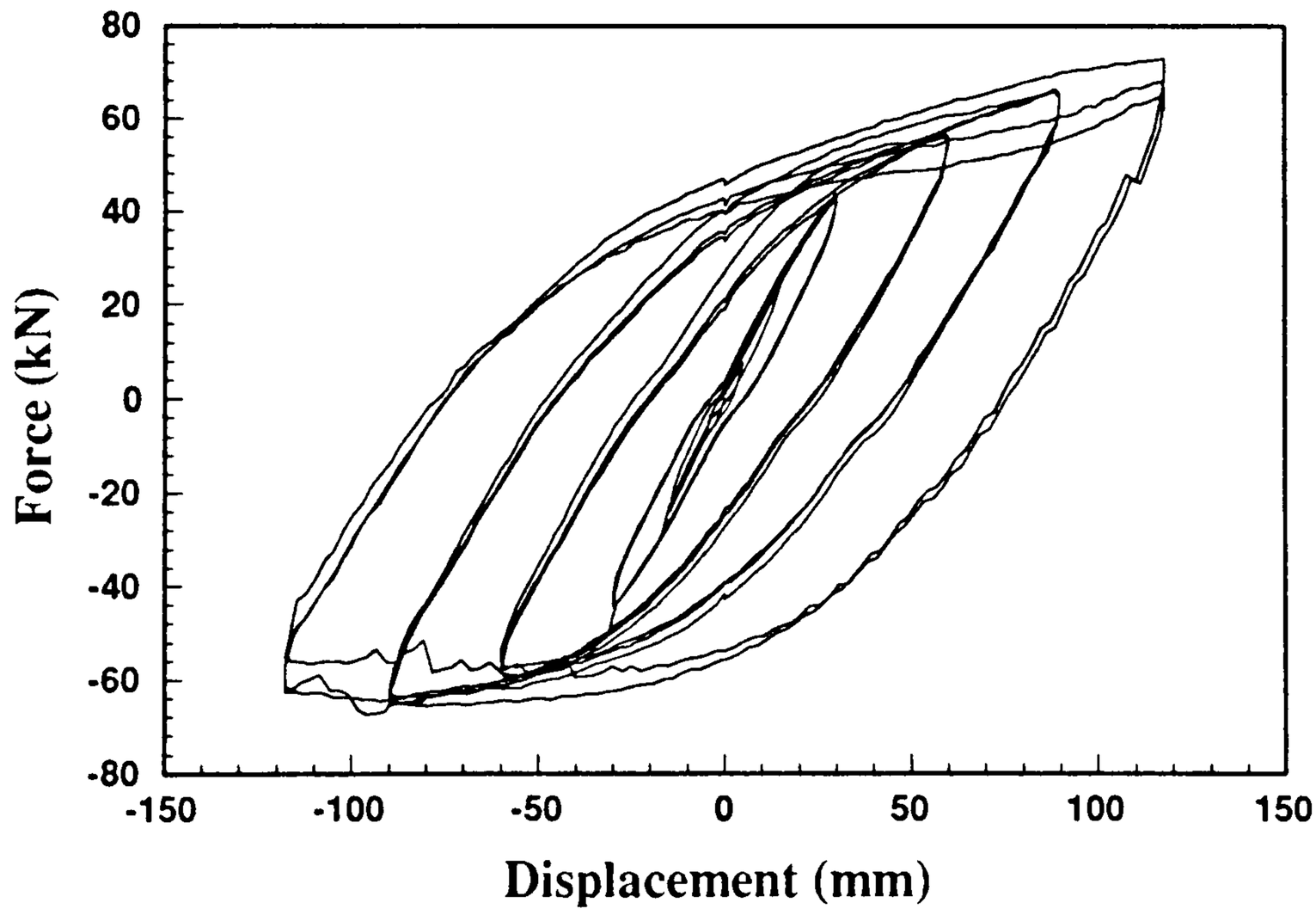

Figure 4.28 Experimental force-displacement at the second floor for model CS3

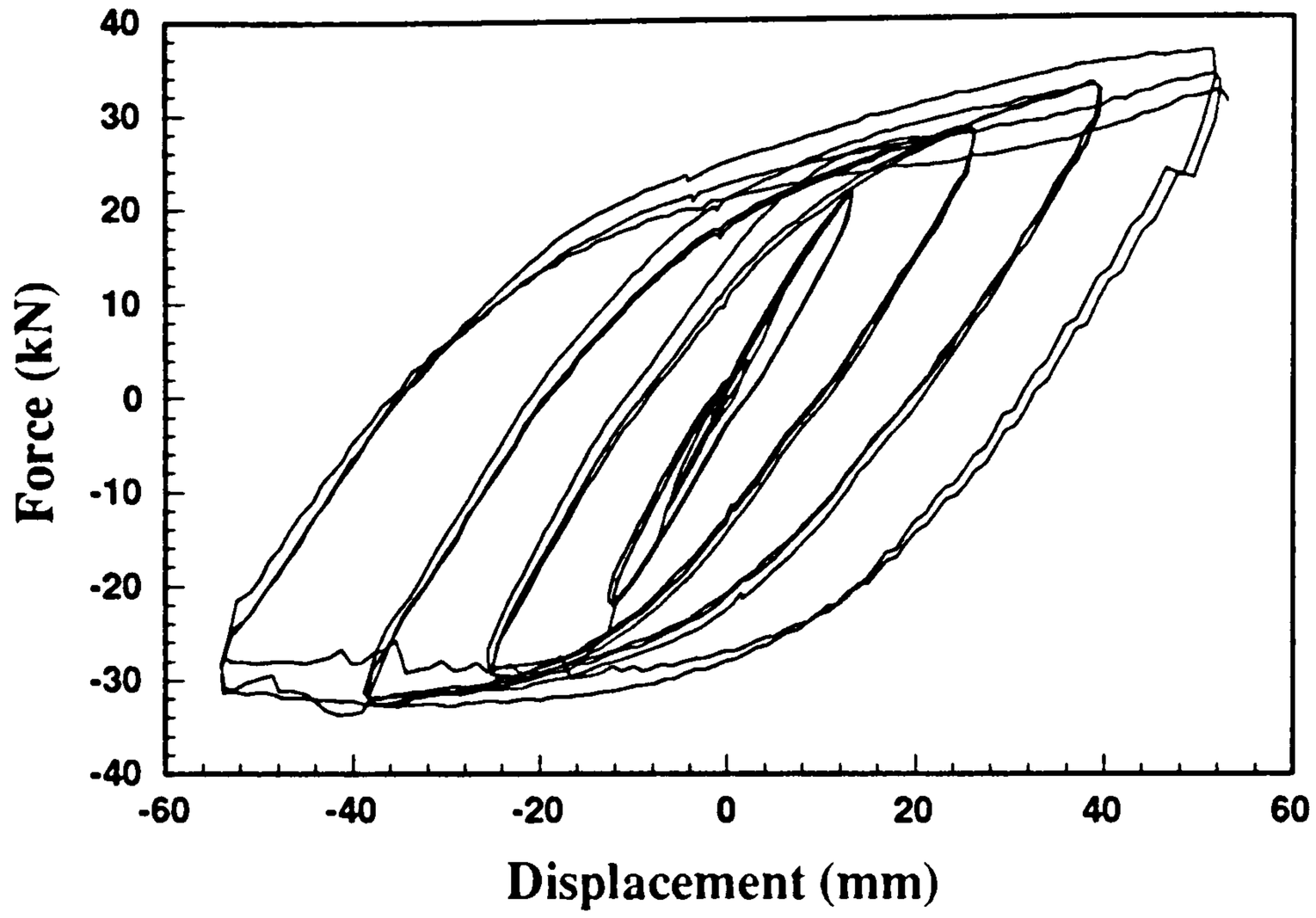

Figure 4.29 Experimental force-displacement at the first floor (model CS3)

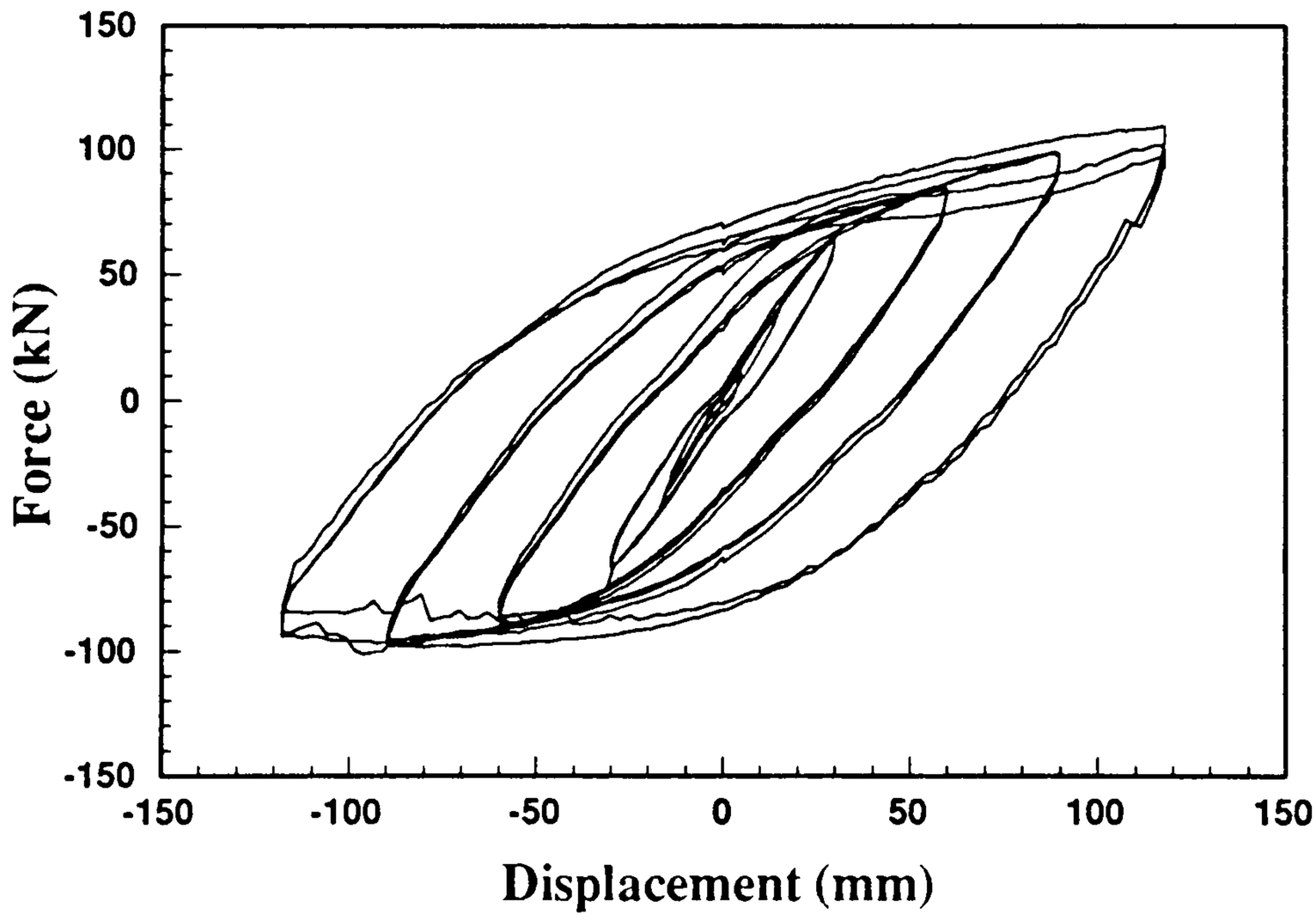

Figure 4.30 Experimental base shear versus top frame displacement (model CS3)

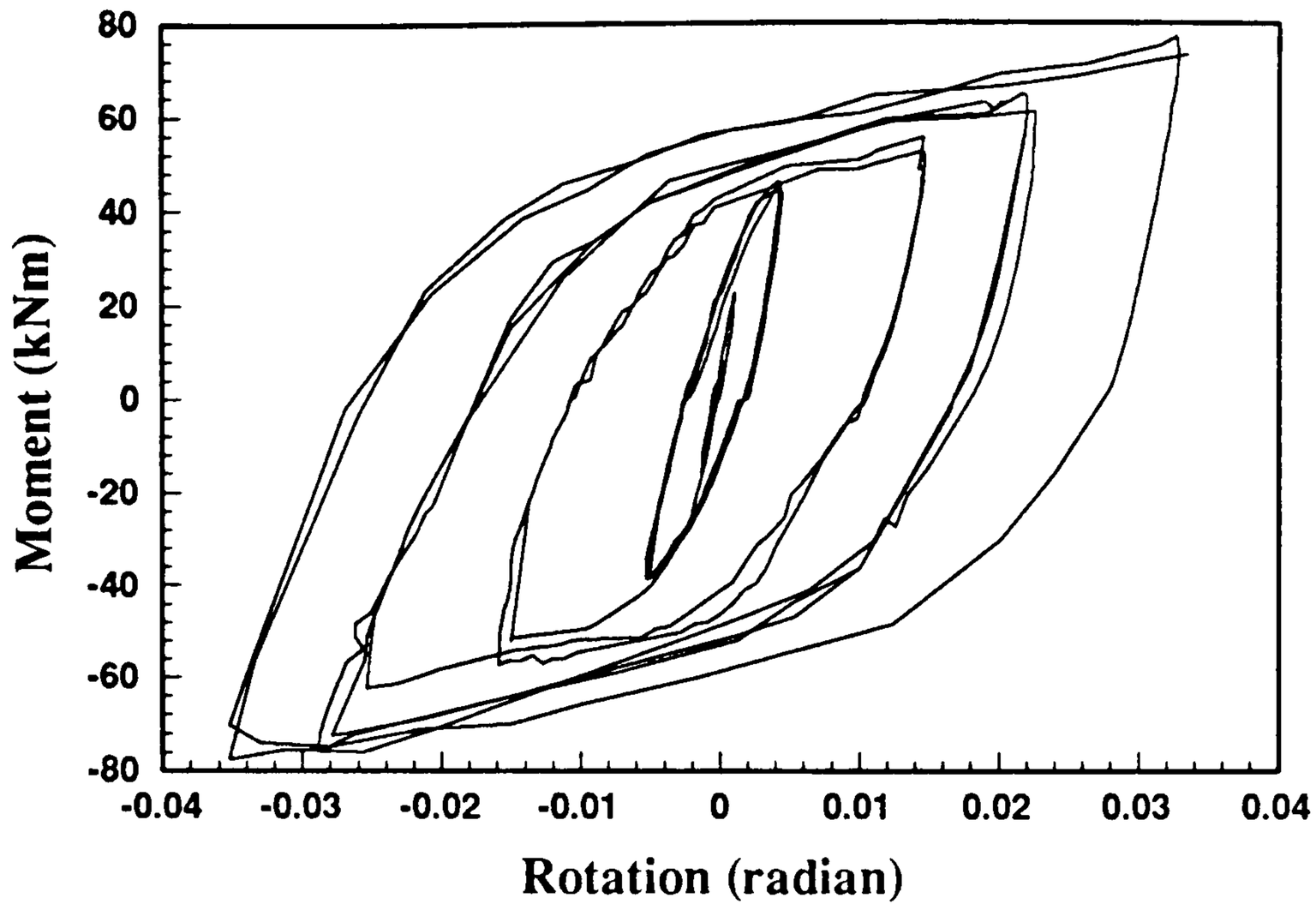

Figure 4.31 Experimental moment-rotation relationship of the connection in the first floor for model CS3

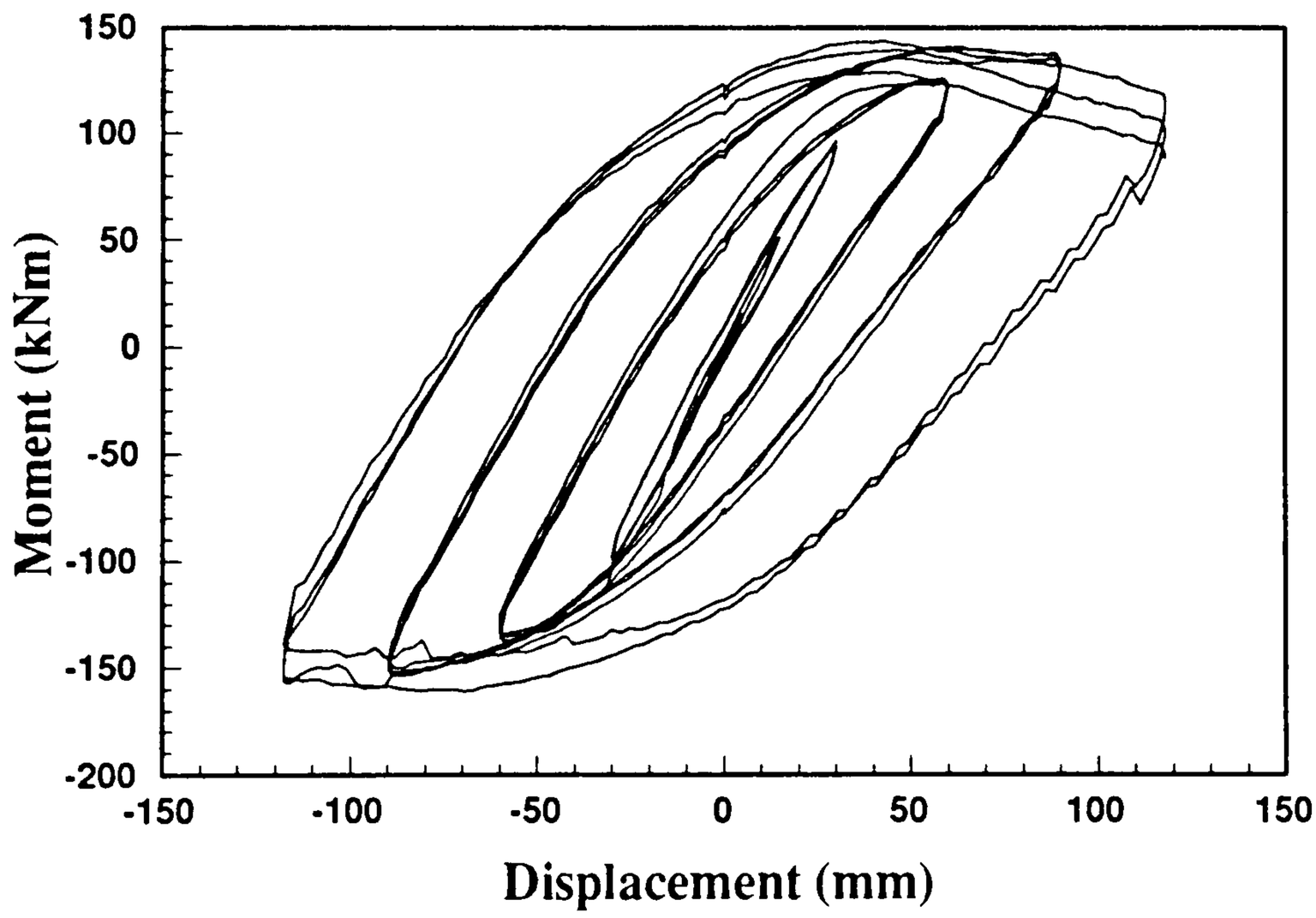

Figure 4.32 Experimental moment at the base of the column versus top frame displacement for model CS3

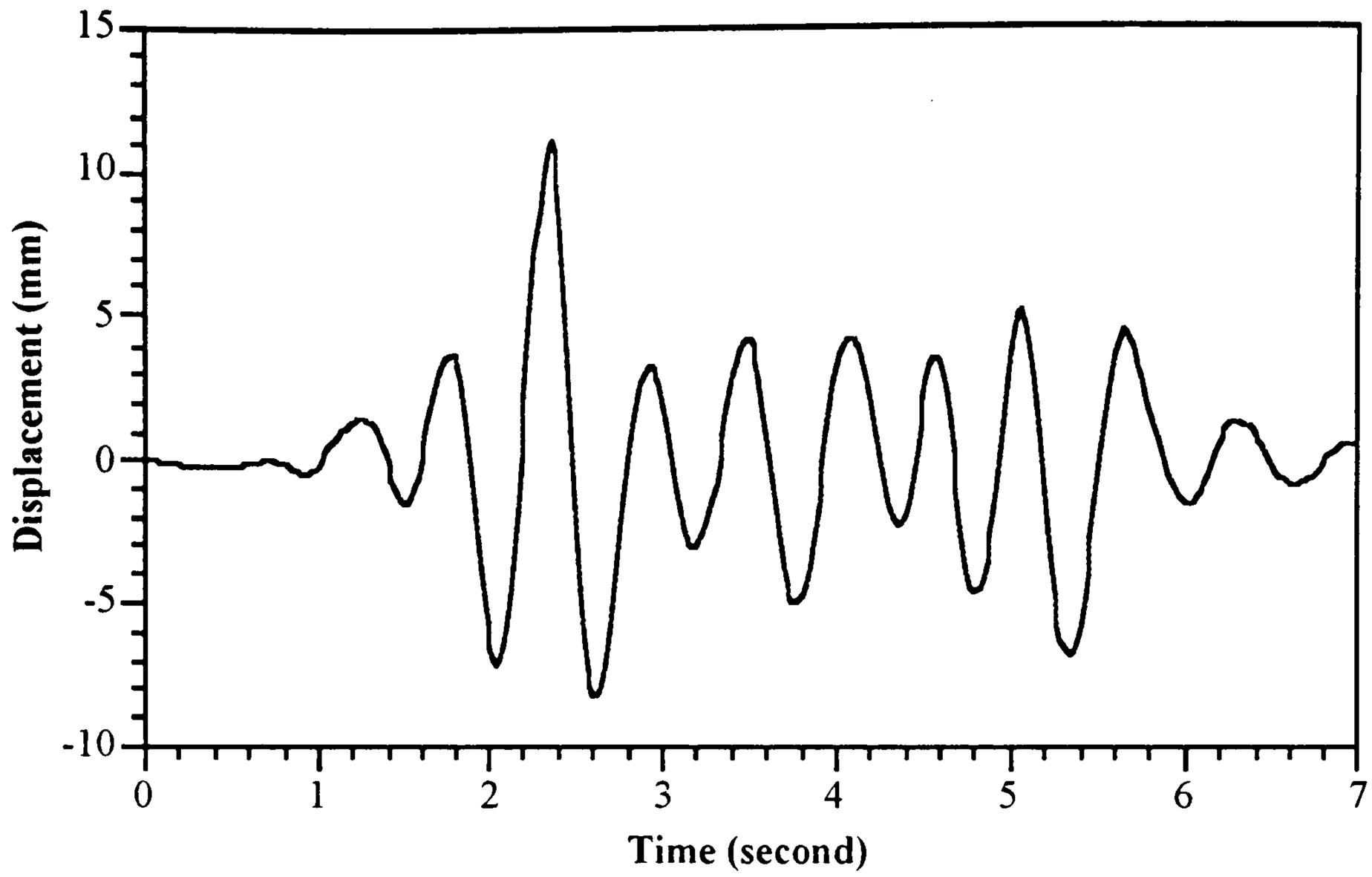

a) Displacement response of model DS1 at the second floor

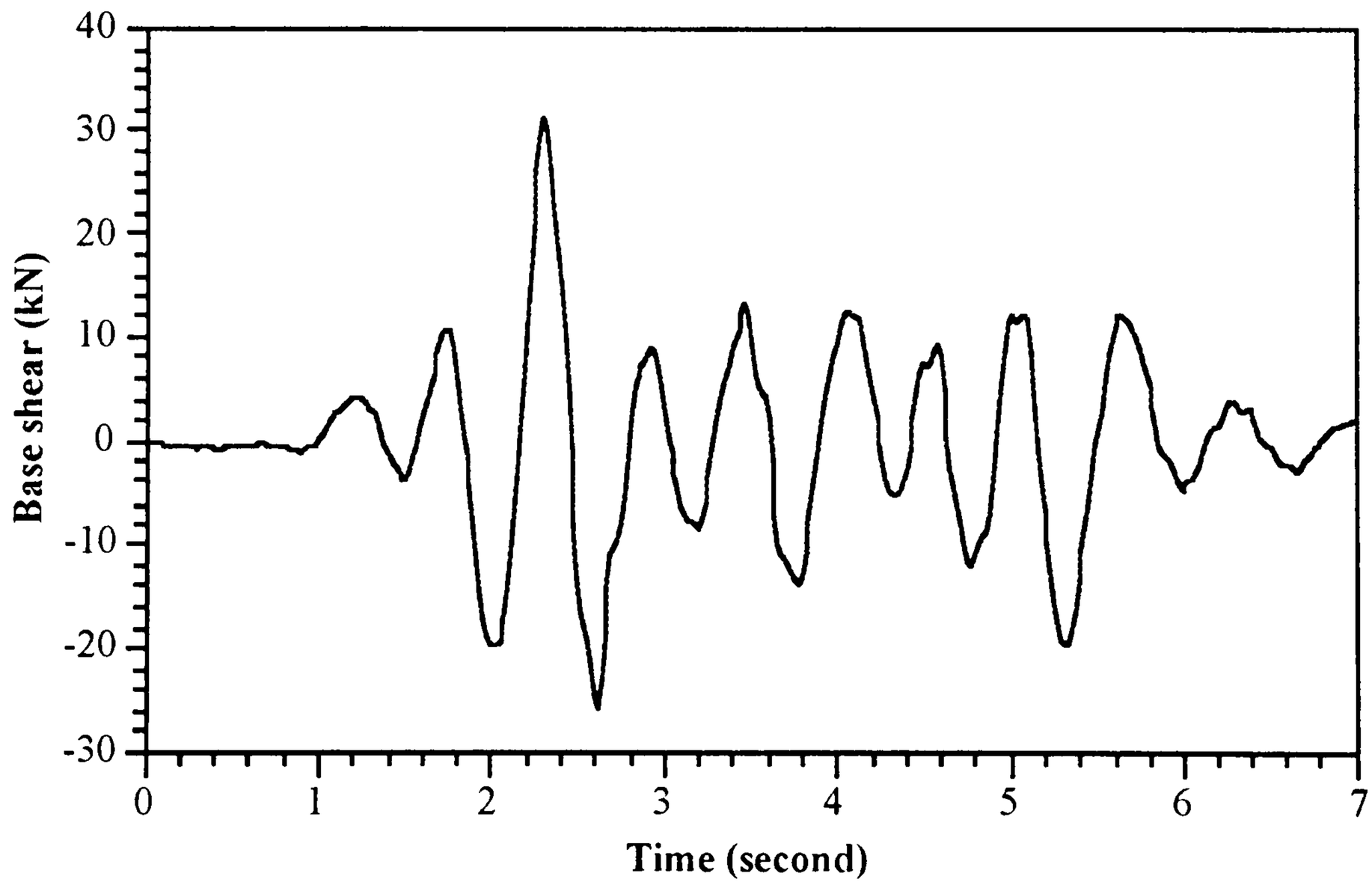

b) Base shear response of model DS1

Figure 4.33 Experimental response of model DS1 subjected to 15% of El Centro record

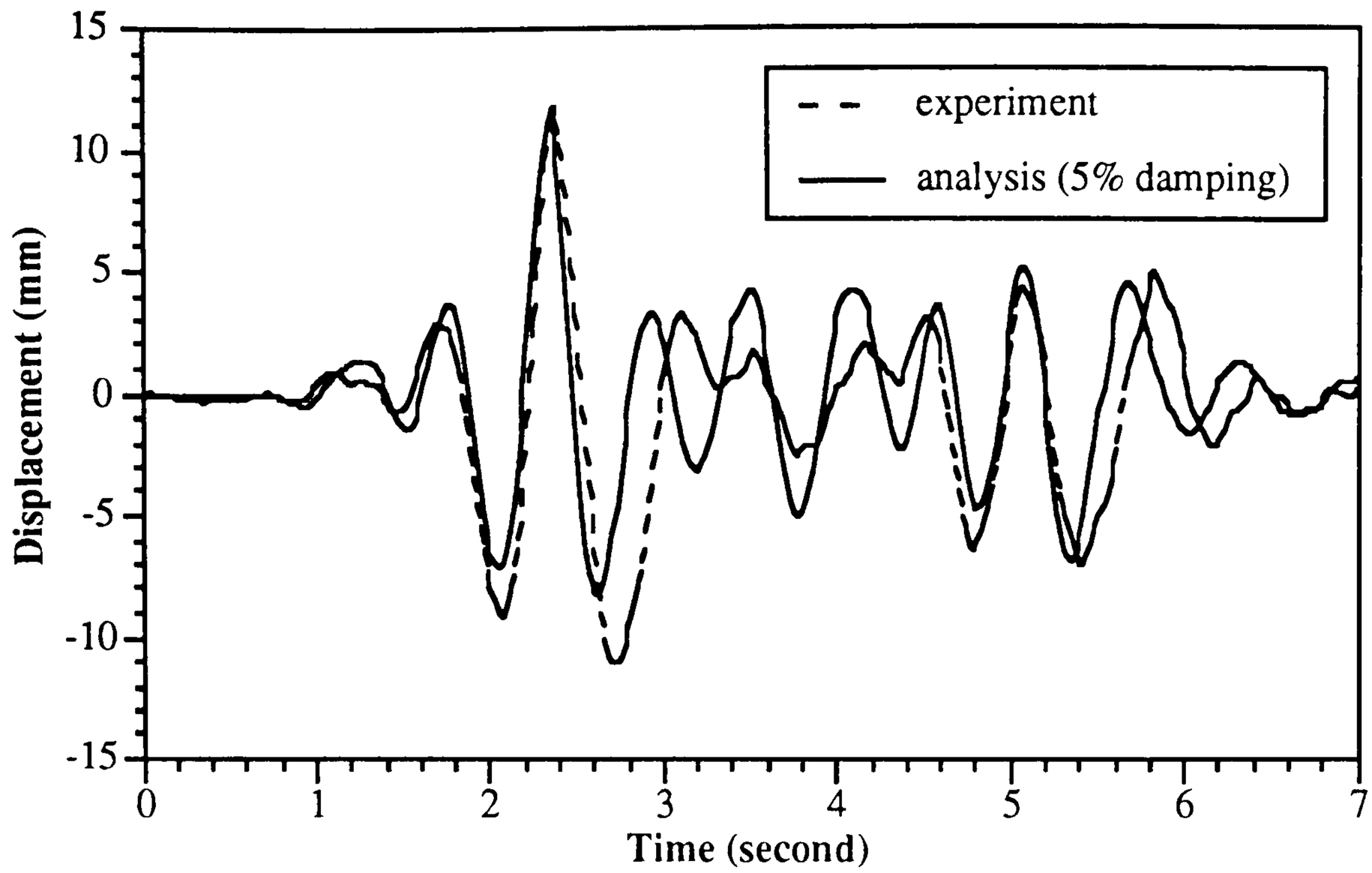

a) Displacement response of model DS1 at the second floor

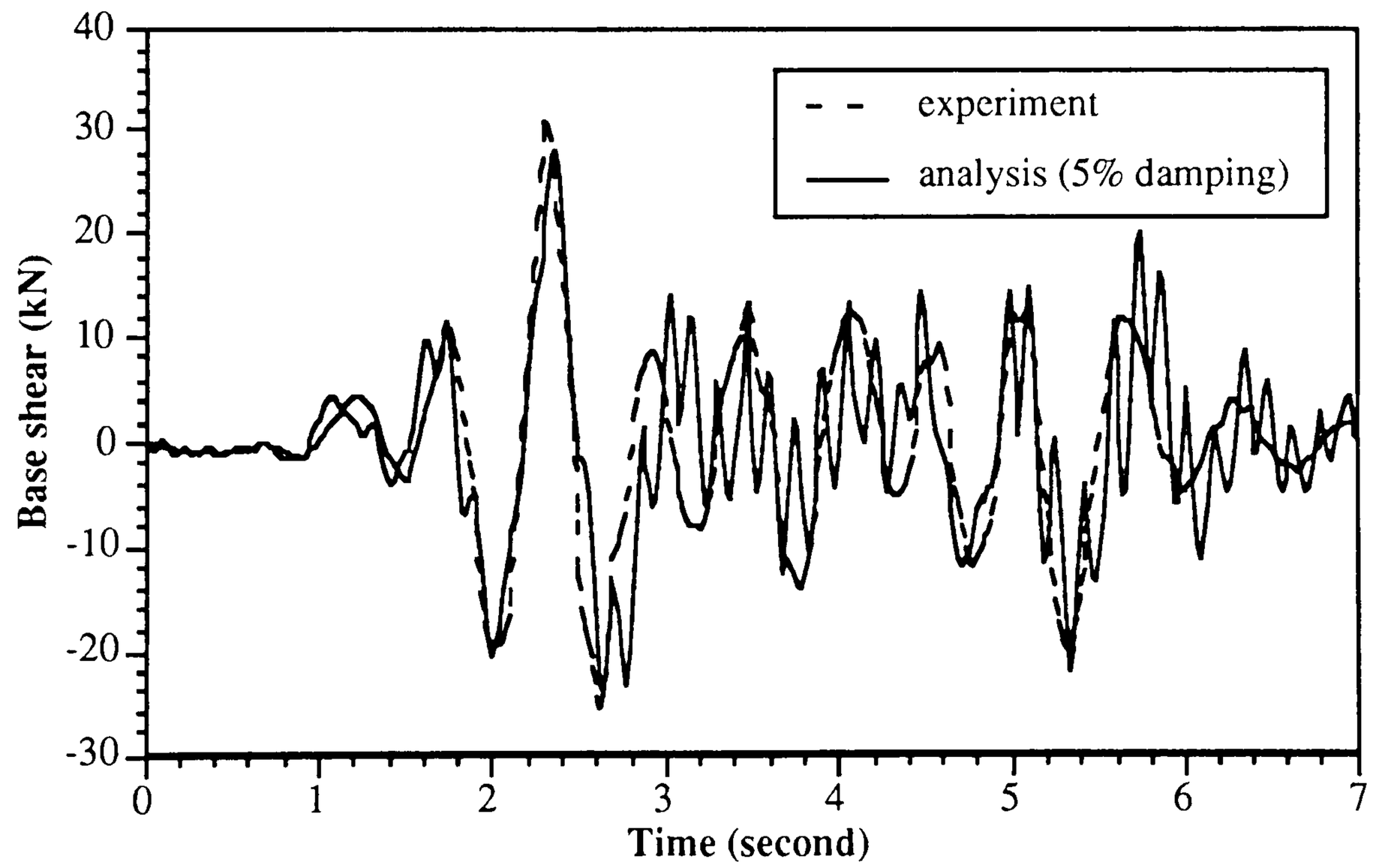

b) Base shear response of model DS1

Figure 4.34 Comparison between experimental and analytical responses of model DS1 subjected to 15% El Centro record

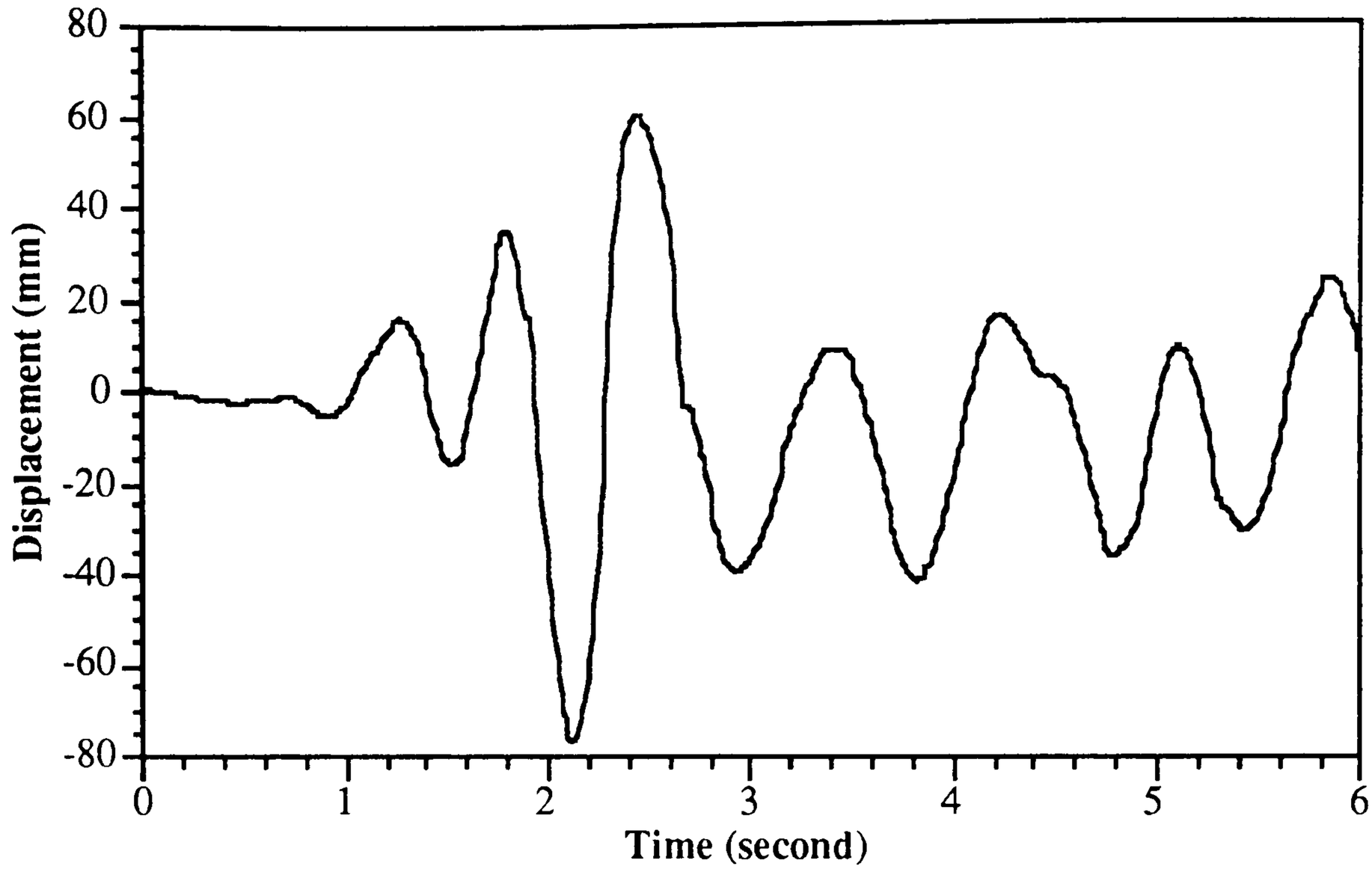

Figure 4.35 Experimental displacement response at the second floor of model DS1 subjected to 120% of El Centro record

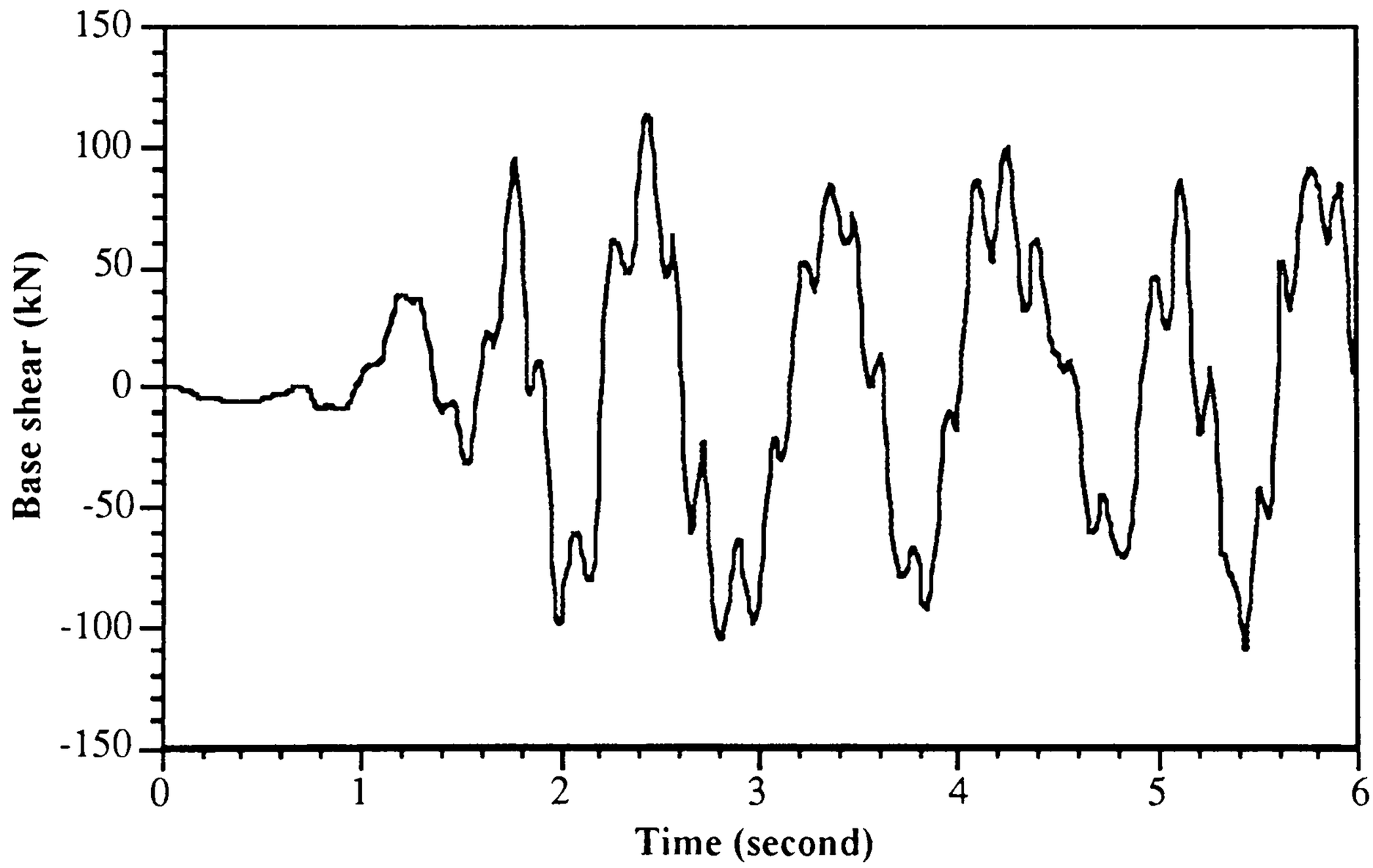

Figure 4.36 Experimental base shear response of model DS1 subjected to 120% of El Centro record

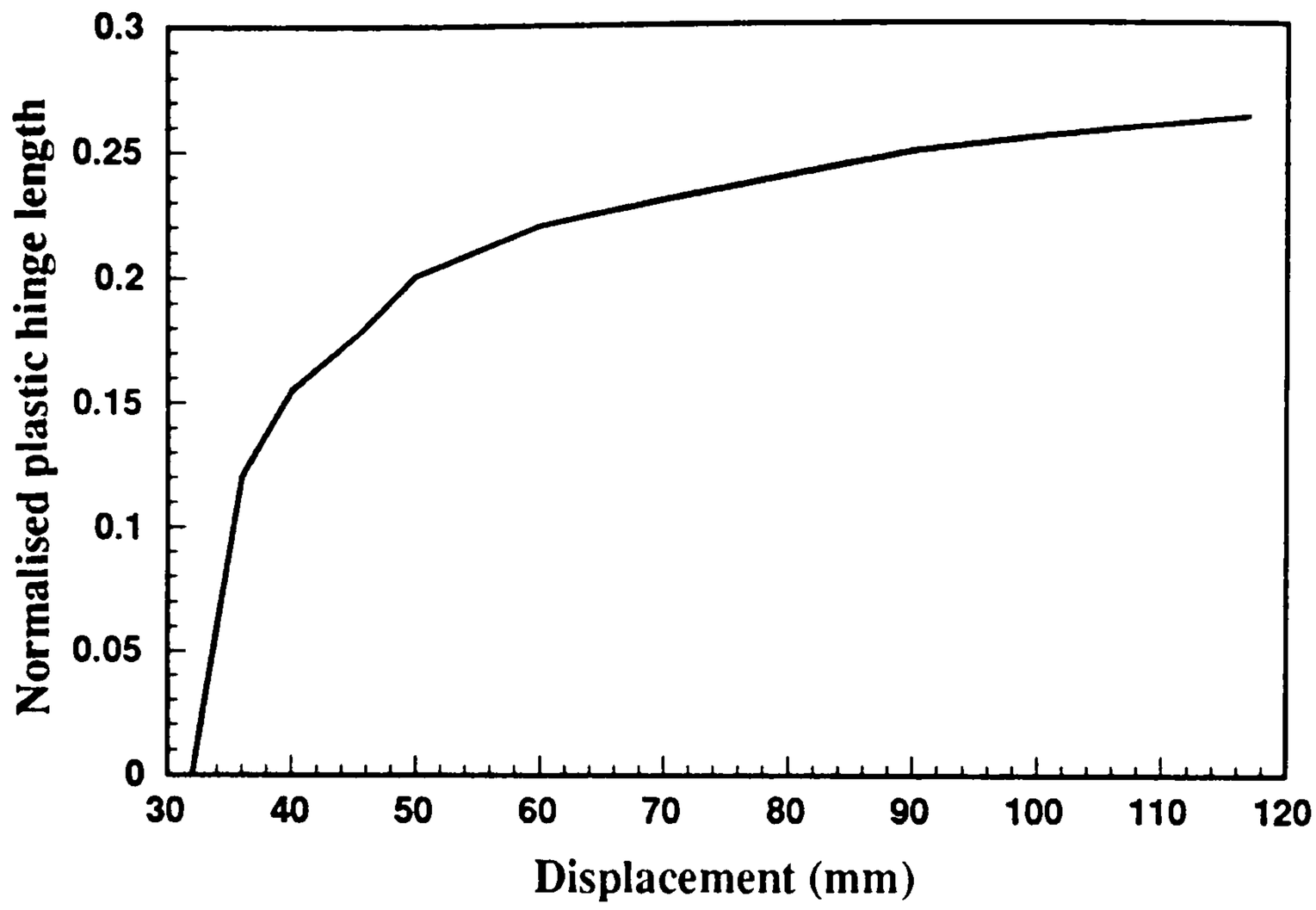

Figure 4.37 Relationship between second floor displacement and plastic hinge length normalised by the height of the first storey (model CR1)

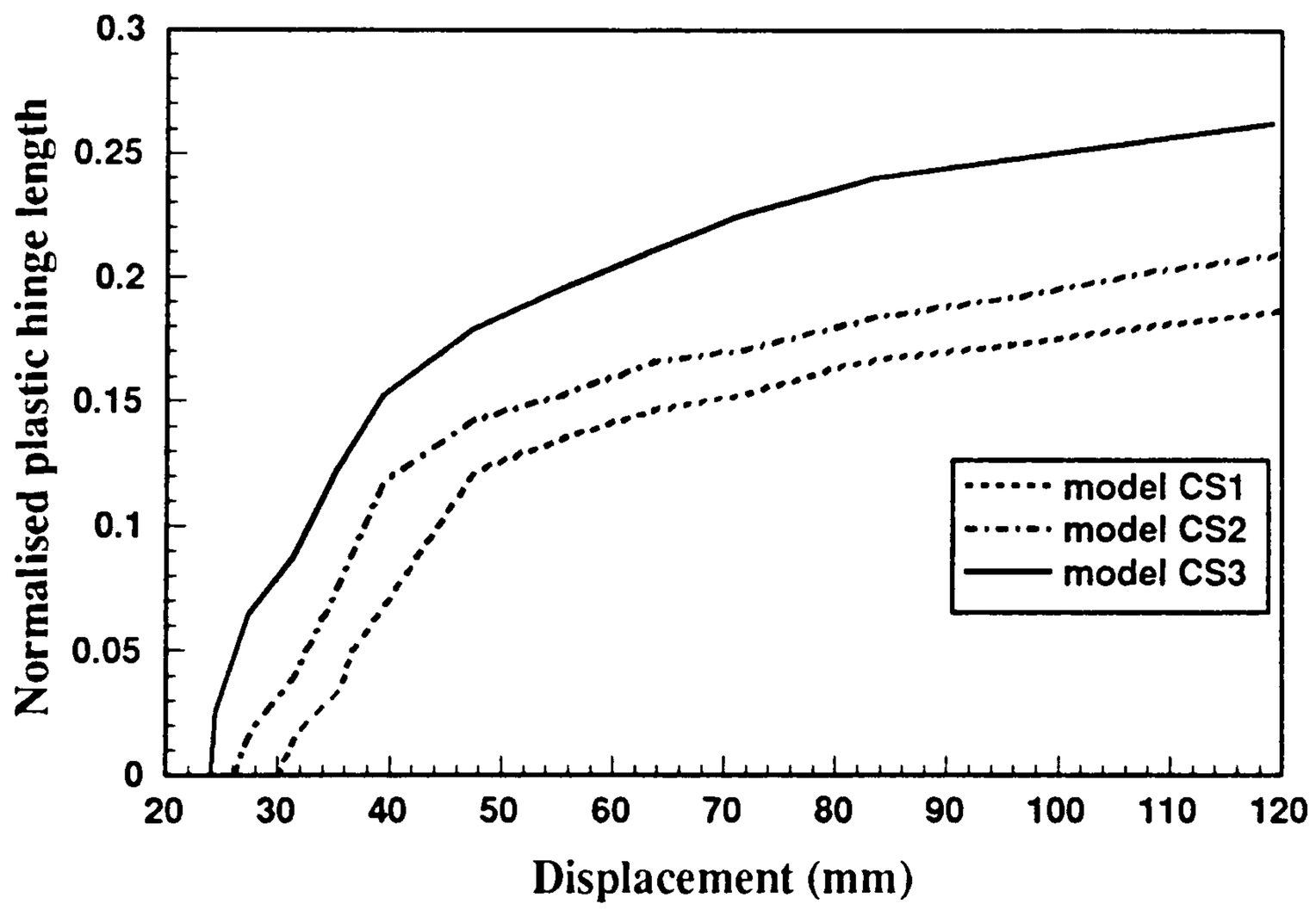

Figure 4.38 Relationship between second floor displacement and plastic hinge length normalized by the height of the first storey for three semi-rigid models

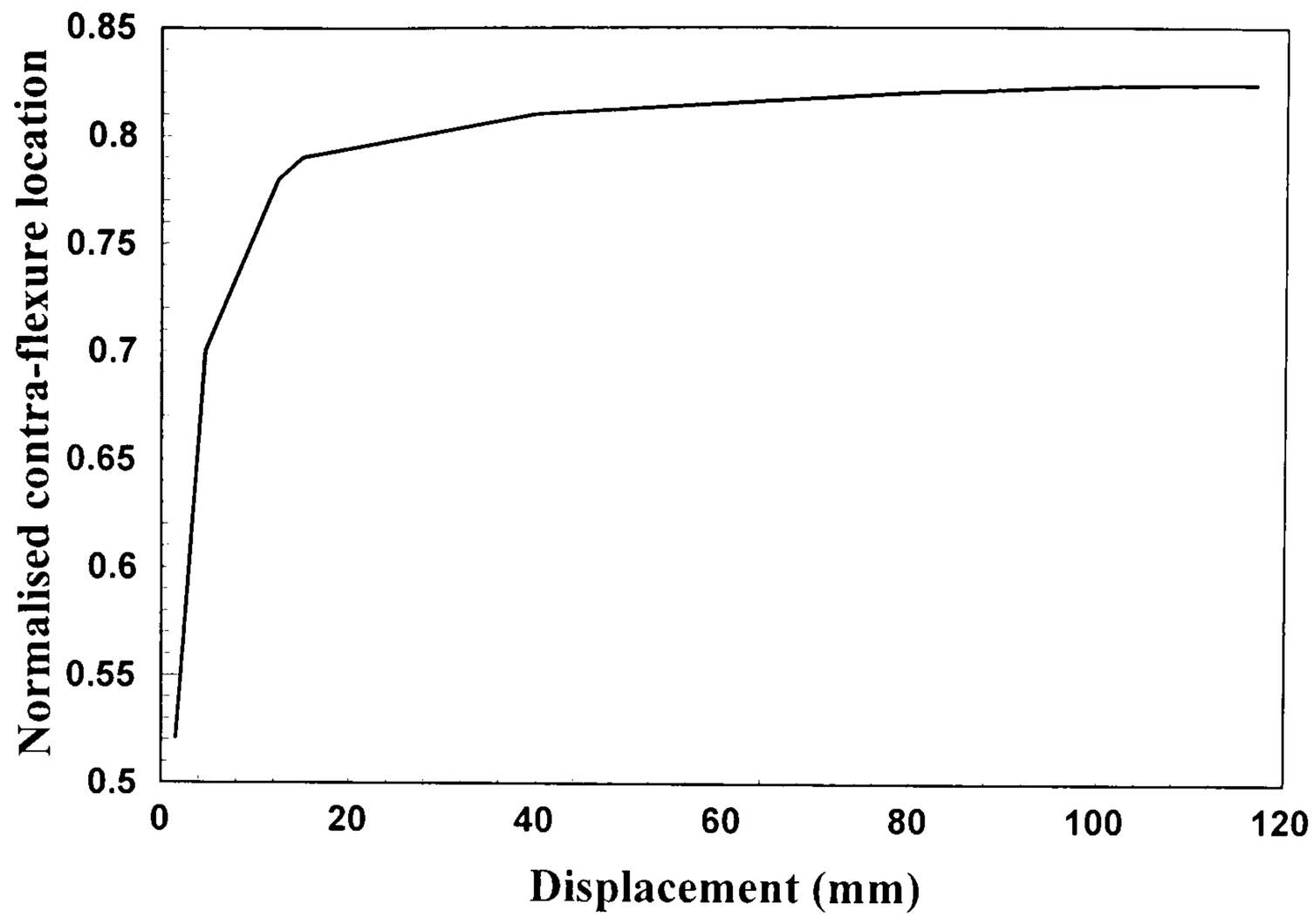

Figure 4.39 Relationship between second floor displacement and the normalised position of the point of contra-flexure in column (model CR1)

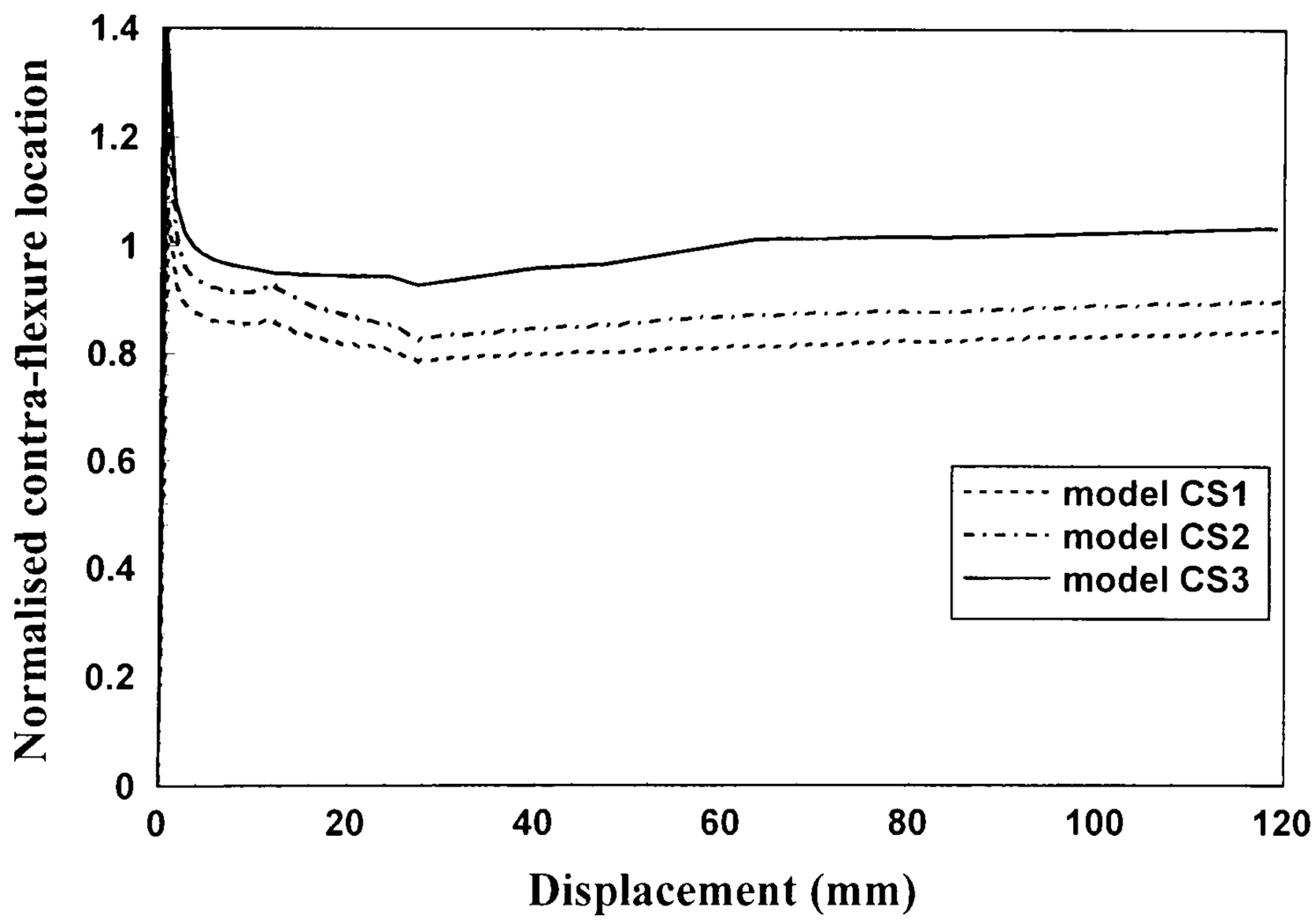

Figure 4.40 Relationship between second floor displacement and the normalised position of the point of contra-flexure for three semi-rigid models

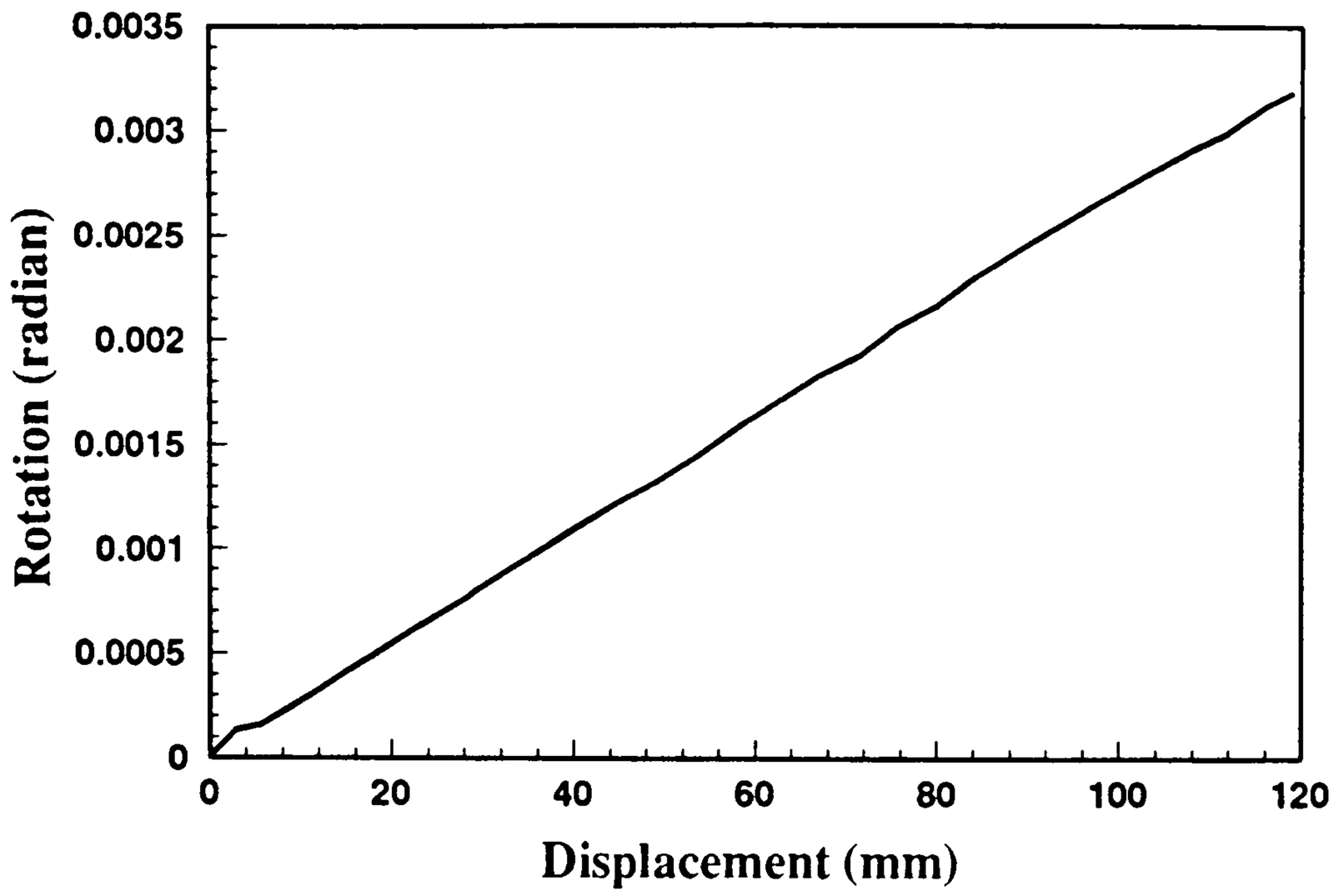

Figure 4.41 Experimental rotation of panel zone versus top frame displacement in semi-rigid frame (model CS1)

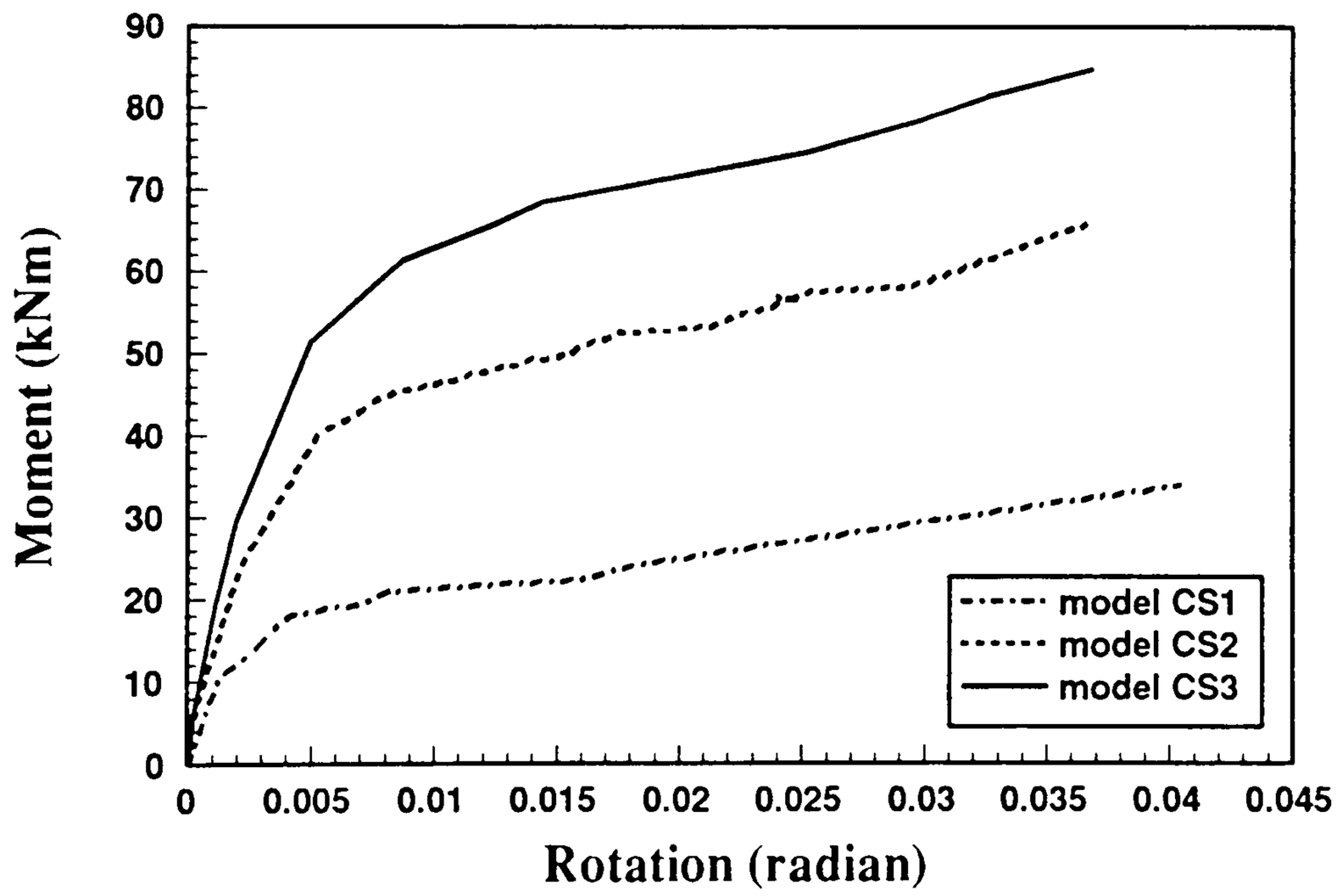

Figure 4.42 Experimental moment-rotation curve of connection obtained from cyclic tests in three semi-rigid models

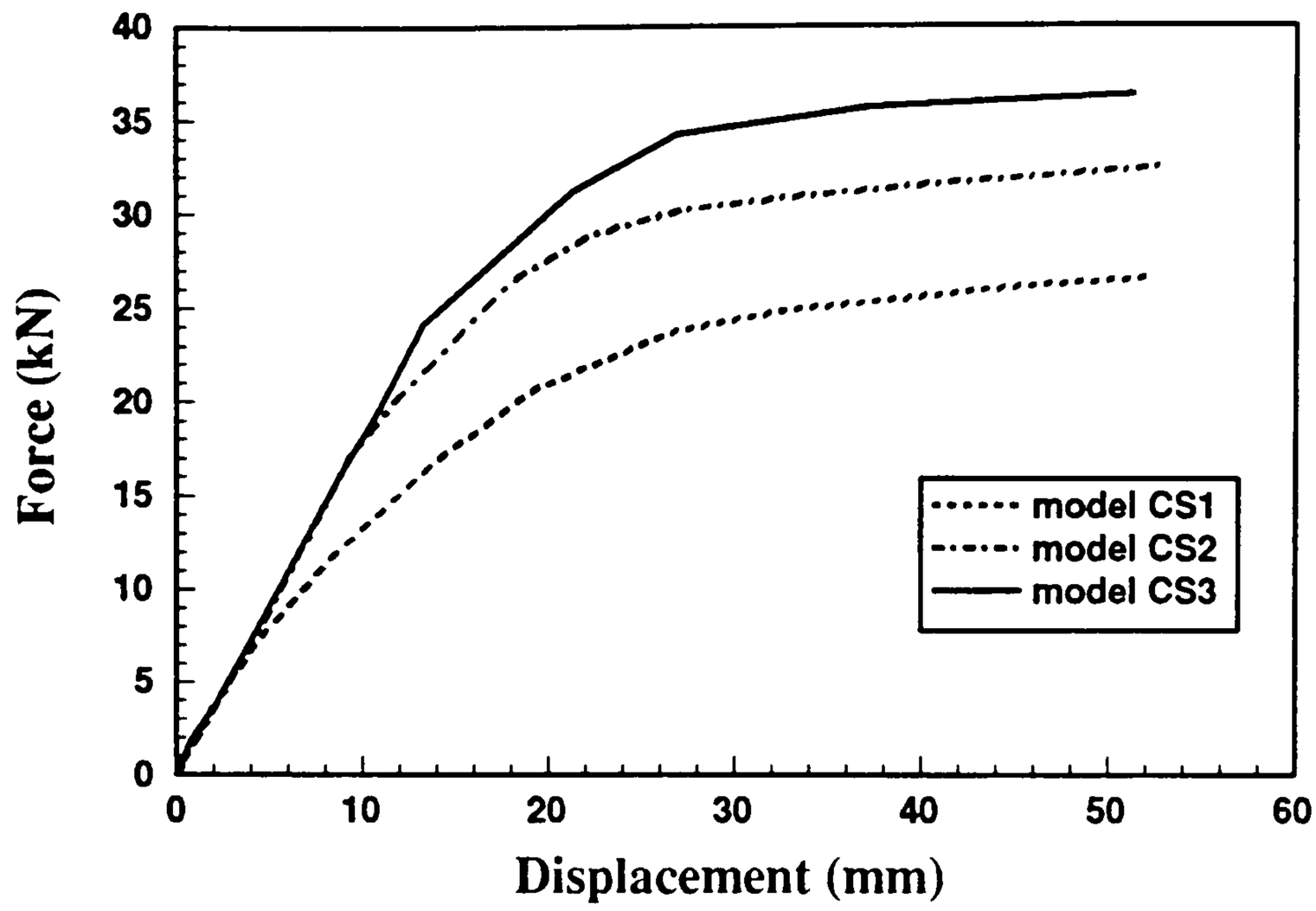

Figure 4.43 Experimental force-displacement at the first floor for three semi-rigid models obtained from cyclic tests

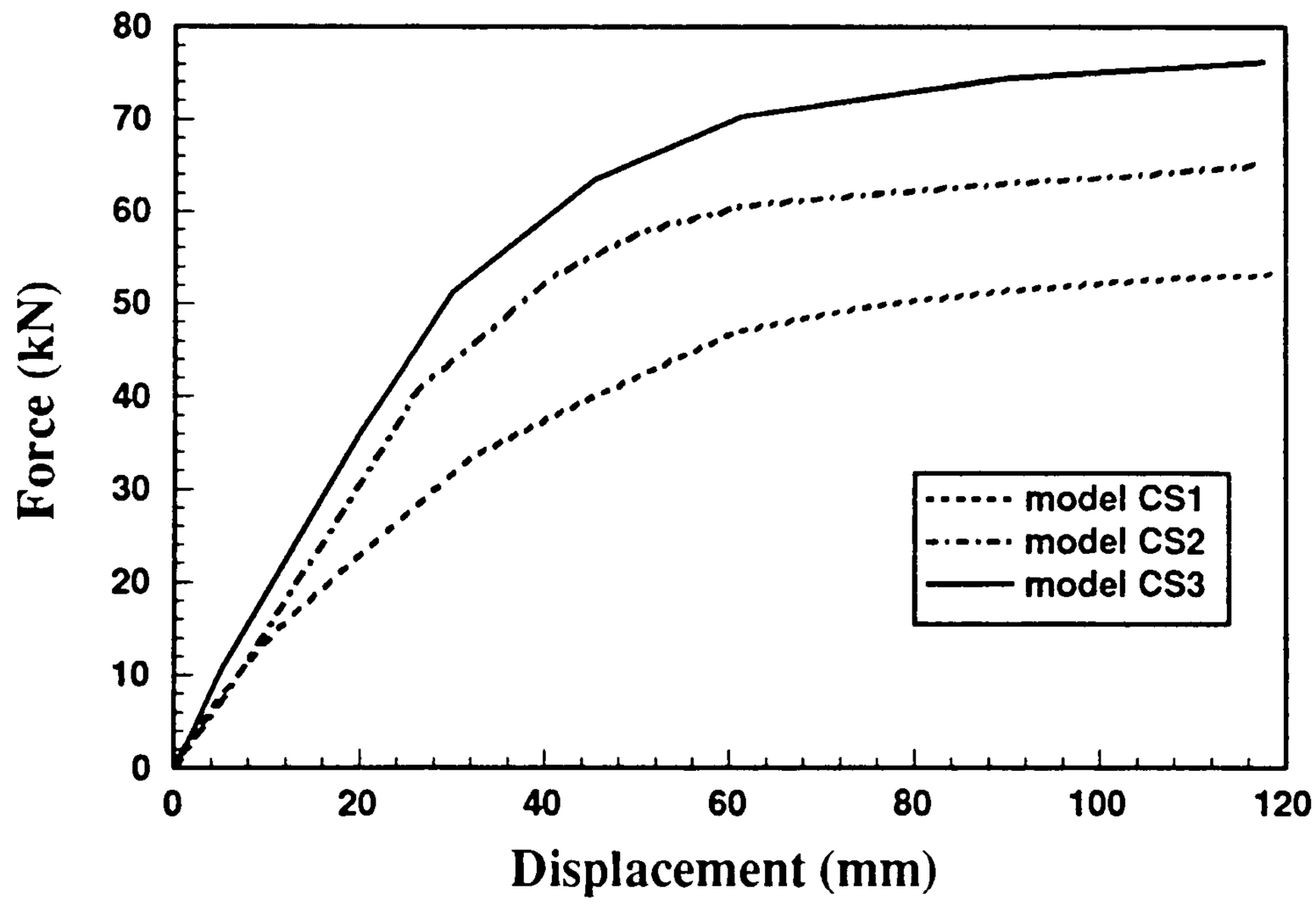

Figure 4.44 Experimental force-displacement at the at the second floor for three semi-rigid models obtained from cyclic tests

CHAPTER 5

5 ANALYSIS OF SEMI-RIGID STEEL FRAMES

5.1 The Non-linear Dynamic Analysis Program 'ADAPTIC'

The ADAPTIC program was developed for the analysis of non-linear steel, reinforced concrete and composite frames. The program is capable of analysing two and three dimensional frames, taking into account both geometric and material nonlinearities. A variety of elements can be used ranging from a plastic hinge element to an elasto-plastic cubic formulation, the latter of which can account for the spread in plasticity through the section and along the member length.

In this program, static, dynamic and eigenvalue analyses are available. For static analysis, the program has the capability to predict the post-ultimate response of frames subjected to proportional loading and has an option for varying loads independently in the pseudo-time domain. The formulations employed in the program are beam-column finite elements, accounting for large nodal displacements using an Eularian system with cubic or quartic shape functions.

For dynamic analysis, separate non-structural elements are available for calculating inertia and damping forces. The forcing function may be in the form of either load or displacement time histories. Independent support motion is also possible using, as input data, displacement, velocity or acceleration. The solution procedure used is iterative, utilising either the full or modified Newton-Raphson method or a combination of both. Several cross-section configurations can be analysed. Bilinear and trilinear cyclic models have also been developed within ADAPTIC to account for the detailed behaviour of beam-to-column connections.

The accuracy of this program has been verified elsewhere (Izzuddin and Elnashai, 1989; Madas and Elnashai, 1989; Elnashai et al, 1989; Izzuddin, 1990 amongst others). Subsequent sections of this chapter give a brief description of the non-linear

material models for steel, the cubic plastic element and the general description of the models which predict connection behaviour.

5.2 The Elasto-Plastic Cubic Element

This element assumes a cubic shape function in the chord system and monitors stresses and strains at various points across two Gaussian sections, allowing for the spread of plasticity throughout the cross-section. The element is defined with two nodes and the cross section is divided into a number of monitoring stations. The stresses are calculated at each monitoring station and for the two Gaussian sections. The basic characteristic of the element is that it is capable of tracing member behaviour based on material stress-strain relationships and large displacements. The accuracy of the analysis increases by introducing more elements in the plastic zones of the member and by increasing the number of monitoring stations.

Three degrees of freedom are used in 2D analysis whereas six degrees of freedom are employed in the 3D formulation, as shown in Figure 5.1. The strain state within the cross-section is determined by the four generalised strains: centroidal axial strain, curvature strains about the two principal axes and the rate of twist. The centroidal axial strain is assumed constant along the element length. In the presence of material plasticity, this condition does not necessarily imply a constant axial force along the element length. However, if the element is used to model short length of elasto-plastic members, it has been shown that the variation of the axial force is insignificant.

Since the relationship between the generalised stresses and strains cannot be established explicitly in the presence of material plasticity, the integration of the virtual work equation is performed numerically to obtain the element forces. Only two Gauss integration sections are employed along the length. The positions of the Gauss sections, as shown in Figure 5.2, are chosen such that the exact integration of the virtual work equation is obtained for the elastic element. Each Gauss section is divided into a number of areas across which stresses and strains are monitored. The effect of shear strains on the material plasticity is neglected and only direct strains are

established at the monitoring points using appropriate uniaxial stress-strain relationships.

To establish the global response of the cubic element, transformations from the chord to the global system are applied. In the calculation of direct stresses at the monitoring points, strains are considered incrementally from the last equilibrium state.

5.3 Material Model

For structural steel, different models were developed to represent its cyclic behaviour. A review of the available relationships and their merits is given by Izzuddin (1990), whilst their applicability to seismic analysis has been assessed by Elnashai and Izzuddin (1993).

The uniaxial behaviour of mild steel in its virgin state is essentially linear elastic up to the point of first yield. Under monotonic loading, the characteristic yield plateau is followed by a region of increased strain hardening, as shown in Figure 5.3. When subjected to constant strain amplitude cycling, steel exhibits a response which always converges to a stabilised saturation loop which is dependent only on the amplitude of cycling. The curve joining the tips of the stabilised cycles is known as the 'cyclic stress-strain curve', as shown in Figure5.4.

Due to the difference in shape between the cyclic and virgin curves, the transient response under constant strain amplitude cycling is characterised by softening for small amplitudes and hardening for large amplitudes.

Two cyclic models for mild steel are implemented within the elasto-plastic cubic formulation in ADAPTIC. The first is the bilinear model with kinematic strain-hardening, while the second is the uniaxial case of the multi-surface model originally proposed by Popov and Petersson (1978).

In the bilinear model, the elastic range remains constant throughout the various loading stages and the kinematic hardening rule for the yield surface is assumed to be a linear function of the increment of plastic strain, as shown in Figure5.5.

In the multi-surface model, a number of surfaces enclosing the yield surface are each associated with a value for an increment of plastic strain. The expansion or contraction and translation (kinematic hardening) of these surfaces are governed by pre-specified hardening rules.

5.4 Modelling of Connections

In analysing the semi-rigid connections of steel frames, the joint elements of ADAPTIC are utilised. Three different models, a linear elastic curve, a trilinear symmetric elasto-plastic curve, and a trilinear asymmetric elasto-plastic curve are available.

In non-linear analysis, both the trilinear symmetric and asymmetric elasto-plastic curves can be selected for predicting the response of semi-rigid steel connections. Figure 5.6 shows the behaviour of the joint elements. The accuracy of these models depends on determining the stiffness parameters K_0, K_1, and K_2. By using zero value for parameter K_2, the trilinear model can be used as a bilinear model.

5.4.1 Proposed Bilinear Moment-Rotation Curve

As discussed in Chapter 2 of this thesis, the behaviour of a beam-to-column connection is characterised by its moment-rotation relationship. Experimental results show that most moment-rotation curves for the top and seat angle connections with double web angles exhibit elastic-plastic behaviour with hardening characteristics. Therefore, based on this behaviour, for the design of semi-rigid steel frames and for simple implementation in the computer program a bilinear model for predicting the moment-rotation curve for the top and seat angle connection with double web angles is proposed in this study.

5.4.1.1 Theory and Assumptions

A typical top and seat angle connection with double web angles and its deformed pattern are shown in Figure 5.7. As indicated in this Figure, the vertical leg of the top

angle attached to the column flange is pulled off the column surface by the beam and the outstanding leg of the seat angle is bent as a cantilever beam around the centre of rotation. Finally, a plastic failure mechanism is formed in the vertical leg of the angle attached to the flange of the column.

Figure 5.8 represents the collapse mechanism in the top angle. As shown in this Figure, two plastic hinges form. One of the hinges forms along the line of the nut edge of the fasteners and the second is located along the line of the toe of the fillet.

To calculate the moment capacity of the connection, it is necessary to define first the location of the centre of rotation. An analysis of the available experimental research data indicated that most semi-rigid connections rotate about a point between the beam compression flange and the centre of gravity of the connection. This point then normally moves down to the beam compression flange as the connection undergoes inelastic behaviour. Therefore, the assumption that the centre of rotation is located in the compression flange of the beam can be used for calculating the moment capacity of the connection.

In order to consider yielding of the outstand leg of the angle for determining the moment capacity of the connection, it is important that the bolt slippage is avoided since this will cause a significant reduction in its ability to dissipate energy. This was observed from experimental results by Bernuzzi et al. (1992). For this purpose, the design philosophy should consist of sizing the bolt diameter and the pretensioning force such that yielding of the angle legs precedes bolt slip. In addition, it is assumed that the flexural stiffness of the web angle could be neglected in the evaluation of the moment capacity of the connection. The primary reasons for this assumption are as follow:

- The web angles are expected to carry a large proportion of the shear load. And since large moments are usually accompanied by large shear forces, shear connections are expected to yield in shear. Thus, the remaining area for carrying bending moments is very small and hence contribute little to the moment capacity of the connection. This behaviour was observed in the cyclic

tests for models CS2, CS3 and DS1 and also in the tests undertaken by Astaneh et al. (1989) and Nader et al. (1988).

- This part of the connection should be able to resist shear forces when the semi-rigid connection loses its moment capacity at the ultimate limit state. Therefore, it is recommended that the flexural stiffness of the web angle connection be much less than the top and seat angles.

By considering the theory and assumptions presented above, M_y, θ_y, K_1, K_2, and $\theta_{max.}$ should be determined in order to construct the bilinear moment-rotation model.

5.4.1.2 Calculation of Yield Moment

As described in the previous section, when the connection responds in the inelastic range, two plastic hinges occur in the vertical leg of the top angle. The virtual work equation for the top angle at the collapse state is given by:

$$2M_{pt}\,\theta = F_{pt}\,L\theta \tag{5.1}$$

where

M_{pt} = Plastic moment of the top angle

F_{pt} = Plastic shear force in the vertical leg

d_1 = Distance from centre of the bolt to the heel of the angle

k = Distance from heel to toe of fillet of angle

D = Width of nuts across the flat sides for bolt fasteners

L = Distance between two plastic hinges (is given by d_1-k-D/2)

To evaluate the shear force, the bending moment versus shear interaction should be considered in the analysis. This is because the distance between the two hinges is very short when compared with the thickness of the angle. For this purpose, the bending

moment-shear interaction formula for the yield criteria as proposed by Drucker (1956) is used:

$$\frac{M_p}{M_o} + \left(\frac{F_{pt}}{F_o}\right)^4 = 1 \tag{5.2}$$

where M_o and F_o are the plastic bending moment and the plastic shear force without coupling and are determined from equations (5.3) and (5.4).

$$M_0 = \frac{\sigma_y l_t (t_t)^2}{4} \tag{5.3}$$

$$F_o = \frac{\sigma_y l_t t_t}{2} \tag{5.4}$$

in which σ_y is the yield stress, l_t is the length of the top angle and t_t is the thickness of the angle. By substituting M_p and M_o from the above equations into (5.2), F_{pt} can be determined, using an iterative procedure, from:

$$\left(\frac{F_{pt}}{F_o}\right)^4 + \frac{L}{t_t}\left(\frac{F_{pt}}{F_o}\right) = 1 \tag{5.5}$$

Having evaluated F_{pt}, M_{pt} can then be calculated from Equation (5.1). The moment capacity contributed by the top angle M_{ut} is obtained by taking moments about the centre of rotation as follow:

$$M_{ut} = M_{pt} + F_{pt}\, d_2 \tag{5.6}$$

where $d_2 = d_B + t_t$ and d_B is the depth of the beam.

To evaluate the moment capacity of the seat angle, it is assumed that the bearing pressure is uniformly distributed over the outstanding leg of the seat angle and thus the plastic moment capacity of the seat angle M_{us} is,

$$M_{us} = \frac{\sigma_y l_s (t_s)^2}{4} \tag{5.7}$$

$$M_{yc} = \frac{\sigma_y l_s (t_t)^2}{4} + \frac{F_{pt} L}{2} + F_{pt}(d_B + t_t) \tag{5.8}$$

where l_s and t_s are the length and the thickness of the seat angle respectively. By using Equations (5.6) and (5.7), the moment capacity of the top and seat angle connection with the double web angle can be obtained from Equation (5.8).

5.4.1.3 Yield Rotation

The relationship between the deformation of the top and seat angles corresponding to the yielding of the connection and the thickness of the angles was developed by Harper et al. (1990). For a wide range of different angle thicknesses it was observed that the deformation of the angles was almost constant and approximately equal to 1.4 mm. This behaviour was noted in the experimental results of models CS1, CS2 and CS3 with different thickness of the top and seat angles.

Considering this value of deformation and making the assumption that the location of the centre of rotation is in the compression flange of the beam, the yield rotation can then be evaluated as shown in Equation (5.9):

$$\theta_y = \frac{1.4}{d_B} \tag{5.9}$$

where θ_y is the yield rotation and d_B is the depth of the beam. In this Equation the unit of d_B is in mm.

5.4.1.4 Evaluation of the Elastic and Post Elastic Stiffness

By determining the moment and rotation from equations (5.8) and (5.9), the elastic stiffness of the connection is obtained by dividing the yield moment by the yield rotation.

Experimental results for semi-rigid models subjected to cyclic tests indicate that the top and seat angles with double web angle connection exhibit significant post-elastic stiffness. As mentioned previously, in the inelastic range larger forces of approximately twice the yield value were observed in the tests. Similar observation was also made in experimental studies carried out by Azizinamini et al. (1985). Such behaviour can be attributed to the material strain hardening.

From experimental moment-rotation curves, it was concluded that a value between 8% and 15% of the elastic stiffness reasonably represents the post-elastic stiffness. According to the results and observations from the moment-rotation curves obtained in three cyclic tests, a value of 10% of the elastic stiffness is recommended for a bilinear representation of the connection response.

5.4.1.5 Maximum Rotation of the Connection

The maximum rotation of the connection is related to the ratio of its moment capacity to the plastic moment of the beam. It is also inversely proportional to the stiffness of the connection. In the three cyclic tests, it was observed that the top and seat angle connection underwent large rotations (greater than 0.04 radian) without failure. In the monotonic tests of Harper et al. (1990), these connections were capable of undergoing rotations of up to 0.04 radian with no significant reduction in the moment capacity.

According to studies carried out by Nader and Astaneh (1992), the maximum rotation of the top and seat angle connection with double web angle should not exceed 0.05 radians. Therefore, the value of 0.04 radians observed from the tests is selected as a maximum rotation of the connection in analysis of semi-rigid steel frames.

5.4.2 Verification of Proposed Bilinear Model

As mentioned in Chapter 2 of this thesis, the thickness of the top and seat angles and the depth of the beam are the key parameters that influence the behaviour of the moment-rotation curve of this type of connection. To investigate the effect of the

thickness of the angles and for verification of the proposed model, the three types of connection that were used in the cyclic tests are examined

In these examples, only the sizes of the angles are varied with the other parameters, depth of the beam and diameter of the bolts, remaining constant. The details of these connections are given in Figure 4.5 of Chapter 4.

The yield moment, rotation and the elastic stiffness of the connections are illustrated in Table 5.1. The bilinear moment-rotation curves for each example are shown in Figure 5.9. As indicated in this Figure, the thickness of the top and seat angles has a significant effect on the moment capacity of the connection.

Table 5.1

Calculated yield parameters of the connections

Model	Thickness of top and seat angles (mm)	Yield moment (kNm)	Yield rotation (radian)	Elastic stiffness kNm /rad.	Moment at $\theta = 0.04$ rad. kNm
CS1	8	19.29	0.0055	3500	31.36
CS2	12	45.75	0.0055	7340	71.07
CS3	15	55.75	0.0055	10100	90.615

To demonstrate the influence of the beam depth and the length of the top and seat angle on the behaviour of this type of connection, three models (8S5, 8S7 and 14S3) which were studied by Azizinamini et al. (1985) are presented. The details of these models are given in Table 5.2 and the moment-rotation curves using the proposed bilinear model are shown in Figure 5.10.

Table 5.2

Details of tested connections (Azizinamini et al, 1985)

Model	Depth of beam (mm)	Thickness of angle (mm)	Length of the angle (mm)	Stress N/mm^2
8S5	209.55	9.52	203.2	280
8S7	209.55	9.52	152.4	280
14S3	358.77	9.52	203.2	280

Table 5.3 represents the calculated yield moment, rotation and the elastic stiffness of this type of connection. As shown in Figure 5.10 and Table 5.3, by increasing the depth of the beam in model 14S3, the yield moment of the connection increases significantly. In addition, it is observed that the yield rotation was inversely proportional to this parameter.

Table 5.3

Calculated yield parameters of test specimens using the proposed model

Model	Yield moment (kNm)	Yield rotation (radian)	Elastic stiffness (kNm /rad.)	Moment at (θ = 0.04 rad.) kNm
8S5	26.89	0.0067	4014	42.95
8S7	20.16	0.0067	3009	32.16
14S3	43.46	0.0039	11140	88.02

To investigate the effect of the length of the angle on the behaviour of the connection, the bilinear moment-rotation relationship for model 8S5 is compared with model 8S7 in Figure 5.11 and Table 5.3. It is demonstrated that the decrease in the length of the angle in model 8S7 causes a reduction in the moment capacity. However this effect is insignificant when compared with the effect of changes in the angle thickness or the beam depth.

5.5 Comparison with Experimental Results

The accuracy of the ADAPTIC program in simulating the non-linear behaviour of different frames has been studied elsewhere (Izzuddin and Elnashai, 1989; Elnashai, and Elghazouli, 1994). In this section, some of the experimental monotonic moment-rotation curves are compared with the proposed bilinear model. This is followed by a comparison of the experimental results (from cyclic and dynamic tests) with the analytical response using the proposed model with ADAPTIC.

5.5.1 Monotonic Tests

In order to compare the results of the proposed bilinear model with the tests results, it is instructive to first examine the monotonic moment-rotation curves obtained from cyclic tests. Furthermore, the accuracy of the model is checked (for changes in the key parameters of the connection) via comparisons with the results of experimental tests carried out by Azizinamini et al. (1985). Details of these connections are given in Table 5.4.

Table 5.4

Details of the different connection models (Azizinamini et al, 1985)

Model	Depth of beam (mm)	Thickness of angle (mm)	Length of the angle (mm)	Stress N/mm^2
8S2	209.55	9.52	152.4	280
8S5	209.55	9.52	203.2	280
14S8	358.77	15.87	203.2	280

The experimental moment-rotation relationships of the six models are shown in Figures 5.12 and 5.13. These Figures confirm that there is good agreement between the model prediction (of the moment-rotation relationship) and the experimental results. This agreement is even more significant in the post-elastic region of the curves.

Table 5.5 gives the analytical and experimental yield moments, the elastic stiffness and the moment at a rotation equal to 0.03 radians for all the models. The differences between the calculated parameters (using the proposed model) and the test results are less than 10%.

Table 5.5

Comparison of analytical and experimental parameters of different connections

Parameters	Method	CS1	CS2	CS3	8S2	8S5	14S8
Yield	test	18.7	39.70	52	35.8	27.20	114.31
moment	analysis	19.29	40.37	55.77	32.85	26.89	113.12
(kNm)	differences (%)	+3.15	+1.68	+7.25	-8.24	-1.14	-1.04
Elastic	test	3600	7270	10400	5340	4059	29310
stiffness	analysis	3500	7340	10100	4900	4014	29000
(kNm/rd.)	differences (%)	-2.77	+1.00	-2.88	-8.23	-1.10	-1.05
Moment	test	29.4	59.3	79.5	44.20	39.65	185.34
at	analysis	29.79	62.39	86.07	47.55	38.90	200.12
$\theta = 0.03$	differences (%)	+1.32	+5.21	+8.26	+7.58	-1.89	+7.97

It is therefore concluded that the proposed bilinear moment-rotation curve represents with reasonable accuracy the yield and ultimate values and hence it may be used with confidence.

5.5.2 Cyclic Tests

In an effort to compare the analytical results of the ADAPTIC program (using the proposed bilinear model) with the tests results, the experimental data from three cyclic tests are examined.

Figures 5.14 through 5.19 show the comparison between the analytical and experimental data for three specimens (CS1, CS2 and CS3) relating to the second storey restoring forces and the base shears versus the top storey displacements. As indicated in these Figures, the hysteretic behaviour of the curve for all the models is in good agreement with the tests in terms of force and displacement.

It was observed that under cyclic loading there was an abrupt reduction in stiffness during the unloading phase. This related to the fact that the connection elements (the top and seat angles) were subjected to bending. An increase in the stiffness during loading phase that is associated with the connecting elements acting in compression (the gap between the column flange and the top or seat angle) was also observed.

Table 5.6

Comparison of analytical yield and ultimate values with experimental results

Specimens	Method	Yield displacement (mm)	Yield base shear (kN)	Ultimate base shear (kN)	Ultimate Moment of col.(kNm)
CS1	Test	30	45	70	145.94
	Analysis	30.59	47.7	70.47	149.32
	Differences (%)	+ 2	+ 6	+ 0. 67	+ 2.3
CS2	Test	26	60	94	161.83
	Analysis	27.5	61.2	95.5	158.20
	Differences (%)	+ 5.8	+ 2	+ 1.5	- 2.24
CS3	Test	24	65	104.5	162
	Analysis	23.70	68.39	110.82	160.13
	Differences (%)	- 1.25	+ 5.20	+ 6	- 1.15

Table 5.6 demonstrates the differences between the analytical and experimental yield and the ultimate parameters. As noted in Chapter 4, the maximum 3% interstorey drift has been identified as an ultimate limit state for each model. As Table 5.6 indicates, the maximum discrepancy between the values obtained from the analyses to the values observed in the tests is less than 6%.

It is also observed that the analytical yield and the ultimate parameters in the three models are in good agreement with the test results. This therefore engenders further confidence in the use of ADAPTIC with the bilinear model approach for the analysis of semi-rigid steel frames.

5.5.3 Dynamic Tests

The experimental results and analytical simulations for model DS1 which was tested using the El-Centro earthquake record are given in Figures 5.20 and 5.21. Figure 5.20 shows the displacement response history obtained from experimental and analytical investigations whilst the comparison for the experimental and analytical base shear response is presented in Figure 5.21. Good agreement is observed between the experimental and analytical results. The analytical displacement response shows good agreement with the results of the test especially during the first 2.5 seconds of the record. The discrepancies observed when the model has achieved its maximum displacement may be attributed to the cumulative errors of the pseudo-dynamic test.

Table 5.7

Dynamic response of model DS1

Method	Record	Acceleration P.G.A.	Yield displacement	Maximum displacement	Maximum base shear
Test	El Centro	0.4 g	23 mm	76 mm	110
Analysis	El Centro	0.4 g	24 mm	73 mm	115
Differences	-	-	+ 4 %	- 4 %	+ 4.5 %

The yield and maximum time history response of this model calculated from ADAPTIC are compared with the values obtained from the test in Table 5.7. As indicated in the Table, the predicted yield and maximum response are in good agreement with the test values, with differences less than 5 % .

In general, both the displacement response and the shear forces show very good correlation between the pseudo-dynamic test results and the non-linear dynamic analysis simulations.

5.6 Remarks

In this Chapter, an analytical bilinear model for predicting the moment-rotation curve of the top and seat angles with double web angles connection is presented. The key parameters which influence the behaviour of the moment-rotation curve for this type of connection are identified. Analytical results, using the proposed bilinear model in the non-linear finite element program ADAPTIC, are in good agreement with the results of momotonic, cyclic and dynamic tests.

It is therefore concluded that by incorporating the proposed bilinear model into ADAPTIC the latter may be used as an effective tool for the inelastic analysis of semi-rigid steel frames with top and seat angles with double web angles connections. Consequently, this program is utilised for carrying out the parametric study described in Chapter 6 to examine the real behaviour of semi-rigid steel frames and the influence of the flexibility of this type of connection on the overall behaviour.

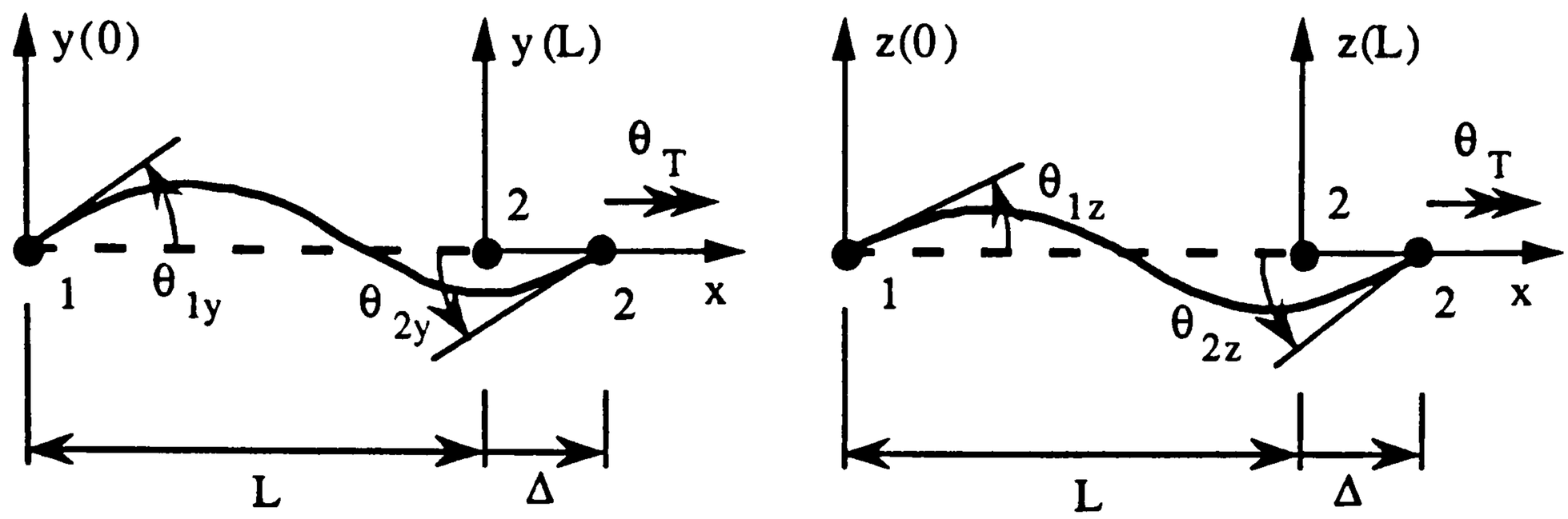

Figure 5.1 Chord freedoms of the cubic formulation (Izzuddin, 1990)

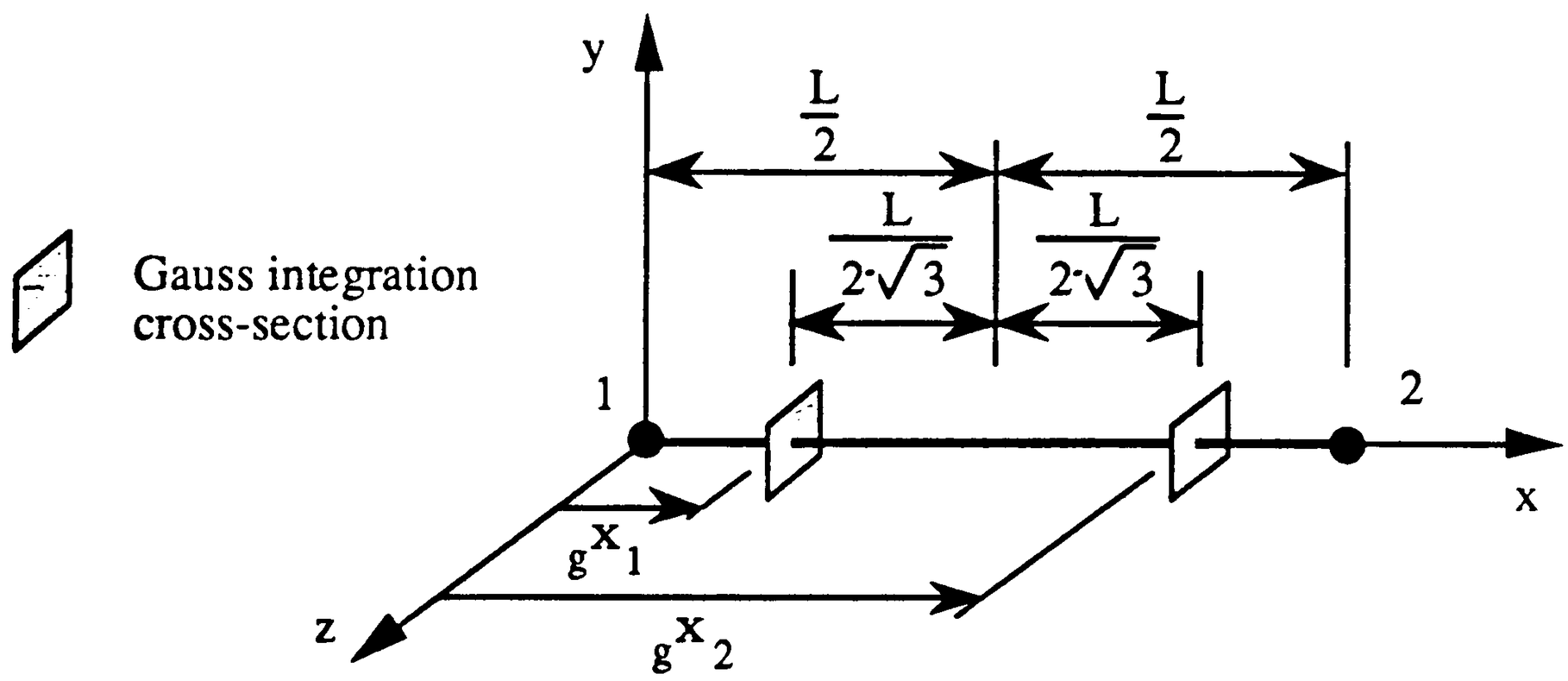

Figure 5.2 Location of the two Gauss integration sections (Izzuddin, 1990)

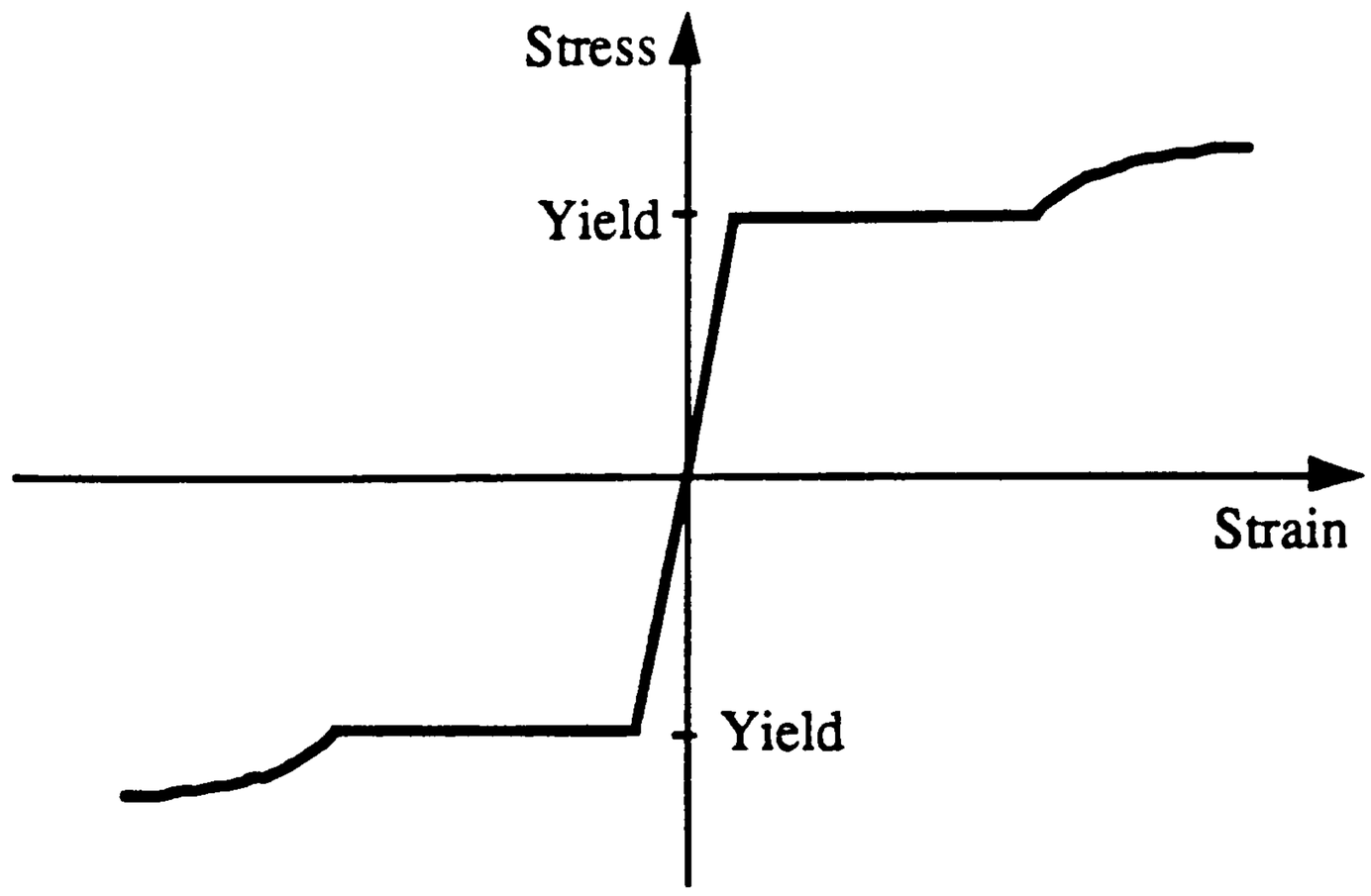

Figure 5.3 Virgin monotonic response of mild steel (Izzuddin, 1990)

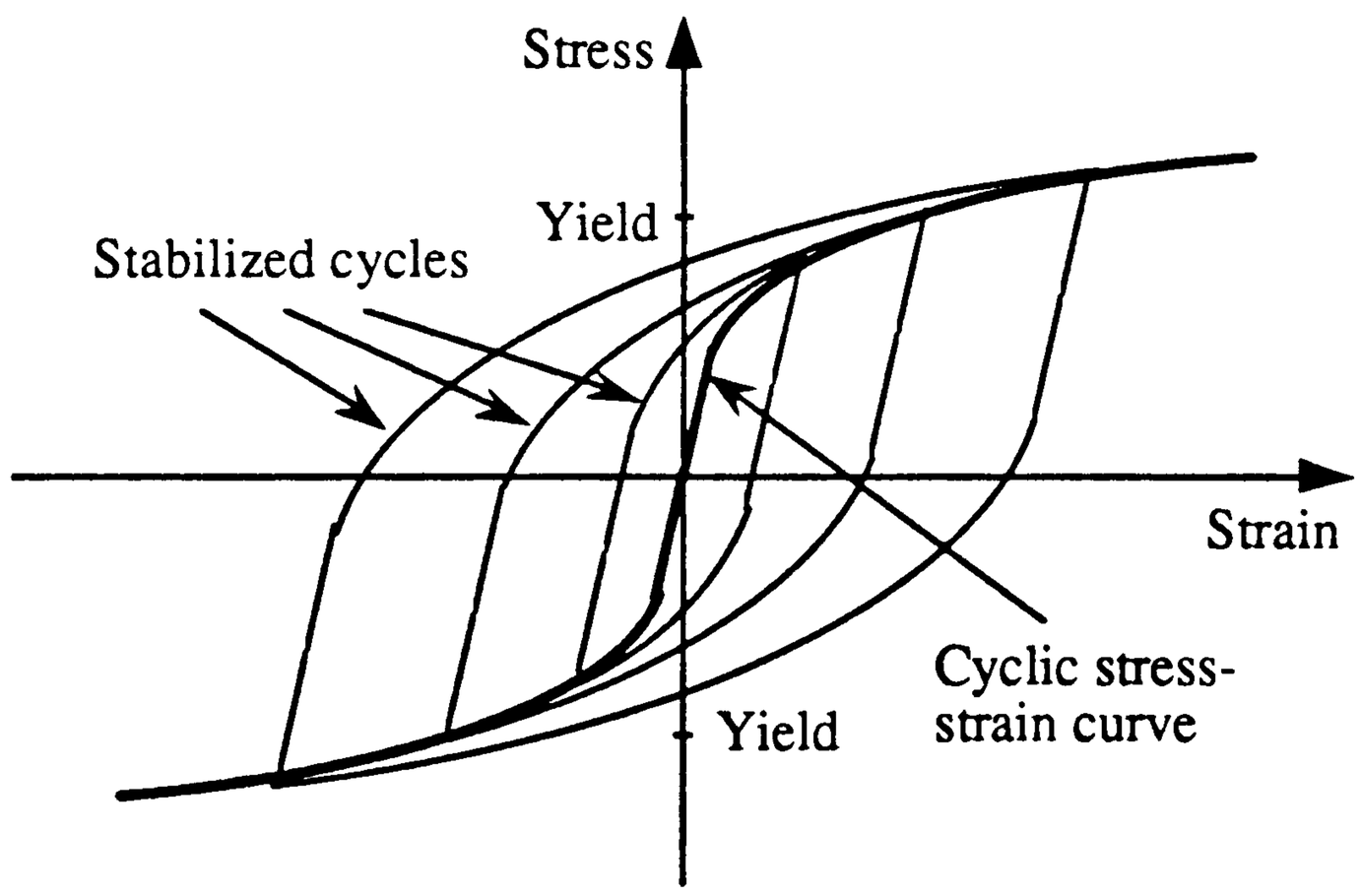

Figure 5.4 Steady state cyclic response of mild steel (Izzuddin, 1990)

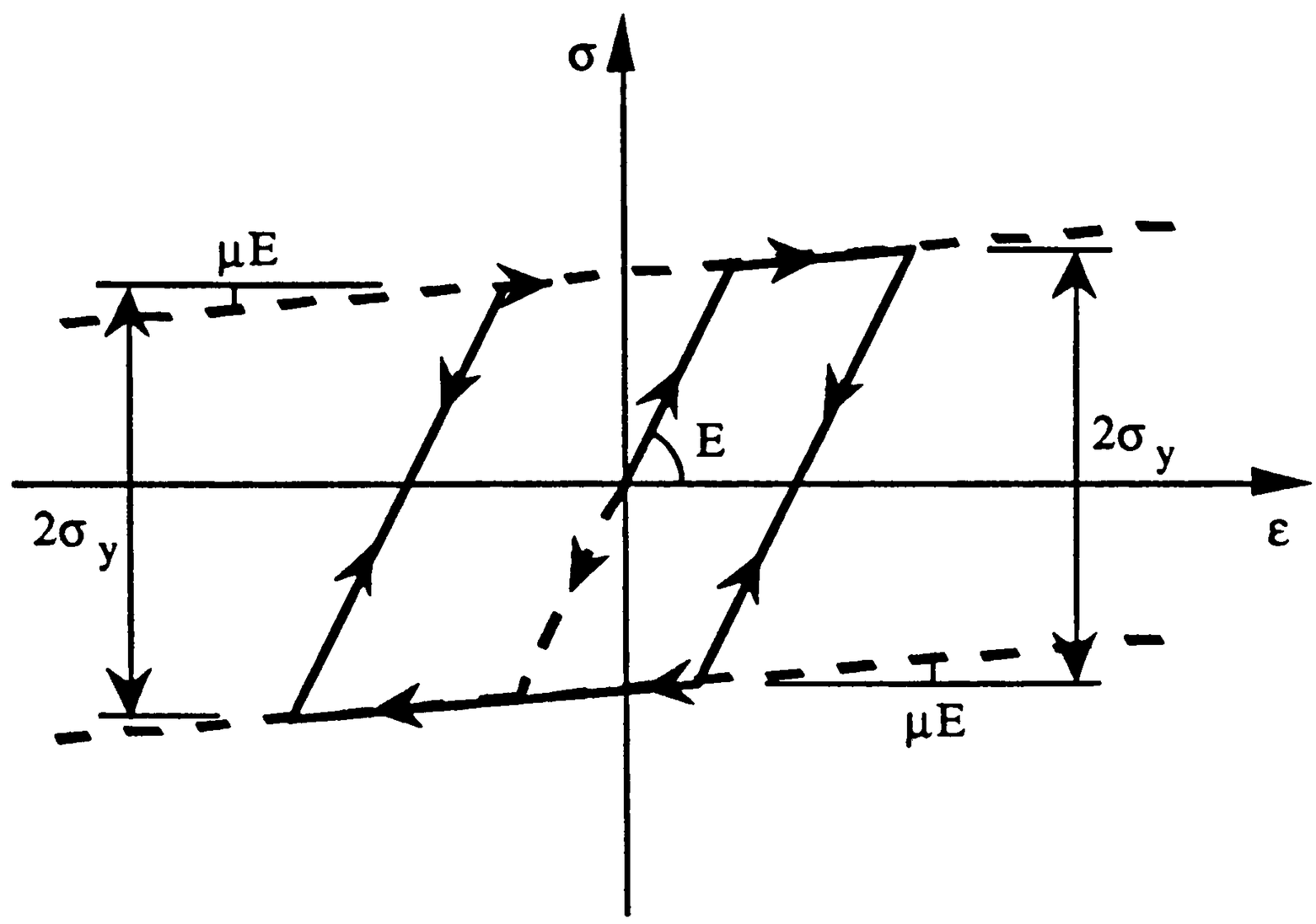

Figure 5.5 Loading and unloading paths of bilinear kinematic model (Izzuddin, 1990)

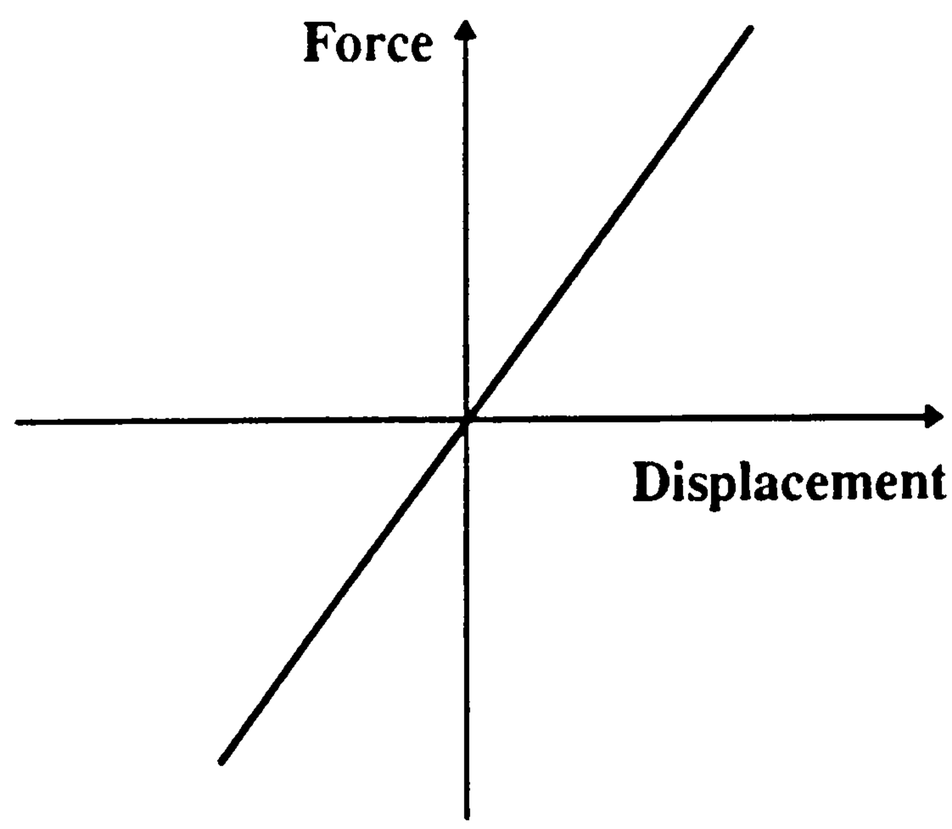

Figure 5.6(a) Linear elastic curve

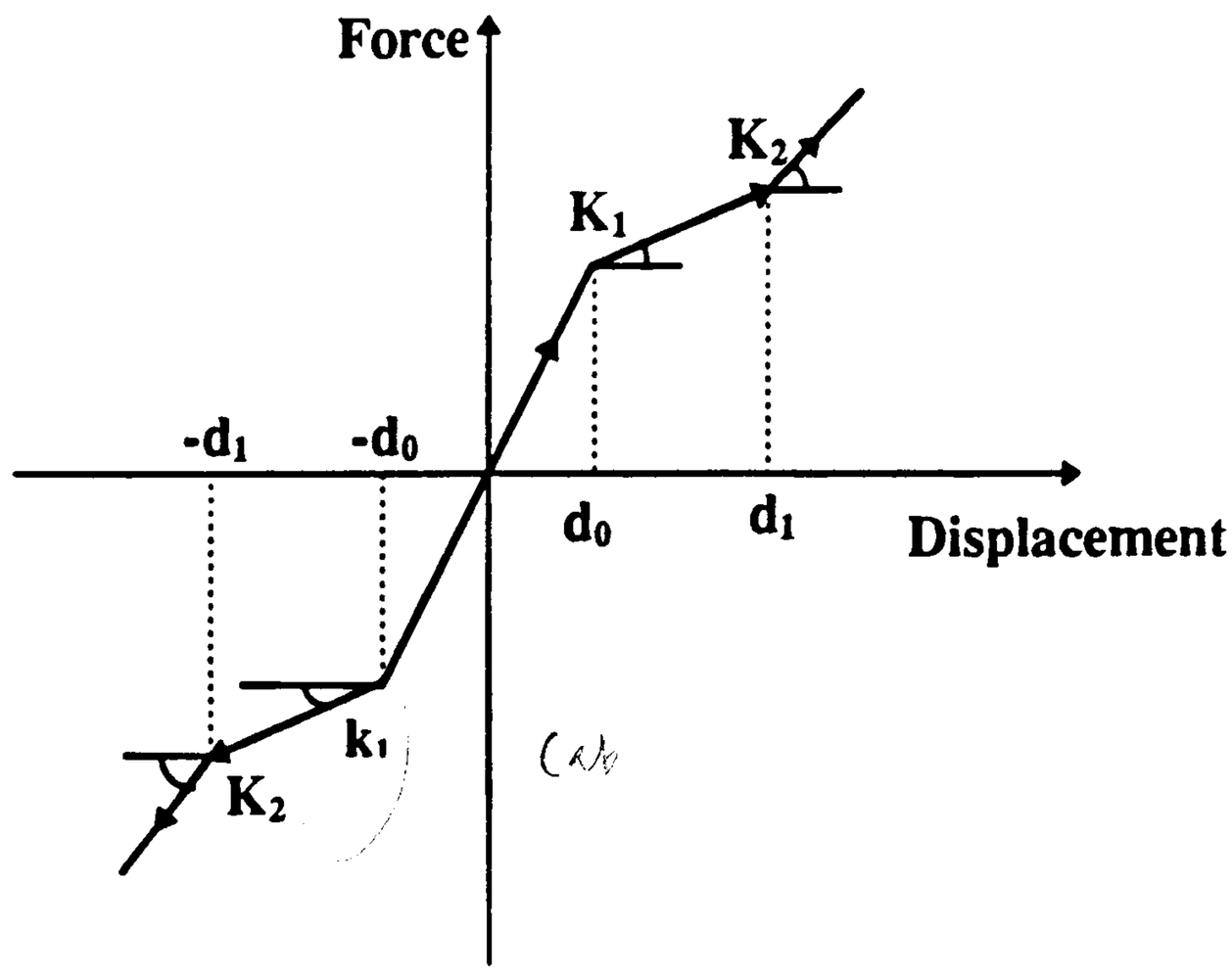

Figure 5.6(b) Trilinear symmetric elasto-plastic curve

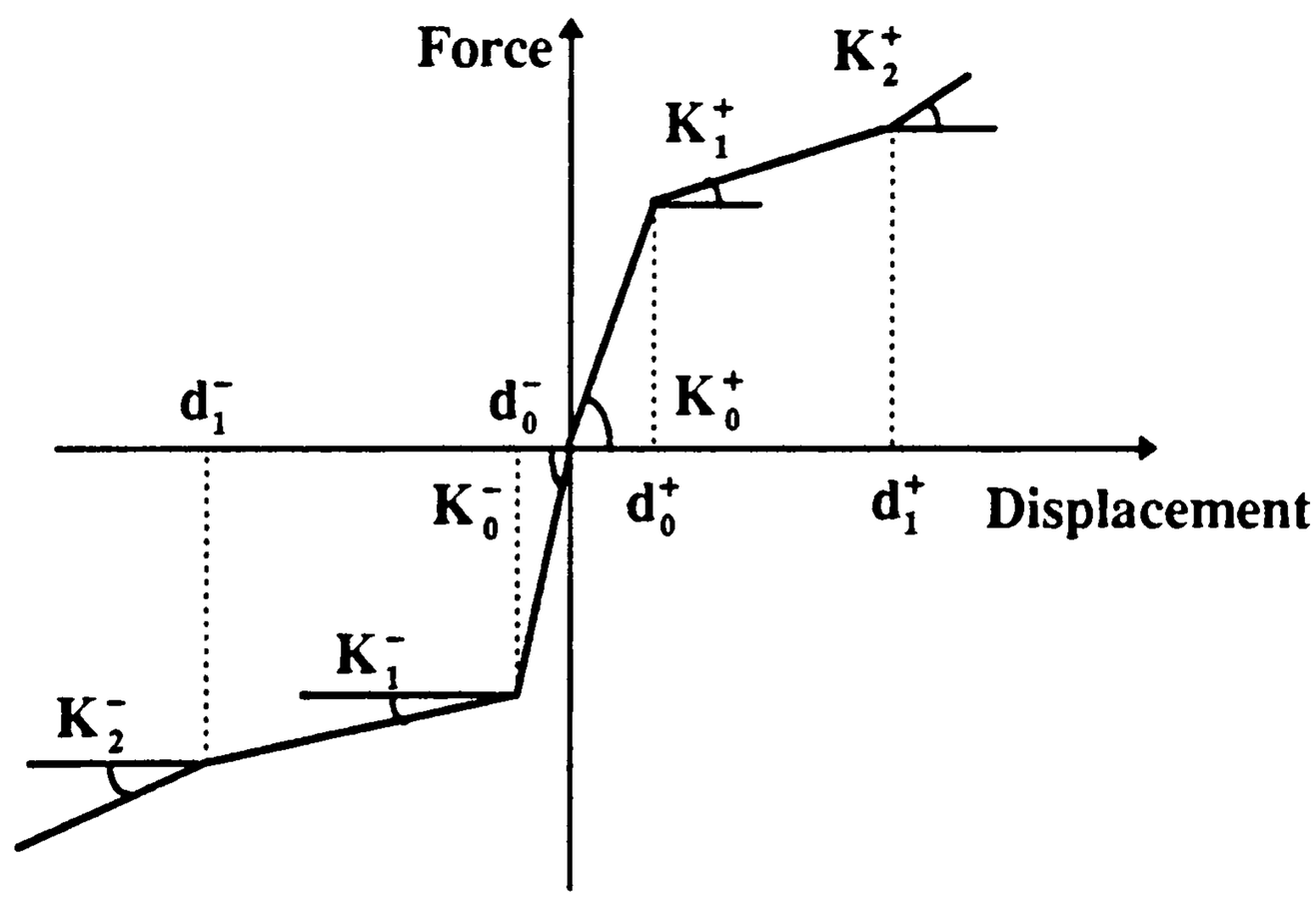

Figure 5.6(c) Trilinear asymmetric elasto-plastic curve

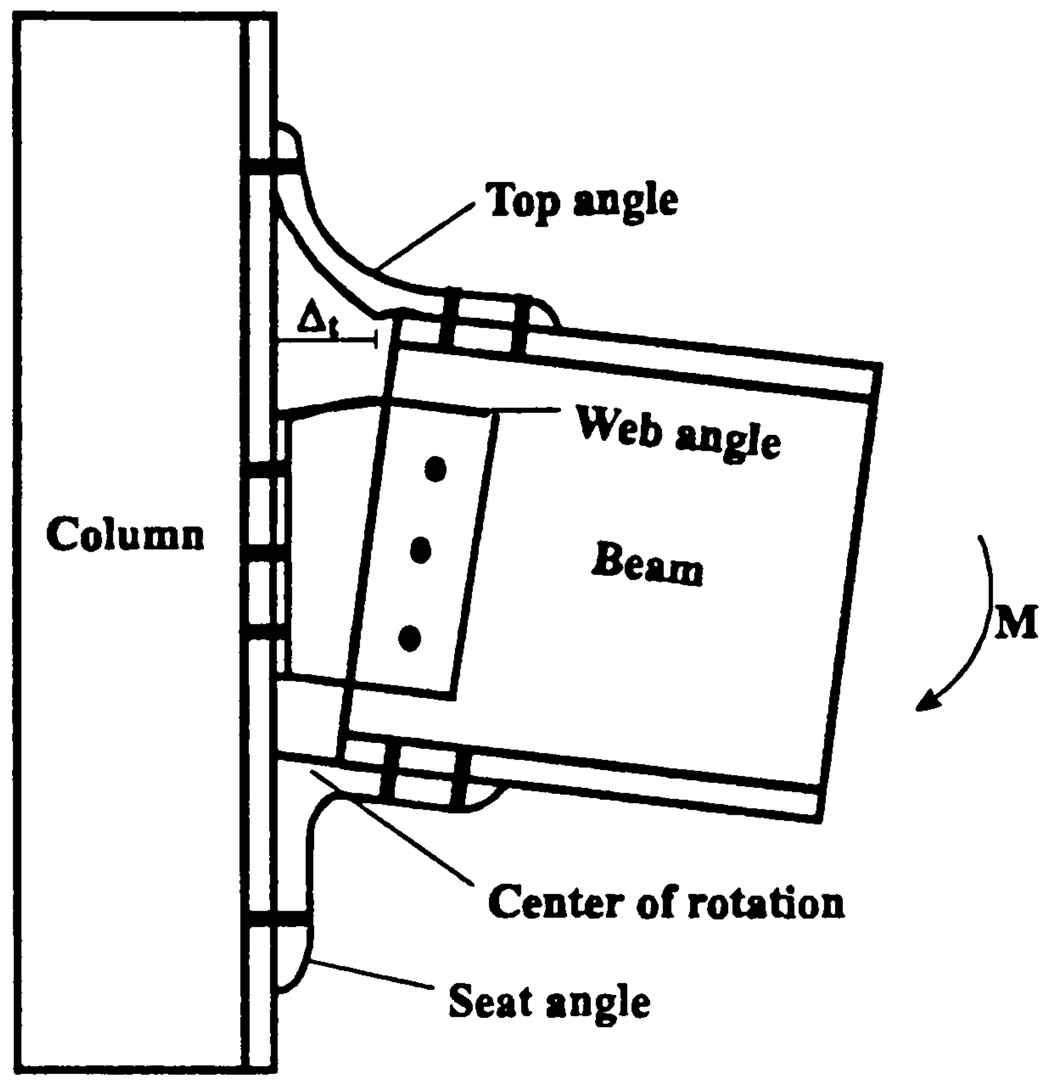

Figure 5.7 Deflected pattern of top and seat angle connection with double web angle

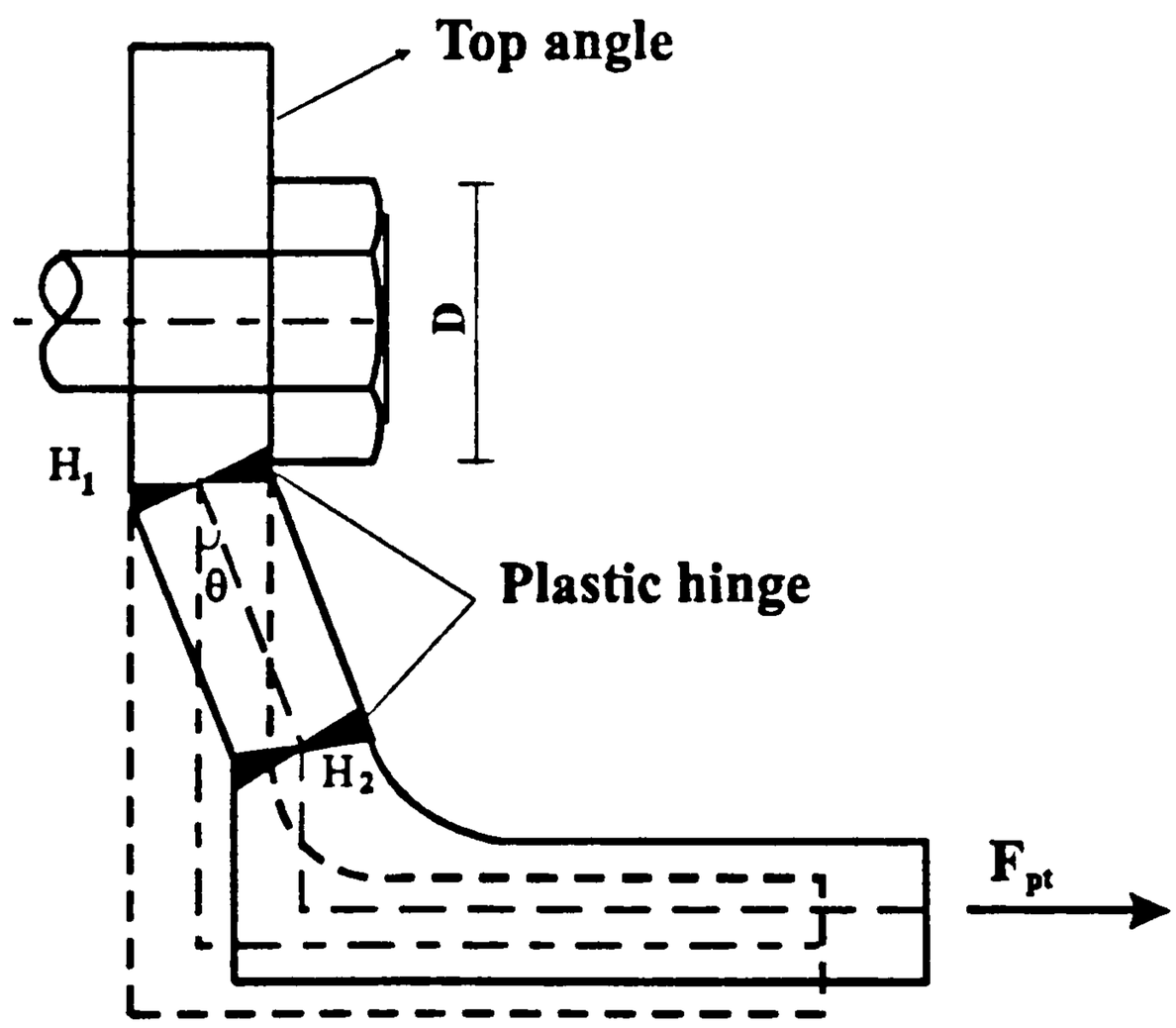

Figure 5.8 Mechanisms formed in top angle

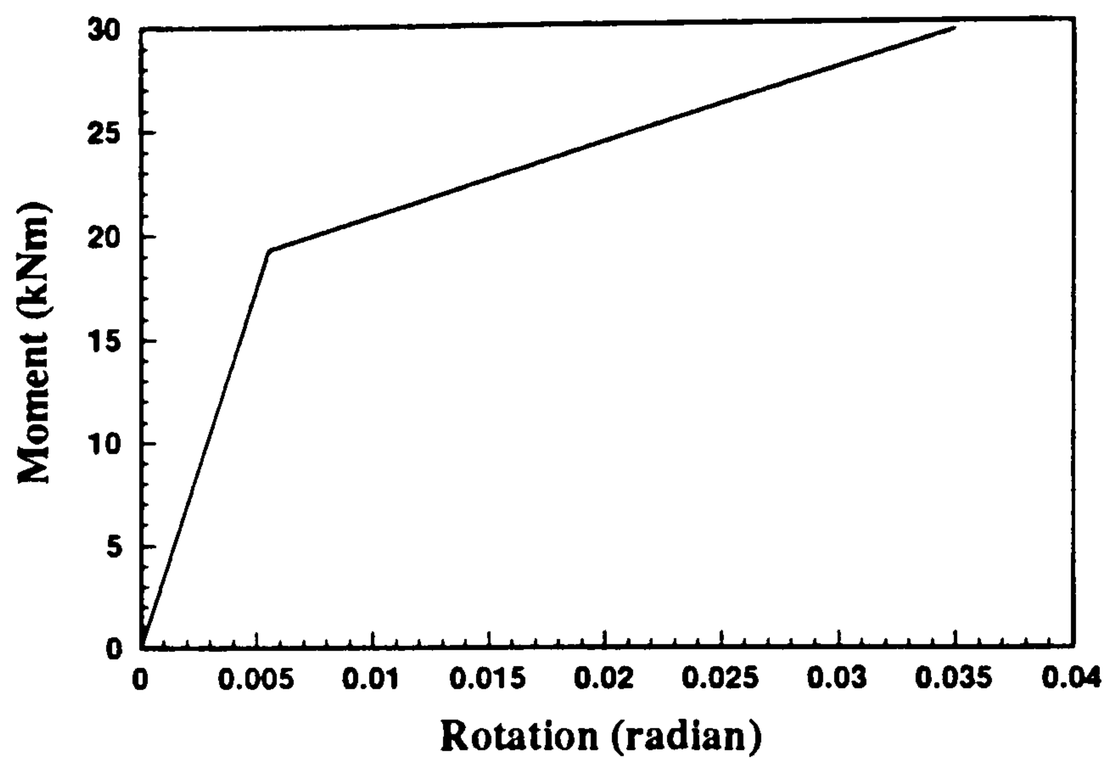

a) Bilinear moment-rotation curve of connection for model CS1

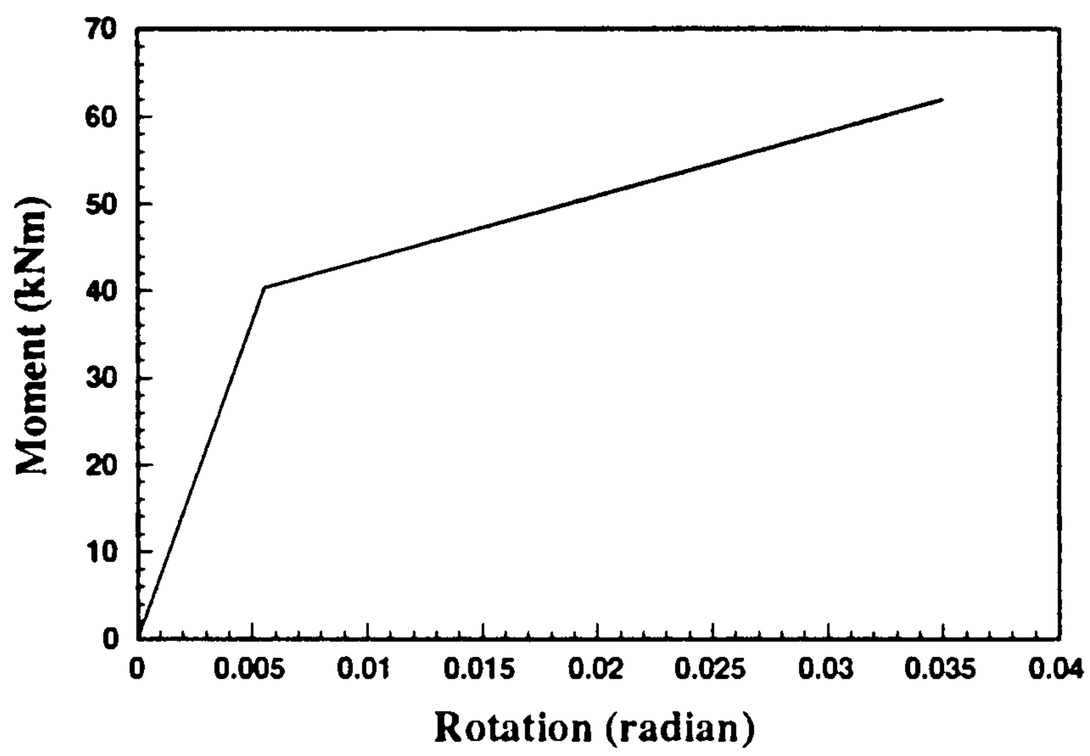

b) Bilinear moment-rotation curve of connection for model CS2

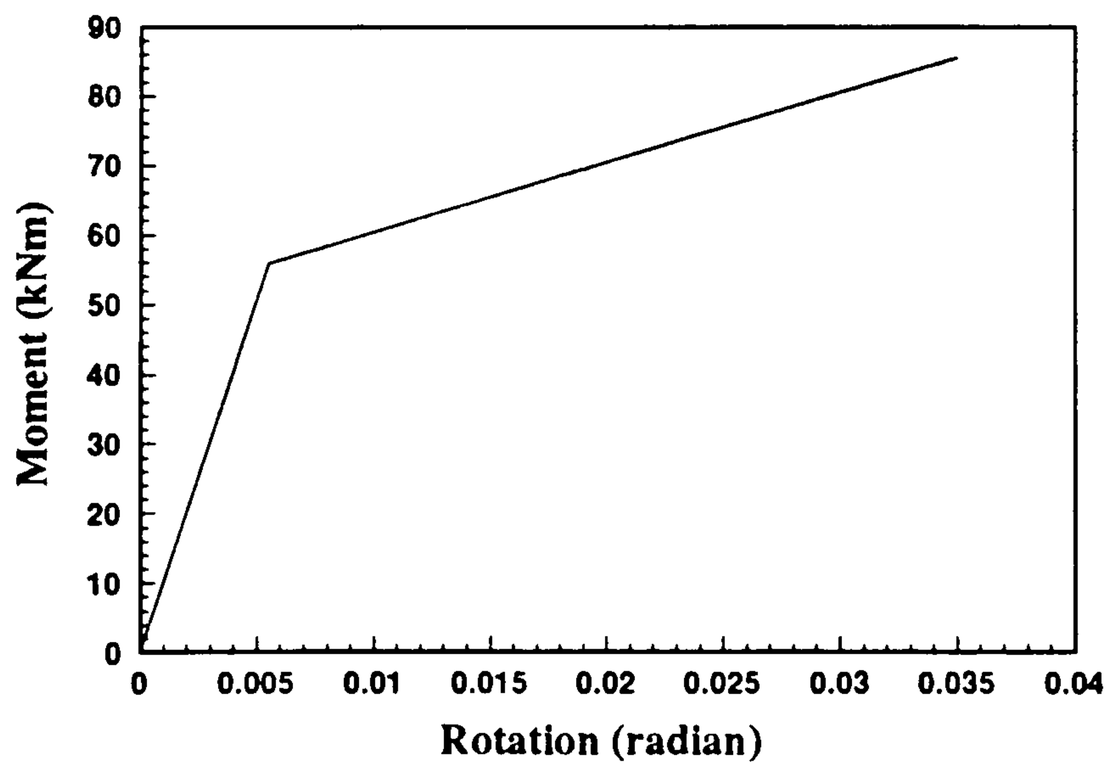

c) Bilinear moment-rotation curve of connection for model CS3

Figure 5.9 Proposed bilinear moment-rotation for three models

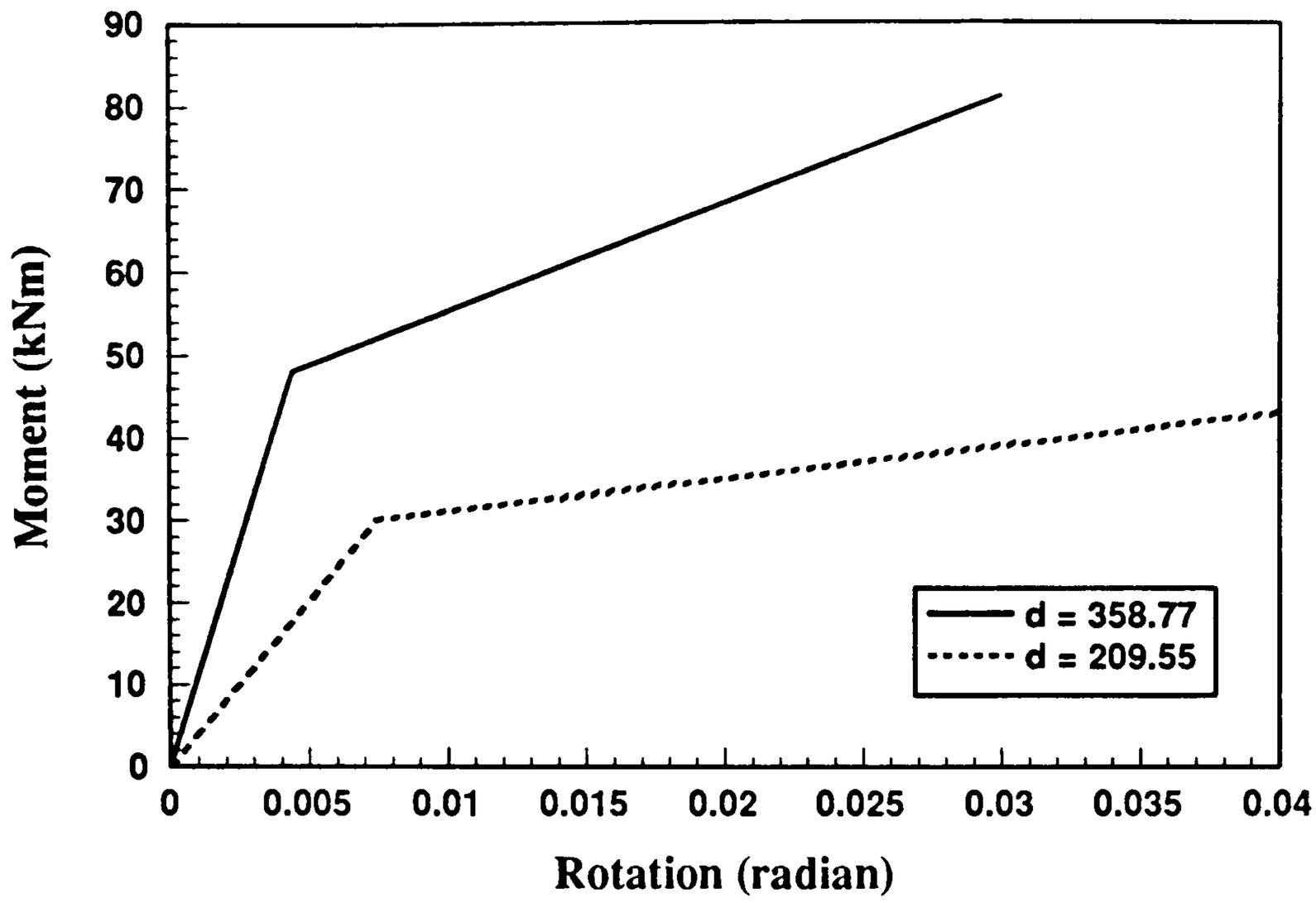

Figure 5.10 Comparison of bilinear moment-rotation relationship of connection for models 8S5 and 14S3 with different depth of the beam

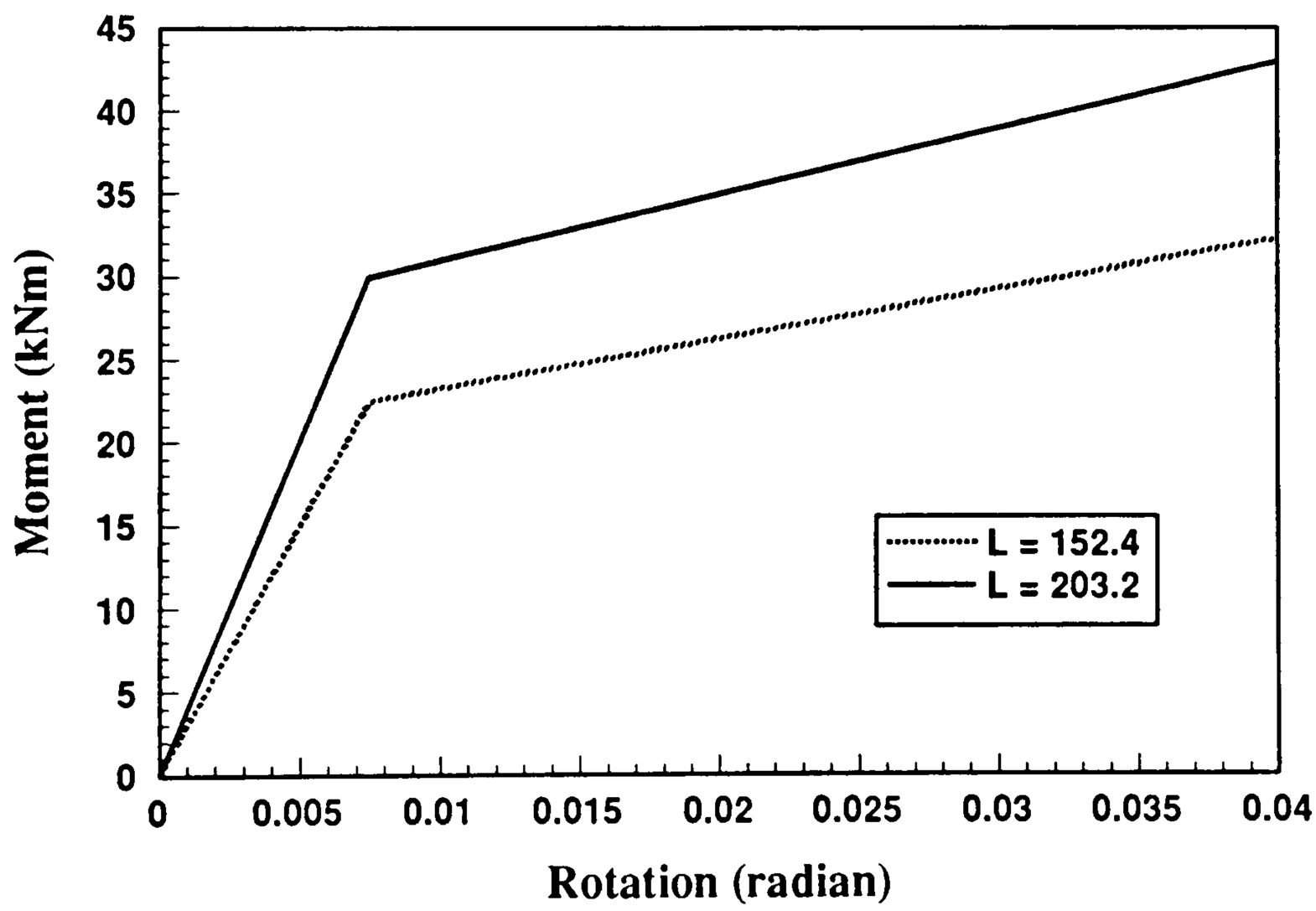

Figure 5.11 Comparison of bilinear moment-rotation curve of connection for models CS5 and CS7 with different length of the angles

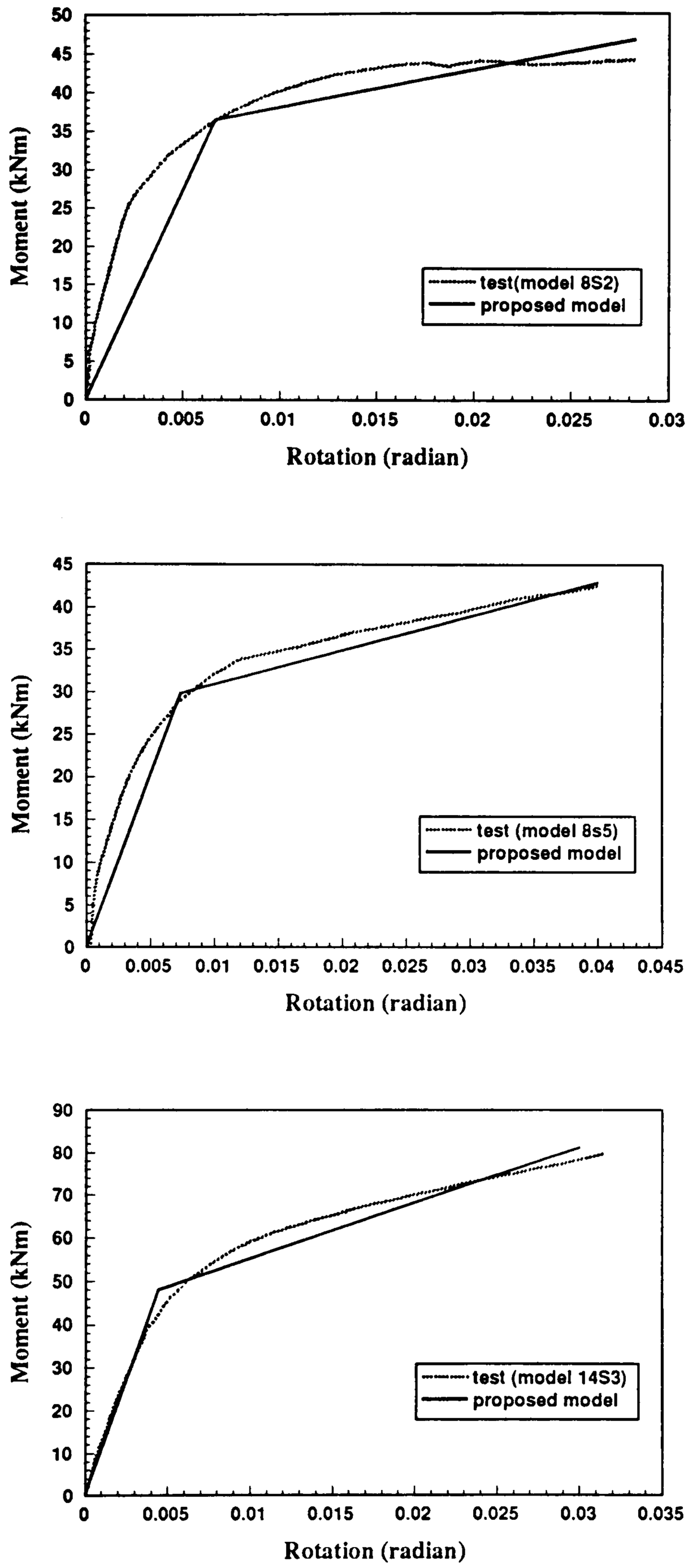

Figure 5.12 Comparison of analytical and experimental moment-rotation curve of connection for three models tested by Azizinamini et al. (1985)

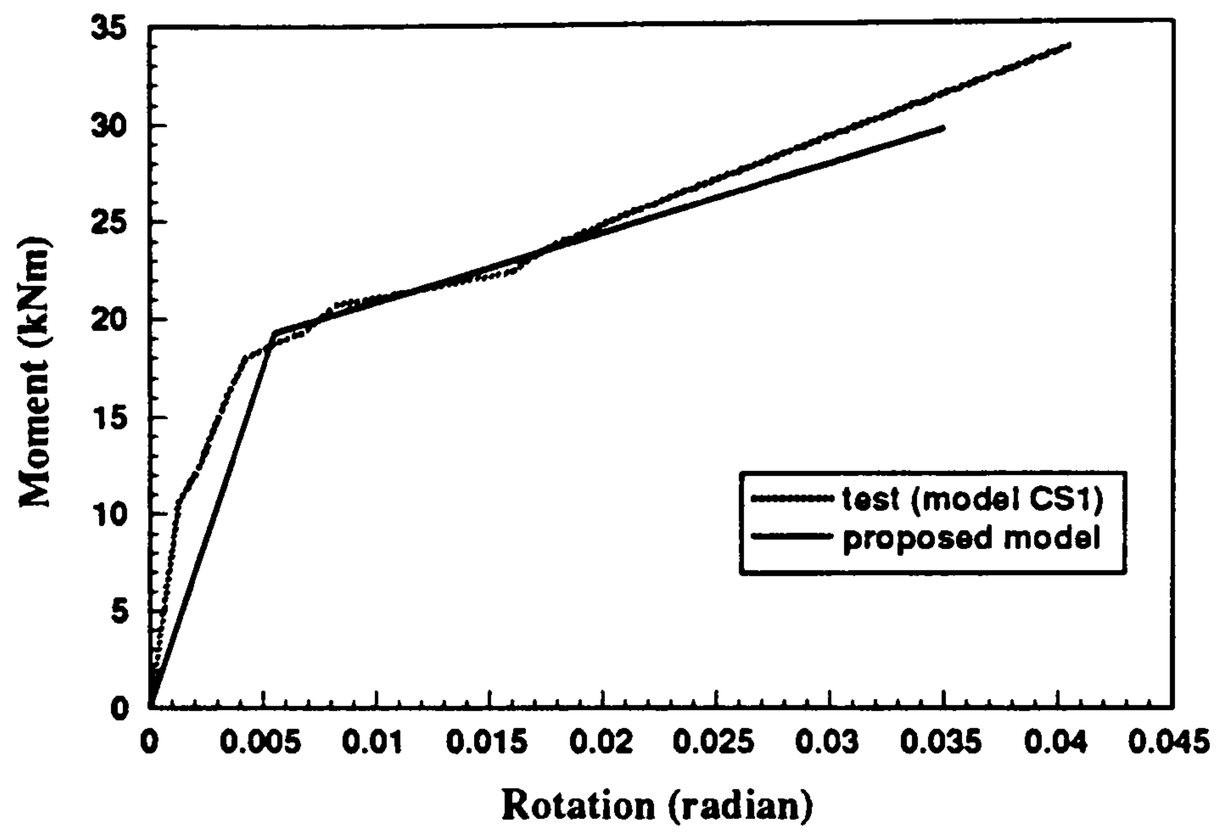

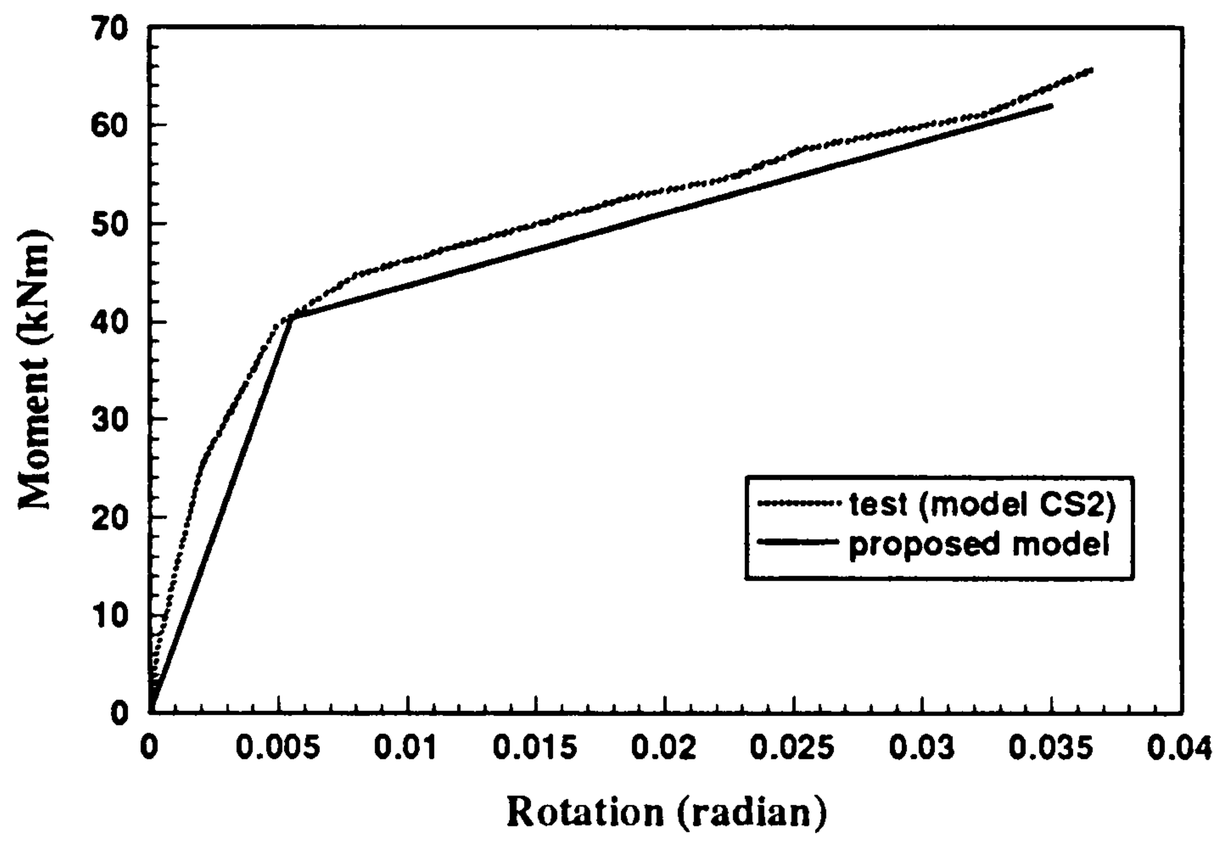

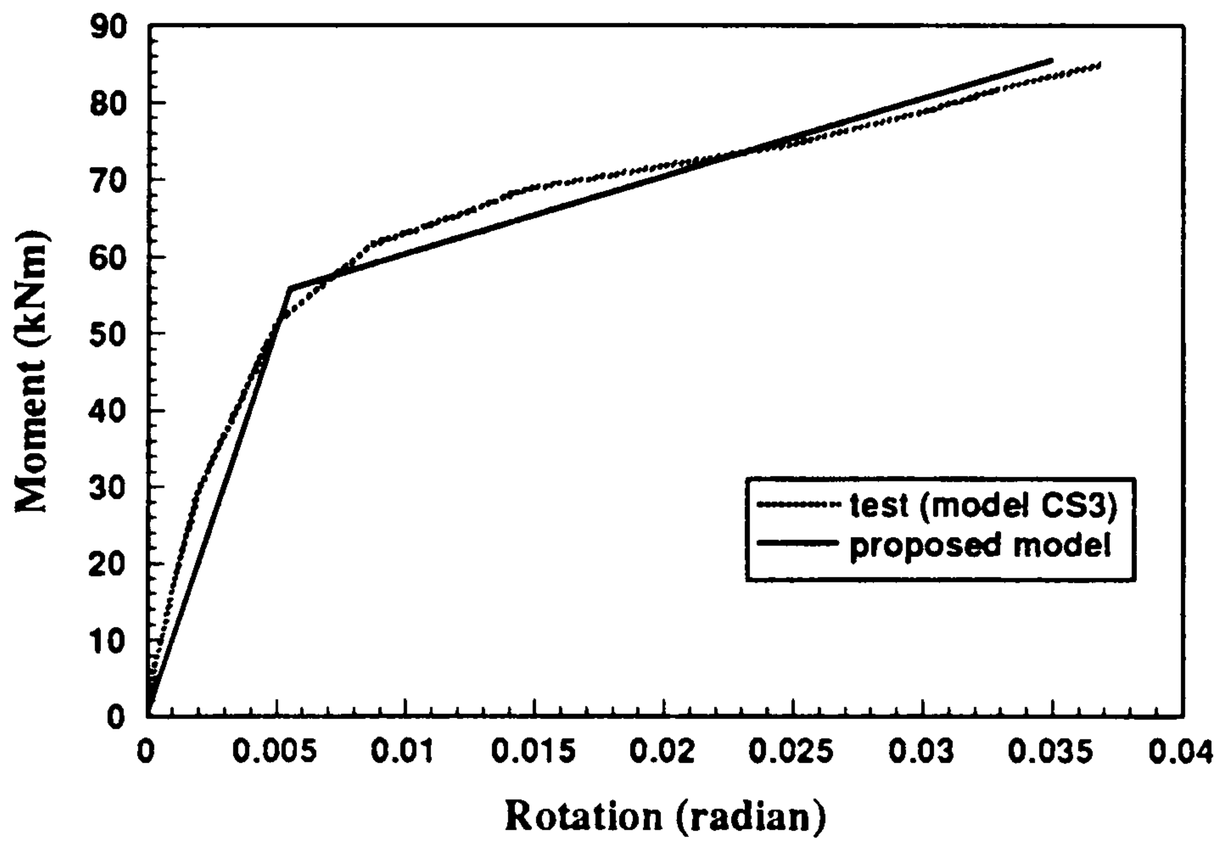

Figure 5.13 Comparison of analytical and experimental moment-rotation curves of connections obtained from three cyclic tests

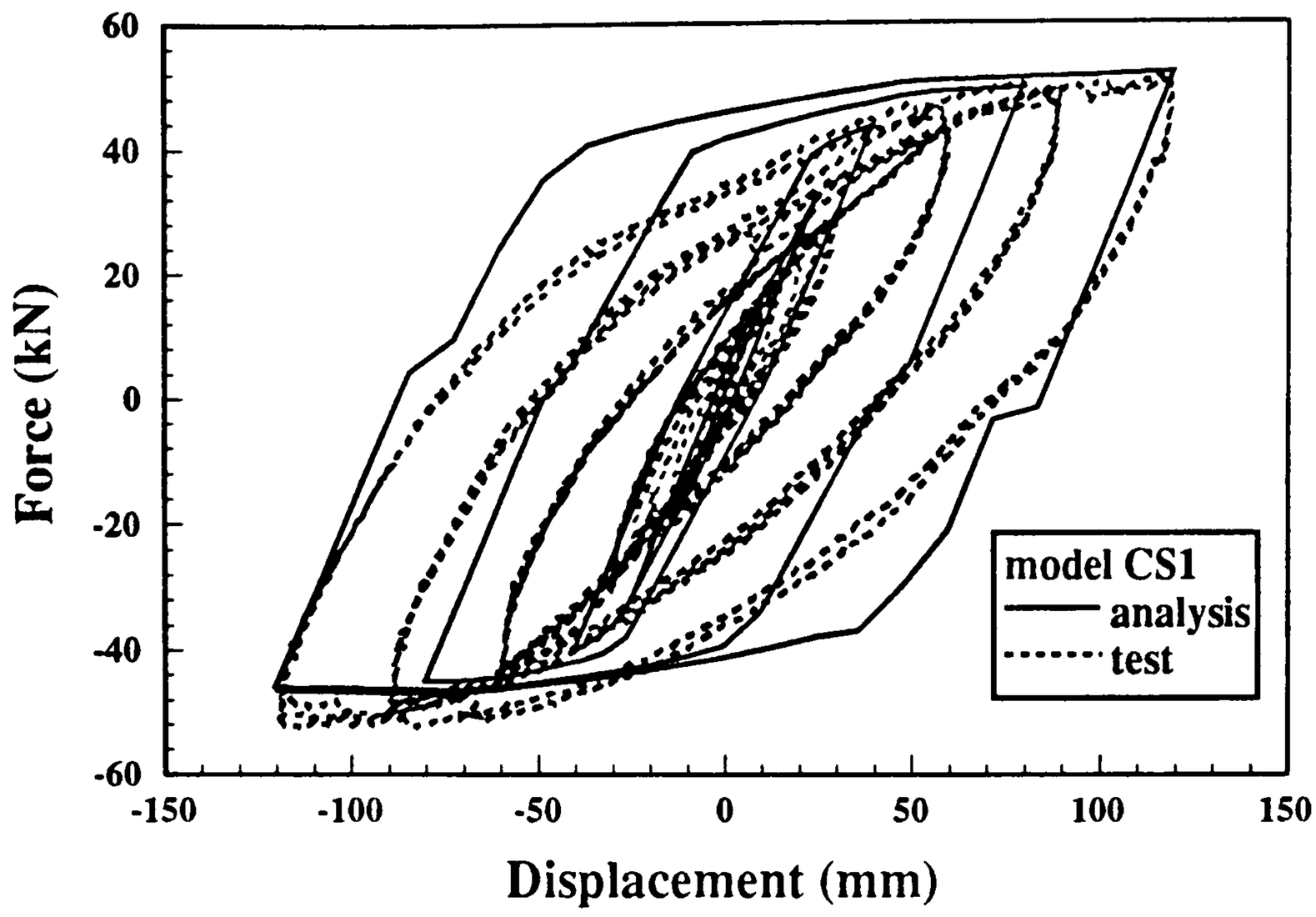

Figure 5.14 Comparison of analytical and experimental force at the second floor versus top frame displacement for model CS1

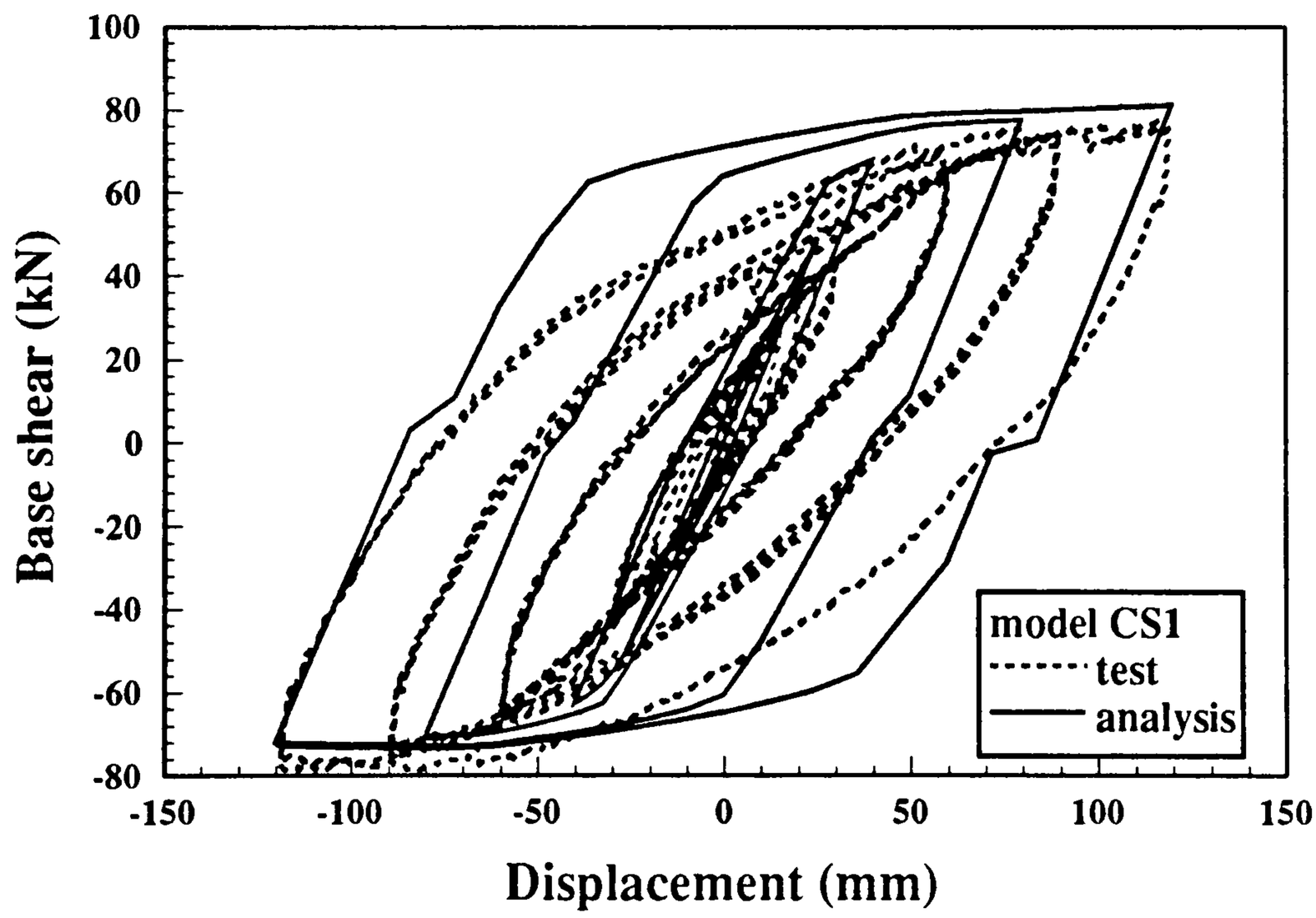

Figure 5.15 Comparison of analytical and experimental base shear versus top frame displacement for model CS1

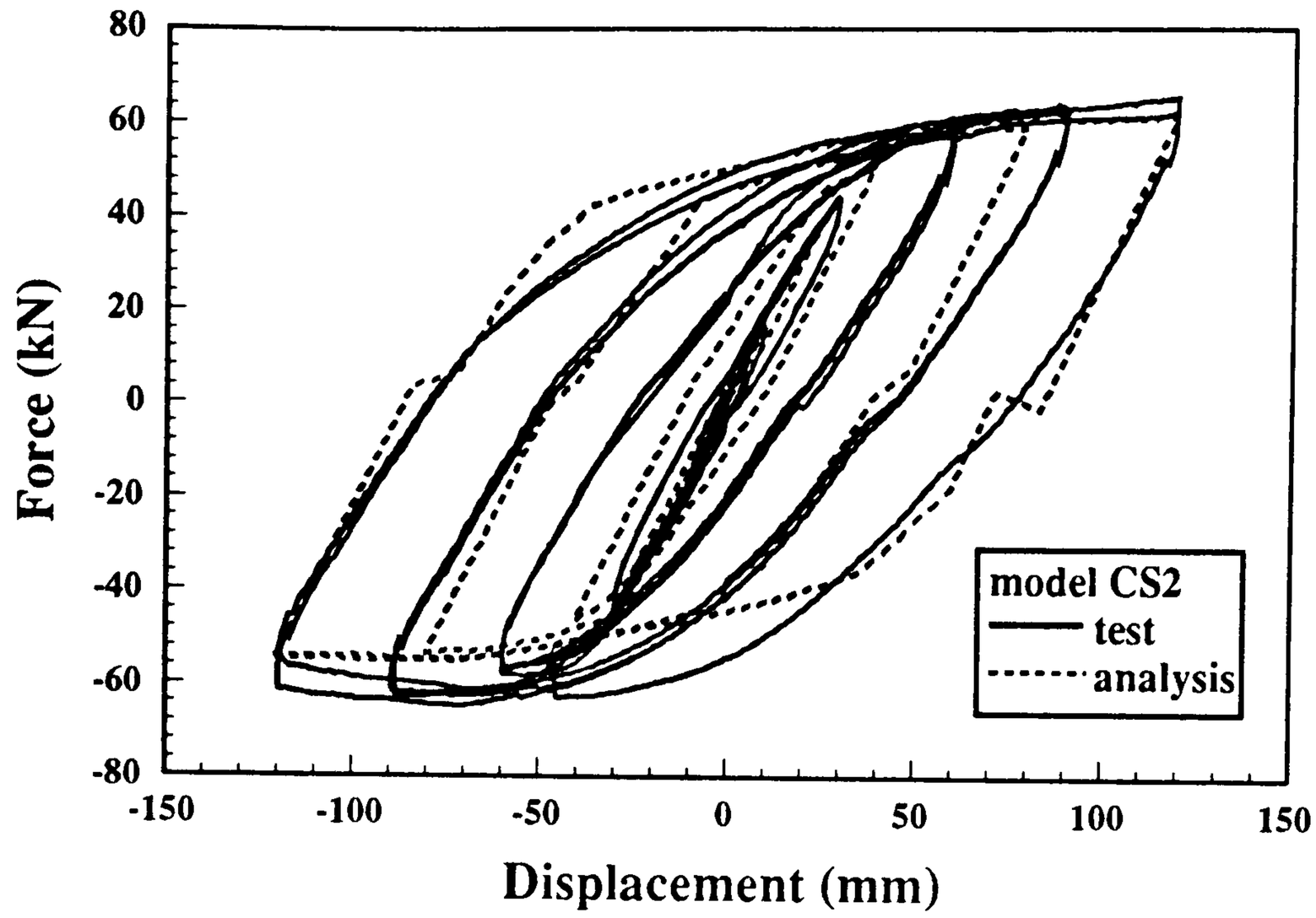

Figure 5.16 Comparison of analytical and experimental force at the second floor versus top frame displacement for model CS2

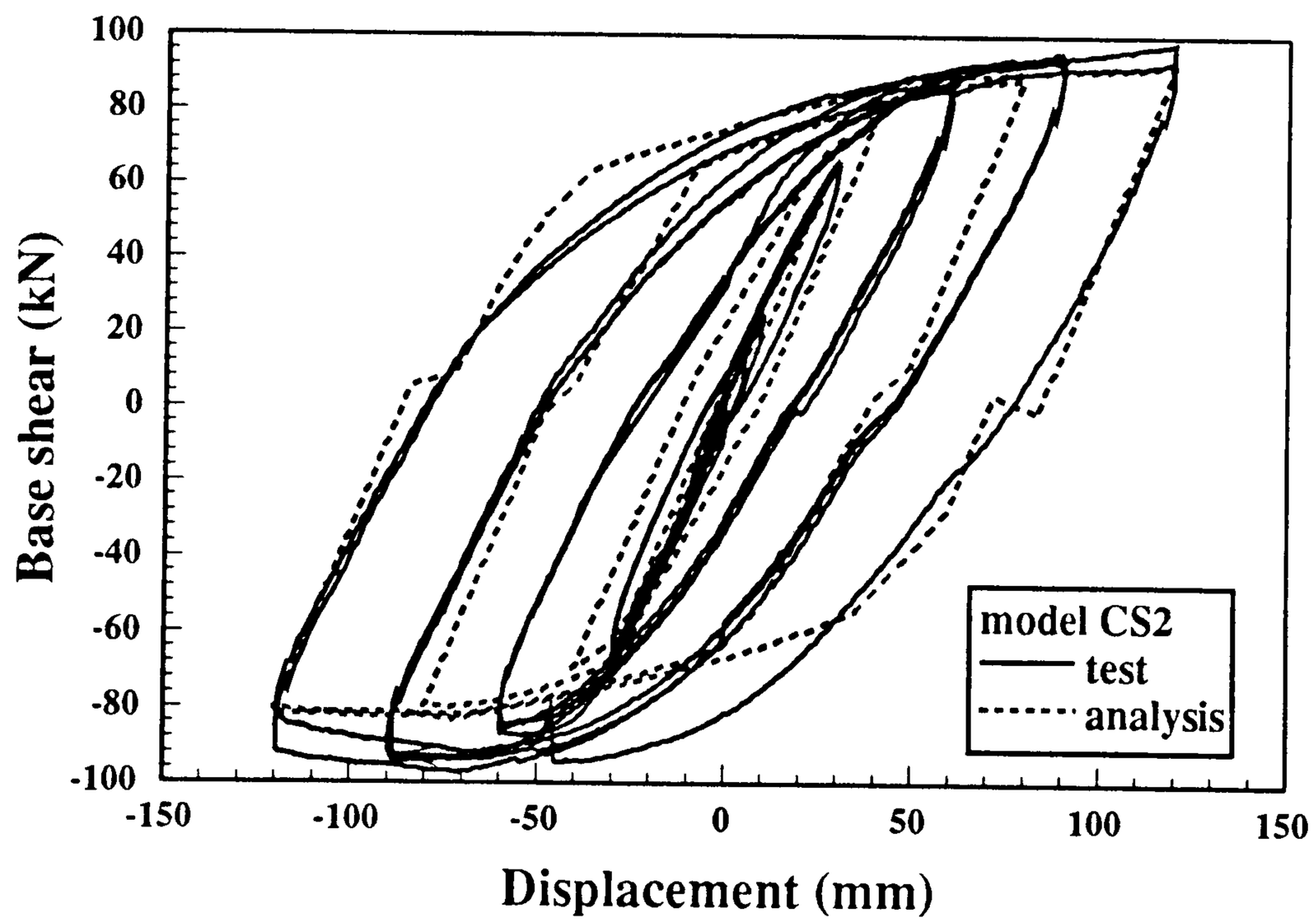

Figure 5.17 Comparison of analytical and experimental base shear versus top frame displacement for model CS2

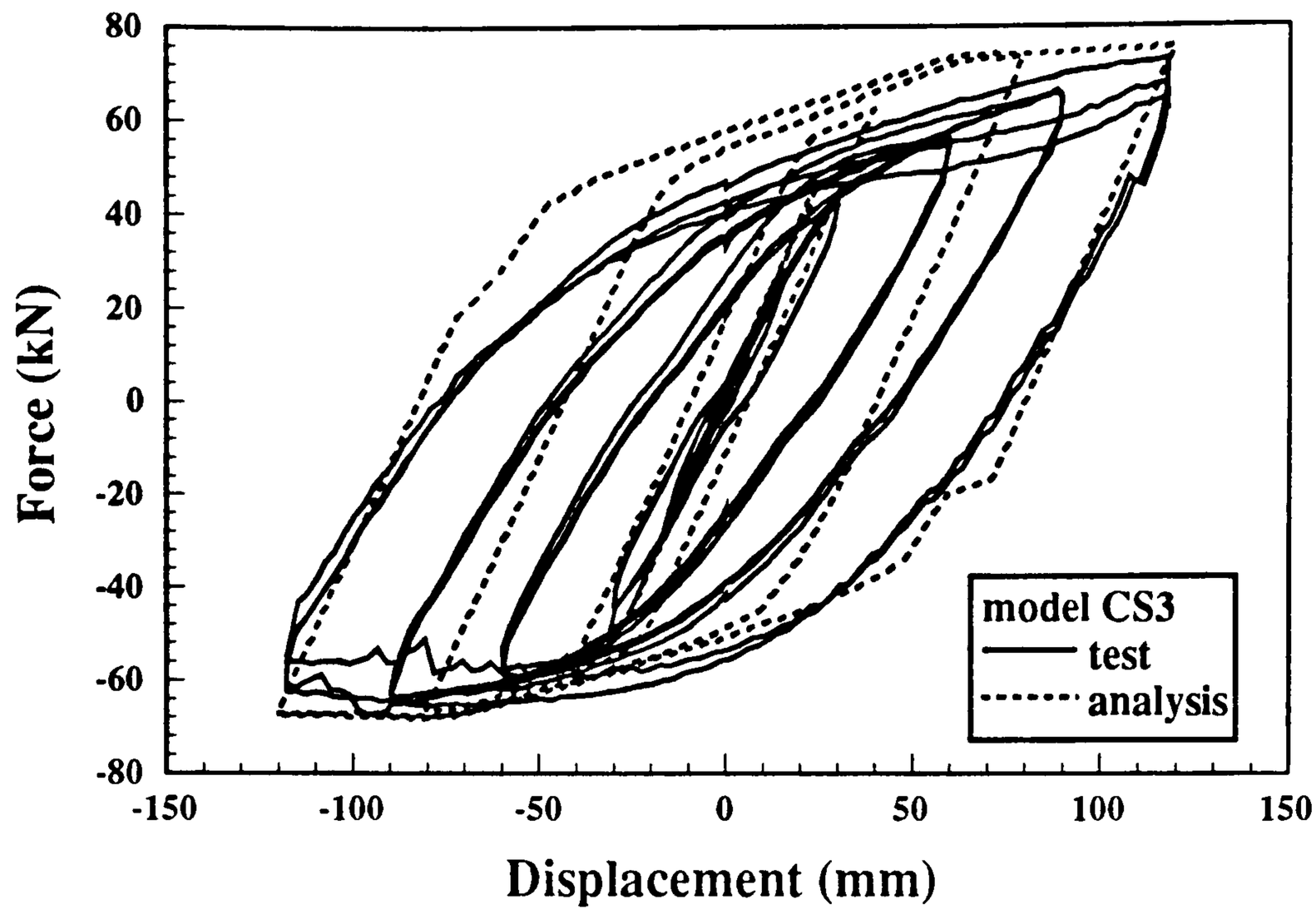

Figure 5.18 Comparison of analytical and experimental force at the second floor versus top frame displacement for model CS3

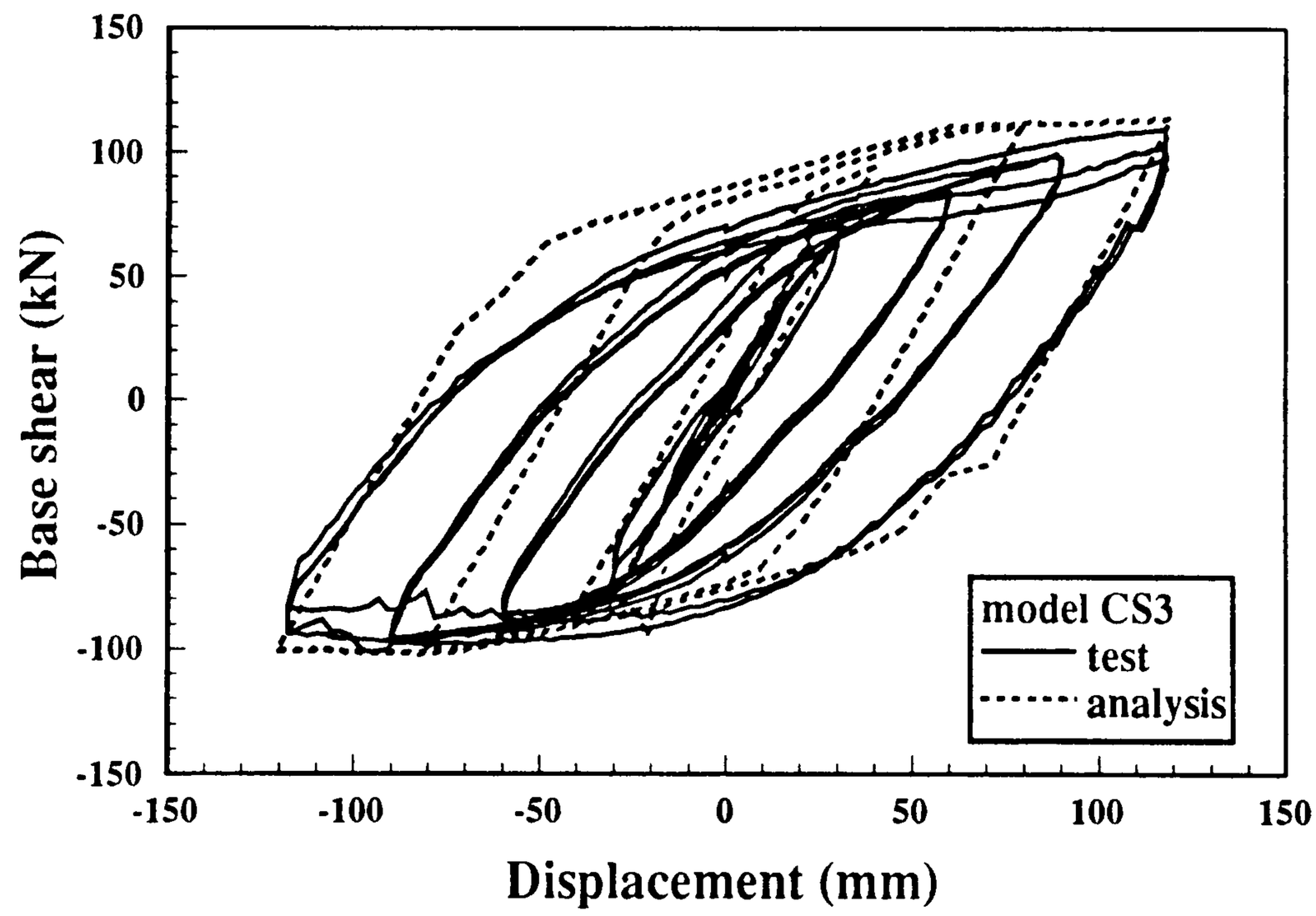

Figure 5.19 Comparison of analytical and experimental base shear versus top frame displacement for model CS3

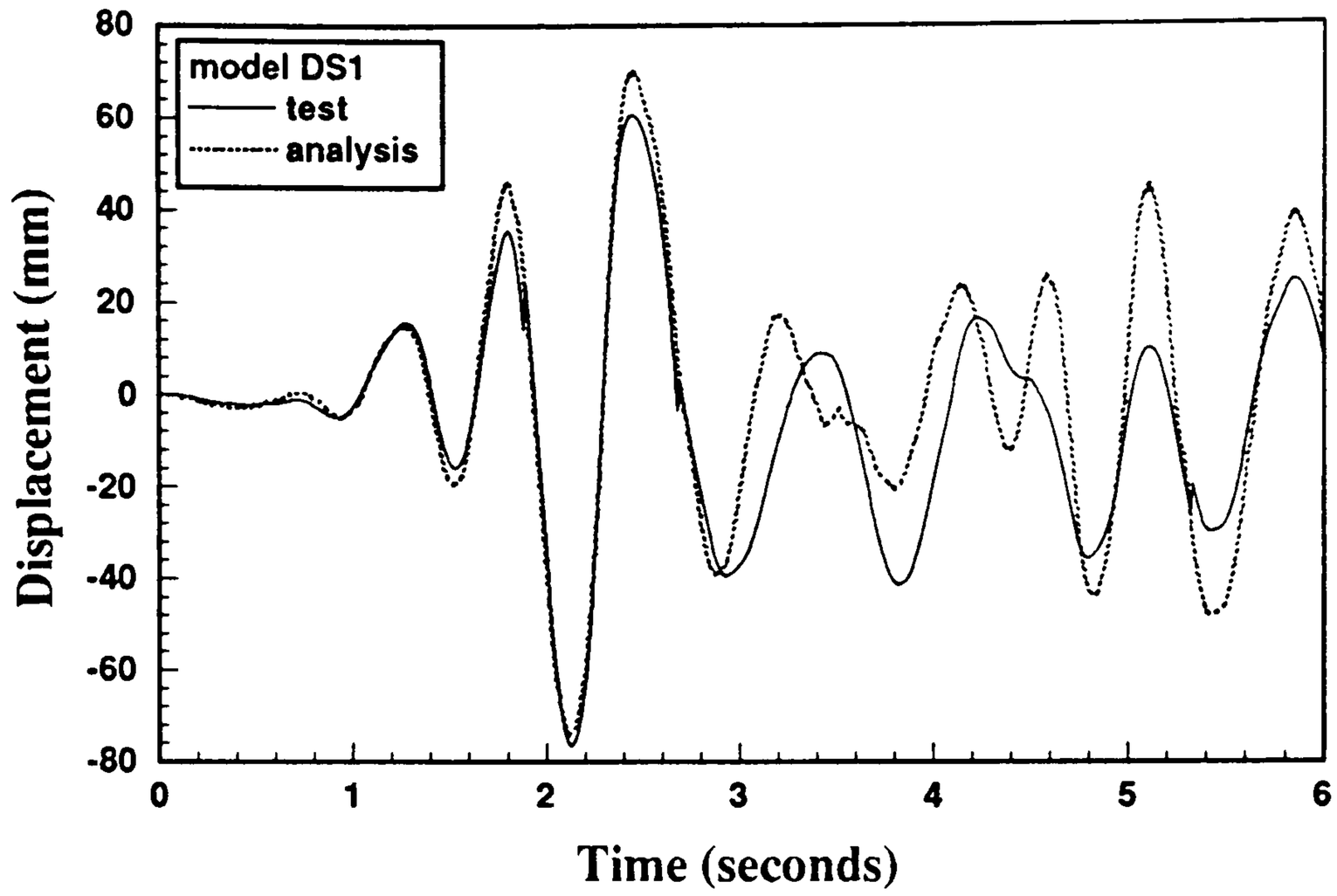

Figure 5.20 Comparison of experimental displacement response at the second floor with analysis for model DS1

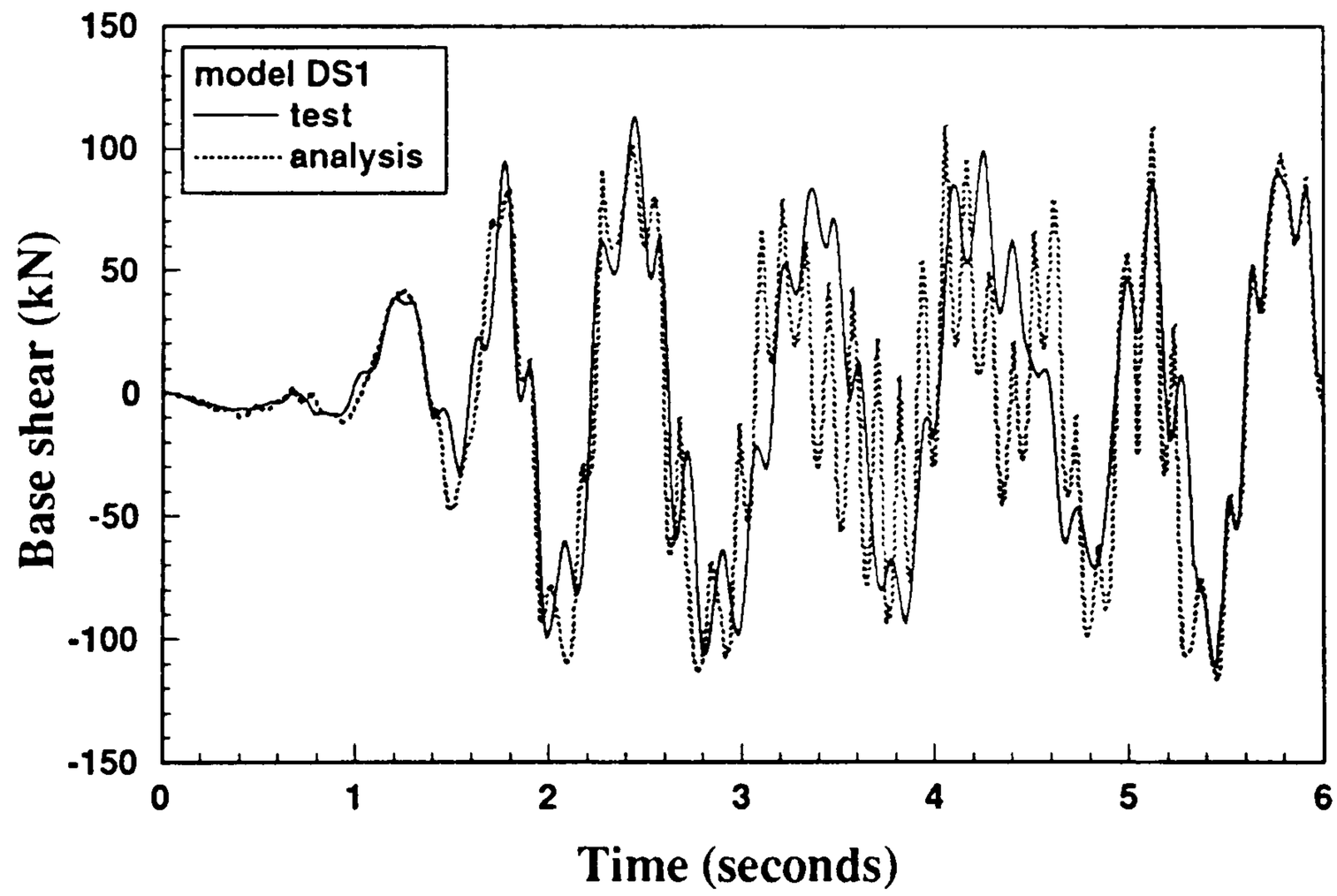

Figure 5.21 Comparison of experimental base shear response with analysis for model DS1

CHAPTER 6

6. ANALYTICAL PARAMETRIC STUDY

6.1 Introduction

As noted previously, one of the aims of the experimental work was to investigate the influence of the flexibility of semi-rigid connections on the overall behaviour of steel frames. In this experimental programme, three semi-rigid frames with different connection capacities were used for the cyclic tests and one for the dynamic test. In the dynamic test, the frame was subjected to the El-Centro time history record.

It is noted that the seismic behaviour of this type of structure is influenced by many parameters such as the geometric and strength properties, the dynamic characteristics of the structure and the frequency content of ground motions. These parameters were not included in the experimental work. However, in a effort to consider the effect of such parameters on the behaviour of semi-rigid steel frames, a parametric study was carried out and the results are presented in this chapter.

It was shown in Chapter 5 that the computer programme ADAPTIC, including the proposed bilinear moment-rotation curve for the connection, is especially suited to predicting the dynamic response of semi-rigid steel frames. It stands to reason, therefore, that through correlation between the analytical and experimental results this advanced tool can be used with confidence in conducting accurate dynamic analyses.

The primary purpose of this study is to examine the seismic behaviour of partial strength semi-rigid steel frames with top and seat angles and double web angle connections. In order to investigate the influence of the dynamic characteristics of the frames and time history records, a number of frames with different configurations is studied. All the frames in the study are subjected to different earthquake records. As a result of this study, the behaviour factors of partial strength semi-rigid steel frames are

evaluated and the dynamic response of these frames compared with both rigid and full strength semi-rigid frames.

6.2 The Design of Semi-rigid Steel Frames

In accordance with the design recommendations given in many codes, e.g. EC8 and UBC, it is accepted that ductile behaviour and inelastic energy absorption may occur in the beams and ground floor columns in which flexural hinges may form. Therefore, it was recommended that inelastic behaviour in the connection should be prevented. To ensure that these connections remained elastic during an earthquake, the connection must be strong enough to enable the development of the beam strength in flexure.

The basis of the design philosophy depicted in this thesis for semi-rigid steel frames in seismic zones is that the connection is permitted to experience inelastic deformation and such deformation will occur prior to inelastic behaviour in the beam or column. By adopting this design approach, all of the ductile elements in the beam-column connection will contribute to the required ductility. It is noted that this design method does not depart from the basic design philosophy for the moment resisting steel frame in seismic areas, i.e. it prevents non-ductile failure. The following sections describe the seismic design of semi-rigid steel frames based on this modified capacity design approach.

6.2.1 Design of Beam and Column Sections

In EC8, moment resisting steel frames are designed using the strong-column/weak-beam approach. At a particular connection the flexural plastic capacity of the column should be larger than the flexural plastic capacity of the beams. The primary reason underpinning this assumption is to avoid damage of the columns, which are essential for vertical stability.

In steel frames containing partial strength semi-rigid connection, the connection are permitted to yield before the beams attain their plastic moment capacities. Hence, the maximum moment transferred from the framing beams to the column is less than the

moment capacity of the beams and is related to the moment capacity of the connections.

6.2.2 Effective Length of Column

The most common approach for taking into account the effect of rigidity of the connection on the buckling length of the member in the design process is to use the concept of effective column length. This effective length may be defined as the length of an equivalent pin-ended column having the same load-carrying capacity as the member under consideration provided with its actual conditions of support.

In using this definition for determining the column slenderness ratio, the geometrical length L is replaced by the effective length L_E. Values of effective length factors $k= L_E/L$ for series of standard cases are provided in the codes.

In applying Appendix E of EC3 (Part 1.1) for calculating the effective length of a column in an unbraced frame, the k-factor is obtained from a chart. To use this chart, two parameters η_1 and η_2 that are related to the amount of bending stiffness provided by the members entering the connection at each end of the unbraced segment must be calculated.

To evaluate the k-factor for semi-rigid steel frames, the effect of the rigidity of the connection must be taken into account in the bending stiffness of the connected beam. This may be carried out in a simple way by multiplying the moment of inertia of the connected beam by the ratio of the moment capacity of the connection to the plastic moment of the connected beam. Alternatively, the following formula for calculating the moment of inertia, as given by Nader and Astaneh (1992), can be used;

$$I^* = I\frac{m(m+3)}{(m+2)(m+6)} \tag{6.1}$$

$$m = \frac{K_c}{(EI/L)_b} \tag{6.2}$$

Where K_e is the rotational stiffness of the connection. By replacing the beam moment of inertia with an equivalent inertia (I^*), which is determined using the approach mentioned above and calculating the parameters η_1 and η_2, the effective length of the column in semi-rigid frames can be obtained from the chart given in Appendix E of EC3 Part 1.1.

6.2.3 Panel Zone

In moment resisting frames with fully welded or full strength connections, it is suggested that the shear strength of the panel zone should be calculated using 100% of the moment capacity of the connected girders. However, the provisions of the UBC state that the panel zone shear may be calculated using 80% of the moment capacity of the connected beams. If this approach is adopted, the panel zone is then the weakest link in the system thus causing yielding to occur at an early stage. This undesirable effect may have been demonstrated in the 1994 Northridge Earthquake where cracks were detected in the panel zone. Hence, in order to protect the panel zone against extensive yielding in this type of structure, it would be advisable that the shear strength be calculated using 100% of the moment capacity of the connected beams.

In partial strength semi-rigid steel frames, the beam-column panel zone should have sufficient shear strength in order to allow the connection to undergo some inelastic deformation prior to the commencement of yielding in the top and seat angles in the connection. Moreover, the panel zone should be capable of sustaining a larger moment when compared with the moment capacity of the connection.

Based on this assumption, in semi-rigid steel frames with connections having a moment capacity between 50% to 70% of the moment capacity of the beam, it is recommended that the shear strength of the panel zone should be calculated using a value of about 80% of the beam.

6.2.4 Beam-Column Connection

As mentioned in Section 6.2.1, the connection should be designed such that it can undergo inelastic deformation before the formation of plastic hinges in the beams. In addition, the beam-column connection must be able of providing sufficient strength to resist the gravity load plus the prescribed design earthquake load.

For this purpose, the connection must be designed such that it would yield at some percentage (α) of the plastic flexural capacity of the beam. According to the classification of the connections in EC3, the value of (α) may vary between 30% and 70% when partial strength semi-rigid connections are considered.

It is noted that since most of the inelastic deformation takes place in the connections, there will be a high demand on the ductility of semi-rigid connections. To ensure that a connection is ductile enough and has the capacity to supply the required rotation, it must be capable of providing adequate hinge rotation while sustaining its yield moment capacity. In addition, it should be able to undergo a sufficient number of cycles before failure.

As shown in the experimental results in Chapter 4, top and seat angles with double web angle connections exhibit high ductility during cyclic and dynamic loads. The plastic rotation of this type of connection was approximately 0.03 radians. Hence, such a connection may be used in semi-rigid steel frame structures in seismic zone.

The target supply of rotation is not easily defined. Surtees et al. (1970) have suggested that a hinge rotation requirement of 0.03 radian would be a reasonable value for connections in multi-storey buildings. Popov et al. (1989) have shown that the plastic rotation in a six storey building, when subjected to a 0.5g ground acceleration of the Parkfield earthquake or to a 0.2g ground acceleration of the Mexico earthquake, is about 0.015. Therefore, the value of 0.03 can be used as a reasonably conservative estimate for the required rotation capacity in semi-rigid steel frames when considered for seismic design.

6.2.5 Bolts Design

The bolts in semi-rigid connections must behave as non-dissipative components to allow ductile elements to undergo inelastic deformation and dissipate energy. The reason for this is that bolt fracture is very similar to weld fracture and its failure is relatively sudden, brittle and dissipates only a very small amount of energy. Thus, the bolts should be designed such that this failure mode not be realised while the ductile elements in the connection undergo inelastic deformations.

On the other hand, slippage of the bolts in the connection can be used to work as a fuse during earthquakes. By designing the bolts to slip under specific forces, the bolted connection can limit the force which is transmitted to the columns. In addition, the friction slippage results in significant energy dissipation and damping.

One of the key questions facing designers is the value of slip displacement aimed at. Experimental tests carried out by Bernuzzi (1992) show that, when slippage occurs at low level of force the rotation due to slip increases as the connection is subjected to more than one constant amplitude deformation cycle. This effect becomes dominant if the connection is subjected to large cyclic loading thus influencing the overall structural response.

The results of the three cyclic tests, coupled with the experimental results of other researchers (Azizinamini et al., 1985) indicate that when yielding of the angle legs precedes the bolt slippage, more energy is dissipated during cyclic loads. As a result of this behaviour, the diameter of the bolts and pretensioning forces should be designed such that the sum of the forces on the bolts subjected to shear are larger than the force corresponding to yielding in the angle.

6.3 Limit State Criteria

To evaluate the seismic response of semi-rigid steel frames, together with the other parameters such as the behaviour factor, it is essential to define the yield and ultimate

criteria for each frame. The following sections describe the definitions of each limit state employed in monitoring the performance of the frames analysed.

6.3.1 Yield State

The yield criterion is defined in the structure as a state at which the inelastic deformation begin to contribute to the dissipation of input seismic energy. In the case of the ADAPTIC program, extreme fibre stress and strain data are available for both gauss points in each element of the structural model and for each time step of the response. Therefore, the yield state may be defined when the stress in the structural member at any gauss point in the finite element model, both in compression and in tension, reaches the yield strength. This criterion has been successfully applied in the past (Elghazouli, 1992; Broderick, 1994)

6.3.2 Ultimate State

To evaluate behaviour factors, a set of failure criteria (which describes structural failure) are defined. These failure criteria are arranged in two groups; the first relates to failure on a global (storey) and the second defines the limits of response for individual members.

6.3.2.1 Storey failure criteria

i. Interstorey drift

To limit the damage which may occur in structural and non-structural elements, it is necessary to control the maximum interstorey drift in the structure. The upper limiting value of interstorey drift commonly used as an ultimate limit state is:

$$\Delta_i = \frac{\delta_i - \delta_{i-1}}{h_i} \leq 0.03 \qquad (6.3)$$

where δ_i is the displacement at floor level i and h_i is the height of the storey under consideration. This limit has been widely used in the literature and is supported by field evidence correlating interstorey drift with damage.

ii. Storey stability

EC8 requires that the stability index of the structure should be evaluated for each storey using the following equation:

$$\theta = \frac{P_{tot}\, d_r}{v_{tot}\, h} \tag{6.4}$$

where P_{tot} is the total gravity load, d_r is the displacement (product of elastic displacement and q factor), v_{tot} is the total seismic design shear and h is the height. For stability, EC8 recommends a limiting value of 0.30 for this parameter.

iii. Collapse mechanism formation

The allowable deformation in each storey is limited by the interstorey drift. A similar limit on deformation, in terms of the resistance of the structure and gravity loading, is controlled by the stability index. To guarantee that the strength demand imposed on a structure are not excessive, the soft storey mechanism must be inhibited.

This mechanism of failure in the structure is defined when plastic hinges occur at the upper and lower ends of each column. In this regard, the occurrence of a plastic hinge is identified by the exceedance of the yield strain in both the tension and the compression flanges of the column. This criterion is included for completeness, but it is likely that it will be associated with the satisfaction of either the interstorey drift or the stability index criteria.

6.3.2.2 Local failure criteria

The maximum deformation allowed in the structural members is defined as a local failure criterion. The evaluation of these limits for semi-rigid steel frames is based on

maximum rotation in the connection or the rotation capacity of the members as detailed hereafter.

i. Maximum rotation of the connection

As mentioned in Chapter 5, experimental studies show that top and seat angles with double web angles connections can undergo large rotations without failure when they are designed such that the top and seat angles are allowed to yield prior to other modes of failure. It has been observed that this type of connection is capable of supplying a plastic rotation which exceeds 0.030 radian. However, it has also been recommended that the maximum total rotation should not exceed 0.05 radian (Astaneh et al., 1992).

ii. Column failure

Column failure is defined as the occurrence of local buckling due to excessive compression strain. Given that the rotation capacity of steel members is limited by local buckling, the rotation capacity of the member can be used to identify column failure in structures. The rotation capacity is determined in accordance with the procedure given by of Kato (1989) as described below.

The rotation capacity of the member can be evaluated using an accurate approach which accounts for the change from elastic to inelastic material properties along the length of the member. It can also allow for the yield plateau in the stress-strain response. For this purpose, a simplified model of an I-section which consists of two flanges having the same combined area and moment of inertia as the actual section is used (Kato, 1989).

Figure 6.1 shows this section and the material behaviour which is represented by a rigid-plastic strain hardening model. These models are employed to determine the moment-curvature response related to elastic, plastic-flow and strain hardening states in both the tension and compression flanges.

By performing double integration of the curvature distribution the rotations and displacements can be evaluated. The magnitude of the axial load on members can significantly influence the rotation capacity of the members. Based on the level of axial loads, different formulae are developed. In these expressions, the axial load is expressed in terms of the stress ratio ($\alpha = \sigma_o/\sigma_y$) where σ_o is the applied axial stress and σ_y is the yield stress.

For the condition $(R-1)/2<\alpha$, where R ($= \sigma_{cr}/\sigma_y$) represents the normalised critical stress, the response of the tension flange will be in the elastic range when the compression flange reaches its critical buckling stress. When $\alpha<(R-1)/2$, the tension flange will yield prior to failure. The condition $\alpha=0$ implies that no axial load is applied to the member and hence the element behaves purely in flexure.

For $(R-1)/2<\alpha$:

$$\mu_\theta = \frac{(R-1)}{2(1-\alpha)(R-\alpha)}\left[\frac{E}{E_{st}}(R-1)+2\left(\frac{\varepsilon_p}{\varepsilon_y}\right)\right] \tag{6.5}$$

For $(R-1)/2\geq\alpha>0$:

$$\mu_\theta = \frac{1}{(1-\alpha)(R-\alpha)}\left\{\frac{E}{E_{st}}\left[(R-1)^2+2\alpha^2\right]+2\frac{\varepsilon_p}{\varepsilon_y}(R-\alpha-1)\right\} \tag{6.6}$$

For $\alpha=0$:

$$\mu_\theta = \frac{(R-1)}{R}\left[\frac{E}{E_{st}}(R-1)+2\frac{\varepsilon_p}{\varepsilon_y}\right] \tag{6.7}$$

where, E is the modulus of Elasticity, E_{st} is the strain-hardening modulus, ε_p and ε_y are the plastic and yield strain, respectively.

The normalised maximum strength $R = \sigma_{cr}/\sigma_y$ obtained from stub-column tests is related to the slenderness parameters α_f and α_w and for mild steel can be evaluated as below (Kato, 1989):

$$\frac{1}{R} = 0.689 + 0.651(1/\alpha_f) + 0.0553(1/\alpha_w) \pm 0.0303 \qquad (6.8)$$

Where $\alpha_f = E(t_f / b^2)/\sigma_{yf}$ and $\alpha_w = E(t_w / d)^2 / \sigma_{yw}$ represent the slenderness of the flange and the web, respectively.

To demonstrate the accuracy of this method the calculated rotation capacity of the column section used in the three cyclic tests are compared with the rotation capacity obtained from the test. Table 6.1 shows that the analytical rotation capacity is in good agreement with the test results. Hence, the expressions can be applied for calculating the rotation capacity required for defining the failure criterion in a member. These expressions were also verified by Broderick (1994).

Table 6.1

Comparison of the calculated rotation capacity of the member with the test

Rotation	θ_y (radian)	θ_u (radian)	μ_θ
Test	0.0064	0.0365	4.71
Local buckling	0.0065	0.0377	4.80
Difference	+1.5 %	+3.29 %	+1.91 %

In an effort to avoid this type of failure, and to dissipate energy in the ductile elements during earthquake loading, the critical member must be designed so that it is capable of attaining a level of strain in its compression flange which is in excess of that at strain hardening. EC8 recognises this hence classifies the steel section based on the level of behaviour factor to be employed. Accordingly, the code recommends the use of class 1 cross-sections with low b/t ratio for structures which are designed for a high level of ductility demand.

6.4 Selection and Scaling of Earthquake Ground Motion

In order to investigate the seismic behaviour of semi-rigid steel frames, it is necessary to subject frames to a wide range earthquake records. This is because the forces, displacements and ductility demand of the structure are highly dependent on the dynamic characteristic of the frames as well as the input ground motion.

In general, one record may possess significant energy over a broad range of frequencies, while another record may produce many large amplitude, high frequency oscillations and the a third record may demonstrate a significant response which is contained in a few long duration acceleration pulses. To consider the influence of all of these parameters on the behaviour, records with different characteristics would have to be selected.

In addition, to compare the response of the structure subjected to different records, the time history acceleration of the ground motions should be scaled such that all of the employed ground motions possess comparable intensities. The following sections describe the approach adopted for scaling the ground acceleration records for this parametric study.

6.4.1 Selection of Records

The peak ground acceleration to peak ground velocity ratio (a/v) was proposed by Zhu et al. (1988) as a simple tool for identifying the characteristics of individual accelerograms.

The velocity response is obtained from an integration of the ground acceleration. Thus, while the peak ground acceleration may be associated with high frequency waves, the peak ground velocity is associated with moderate to low frequency waves of the accelerogram. It is therefore the ground motion with large amplitude, high frequency oscillation which will possess a high a/v ratio while the long duration acceleration pulses will be of low a/v ratio.

The a/v ratio will also reflect the range of possible soil types. For example, the records obtained on rock and firm soils will oscillate with shorter duration and higher frequency than those measured on softer media. In such a way, the high a/v ratio records represent firm ground and probably firm travel path, whilst the converse is true for low a/v ratio.

A statistical study on a selection of Japanese earthquake records performed by Sawada et al. (1992) indicates that a lower a/v ratio will be exhibited by an earthquake with lower predominant frequencies, broader response spectra, larger duration and greater magnitudes, epicentral distances and predominant site periods.

According to the above discussion, the effect of the dynamic characteristics of records on the dynamic response of structures can be taken into account by selecting the ground acceleration with different levels of a/v ratios. In this regard, if the ground acceleration is expressed in terms of 'g' (percentage of gravitational acceleration) and the velocity in metres per second, the three levels of a/v ratio would be defined in the following ranges:

low	:	$a/v < 0.8\ g/ms^{-1}$	(6.9)
normal	:	$0.8\ g/ms^{-1} \leq a/v \leq 1.2\ g/ms^{-1}$	(6.10)
high	:	$1.2\ g/ms^{-1} < a/v$	(6.11)

Selection of records for the analysis of semi-rigid steel frames are based on the classification of accelerograms according to the level of a/v ratio. For this purpose, six earthquake records, consisting of two records in each of the a/v ratio, are selected. The location and dates of each record are given in Table 6.2.

Figures 6.2 to 6.7 show the corrected acceleration time histories and acceleration response spectra for the six selected records. Comparison between the elastic response spectrum of EC8-1 and these response spectra is indicated in Figure 6.8.

Table 6.2

Ground motion records

Records	Earthquake event	Recording station	Component direction
IR02	Irpinia, Italy (23 Nov 1980)	Bagnoli	E-W
IP24	Mexico City, Mexico (15 Oct 1979)	Cerro Prieto	S57W
S152	San Fernando, USA (9 Feb 1971)	Griffith Pk.	S00W
A931	Coalinga, USA (2 May 1983)	Slack Canyon	N45E
FR11	Friuli, Italy (6 May 1976)	Tolmezzo	N-S
MH04	Morgan Hill, USA (24 Apr 1984)	Gilory-6	N-S

Further details, giving the peak ground motion, are indicated in Table 6.3.

Table 6.3

Ground motion record properties

Records	Peak Acceleration (g)	Peak Velocity (m/s)	a/v Ratio
IR02	0.185	0.33	0.56
IP24	0.155	0.190	0.81
S152	0.185	0.21	0.88
A931	0.172	0.154	1.12
FR11	0.36	0.23	1.56
MH04	0.227	0.11	2.02

As shown in Figures 6.2 and 6.3, the Irpinia and the Mexico records contain a number of large amplitude cycles with long duration and contribute proportionally more to the ground velocity, decreasing the a/v ratio. On the other hand, the Friuli and Morgan Hill records (Figures 6.6.and 6.7) contain a number of large amplitudes with short duration and hence they contribute less to the ground velocity thus causing the a/v ratio to increase

The large number of high frequency acceleration cycles in the Morgan Hill record causes it to possess the lowest predominant response frequencies. With the exception of this record, all of the remaining records possess a high spectral acceleration in the range of 0.5-1 second. This is the range of natural periods for the semi-rigid steel frames whose analytical response are presented in the following sections.

6.4.2 Scaling of the Selected Records

To validate the performance of a structure, which is designed in accordance with a code through the inspection of its response to the actual ground motions, the seismic energy imposed on the structure by the records should be comparable to that implied in the code design spectrum.

It has been observed that short period structures ($T < 0.5$ sec) will be sensitive to peak ground acceleration values, whilst structures with periods in the range, 0.5 sec $< T <$ 3 sec will be sensitive to peak ground velocity.

The natural period of semi-rigid steel frames are usually larger than 0.5 second and therefore they should be more sensitive to peak ground velocity rather than peak ground acceleration. Thus, it would seem appropriate to scale earthquake records to possess equal values of velocity spectrum intensity SI which is defined as the area under a pseudo-velocity spectrum between the periods of 0.1 and 2.5 seconds (Housner, 1952):

$$SI(\beta) = \int_{0.1}^{2.5} S_v(T,\beta)\,dT \qquad (6.12)$$

where β represents the fraction of critical damping, S_v is the pseudo-spectral velocity and T is the response period. If the acceleration record is not available, such as in the case of a design acceleration spectrum, then the pseudo-spectral velocity is obtained from

$$S_v = \frac{2\pi}{T} S_a \qquad (6.13)$$

where S_a is the spectral acceleration. The spectral intensity is integrated as the area under the velocity spectrum between two limits of frequency or period.

Table 6.4

Scaling of ground motion accelerations

Records	Peak Acceleration(g)	Spectral Intensity	Scaling Factor	Scaled Acceleration
IR02	0.185	122.7	0.778	0.144
IP24	0.155	87.1	1.096	0.170
S152	0.185	63.1	1.513	0.280
A931	0.172	81.4	1.173	0.200
FR11	0.360	93.4	1.022	0.368
MH04	0.227	46.6	1.965	0.446

To scale all of the selected records according to this procedure, a design peak ground acceleration of 0.3g is defined and the spectral intensities of the natural records are evaluated by using the above equations. The pseudo-velocity spectral intensity of the design spectrum given in EC8 and scaled to 0.3g is 95.5 cm. Table 6.4 shows the spectral intensity, scaling factor and the scaled peak ground acceleration for each selected record.

6.5 Design and Modelling of Frames

The response of the frames subjected to seismic forces is dependent on the interaction of the dynamic characteristics of both structure and loading. Thus, to obtain a comprehensive view of the seismic performance of steel frames with partial strength semi-rigid connections, it is necessary to design a wide range of steel frames with different configurations and connection capacity. The dimensions and design details of these frames are described in this section.

6.5.1 Design of Frames

All the frames were designed according to the requirements specified in the structural Eurocodes for the seismic design of moment resisting steel frames. The controlling design criterion in each case, except for the two storey rigid frame, was the need to limit interstorey drift to the maximum value allowed in the code.

One approach which can be used to control the above criterion in semi-rigid steel frames is to select beam sections which are larger than column sections. Therefore, in all the semi-rigid frames in this study, the size of the beams are larger than those for rigid frames. On the other hand, the size of the column in the rigid frames are larger than the column sections in the semi-rigid frames. This is because the weak-beam/strong-column principle must be observed in the design of rigid frames.

In the case of rigid frames, members are designed such that the plastic hinges form in the beams and not in the column, except at the base of the column. On account of this, the requirement for the column sections at any node is that the sum of the design values for the bending moments in the adjacent cross-sections of the column are not less than the sum of the resisting moments of the beams connected to the column.

This requirement results in a very small over-strength between the column and beam. However, when the design moments for the column (as recommended by EC8) are considered in the stability checks required by EC3, an additional bending resistance for the column will be provided.

In semi-rigid steel frames, as discussed previously, the plastic hinges form in the connections and therefore it is not necessary to follow the weak-beam/strong-column approach. Consequently, the beams and columns are proportioned using direct design (sections selected to satisfy strength requirements under the applied actions with no over-strength). In this approach and throughout this study, the connection strength is calculated such that it is the first yield zone. Hereafter, this will be referred to as 'direct design'.

The shear capacity requirement controls the beam sections in both rigid and semi-rigid frames. In addition, larger beam sections were selected primarily to control the interstorey drift in semi-rigid frames. In all frames, the stiffness of the roof beams was reduced relative to those employed in the lower storeys.

The range of rigid and semi-rigid frames investigated in this study is described in Table 6.5. Figure 6.9 represents the frame configurations and the full details of the section sizes of the members and the properties of connections for the frames are given in Appendix B. Two groups of frames, A and B, were designed. In the design of the frames in group A, the controlling interstorey limit criterion for semi-rigid frames was violated. However, this limit criterion was observed in the design of frames in group B.

Table 6.5

Frame dimensions and connection types

Frame Reference	No of Storeys	No of Bays	Storey Height (m)	Bay Width (m)	Connection Type
R22	2	2	3.0	5.0	Rigid
S22	2	2	3.0	5.0	Semi-rigid
R23	2	3	3.60	6.0	Rigid
S23	2	3	3.60	6.0	Semi-rigid
R42	4	2	3.0	6.0	Rigid
S42	4	2	3.0	6.0	Semi-rigid
R63	6	3	3.0	6.0	Rigid
S63	6	3	3.0	6.0	Semi-rigid

The numbers (30, 50 and 70) given in Appendix B for the reference code of frames with semi-rigid connections represent the percentage of the moment capacity of the connections to the plastic moment of the related beams. 'D' denotes that the 'direct design' method was used for these frames. 'C' represents capacity design requirement. Each frame is identified by the number of storeys and bays and the first letter shows the type of connection used in frames. Thus, frame S22D30 is a two storey two bay semi-rigid frame having a connection moment capacity of 30% of the plastic moment of the beam and was designed following the direct design method. Frame R22C, is an equivalent rigid frame following the strong-column/weak beam design.

6.5.2 Modelling of Frames

The ADAPTIC finite element program was employed in all the analyses. Four cubic elements were used for each column, including two short elements at either end. A similar assembly of beam elements with five cubic elements was adopted in each span.

A conventional bilinear model with a strain hardening modulus of 1% was employed to represent the material response in the steel sections. The mass of the structure was evaluated assuming a frame spacing normal to the direction of loading of 4.0 m and on the basis of the thickness of the floor slabs. The storey gravity load is modelled along the beam length, whilst the storey mass is lumped at the connections.

6.6 Results of Dynamic Analysis

To determine the response of the different structures, each frame was subjected to the earthquake ground motions selected in section 6.3. In order to identify the yield and failure criteria for each frame, the selected records were scaled and repeatedly applied to the frames until each of the limit state criteria was satisfied. Due to the volume of the obtained results, only the salient aspect of the response, which is relevant to the objective of this study, will be presented here.

6.6.1 Two-Storey Frames

In design of the two storey frames in group A, it was the gravity loads which governed the design of the beams and columns. This arose as a result of the combination of long beam spans and low number of building stories. Conversely, in group B the limit state of 1.5% drift controlled the design of the elements in all the semi-rigid frames. The section size of these elements and the properties of the connections are given in Appendix B.

Table 6.6 shows the interstorey drift and forces of the semi-rigid frames in group A and an equivalent rigid frame. These frames were subjected to time-history records of EC8-1 with a maximum peak ground acceleration (pga) of 0.3g. It is seen that the maximum interstorey drift in frame S22C30, is larger than that for frame S22D30. This is due to the effect of the longer period of frame S22D30 which attracted lower forces.

Table 6.6

Time history response of two-storey frames in group A

Frame References	Interstorey Drift (%)	Max. Moment of column (kNm)	Base Shear (kN)
S22D30	0.024	72.5	41
S22C30	0.028	155.5	64.1
R22C	0.015	161.38	91.14
S23D30	0.025	162.9	74.2
S23D70	0.022	238	123.35
R23C	0.018	356.2	187.34

As indicated in Table 6.6, when the ultimate moment at the base of the column in the first storey, and the base shear, in semi-rigid frames are compared to rigid frames, it is

noted that as the flexibility of the connection increases the forces in the column members decrease.

On the other hand, the interstorey drift in all semi-rigid frames is larger than the limit criterion in the code. This is because in the design of semi-rigid frames in group A, this limit state was intentionally violated.

Table 6.7 demonstrates the time history response of the two-storey frames in group B that were subjected to the EC8-1 with a pga of 0.3g. It is noted that in the design of these frames, the interstorey drift was limited to 1.5%, which dominated the design of beams and columns. In this regard, the size of the columns in the semi-rigid frames are larger than the rigid frame particularly for frame S23D30.

Table 6.7

Time history response of two-storey frames in group B

Frame References	Interstorey Drift (%)	Max. Moment of Column (kNm)	Base Shear (kN)
S23D30	1.60	277.10	468.79
S23D50	1.70	309.18	556.13
S23D70	1.76	282.16	514.18
S23C70	1.84	354.70	497.80
S23C100	1.75	357.04	529.40
R23C	1.40	356.60	542.33

It is seen that the values of interstorey drift in all the semi-rigid frames are reasonable and not far from the value required by the code. As illustrated in Table 6.7 the drift of the semi-rigid frame with 30% moment capacity is 1.6% (which is close to the value of 1.5% and less than the drift of the other semi-rigid frames). To confirm this, all of the

frames were subjected to three natural time history records. These three records are more critical for these frames when compared with the selected records in section 6.4.1 of this chapter.

The interstorey drift of the rigid and the semi-rigid frames are given in Table 6.8. Once again, except for the IR02 record, the value of the drift in the semi-rigid frame with 30% moment capacity is less than the values of the drifts observed for other frames when subjected to the S152 and MH04 records. This would suggest that partial strength semi-rigid steel frames are capable of sustaining larger earthquakes when compared with the partial strength semi-rigid frames with a higher moment capacity or with full strength semi-rigid steel frames. This is due to the longer period of this type of structure as well as to the large amount of energy dissipated in the inelastic range during earthquake loading.

Table 6.8

Maximum drift of two-storey frames subjected to different records (0.3g)

Frame reference	EC8-1	IR02	S152	MH04
S23D30	1.60	0.71	1.20	1.20
S23D50	1.70	0.66	1.40	1.43
S23D70	1.76	0.74	1.34	1.55
S23C70	1.84	0.69	1.33	1.25
S23C100	1.75	0.63	1.49	1.45
R23C	1.40	0.49	1.42	1.07

The results of this analysis also suggest that, among the above records, the artificial time-history record of EC8 is more critical than the natural earthquakes. This is shown in the form of acceleration response spectra in Figure 6.8. As indicated in this Figure, the normalised acceleration spectrum of EC8 (between periods of $0.4<T<3$ seconds) covers the acceleration spectra of three natural earthquakes. Thus, the design forces of

the frames calculated based on the spectrum of EC8 would be a conservative when compared to forces evaluated from a natural earthquake spectrum.

To evaluate the ultimate capacity and the behaviour factors for these frames, they were subjected to two artificial records generated from the EC8 spectrum. Table 6.9 presents the scaled collapse ground accelerations (a_u) and the collapse mechanism for each frame.

Table 6.9

Collapse ground acceleration of two-storey frames

Frame references	EC8-1		EC8-2	
	a_u at collapse	collapse mechanism	a_u at collapse	collapse mechanism
S23D30	0.60g	3% drift	0.76g	3% drift
S23D50	0.65g	3% drift	0.70g	3% drift
S23D70	0.80g	soft storey	0.73g	3% drift
S23C70	0.65g	soft storey	0.62g	soft storey
S23C100	0.45g	soft storey	0.48g	soft storey
R23C	0.38g	soft storey	0.40g	soft storey

It is observed that the failure ground acceleration values for all partial strength semi-rigid frames are higher than those for the rigid and full strength semi-rigid frames. As described previously, the design of the rigid frame as well as the full strength semi-rigid frame were governed by the imposed gravity loads and were independent of the design seismic actions. The consequence of this was that these frames were over-designed for the applied seismic loads. As a result, the ground accelerations at yield, of 0.16g for the rigid and 0.20g for the full strength semi-rigid frames, were significantly greater than would be expected if the seismic load case was critical. The values of failure

acceleration do not display a similar increase, given that they are in the low range of 0.38g for rigid frame and 0.45g for the full strength semi-rigid frame. These values are 0.40g and 0.48g respectively for the EC8-2 record. In each case, failure occurs due to the formation of a soft storey in the first floor.

On the other hand, in the case of partial strength semi-rigid frames (except for the frame with 70% moment capacity), interstorey drift is the controlling failure criterion. The yield accelerations are in the range of 0.06g to 0.11g and, as shown in Table 6.9, the failure accelerations are much higher than for rigid frames. This is due to the fact that the former system design is controlled by drift, hence yield under lateral earthquake loading occurs and on. The converse is true for rigid frames which are controlled by gravity. They therefore, exhibit excessive over-strength under transverse loading, hence their yield acceleration is exceptionally high. In addition, in the inelastic range, most of input energy during earthquake loading is dissipated by the connection undergoing large deformations. Thus, the connections act as a fuse to control the forces in the column members and restrict the concentration of high stresses in these parts of the frames.

The behaviour factors have been determined for each frame when they were subjected to two of the records from EC8. These values are given in Table 6.10. The method used for calculating the behaviour factor, q' and q'_D, is described in Chapter 4. As indicated in Table 6.10, the behaviour factors of semi-rigid frames for both records are higher than the values for rigid and full strength semi-rigid frames. They are also higher than the value for the semi-rigid frame with 70% moment capacity (which was designed according to the capacity design method). As mentioned above, the high yield acceleration and the soft storey mechanism in R23C, S23C100 and S23C70 frames lead to the low values of behaviour factor.

Table 6.10

Calculated behaviour factor for two storey frames

Frame references	EC8-1		EC8-2	
	q'	q'_D	q'	q'_D
S23D30	10.0	12.0	12.6	15.2
S23D50	5.9	13.0	7.0	14.0
S23D70	5.7	16.0	6.6	14.6
S23C70	4.3	13.0	4.4	12.4
S23C100	2.2	9.0	3.2	9.6
R23C	2.4	7.6	1.7	8.0

It is observed that the calculated behaviour factor for all semi-rigid frames are fairly close to the design value given in EC8. The value of q'_D, given in the same Table, is a more meaningful measure of the behaviour factor used in the design. In this case, the collapse ground acceleration is compared with design-implied yield acceleration (a_{design} /q_{design}) Based on this method of calculation, the behaviour factors for all the semi-rigid frames are more than twice their design value.

Table 6.11 presents the main response parameters defining the deformation demand for each frame. The base shear at yield V_y and at failure V_u are compared in order to identify the over-strength parameter α_i (=V_y/V_u) employed by EC8 in the evaluation of the design behaviour factors.

As shown in Table 6.11, these over-strength values for the semi-rigid frames are in the range of 1.49 to 3.22 for the EC8-1 record and in the range of 1.62 to 3.48 for EC8-2 record. These values are greater than the 1.2 recommended in the code. The high values of over-strength imply that a greater behaviour factor can be assumed for the design of semi-rigid steel frames.

Table 6.11

Response parameters at yield and collapse (forces in kN)

Frame references	EC8 records	Over-strength α_i			Global ductility			Rotation ductility	
		V_u	V_y	α_i	Δ_{sy}	Δ_{su}	$\mu_{\Delta s}$	$\mu_{\theta col}$	$\mu_{\theta con}$
S23D30	EC8-1	581	181	3.22	0.53	3	5.66	1.57	6.15
	EC8-2	617	177	3.48	0.61	3	4.92	1.64	6.20
S23D50	EC8-1	597	315	1.90	0.90	3	3.33	2.70	6.67
	EC8-2	608	335	1.82	0.90	3	3.33	2.50	5.90
S23D70	EC8-1	629	421	1.49	1.30	2.70	2.08	2.21	6.67
	EC8-2	619	382	1.62	1.30	3	2.31	2.07	5.64
S23C70	EC8-1	599	435	1.38	1.37	2.70	1.97	2.00	4.87
	EC8-2	595	445	1.34	1.60	2.40	1.50	1.78	4.10
S23C100	EC8-1	601	467	1.29	1.59	1.89	1.19	2.00	2.82
	EC8-2	588	475	1.24	1.60	2.40	1.50	2.33	2.10
R23C	EC8-1	583	455	1.28	1.10	1.45	1.32	1.75	-
	EC8-2	569	477	1.19	1.20	1.64	1.37	1.67	-

The maximum interstorey drifts experienced at yield and failure are denoted in Table 6.11 by Δ_{sy} and Δ_{su}, respectively. As mentioned previously, because of the dominant effect of gravity loads in the design of rigid and full strength semi-rigid frames, high interstorey drifts were experienced in these frames before yielding occurred. Consequently, the formation of column hinge mechanism was observed at a drift of 1.44% in the case of the EC8-1 record, and at drift of 1.64% for the EC8-2 record, in rigid frames. Similar behaviour was experienced in the full strength semi-rigid frame and the semi-rigid frame with 70% moment capacity.

The parameter $\mu_{\Delta s}$, evaluated as the ratio of Δ_{sy} to Δ_{su}, represents a measure of the global ductility demand at each storey level. The high value of global ductility in partial strength semi-rigid frames, particularly in the frame with 30% moment capacity, indicates that these structures are capable of dissipating considerable energy in the event of earthquake. It should be noted, however, that the maximum global ductility

value of 1.5 in the full strength semi-rigid frame and the value of 1.32 in the rigid frame do not allow much scope for energy dissipation in these structures.

At member level, deformation demands are demonstrated by the rotation ductility experienced in the column members and connections. As would be expected, in semi-rigid frames, the connections undergo large rotational deformation and hence the rotation ductility demands are very high. As shown in Table 6.11, the rotation ductility of the connection in the semi-rigid frame with 30% moment capacity is 6.15, i.e. 50% of its rotation capacity This value indicates that the connections are capable of dissipating substantial levels of energy during earthquake loading.

Values of rotation ductility at the base of the columns for all the frames are listed in Table 6.11. It is noticed that all of these values are moderate and well within their capacity. The low level of rotation ductility at the base of the rigid and full strength semi-rigid frames is due to the soft storey mechanism occurring in these frames. The low level of rotation ductility in semi-rigid frames is related to the flexibility of the connection which can cause a further delay in local buckling of the column members. However, it must be stressed that this flexibility in the connection causes an increase in the effective length of the column such that the net effect is probably a reduction in member resistance.

6.6.2 Four Storey Frames

In this study, the four-storey two-bay steel frames have been divided into two groups. The limit state of 1.5% drift was violated in series A and observed in design of the frames in group B. For the design ground acceleration of 0.30g, the interstorey drifts for the frames in group B were delimited to a value which was less than the allowable 1.5%. This was achieved by increasing the section size and hence the flexural stiffness of beam and column members.

In this regard, in rigid and full strength semi-rigid frames, increases in the frame stiffness must be achieved by increasing the size of both the beam and column members, since an increase in the beam size alone would induce excessive design

moments on the adjacent column members. However, in partial strength semi-rigid frames, when the direct design method is applied, the controlling drift can be achieved only by increasing the beam section size. The section size of the elements and the properties of the connections of these frames are given in Appendix B.

Table 6.12 shows the interstorey drift and the associated forces for the semi-rigid frames in group A. In comparison the response of the semi-rigid frames, S42C and S42D, which were designed in accordance with the capacity design method, experienced the greater interstorey drifts, base shear and moment at the base of the column in the first storey. The primary reason for this behaviour is that the weaker columns in the S42D frames lead to an increase in the period of these structures hence they attracted lower seismic forces.

Table 6.12

Time history response of four storey frames in group A

Frame references	Maximum drift	Base shear (kN)	Moment (kNm)
S42D30	2.5%	120.9	272.8
S42D50	2%	133.4	280.60
S42D70	2%	155.8	290.3
S42C30	2.6%	147.88	336.9
S42C50	2%	150.43	347
S42C70	1.9%	178	357
R42C	1.8%	218.04	366.7

The longer period in these frames causes a decrease in the interstorey drift. However, these values are usually greater than the limit state value (1.5%) and in some cases the discrepancy may be as high as 60%. This is because the interstorey drift limits were not imposed in the design of these frames and the gravity loads were the governing criterion in the design of the members.

To investigate the seismic behaviour of frames in group B, they were subjected to different earthquake records. In order to compare these results with the results of rigid

and full strength semi-rigid frames, the later frames were also subjected to the same records scaled to the same peak ground acceleration.

The selection of the member sections were controlled by interstorey drift. Generally, the limit state of interstorey drift lead to reasonable member size for the semi-rigid frames. However, for the frame with 30% moment capacity, member sizes were significantly larger than the rigid frame. It is therefore concluded that as the number of storeys increase, the minimum connection strength should also increase. Otherwise, drift control of the more slender structure would lead to gross member dimensions, well above those needed in the rigid frame scenarios (S42D30 results are omitted, for the given reason).

Table 6.13

Time history response of four storey frames in group B

Frame references	Maximum drift (%)	Base shear (kN)	Moment (kNm)
S42D50	1.55	517.53	562.66
S42D70	1.65	621.55	616.79
S42C100	1.66	661.67	627.29
R42C	1.70	683.65	618.78

Table 6.13 shows the maximum interstorey drift, base shear and moment at the base of the column in the first storey for the four storey rigid and semi-rigid frames when subjected to the EC8-1 record. The comparison between the response of these frames are also shown in Figures 6.10 and 6.11. It is shown that the forces and interstorey drift in the semi-rigid frames are less than those values for the rigid frame. To confirm this, all of the frames were subjected to three natural records, IR02, S152 and MH04. The results of these analyses are given in Table 6.14. Except for the record MH04, the interstorey drifts of the partial strength semi-rigid frames are lower than those for the rigid frame.

Table 6.14

Maximum interstorey drift for the four storey frames

Frame references	EC8-1	IR02	S152	MH04
S42D50	1.55	0.58	0.85	1.54
S42D70	1.65	0.59	1.23	1.65
S42C100	1.66	0.55	1.39	1.24
R42C	1.70	0.59	1.00	1.31

As shown in Tables 6.13 and 6.14 and in Figure 6.12, the interstorey drift and the response of full strength semi-rigid connection steel frames are higher than the partial strength semi-rigid frames for two records. This would suggest that the stiffer and stronger connections in frames may not always be an adequate solution for controlling the drift. This observation was also made when the results of two semi-rigid frames, S42D50 and S42D70, were compared.

As a result of this analysis, it is evident that the partial strength semi-rigid connection steel frame with a moment connection capacity in the range of 50% to 70% of the plastic moment of the connected beams are capable of carrying seismic forces in excess of their design without suffering from excessive interstorey drifts.

To calculate the collapse ground motion acceleration and to determine the behaviour factor, each of the frames was subjected to two artificial records of EC8. The exceedance of 3% interstorey drift dominated the failure mode for all of these frames. The yield and collapse accelerations that were obtained from this analysis are given in Table 6.15.

As indicated in Table 6.15, the frame S42D50 yielded at a lower value of acceleration than the rigid frame. On the other hand, the failure mode of this frame occurred at a higher value of acceleration in the EC8-1 record. This suggests that this frame exhibits a high level of ductility and hence dissipates more energy throughout its inelastic deformation range.

Table 6.15

Yield and ultimate acceleration for the four storey frames at 3% drift

Frame References	EC8-1		EC8-2	
	a_y	a_u	a_y	a_u
S42D50	0.14g	0.94g	0.14g	0.89g
S42D70	0.18g	0.99g	0.15g	0.90g
S42C100	0.22g	0.81g	0.21g	0.85g
R42C	0.16g	0.70	0.18g	1.25g

The calculated behaviour factors given in Table 6.16 illustrate this clearly. As shown in this Table, the behaviour factor for frame S42D50 is the highest value for the EC8-1 record. Its value is also higher than the values for frames, S42D70 and S42C100 for the EC8-1 record, falling below that observed for the rigid frame subjected to the EC8-2 record.

Table 6.16

Calculated behaviour factors for the four storey frames

Frame References	EC8-1		EC8-2	
	q'	q'_D	q'	q'_D
S42D50	6.27	18.8	6.36	17.8
S42D70	5.5	19.8	6.00	18
S42C100	3.68	16.2	4.05	17
R42C	4.67	14	6.94	25

To investigate the main response parameters defining the deformation demand for each frame, the over-strength (α_i), global ductility ($\mu_{\Delta s}$) and rotation ductility (μ_θ) were determined and are given in Table 6.17.

Table 6.17

Response parameters at the yield and ultimate states (forces in kN)

Frame references	EC8 records	Over-strength values			Global ductility			Rotation ductility	
		V_y	V_u	α_i	Δ_{sy}	Δ_{su}	$\mu_{\Delta s}$	$\mu_{\theta col}$	$\mu_{\theta con}$
S42D50	EC8-1	385	716	1.86	0.009	0.03	3.3	4.38	8.97
	EC8-2	363	711	1.96	0.01	0.03	3	3.84	7.18
S42D70	EC8-1	443	819	1.85	0.011	0.03	2.7	4.11	7.43
	EC8-2	401	836	2.08	0.01	0.03	3	4.52	7.69
S42C100	EC8-1	537	843	1.57	0.012	0.03	2.5	3.97	6.92
	EC8-2	495	889	1.79	0.01	0.03	3	3.99	6.67
R42C	EC8-1	522	754	1.44	0.011	0.03	2.7	3.15	-
	EC8-2	446	834	1.87	0.01	0.03	3	3.69	-

From the response parameters listed in Table 6.17, it is observed that the yield interstorey drift for all the semi-rigid frames are as high as for the rigid frames. This is attributed to the selection of larger member sections to control the design drift.

The rotation ductility of the columns in semi-rigid frames is higher than that for the rigid frame but lower than its rotation capacity. As shown in Table 6.17, the maximum rotation ductility for the column in frame S42D50 is 4.38 which is only 47% of its rotation capacity. This implies that the local failure does not occur in the column members in semi-rigid frames. However, the flexibility of the connection causes an increase of the effective length of the column, but this is not a significant factor which influences the collapse mechanism of the frames.

The rotation ductility of the connection for each of the semi-rigid frames are also presented in Table 6.17. The high value of the rotation ductility in frame S42D50 suggest that this part of the structure is responsible for a substantial proportion of the energy absorption. It would have been really effective to quote the energy absorption

(area under load-displacement or moment-rotation curves) for members and connections in a sample rigid and semi-rigid, to show the shift of damage from members to connections.

It was observed throughout this investigation that the four storey frames with partial strength semi-rigid connections which were designed on the basis of the 'direct design' method, are capable of sustaining a level of seismic forces comparable with rigid frames. A similar observation was made with regard to their response parameters. In addition, a comparison of the primary dynamic response of this type of structure with the response of full strength semi-rigid frames indicates the former attract less forces, show lower interstorey drift and produce higher behaviour factors.

6.6.3 Six Storey Frames

In the design of the six storey frames, the maximum interstorey drift of 1.5% governed. This lead to an increase in the section size for the column and beam members. The section size of these members and the properties of the connections are given in Appendix B.

The frames were subjected to four records, three natural ground motions and one artificial record derived from the EC8 spectrum. Table 6.18 shows the maximum interstorey drift for each frame for the various records.

Table 6.18

Maximum interstorey drift for the six storey frames for various records

Frame references	EC8-1	IR02	S152	MH04
S63D50	1.20	0.58	1.25	1.37
S63D70	1.50	0.46	1.00	1.16
S63C100	1.80	0.46	0.84	1.24
R63C	1.90	0.42	0.81	1.79

It is observed that the interstorey drift of partial strength semi-rigid frames are less than the corresponding rigid frame for two records, EC8-1 and MH04. Conversely, the rigid frame has a lower value of drift for records IR02 and S152. Figure 6.13 shows the maximum interstorey drift for each storey in the six storey frames for the different records. When the interstorey drift for two of the structures, S63D50 and S63D70, are compared, it is observed that for all of the records (with the exception of EC8-1), the frame with stiffer and stronger connections had a lower value of maximum interstorey drift. This behaviour was also observed in frame S63C100.

The comparison of the response of the partial strength semi-rigid frames with the rigid frame for EC8-1 record is illustrated in Figures 6.14 and 6.15. It is clear that the base shear and the moment at the base of the column in the first storey of the semi-rigid frames are lower than the rigid frame.

Figure 6.16 compares the response of different semi-rigid frames when subjected to EC8-1 record. As shown in the Figure, the frame with more flexible connection attracts lower forces. The maximum values of response are given in Tables 6.19 and 6.20.

Table 6.19

Maximum base shear (kN) of frames for different records

Frame references	EC8-1	IR02	S152	MH04
S63D50	1048	639	1003	1145
S63D70	1294	451	1235	1440
S63C100	1638	451	1113	1487
R63C	1621	482	956	1633

As shown in these Figures and Tables, the flexible connections in Frame S63D50 result in a longer period hence the frame attracts less forces for three of the records. Only for the IR02 record are the forces greater than its counterparts. The reason for this is that the IR02 record has high amplifications in a narrow band of frequency. This leads to

relative low SI values, hence high scaling. If the structure has a period close to the period of high amplification in the record, increased response results.

Table 6.20

Maximum moment (kNm) at the base of the first storey column

Frame references	EC8-1	IR02	S152	MH04
S63D50	1001	554	924	955
S63D70	1168	389	1031	1197
S63C100	1424	375	875	1148
R63C	1499	482	773	1406

The results from this analysis also suggest that among all of these records, the artificial accelerogram is the most critical for these frames.

Table 6.21

Rotation ductility of members and connections for the EC8-1 record

Frame references	$\mu_{\theta col}$	$\mu_{\theta col}/R_{\theta col}$ (%)	$\mu_{\theta con}$	$\mu_{\theta con}/R_{\theta con}$ (%)
S63D50	1.6	14	3.67	27.5
S63D70	1.72	15.4	4.67	40.6
S63C100	2.1	18.7	5.33	64
R63C	2.46	21	-	-

The calculated rotation ductility of the column in the first storey and the maximum rotation ductility of the connection in each of these frames are given in Table 6.21. As shown in this Table, the rotation ductility of the column members in the partial strength semi-rigid frames are less than 15% of their rotation capacity. The rotation ductility of the connections for these frames are also less than the 50% of the rotation capacity of the connections.

In order to evaluate the behaviour factor, the frames were subjected to the two artificial records of EC8. The interstorey drift of 3% determined the collapse state in these frames. The yield and ultimate collapse accelerations are given in Table 6.22. As observed in this Table, the ultimate acceleration for partial strength semi-rigid frames for both records are higher than those for rigid and full strength semi-rigid frames.

Table 6.22

Yield and ultimate acceleration for the six storey frames at 3% drift

Frame References	EC8-1		EC8-2	
	a_y	a_u	a_y	a_u
S63D50	0.11g	0.99g	0.14g	0.90g
S63D70	0.12g	1.05g	0.16g	0.95g
S63C100	0.19g	0.78g	0.26g	1.00g
R63C	0.22g	0.50g	0.20g	0.39g

The calculated behaviour factors and the values of over-strength for these six storey frames are presented in Table 6.23. It is observed that the semi-rigid frames achieved higher over-strength values and also higher behaviour factors when compared with the rigid frame. This means that increasing the number of storeys in this type of structure does not affect significantly its ductility demands.

Table 6.23

Calculated behaviour factors and over-strength values for six storey frames

Frame References	EC8-1			EC8-2		
	q'	q'_D	α_i	q'	q'_D	α_i
S63D50	9.0	19.8	2.90	7.5	18	2.63
S63D70	8.7	21	2.44	6.3	19	2.17
S63C100	4.1	15.6	1.61	3.85	20	1.43
R63C	2.27	10.0	1.62	1.95	7.8	1.05

By considering the response from the time history analysis of the six storey partial strength semi-rigid frames, it is concluded that they possess sufficient strength and stiffness when subjected to different records. The maximum interstorey drift is less than the allowable value for the limit state (1.5%). They exhibited higher behaviour factor than the value recommended in EC8 for steel frames and the maximum rotation in the column members and in the connections are very much less than the rotation supply values. Hence, local failure is not imminent at the drift-controlled collapse state.

It was also observed that the partial strength semi-rigid frame with 70% moment capacity gave lower values of drift when compared with the semi-rigid frame with 50% moment capacity. This would suggest that it is beneficial to use partial strength semi-rigid connections with 70% moment capacity in structures in which the number of storeys is greater than four. However, it should be pointed out that the response of the six storey semi-rigid frame with 50% moment capacity are reasonable and are comparable with those observed for the rigid frame.

6.7 Discussion and Design Implications

In this chapter a number of recommendations for the design of semi-rigid frames are presented. Following these recommendations, two, four and six storey frames with different configurations and different connections were designed. In order to examine the seismic behaviour of partial strength semi-rigid frames and to undertake comparisons with rigid frames, all of the frames were subjected to different earthquake records. The characteristics of these records are given in this chapter and the method of scaling their peak ground accelerations is described. In this section, a general discussion of the results of this parametric study is presented.

6.7.1 Capacity Design for Semi-rigid Steel Frames

As mentioned above, in the design of partial strength semi-rigid steel frames, it is not necessary to observe the strong-column/weak-beam approach for such structures. Indeed, it has been demonstrated that this type of structure can be designed on the

basis of 'direct design' approach. This entails proportioning the beam and columns for the applied actions (with no over-strength) whilst providing connection with partial strength. The results obtained from time history analysis of the semi-rigid frames that were designed according to this approach show that the column members (at the ultimate condition) never reach a critical state and that the rotation ductility of the members are usually less than 30% of their rotation capacity.

On the other hand, the analytical results of the two storey rigid frames that were designed according to the strong-column/weak-beam approach demonstrated that this type of structure suffered from soft storey failure. Therefore, in the design of low rise structures (with long span beams) subjected to seismic loading, the partial strength semi-rigid frames is recommended.

By adopting this approach for the design of semi-rigid frames with partial strength connections, the latter are designed such that the first yield occurs in the connections and not in the beams. Moreover, the connections should have sufficient strength to be stable at the serviceability limit state and possess sufficient ductility to be capable of sustaining large deformations at the ultimate limit state.

For this purpose, the connection should be designed such that the yielding of the angle legs or of the plates precedes the other modes of failure, e.g. shear yielding in the panel zone or fracture in the bolts. In addition, in order to prevent bolt slippage prior to yielding in the angles or the plates, the diameter of the bolts and pretensioning forces should be designed such that the sum of the forces of the bolts subjected to shear be greater than the force corresponding to yielding in the angle.

6.7.2 Frame Configurations

The analytical results of the two storey rigid frames that were designed according to the strong-column/weak-beam approach confirm that this type of structure may suffer from soft storey failure. In the two storey semi-rigid frames, the global mechanism of interstorey drift dominates the collapse state. It was also observed that this type of structure sustained higher peak ground acceleration when compared with the rigid

frame. This confirms the recommendation given in the previous section for the design of low rise structures with long spans.

A comparison between the results for partial strength semi-rigid frames with different moment capacities suggests that the flexibility of the connections leads to a longer period in the structure. As a consequence, the forces in the members (i.e. shear forces and moments in the columns) decreased. Additionally, in some cases, the maximum interstorey drift for frames with more flexible connections were less than that observed for the semi-rigid frames with stiffer and stronger connections.

In semi-rigid frames, it was shown that controlling the interstorey drift governed the design of the members and as such larger size for the column and beam elements were required. However, when the weight of the designed semi-rigid frame was compared with the weight of the rigid frame, it was observed that the differences was less than 2%. In some cases, the weight of the semi-rigid frame was actually less than that for the rigid frame.

Therefore, in the design of partial strength semi-rigid steel frames, the connections with moment capacities in the range of 30%-70% of the plastic moment of the connected beams may be used with confidence. furthermore, it was observed that when the number of storeys in such structures increased, the interstorey drift for the frames with stronger connections were more acceptable. This observation was evident in the response for the six storey semi-rigid frame with 70% moment capacity when subjected to three natural records.

Table 6.24

Recommended values for moment capacity of connection

Number of storeys	Type of connection	Moment capacity
Two-storey frames	Partial strength semi-rigid	30%-50%
Two-Four storey frames	Partial strength semi-rigid	50%-70%
Five-Six storey frames	Partial/full strength semi-rigid	70%-100%

In view of the above discussion, and in an effort to limit the use of large section size for members in partial strength semi-rigid frames, guidance for using partial strength semi-rigid connections with different moment capacity and number of storeys is given in Table 6.24.

6.7.3 Over-strength of Semi-Rigid Frames

The over-strength for the structural system employed to resist the imposed seismic loads α, is defined in EC8 as

$$\alpha_i = \frac{\alpha_u}{\alpha_y} \tag{6.14}$$

Where α_u is the load multiplier at the attainment of the ultimate limit state and α_y is that at limit yield. The design value of the structural behaviour factor to be employed in EC8 for each moment resisting frame is directly proportional to α_i. In calculating the value of α_i for semi-rigid frames, α_u is taken as the lateral resistance at the maximum interstorey drift of 3%, and α_y relates to the base shear at which the first instance of connection yielding is detected. Table 6.25 gives the over-strength values for all the semi-rigid and rigid frames identified in this study.

It is observed that the frames with partial strength semi-rigid connections achieved higher α_i values when compared with the rigid frames. This would suggest that the value recommended by EC8 could be increased when semi-rigid connections are employed in steel frames.

6.7.4 Behaviour Factors

As mentioned previously, the maximum interstorey drift of 3% is the failure criterion for all partial strength semi-rigid frames. Therefore, to determine the behaviour factor

for these frames it is necessary to evaluate the peak ground acceleration at yield as well as at the collapse state. Whilst it is a straightforward procedure to calculate the peak ground acceleration at which the interstorey drift limit of 3% is reached (hence giving a value for $a_{g(collapse)}$), a simple equivalent definition for $a_{g(yield)}$ is not available.

Table 6.25

Over-strength values of moment resisting frames

Frame References	Over-strength α_i	
	EC8-1	EC8-2
S23D30	3.22	3.48
S23D50	1.90	1.82
S23D70	1.49	1.62
R23C	1.28	1.19
S42D50	1.86	1.96
S42D70	1.85	2.09
R42C	1.44	1.87
S63D50	2.90	2.63
S63D70	2.44	2.17
R63C	1.62	1.05

There is, however, a definition for the yield acceleration in terms of the design ground acceleration and the q-factor employed in the design. In this case, the behaviour factor, q'_{drif}, will be that given by equation 4.13 in Chapter 4 [$q'_D = a_{g(collapse)} / (a_{g(design)} / q)$]. Although this definition has the advantage that it relates the intensity of loading at collapse to the design loads, it fails to take cognisance of the influence of different ground motions, structural designs and response periods on the value of the yield acceleration.

To overcome the above problem, the yield acceleration can be determined from the maximum interstorey drift of the structure under each of the selected ground motions scaled to their design value. This value of drift is denoted as $\Delta_{i\,(design)}$. Therefore, as each frame is designed for the maximum interstorey drift of 1.5%, the ratio $\Delta_{i\,(design)}/1.5$, may be used as a correction factor to allow for the ground motion dependence of the displacement response. This correction is employed to define a value for the yield acceleration which can be used in the evaluation of q'_{drift} as follows:

$$a_{y(drift)} = \frac{a_{g(design)}}{\Delta_{i(design)} / 1.5} \tag{6.15}$$

$$q'_{drift} = \left(\frac{a_{g(collapse)}}{a_{y(drift)}} \right) q_{design} \tag{6.16}$$

As mentioned above, among all the selected records, the EC8-1 record was the most critical for the frames which were analysed and designed in this chapter. Therefore, The calculated behaviour factor for this record would be the minimum value of q'_{drift} for these frames. Table 6.26 gives the values of behaviour factors for both the semi-rigid and rigid frames identified in this study.

Table 6.26

Behaviour factors of semi-rigid frames

Frame references	q'_{drift}	q'_{drift}/α_i	q'_D	q'_D/α_i
S23D30	12.8	3.97	12	3.72
S23D50	14.73	7.77	13.0	6.85
S23D70	18.77	12.55	16.0	10.70
R23C	7.09	5.53	7.6	5.93
S42D50	19.43	10.45	18.8	10.11
S42D70	21.78	11.77	19.8	10.70
R42C	15.87	10.97	14.0	9.67
S63D50	15.84	5.47	19.8	6.83
S63D70	21.00	8.61	21.0	8.61
R63C	12.67	7.80	10.0	6.16

As shown in this Table, the behaviour factors for all the semi-rigid steel frames are more than twice the design behaviour factor of EC8. It is also observed that the values of q'/α_i for all the semi-rigid frames (with the exception of S23D30) are much higher than those recommended in EC8 for rigid frames. The lower values for frames S23D30 and S63D50 are related to the higher value of over-strength in these frames (3.22 and 2.90).

The results from the dynamic analyses for the seismic response of partial strength semi-rigid steel frames described herein can be used as a basis for recommending more appropriate behaviour factors than the values of EC8 for rigid frames. Given that no previous research has been conducted in this regard, it is not possible to compare the results achieved with other independent work.

To provide a reasonable value of behaviour factor which should be applied in the design of semi-rigid frames, the ratio of the behaviour factors for semi-rigid frames to those for rigid frames are presented in Table 6.27.

Table 6.27

Comparative behaviour factors (semi-rigid vs. rigid frames)

Frame references	$\left(q'_{semi-rigid}/q'_{rigid}\right)_{drift}$	$q'_{D(semi-rigid)}/q'_{D(rigid)}$
S23D30	1.80	1.58
S23D50	2.08	1.71
S23D70	2.65	2.10
S42D50	1.22	1.34
S42D70	1.37	1.41
R42C	1.00	1.00
S63D50	1.25	1.98
S63D70	1.66	2.1

In addition, the value of $\left[(q'/\alpha_i)\alpha'\right]$ for each semi-rigid frame is evaluated and given in Table 6.28. In this calculation, the value of α' normalised to the over-strength value of the equivalent rigid frame.

Table 6.28

Calculated over-strength factors for rigid and semi-rigid frames

Frame references	$\left[(q'/\alpha_i)\alpha'\right]$	$\left[(q'_D/\alpha_i)\alpha'\right]$
S23D30	9.96	9.34
S23D50	11.50	10.14
S23D70	14.56	12.41
R23C	5.53	5.93
S42D50	13.48	13.04
S42D70	15.06	13.69
R42C	10.97	9.67
S63D50	9.79	12.12
S63D70	13.00	13.00
R63C	7.80	6.16

From this investigation it is clear that the behaviour factor for semi-rigid frames is greater than that for rigid frames, subject to the limitation of the structural forms investigated herein. As indicated in Table 6.27, this behaviour factor is at least 1.22 times the behaviour factor for the rigid frame.

Table 6.28 also show that none of the frames failed below a value of q'/α_i=9.0. Although, more dynamic analyses would be needed to obtain a more accurate value for the behaviour factor for semi-rigid frames, it is concluded herein that a value of 1.2 times the design behaviour factor for the rigid frame would be an acceptable safe limit to apply in the design of the former frames.

6.7.5 Rotation Ductility

The results of the dynamic analyses in this chapter suggest that if the connection is designed to supply the required rotational ductility it can be used to dissipate large amounts of energy (in a stable manner) through its non-linear behaviour while the beams and columns suffer little damage. In all the frames with top and seat angles and double web angles connections, the rotation ductility of the connections at the ultimate state are less than 50% of their rotation capacity. Therefore, this type of connection is capable of dissipating a large amount of energy in the event of a severe earthquake and hence can be used with confidence in seismic areas.

The maximum rotation ductility in column members in all the semi-rigid steel frames is much lower than their rotation capacity. The reason for this is that the flexibility of the connection in these frames causes a decrease in the seismic forces and prior to any yielding in the connection, limits the transfer of forces to the columns

It is noted that whilst the flexibility of the connection increases the effective length of the column, when this effect is accompanied by lower seismic forces, it does not lead to failure. As observed from the results of the time history analyses, the column members in all the semi-rigid frames were subjected to only 20% of their rotation capacity.

6.8 Concluding Remark

Comparison between the response of semi-rigid and rigid frames suggests that the seismic performance of partial strength semi-rigid frames is comparable with that of rigid frames. Although semi-rigid steel structures are generally more flexible, this extra flexibility does not necessarily result in larger drifts. As a whole, a well designed semi-rigid connection can actively participate in absorbing and dissipating energy in the event of a severe earthquake, thus protecting other frame components.

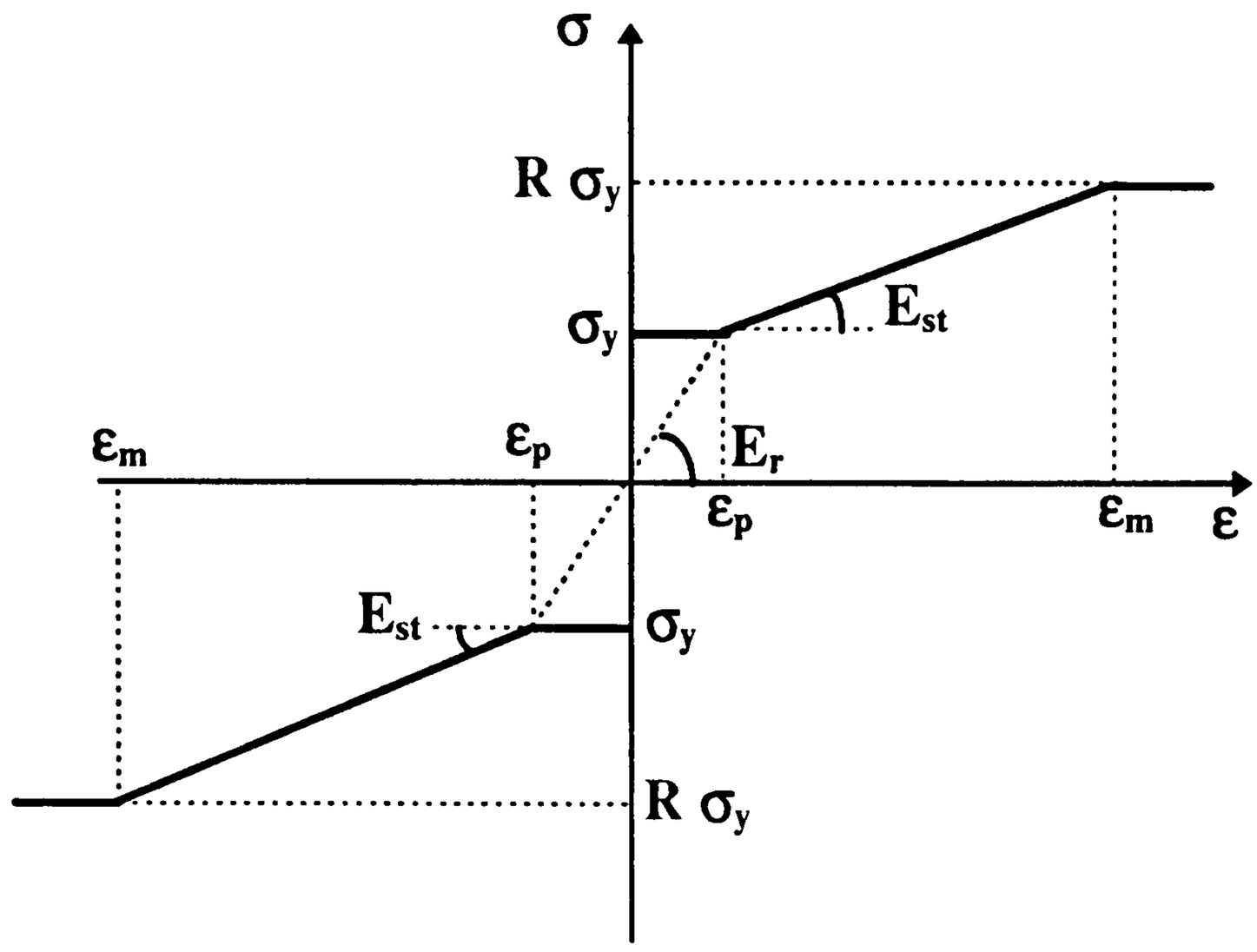

a) Stress-strain relation

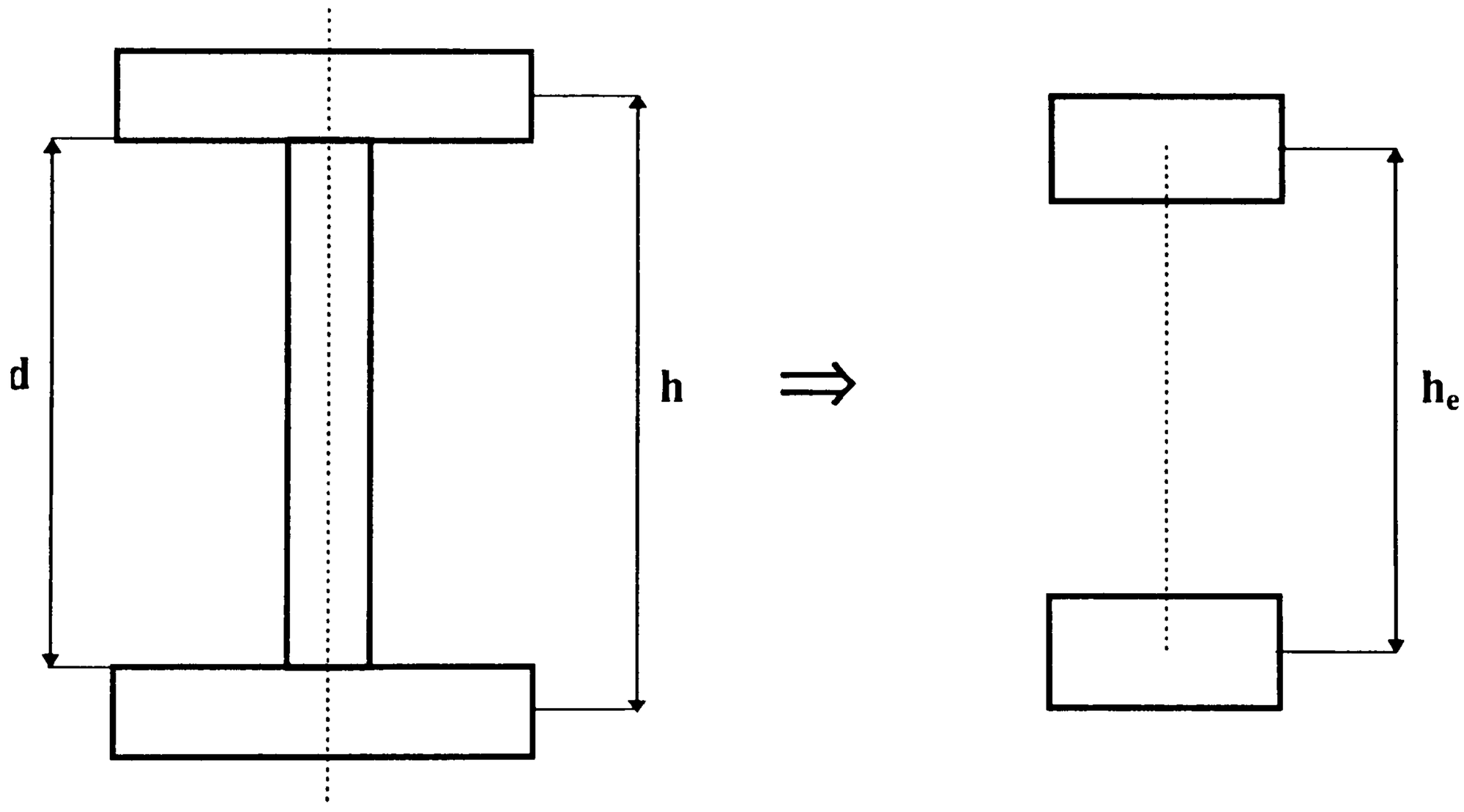

b) Equivalent section

Figure 6.1

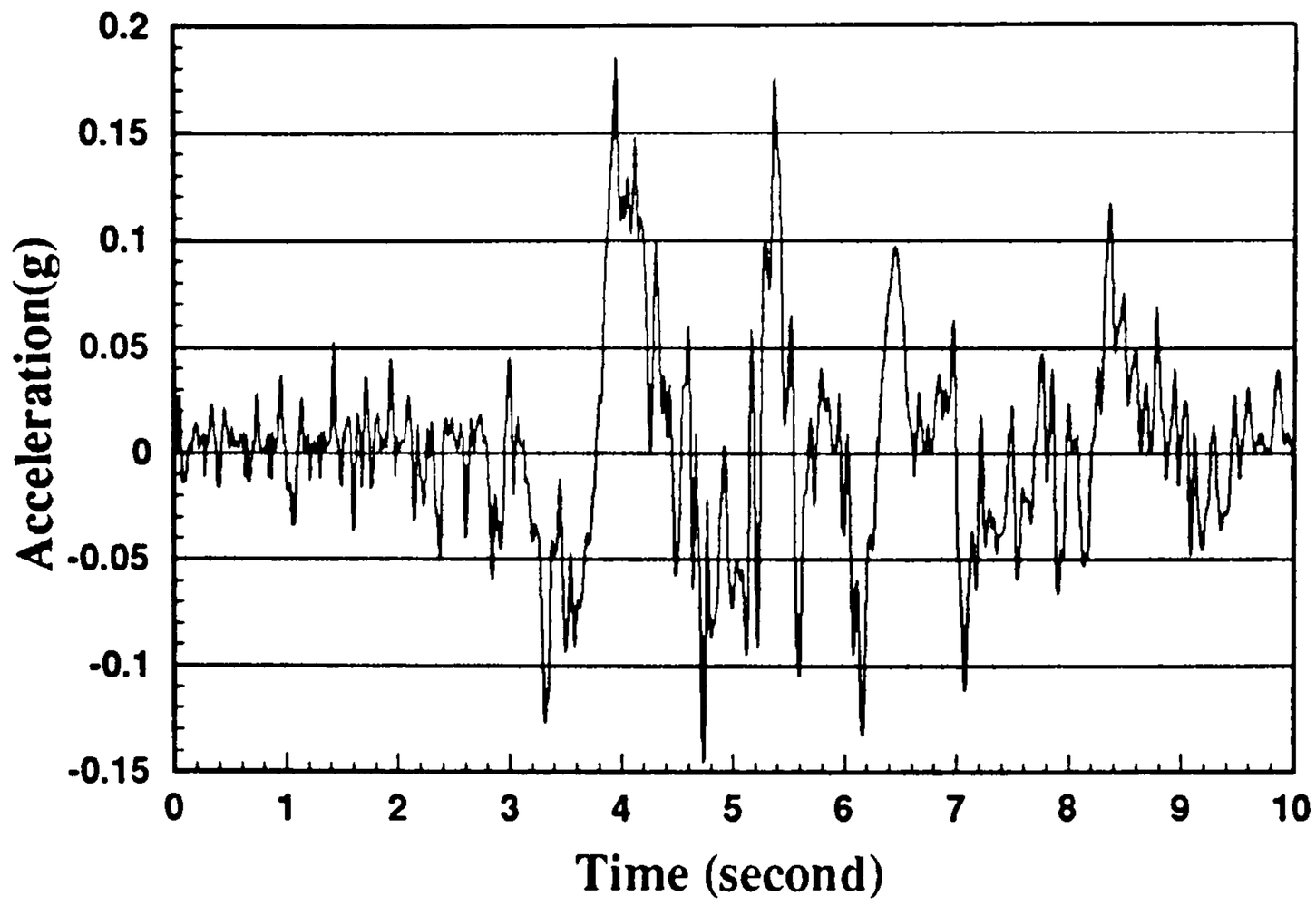

a) Corrected ground accelerations

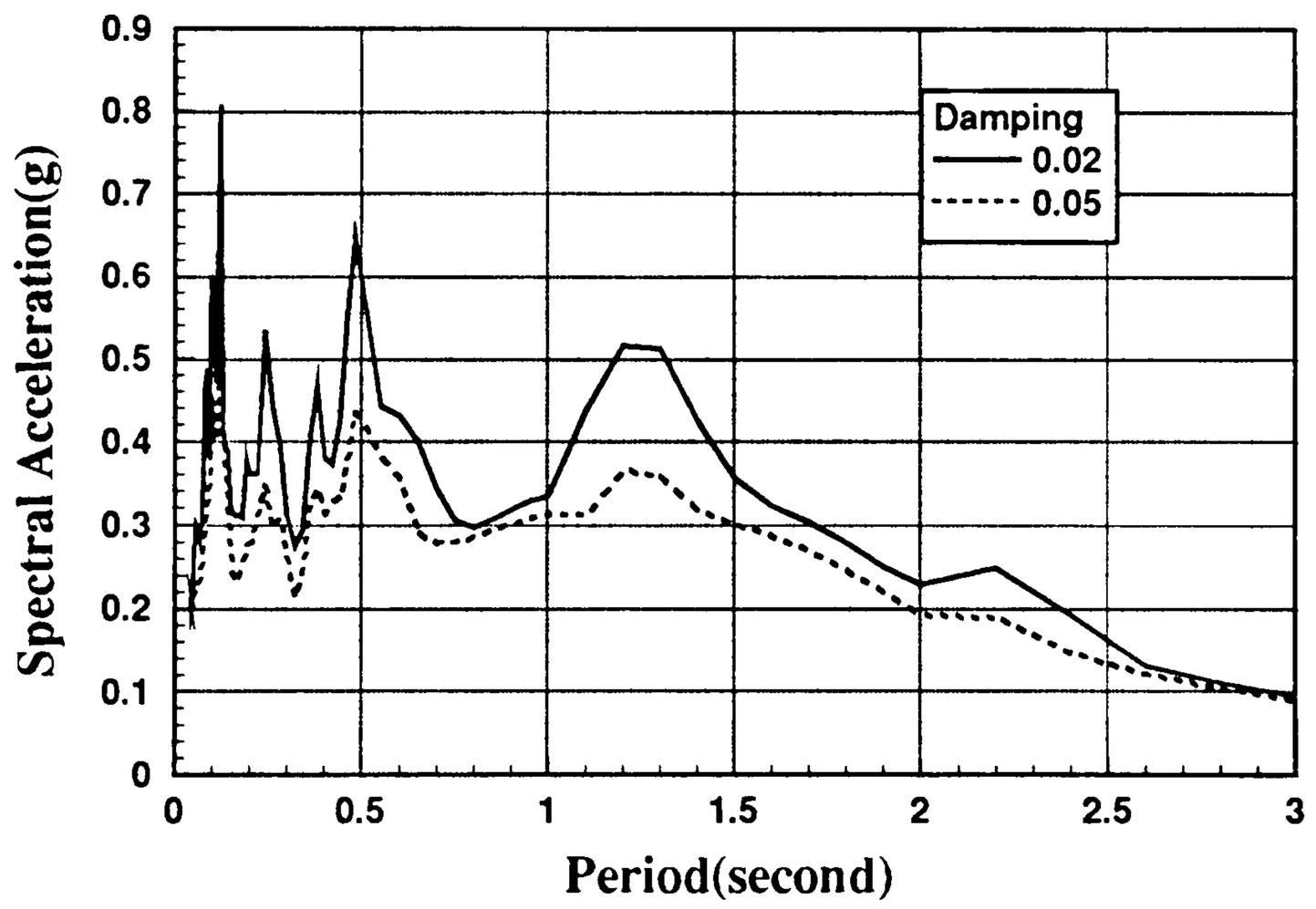

b) Elastic response spectra

Figure 6.2 Acceleration time history and elastic response spectra of Irpinia record

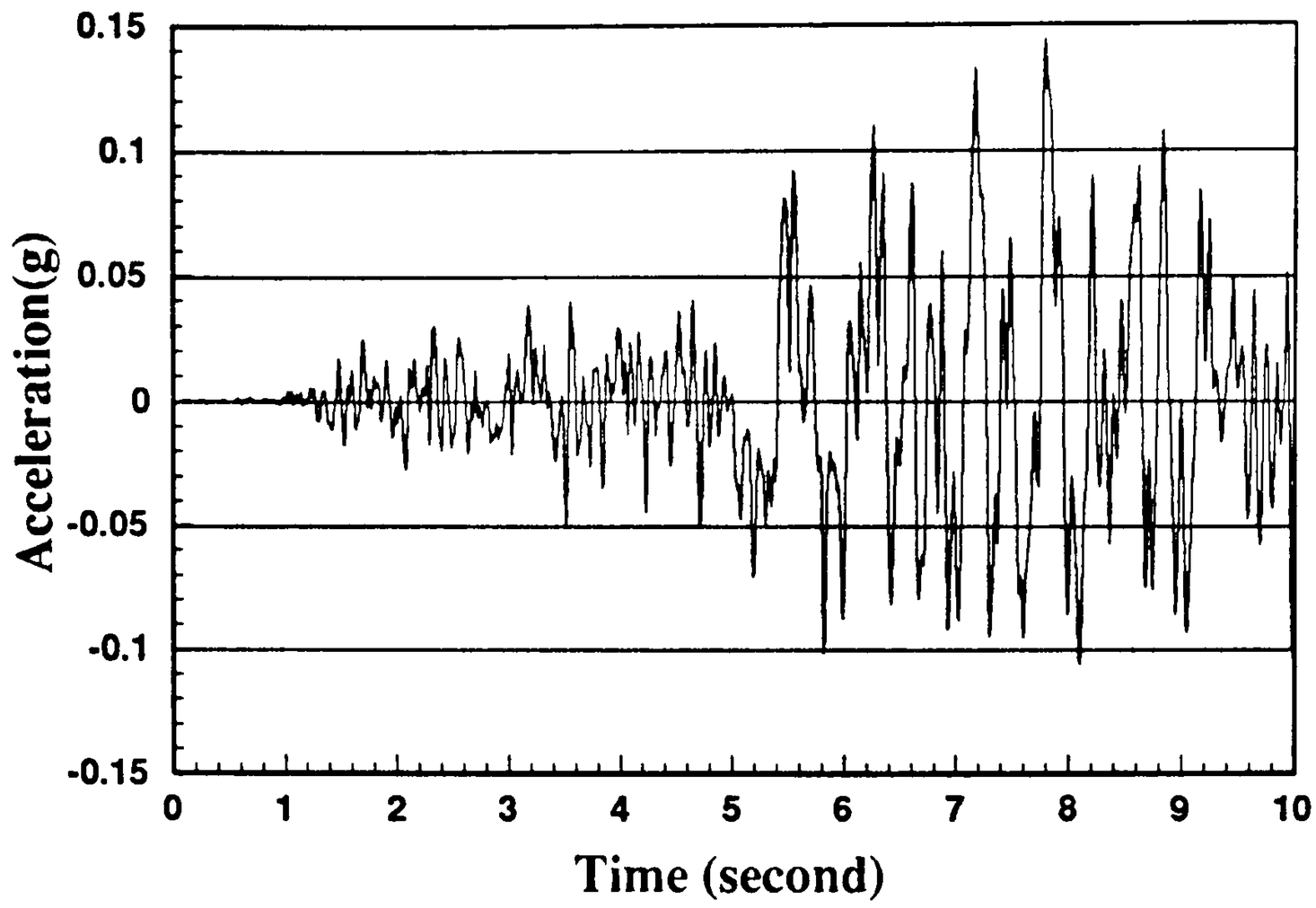

a) Corrected ground acceleration

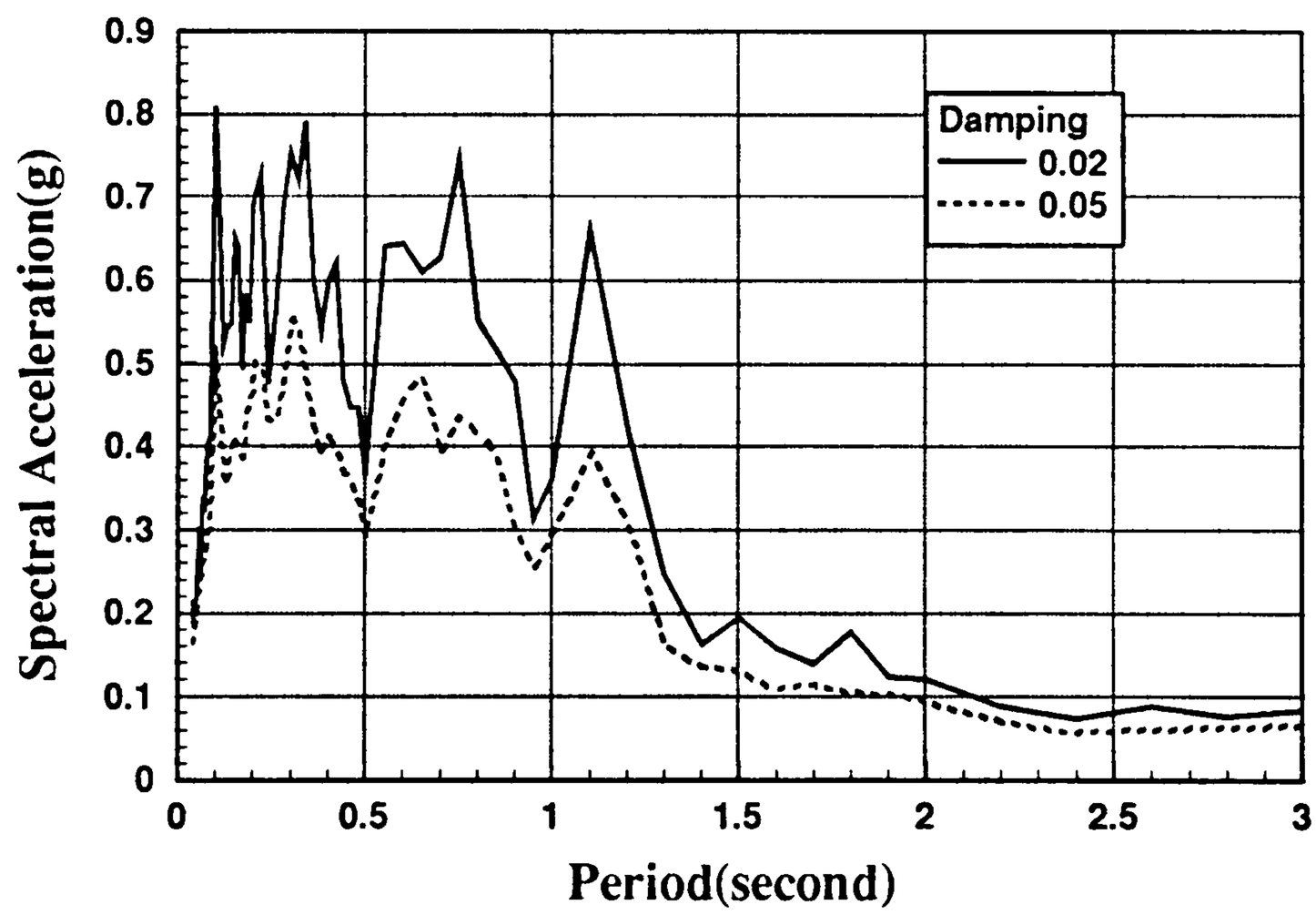

b) Elastic response spectra

Figure 6.3 Acceleration time history and elastic response spectra of Mexico record

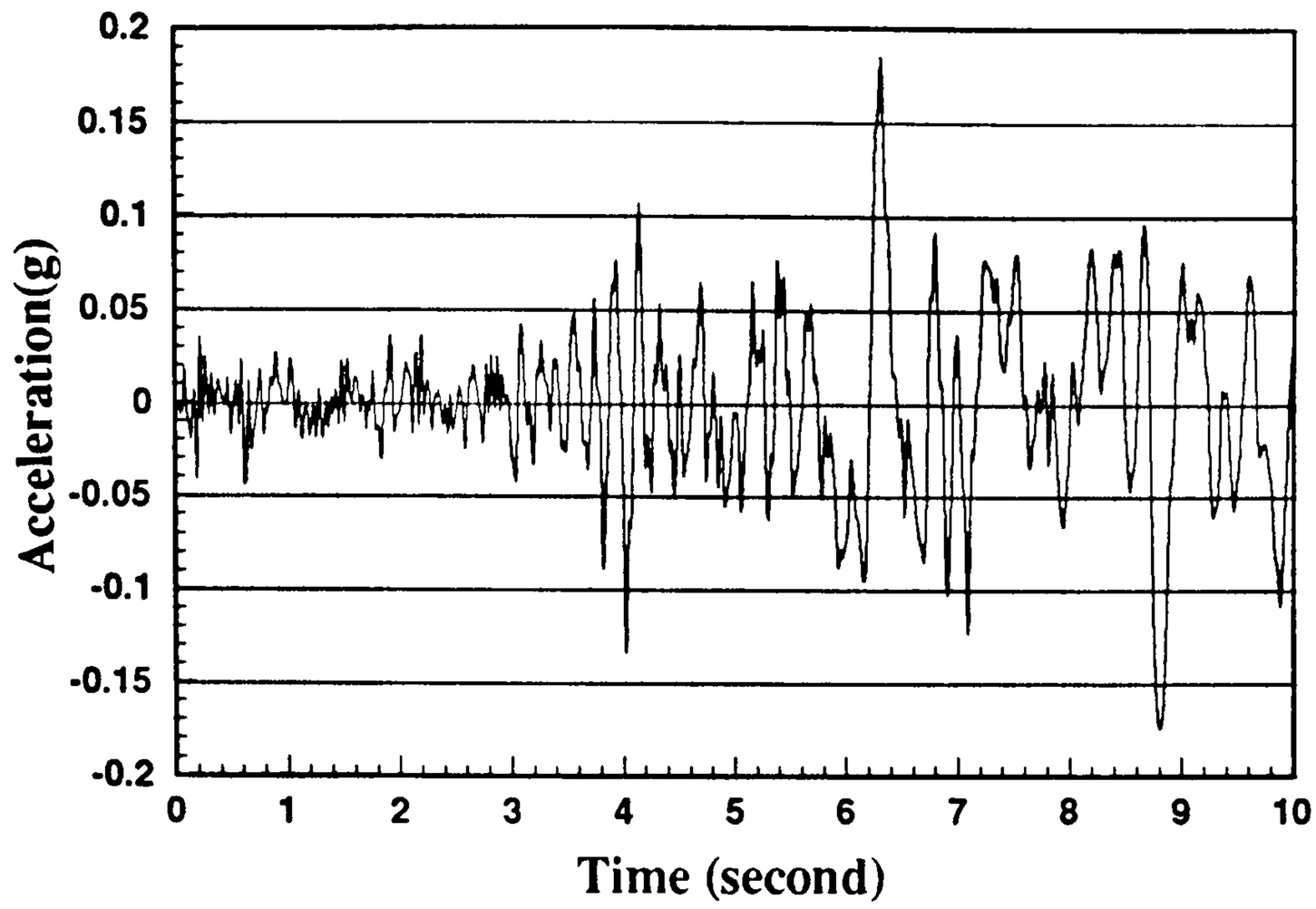

a) Corrected ground acceleration

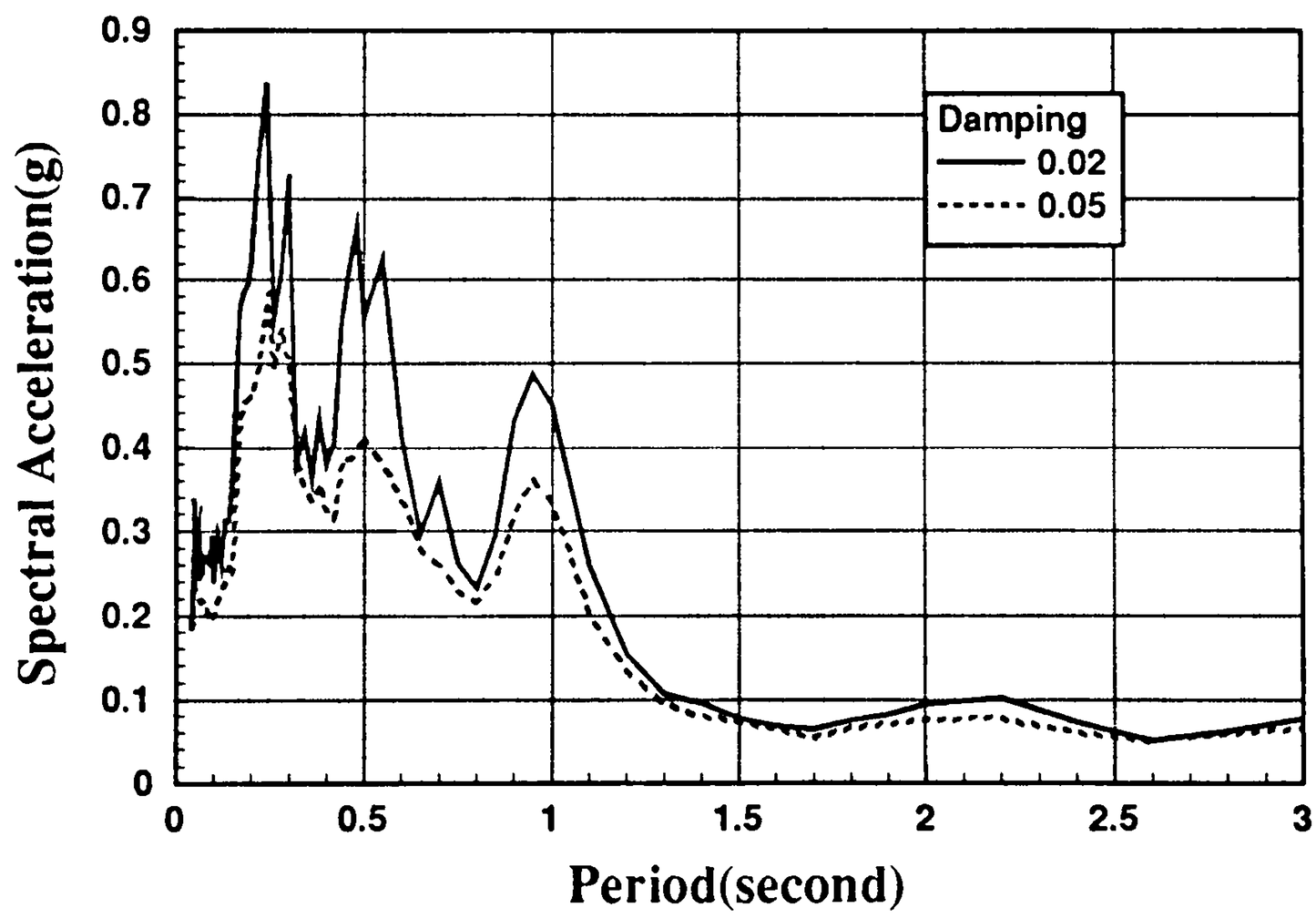

b) Elastic response spectra

Figure 6.4 Acceleration time history and elastic response spectra of San Fernando record

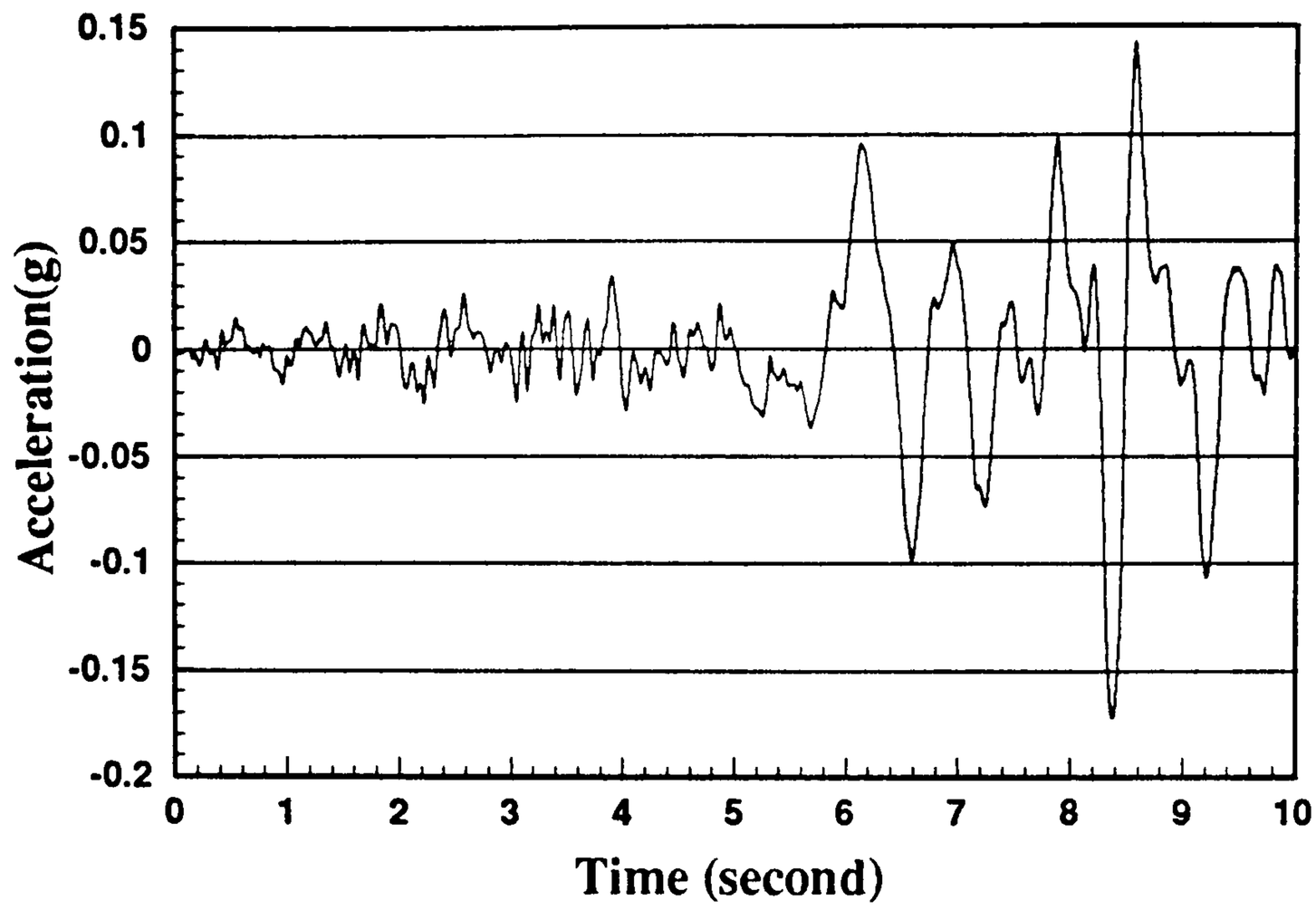

a) Corrected ground accelerations

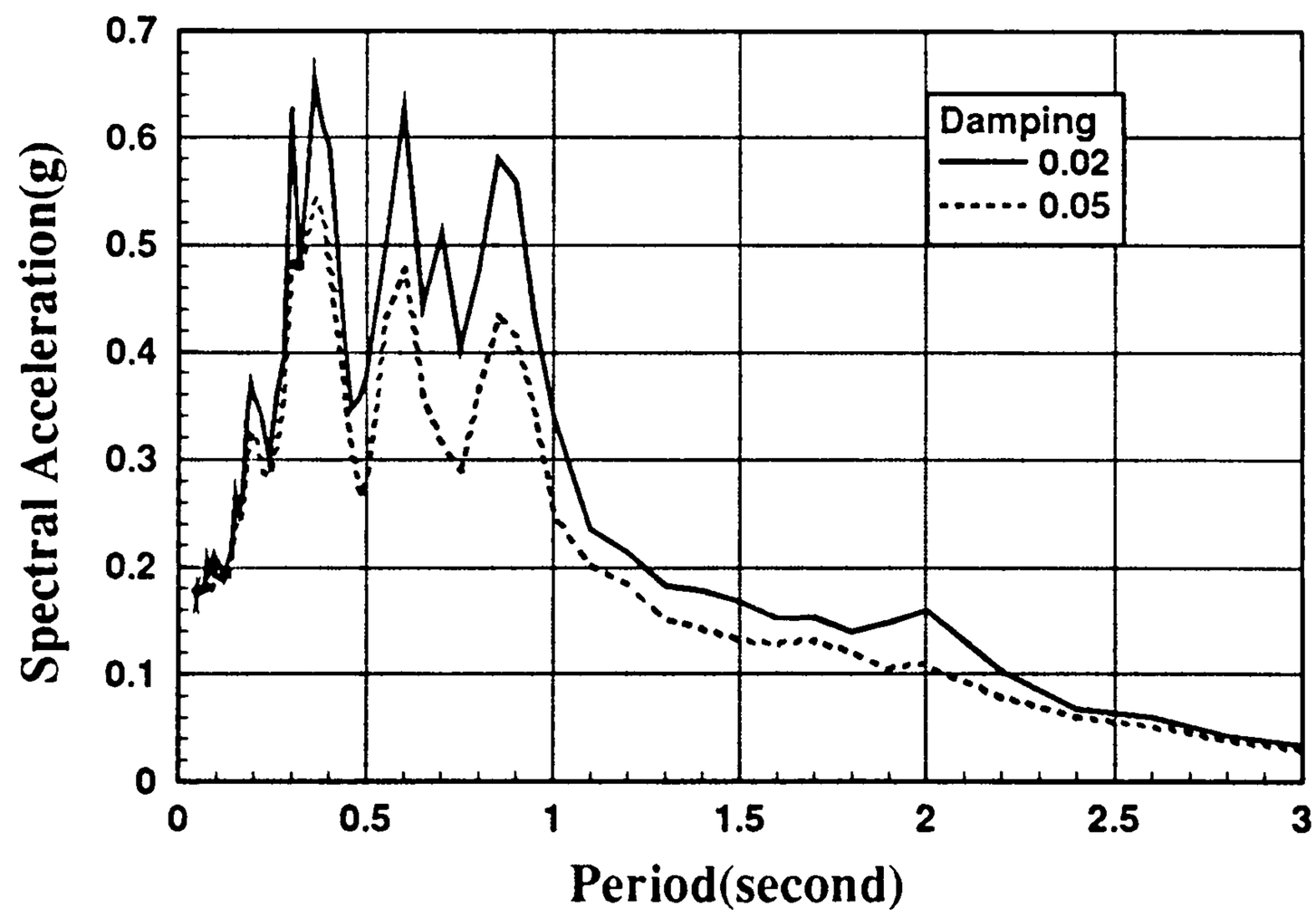

b) Elastic response spectra

Figure 6.5 Acceleration time history and elastic response spectra of Coalinga record

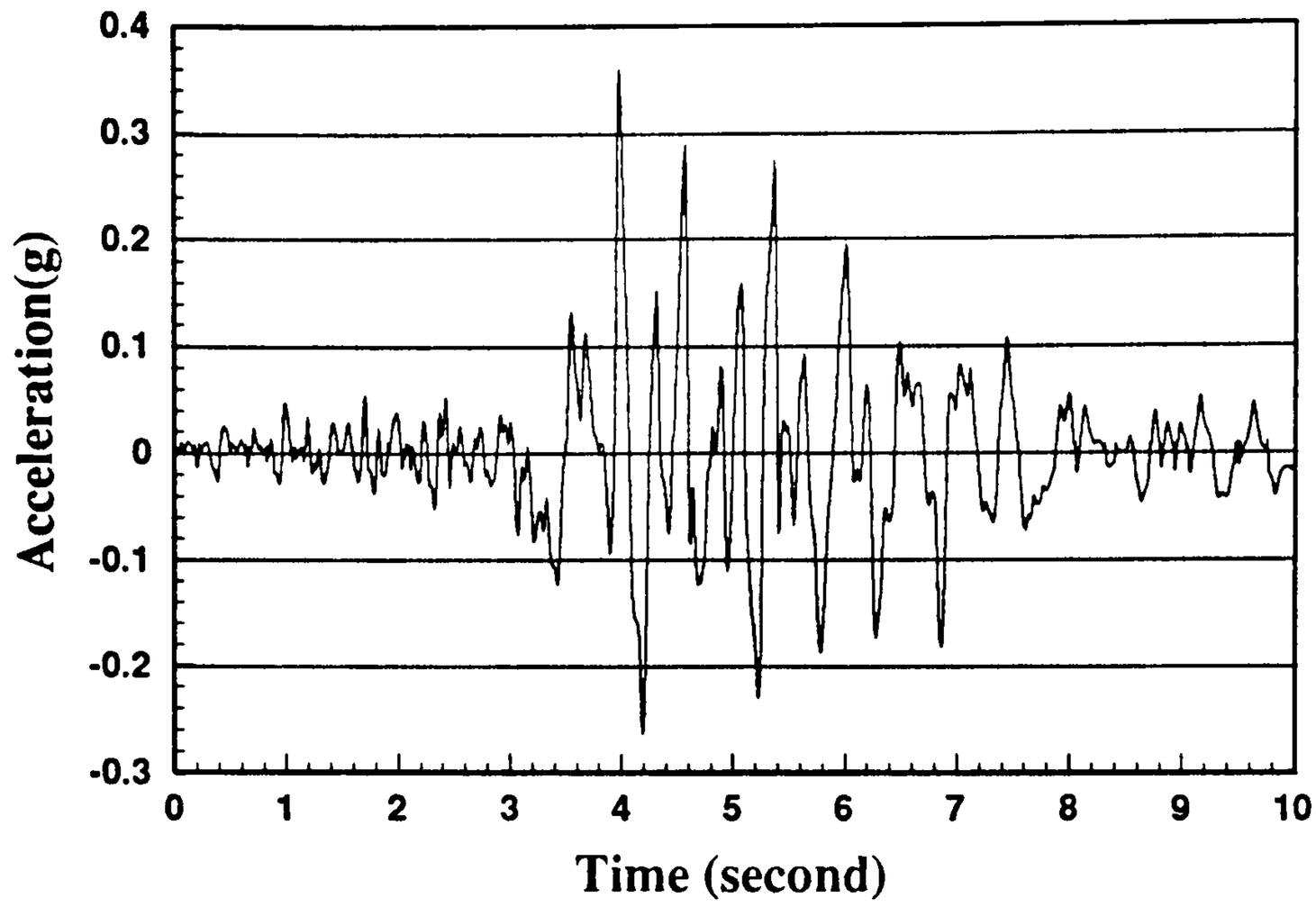

a) Corrected ground accelerations

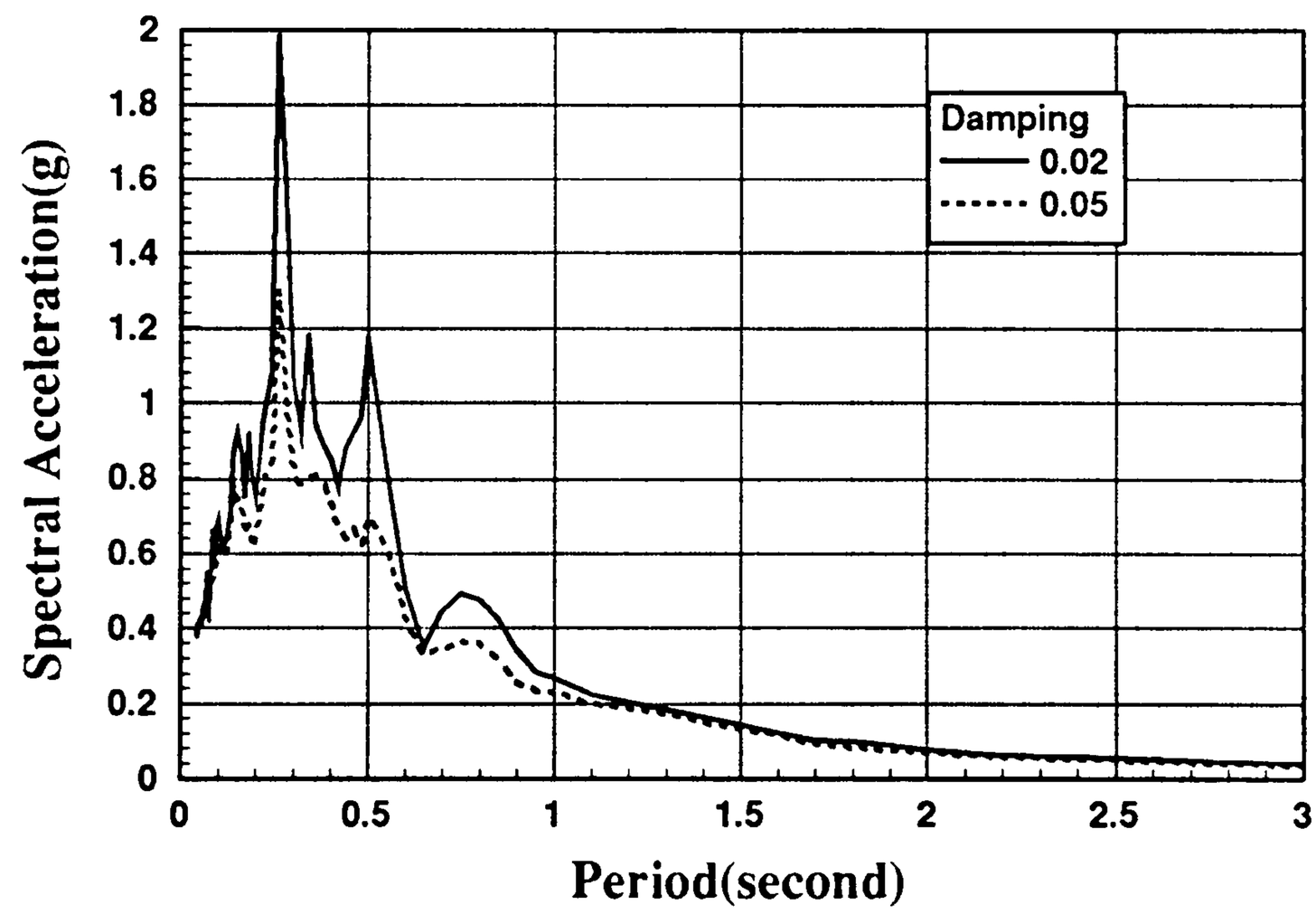

b) Elastic response spectra

Figure 6.6 Acceleration time history and elastic response spectra of Friuli record

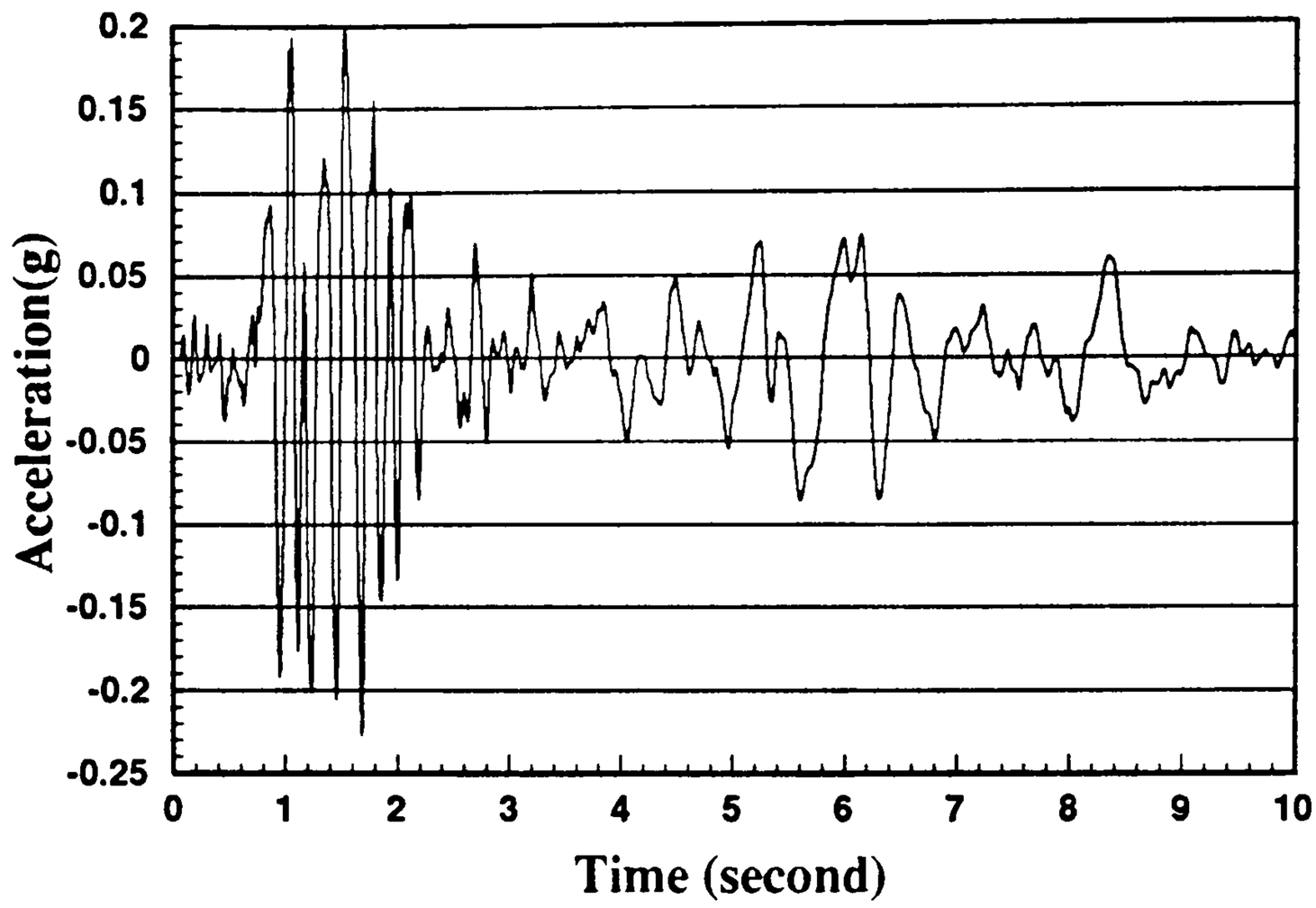

a) Corrected acceleration record

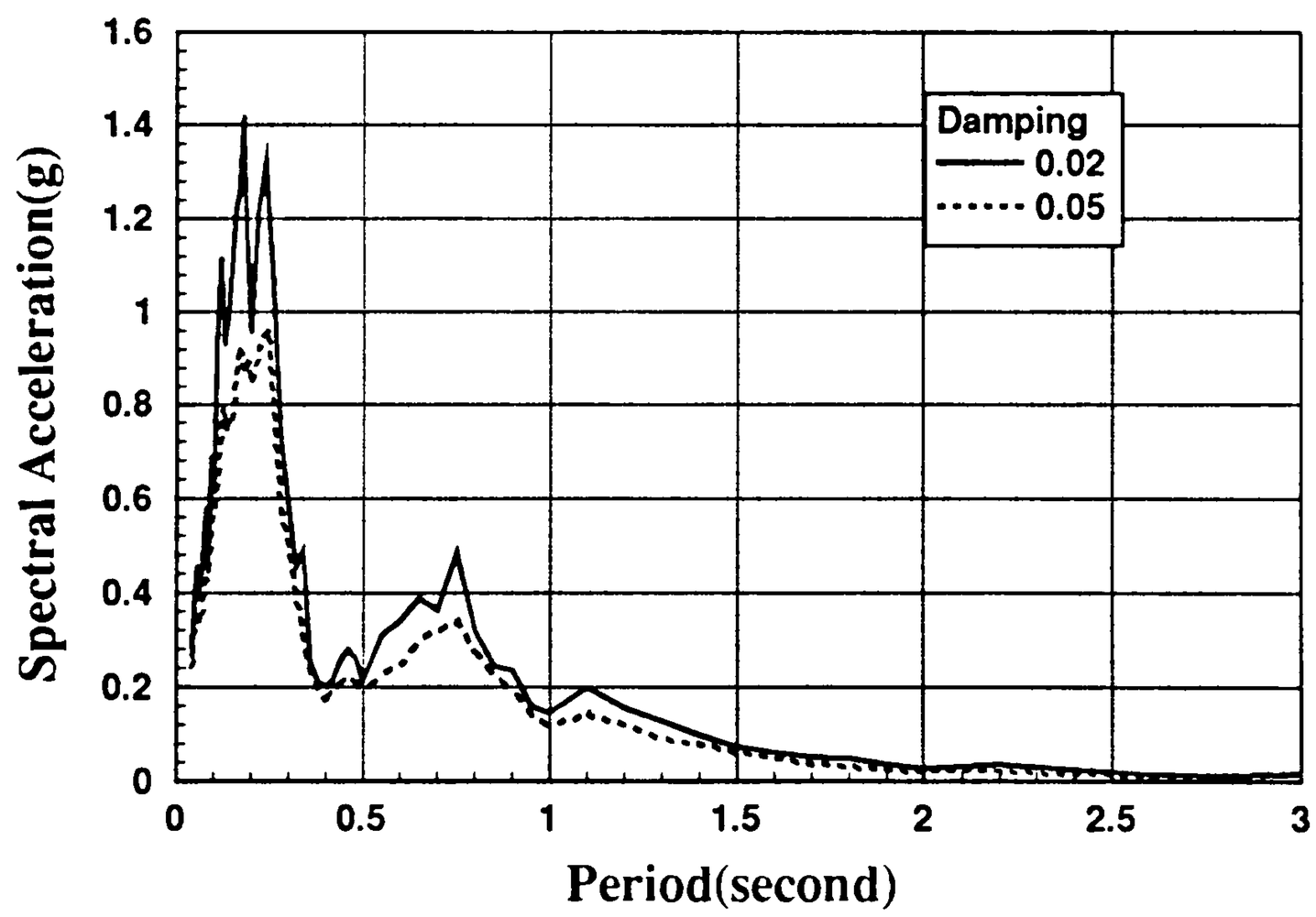

b) Elastic response spectra

Figure 6.7 Acceleration time history and elastic response spectra of Morgan Hill record

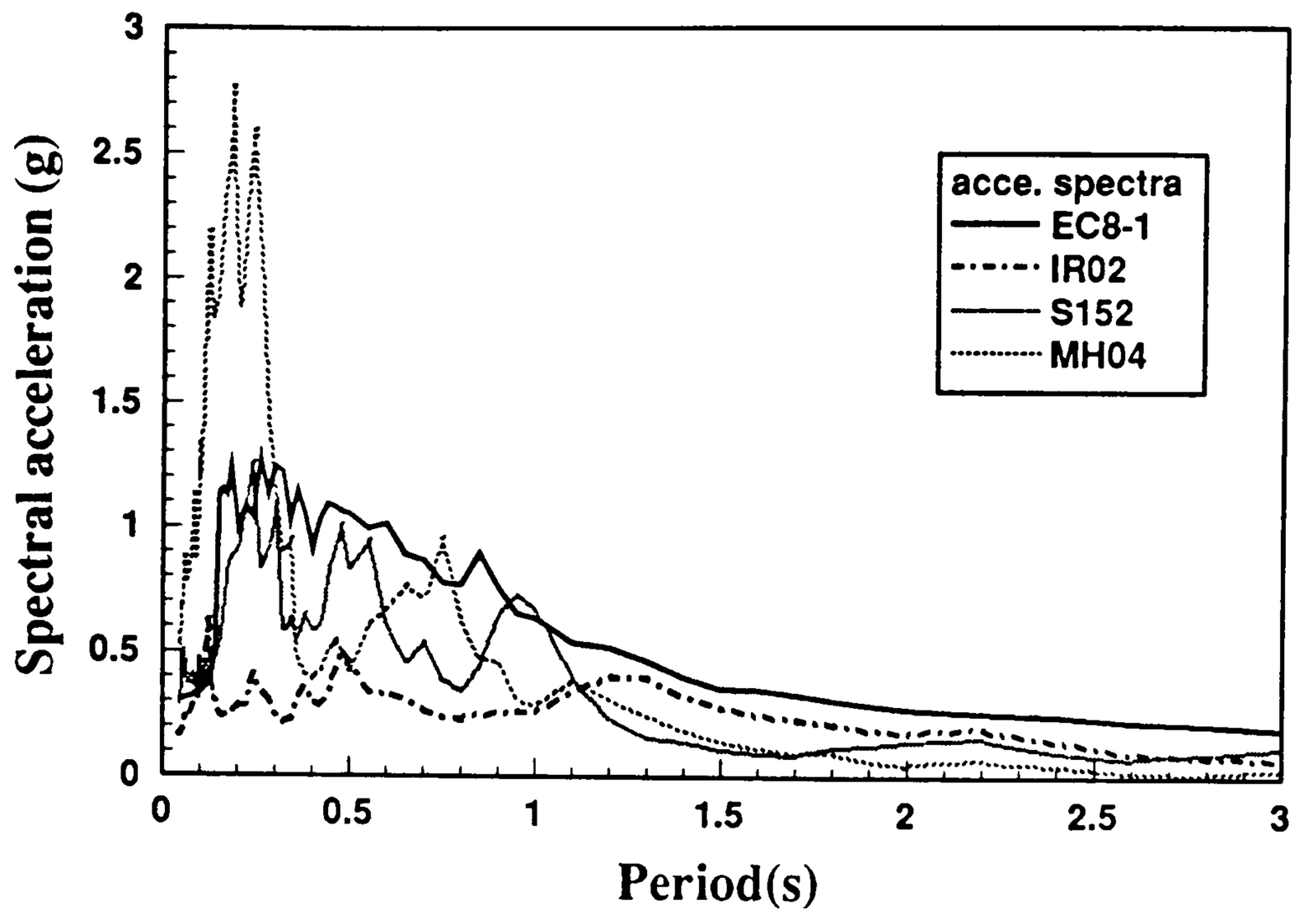

Figure 6.8 Comparison of elastic response spectra of different records

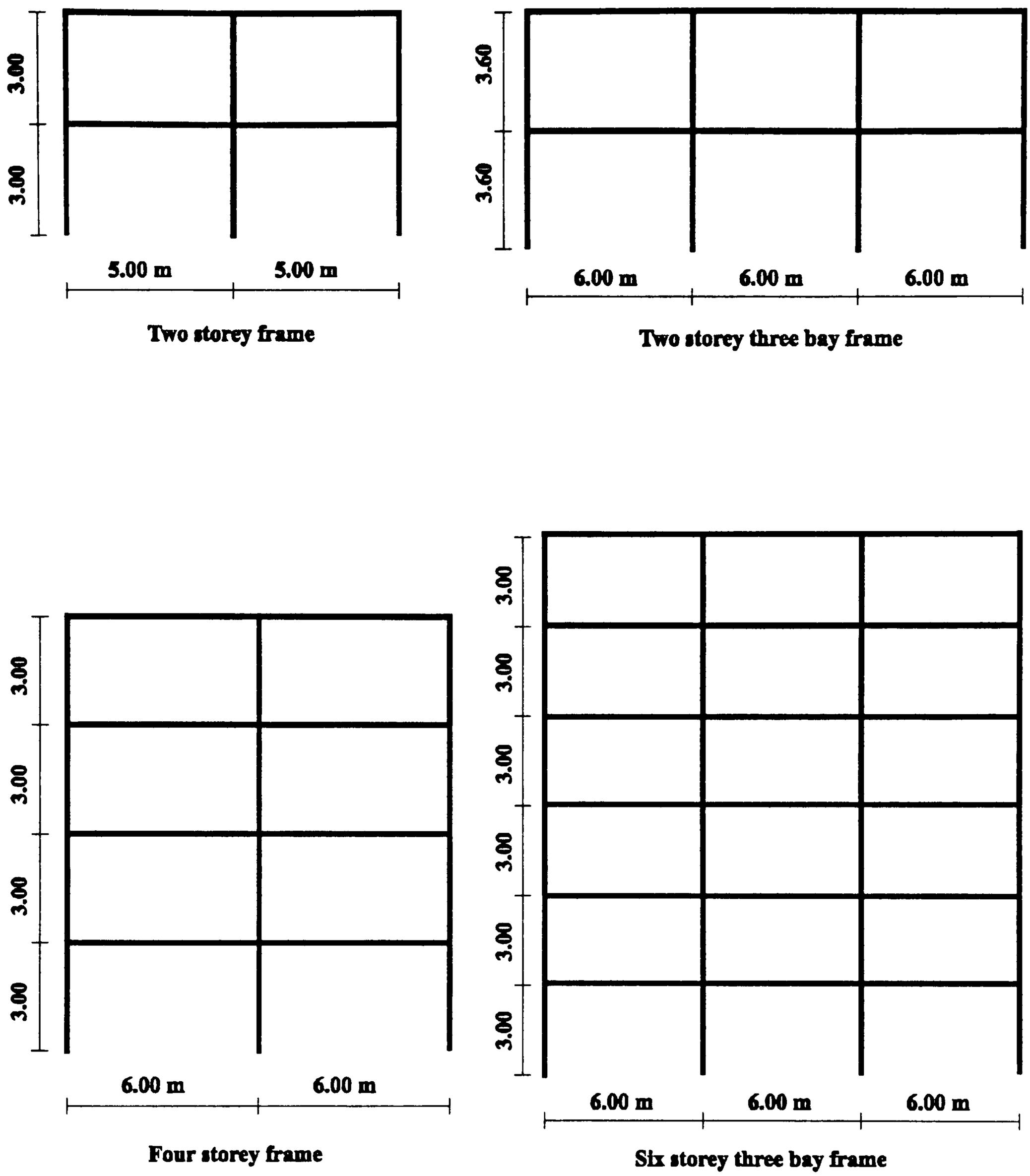

Figure 6.9 Frame configuration

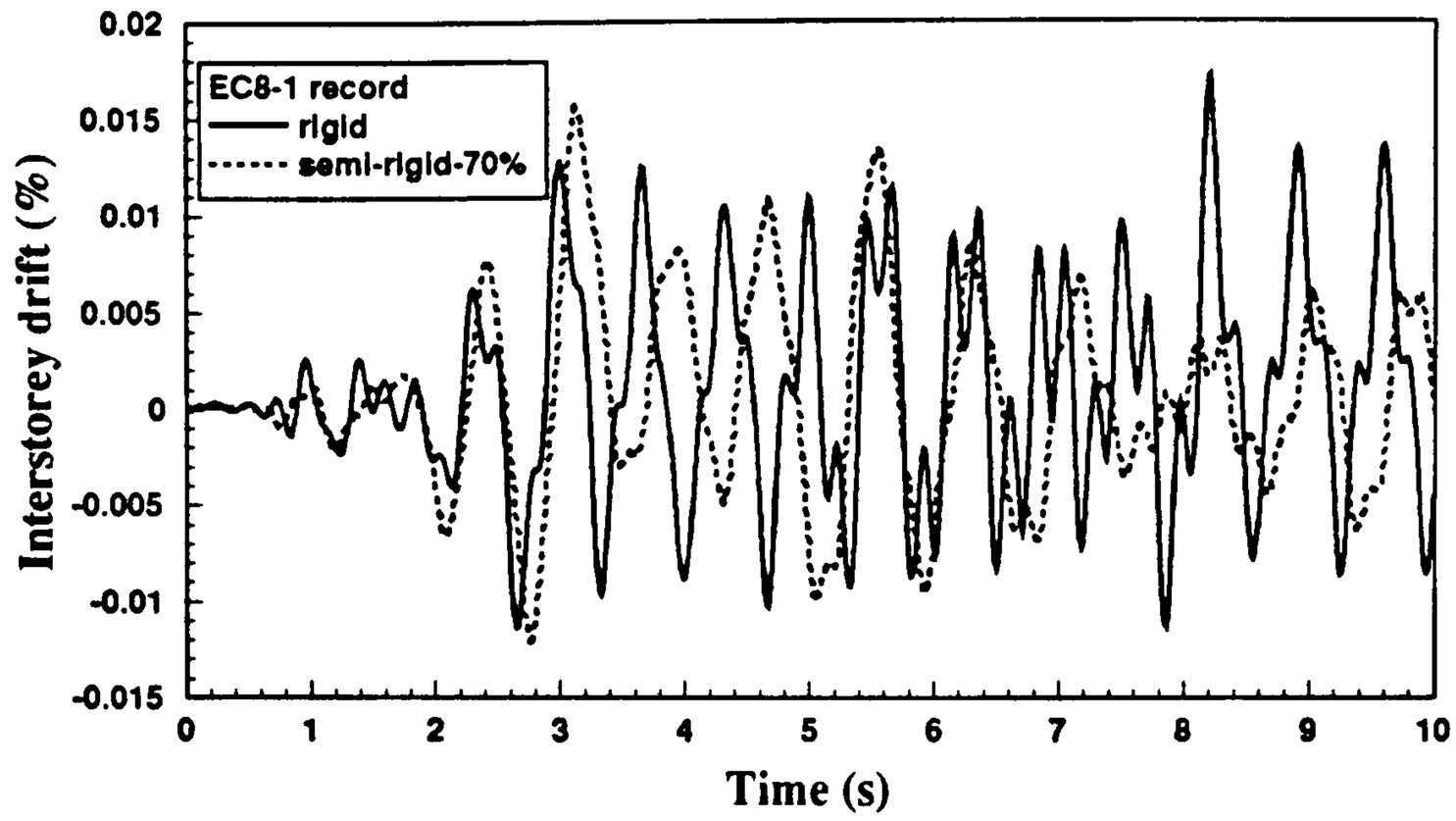

a) Interstorey drift

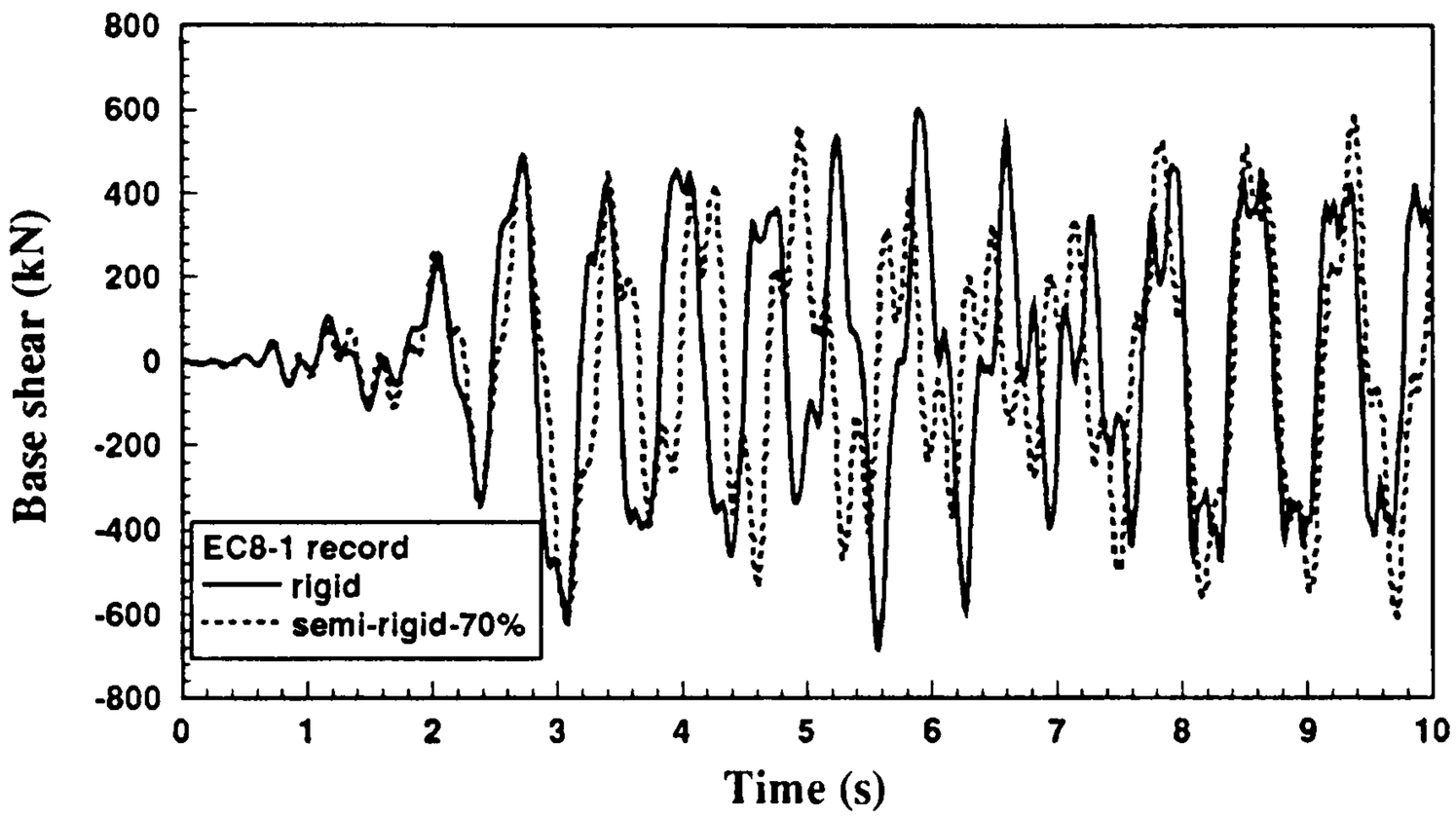

b) Base shear

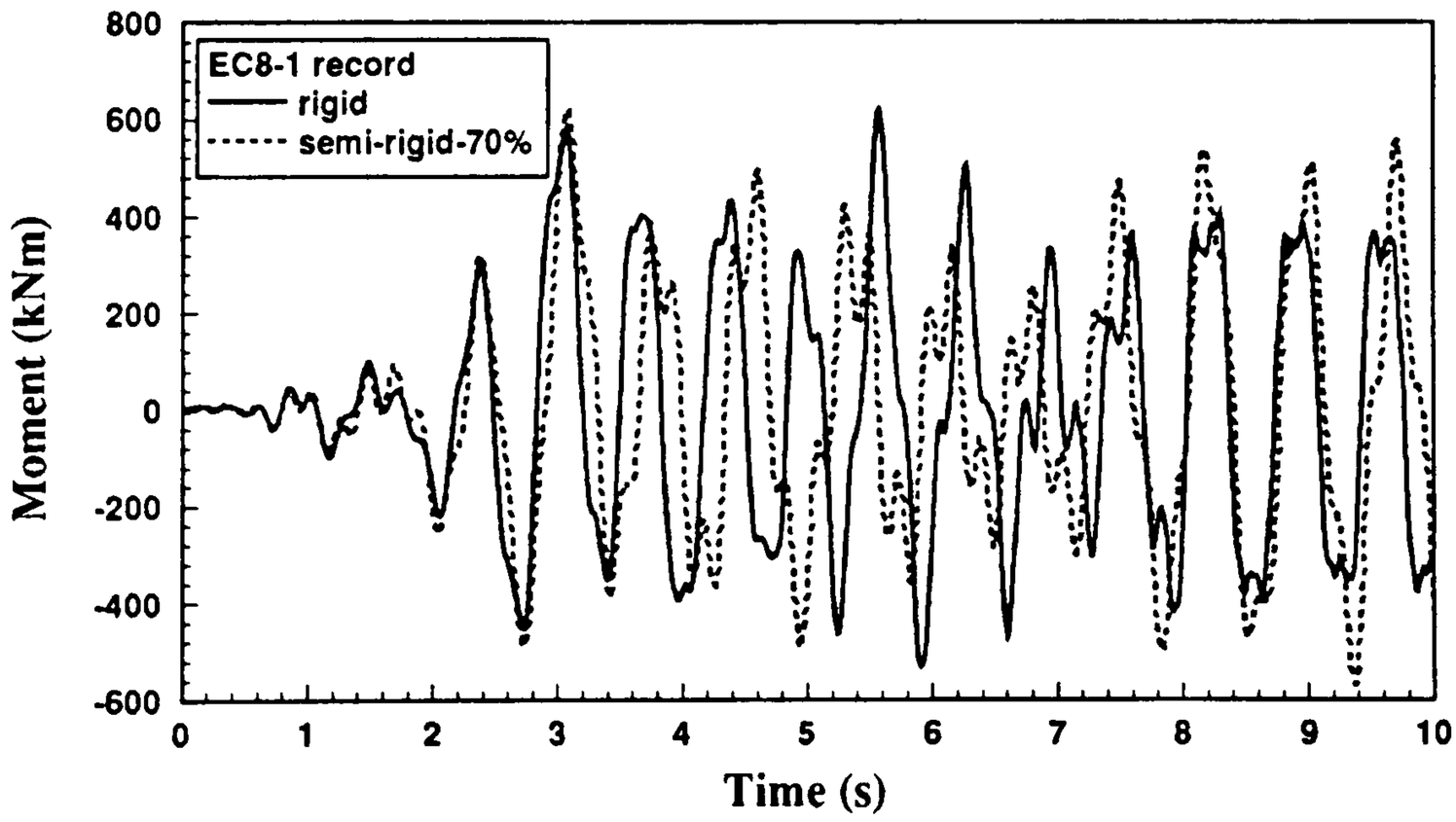

c) Moment at the base of the column in the first storey

Figure 6.10 Comparison of the response of four-storey semi-rigid frame (S42D70) with rigid frame

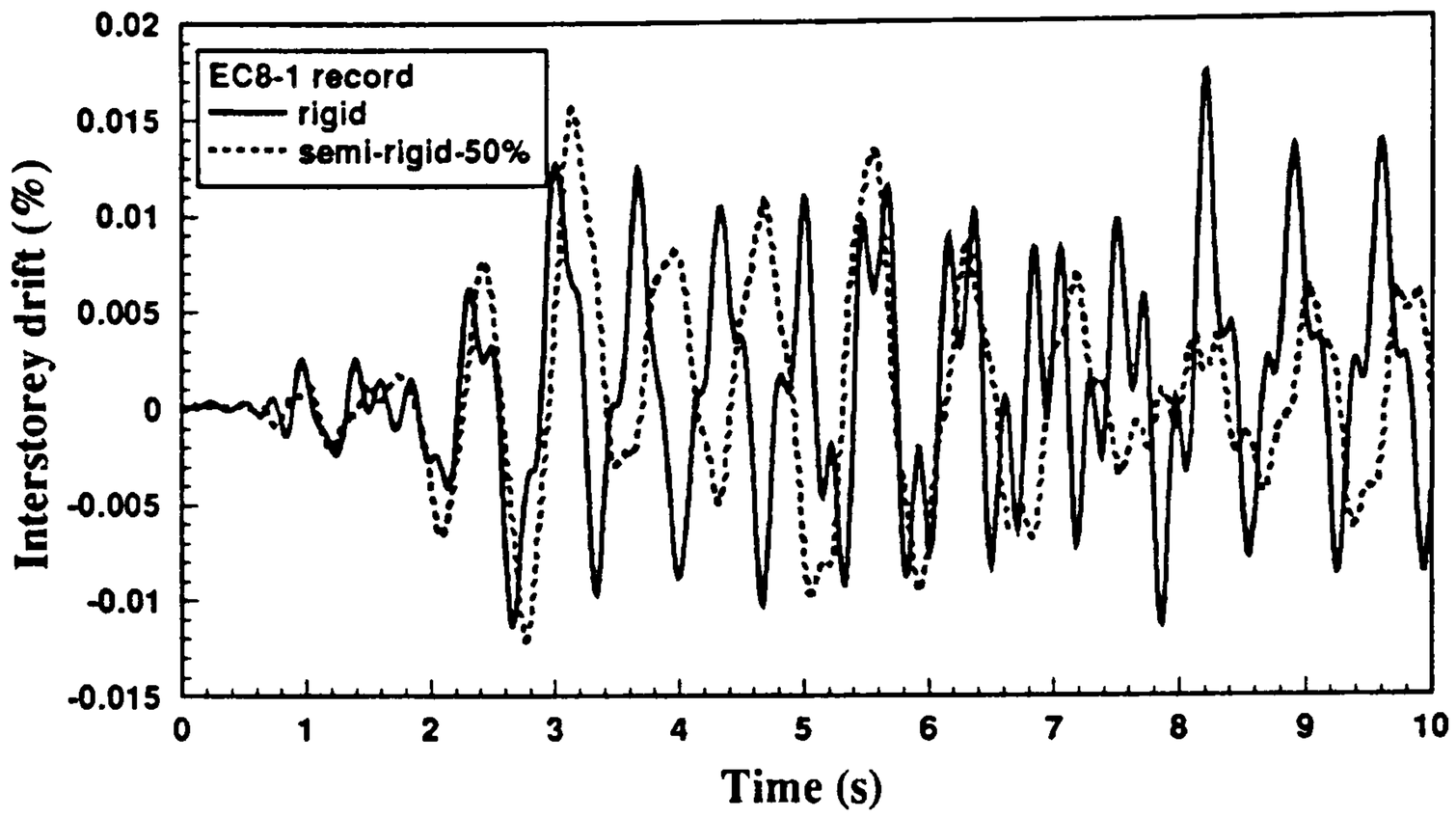

a) interstorey drift

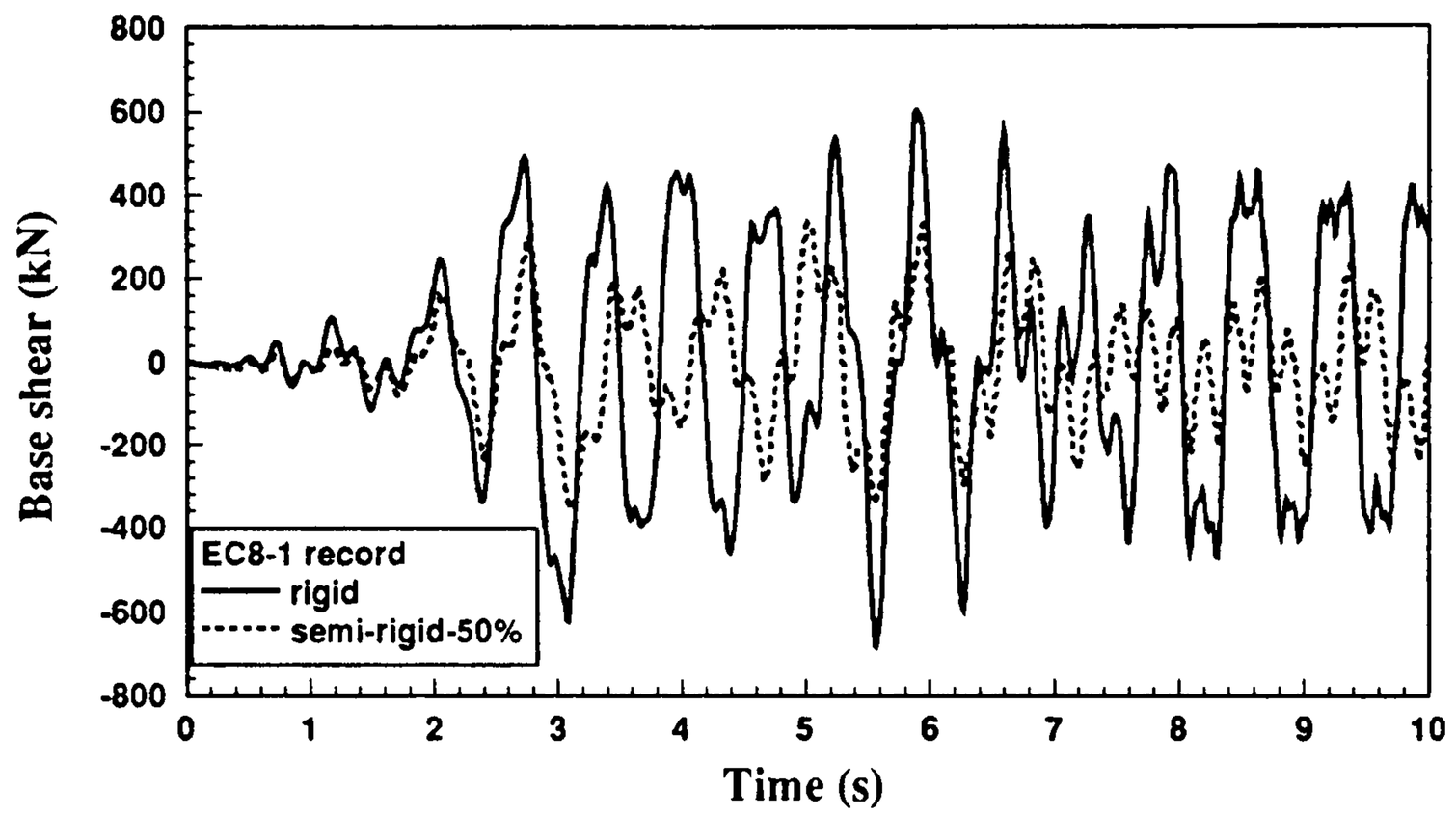

b) Base shear

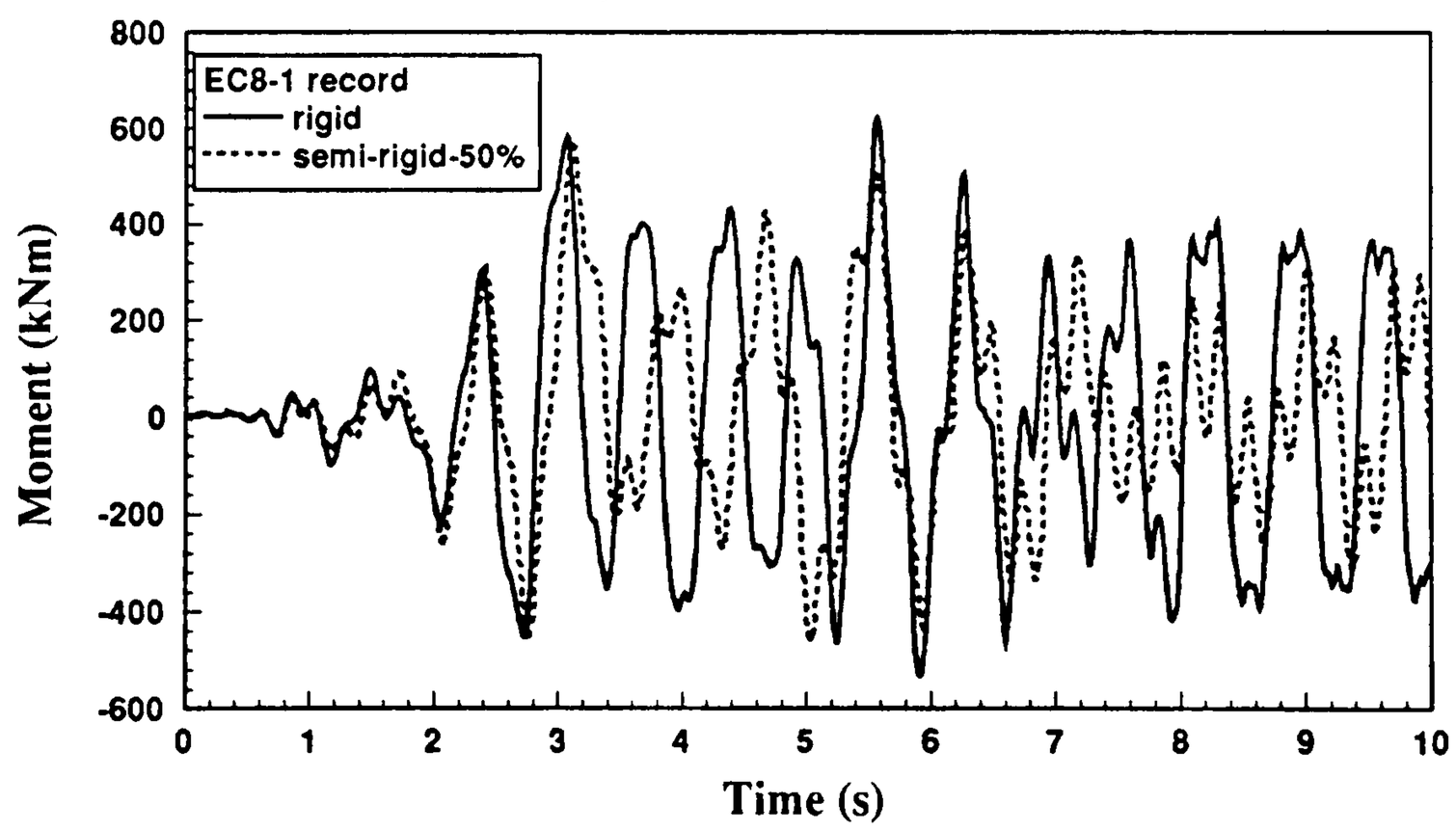

c) Moment at the base of the column in the first storey

Figure 6.11 Comparison of the response of four-storey semi-rigid frame (S42D50) with the rigid frame

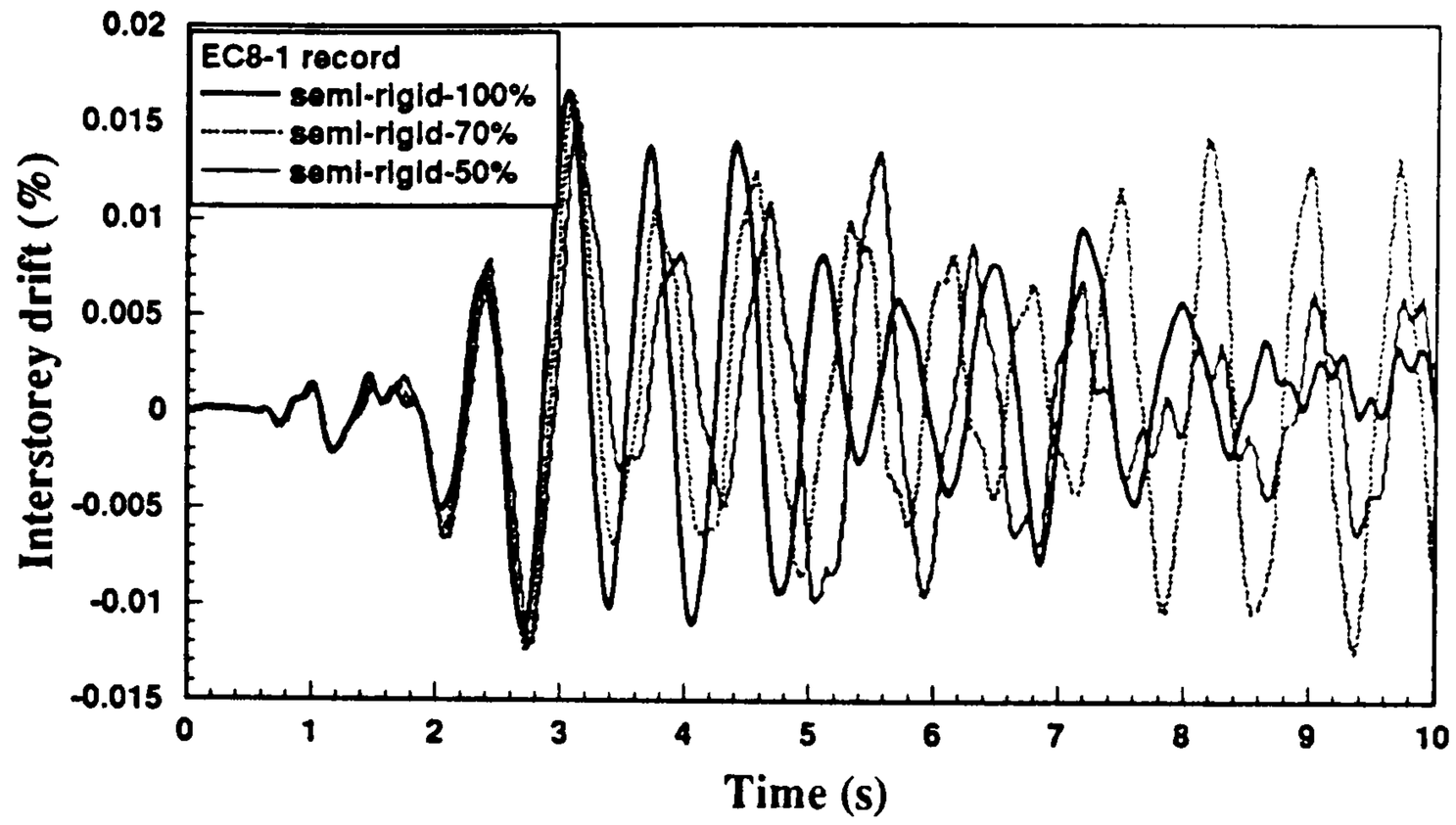

a) Interstorey drift

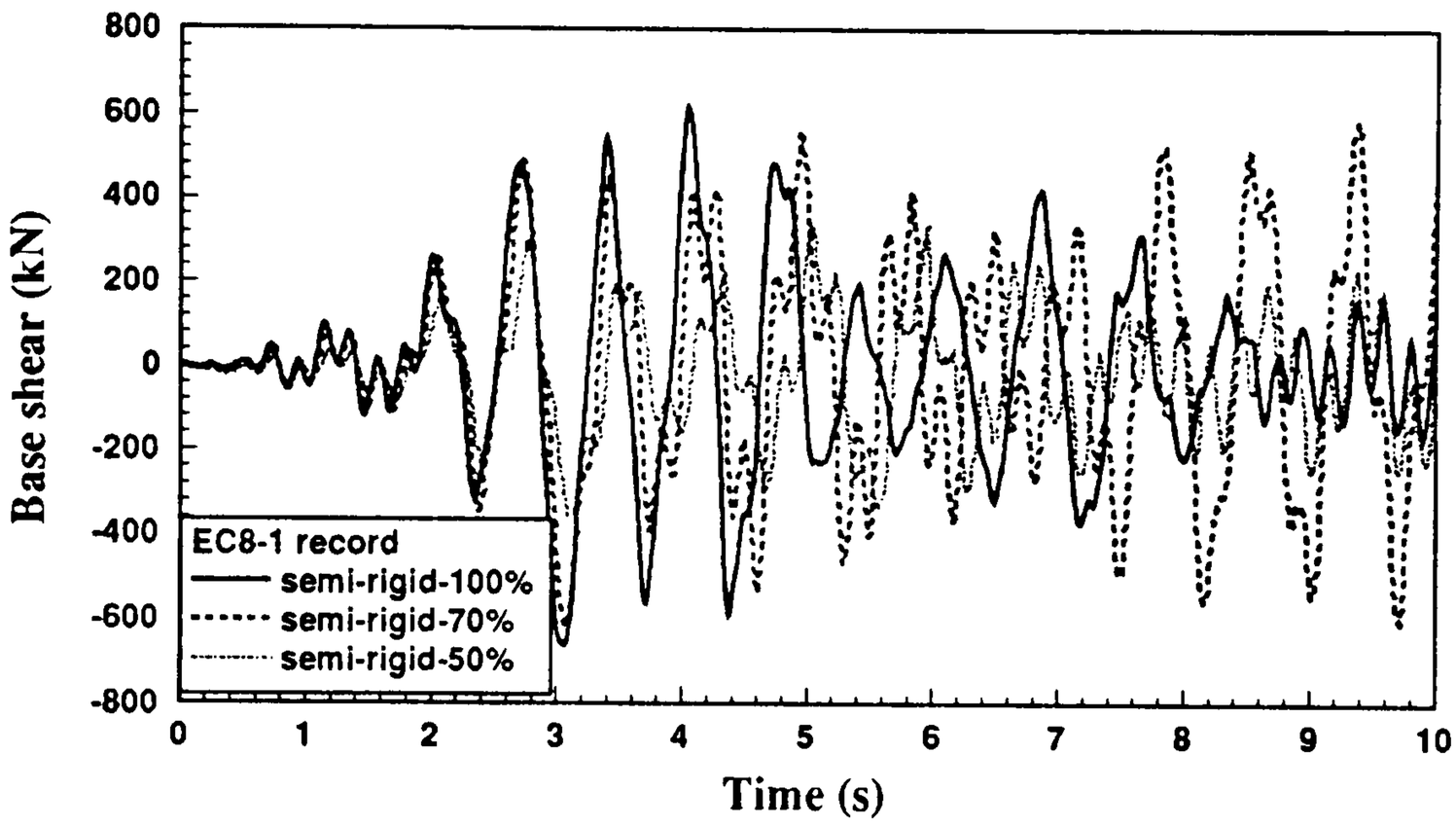

b) Base shear

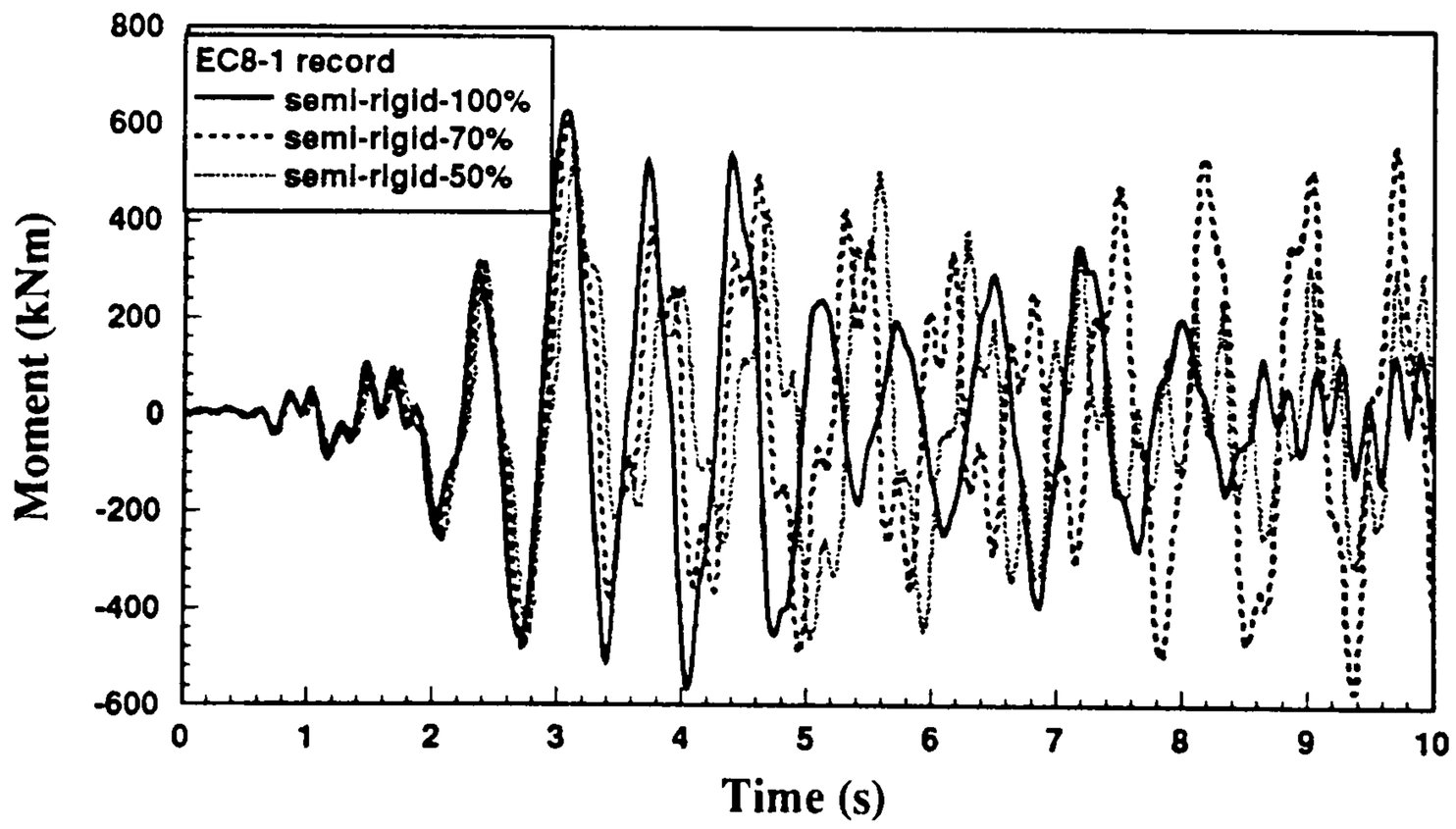

c) Moment at the base of the column in the first storey

Figure 6.12 Comparison of the response of four storey semi-rigid frames

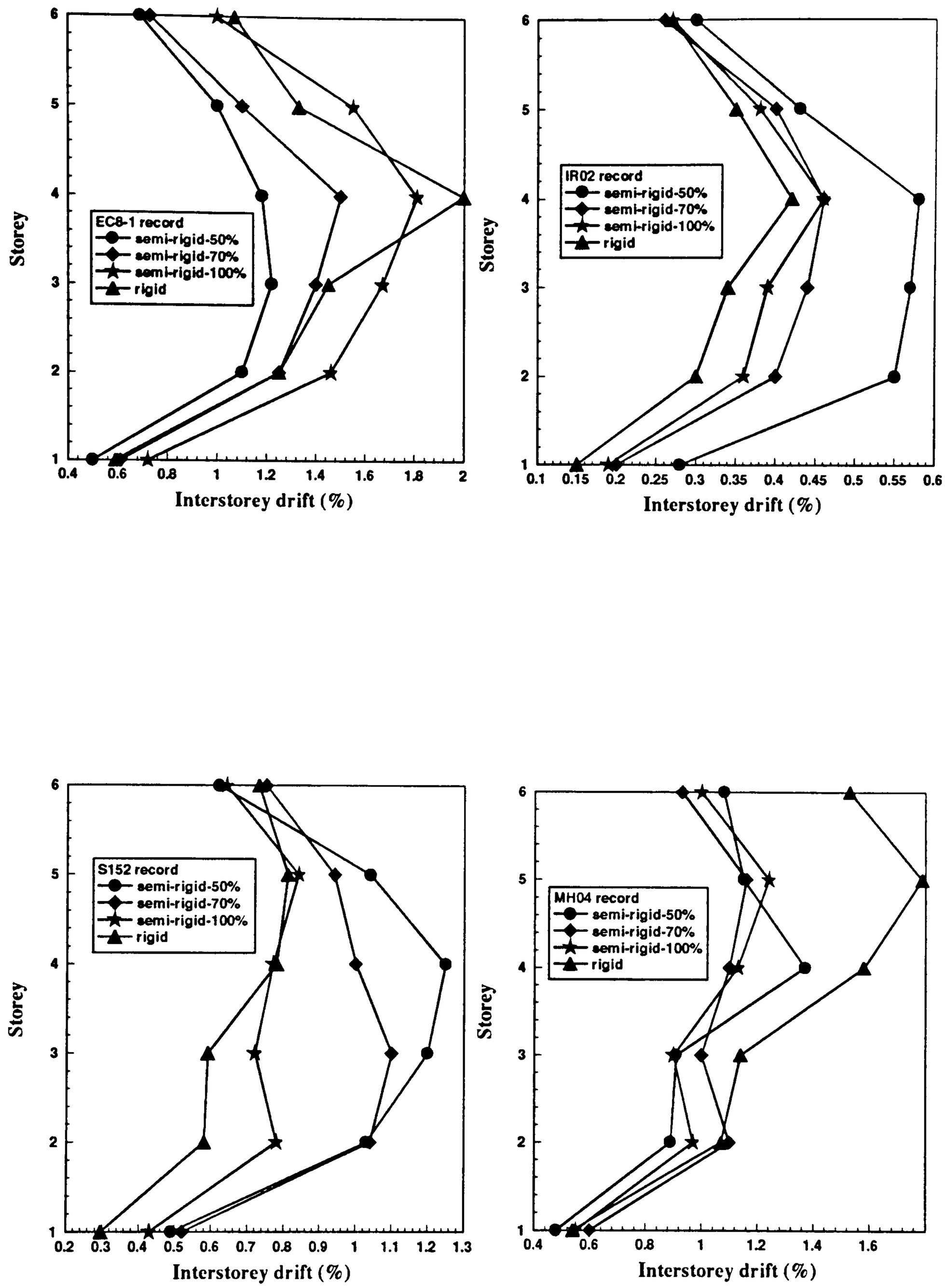

Figure 6.13 Maximum interstorey drift of six storey frames

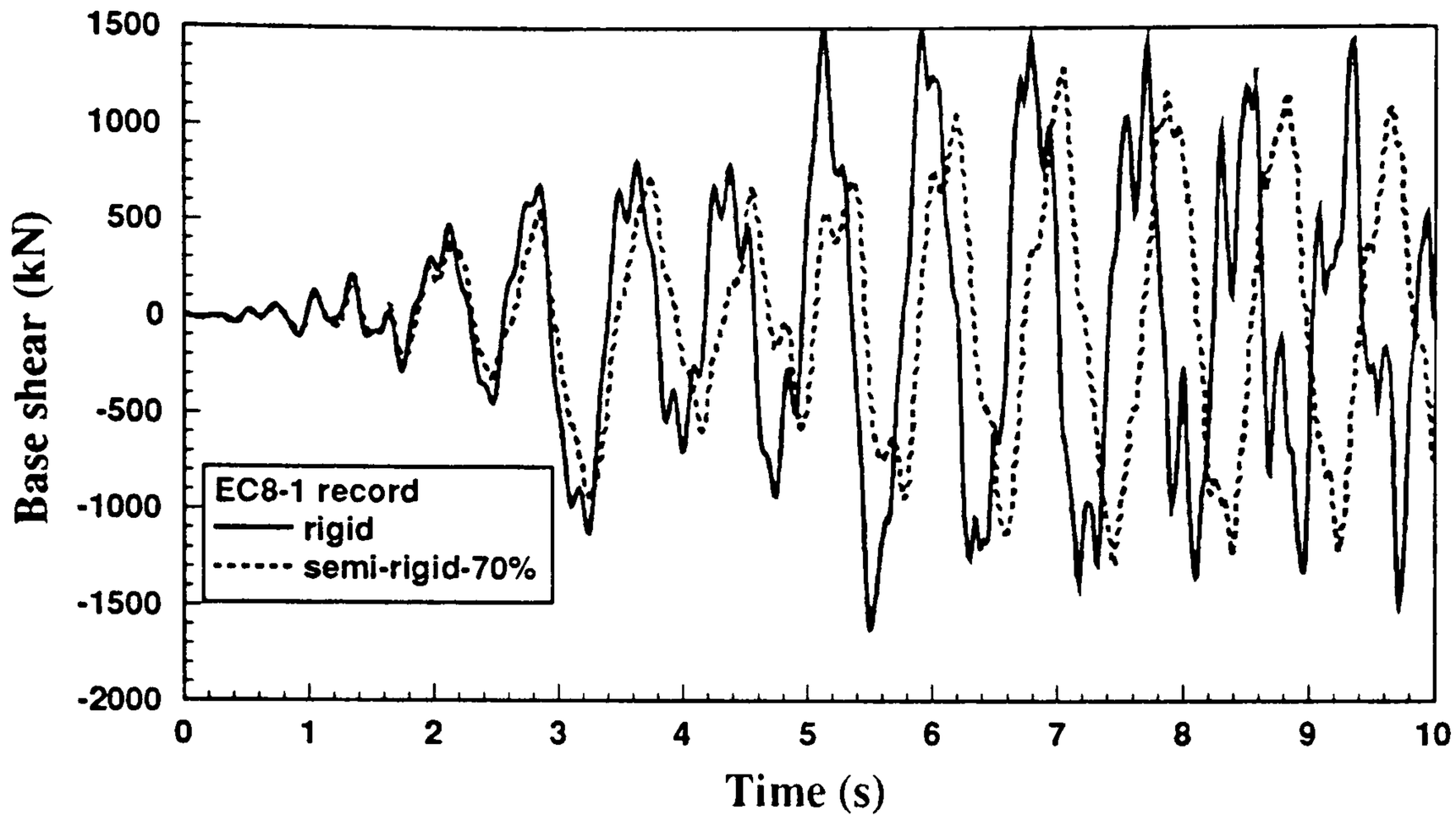

a) Base shear

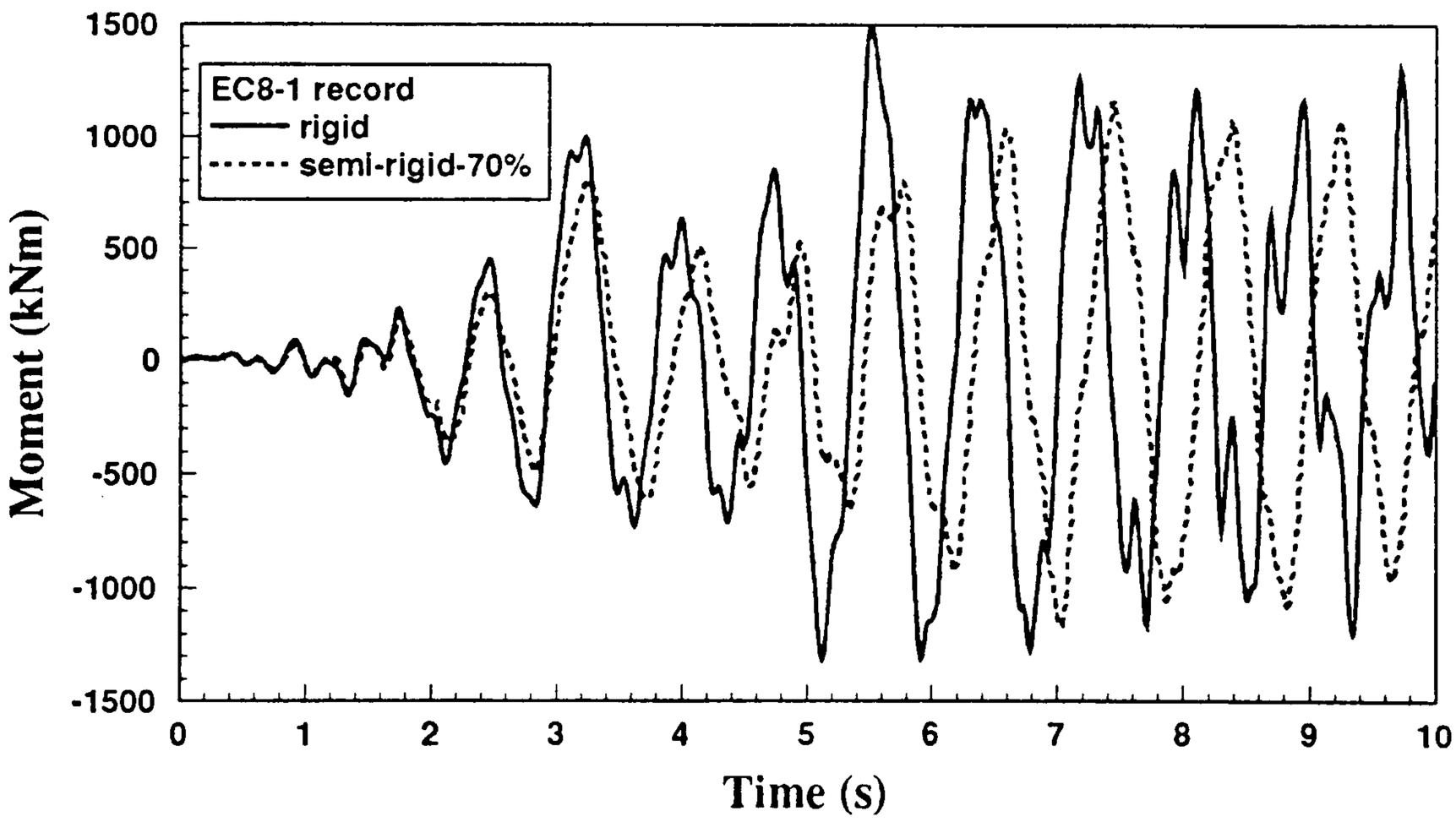

b) Moment at the base of the column in the first storey

Figure 6.14 Comparison of the response of six storey semi-rigid frame (S63D70) with the rigid frame

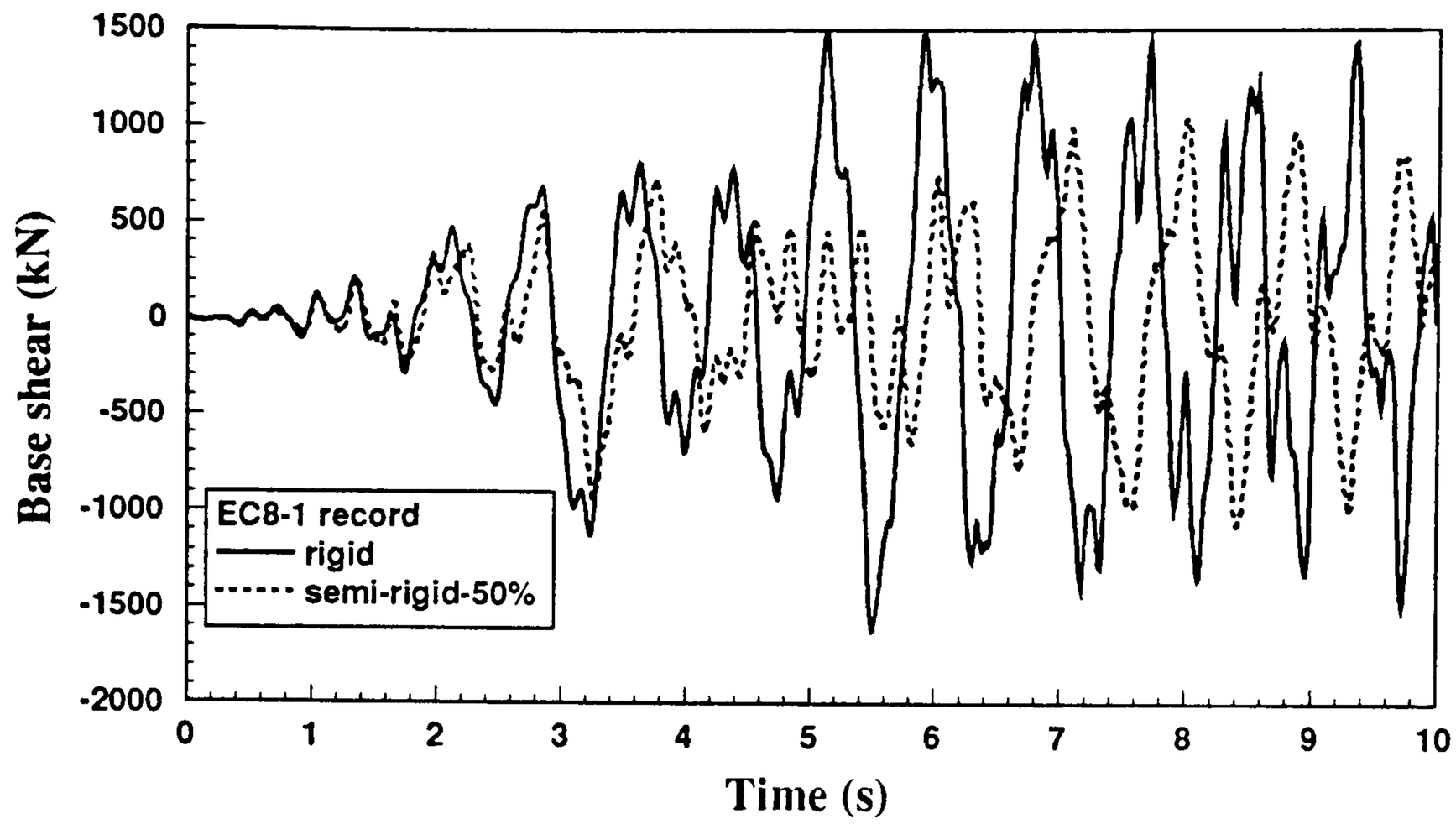

a) Base shear

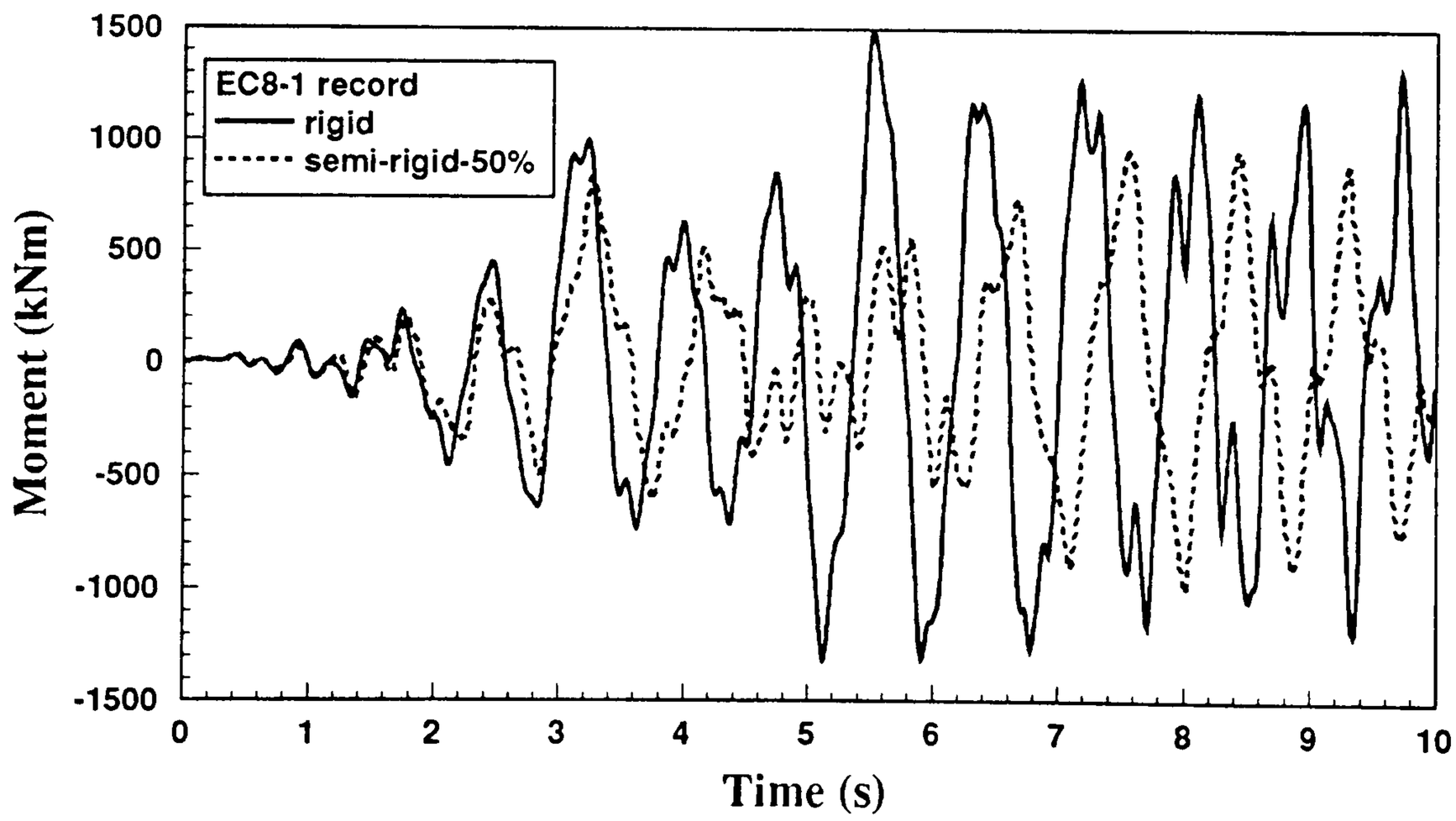

b) Moment at the base of the column in the first storey

Figure 6.15 Comparison of the response of six storey semi-rigid frame (S63D50) with the rigid frame

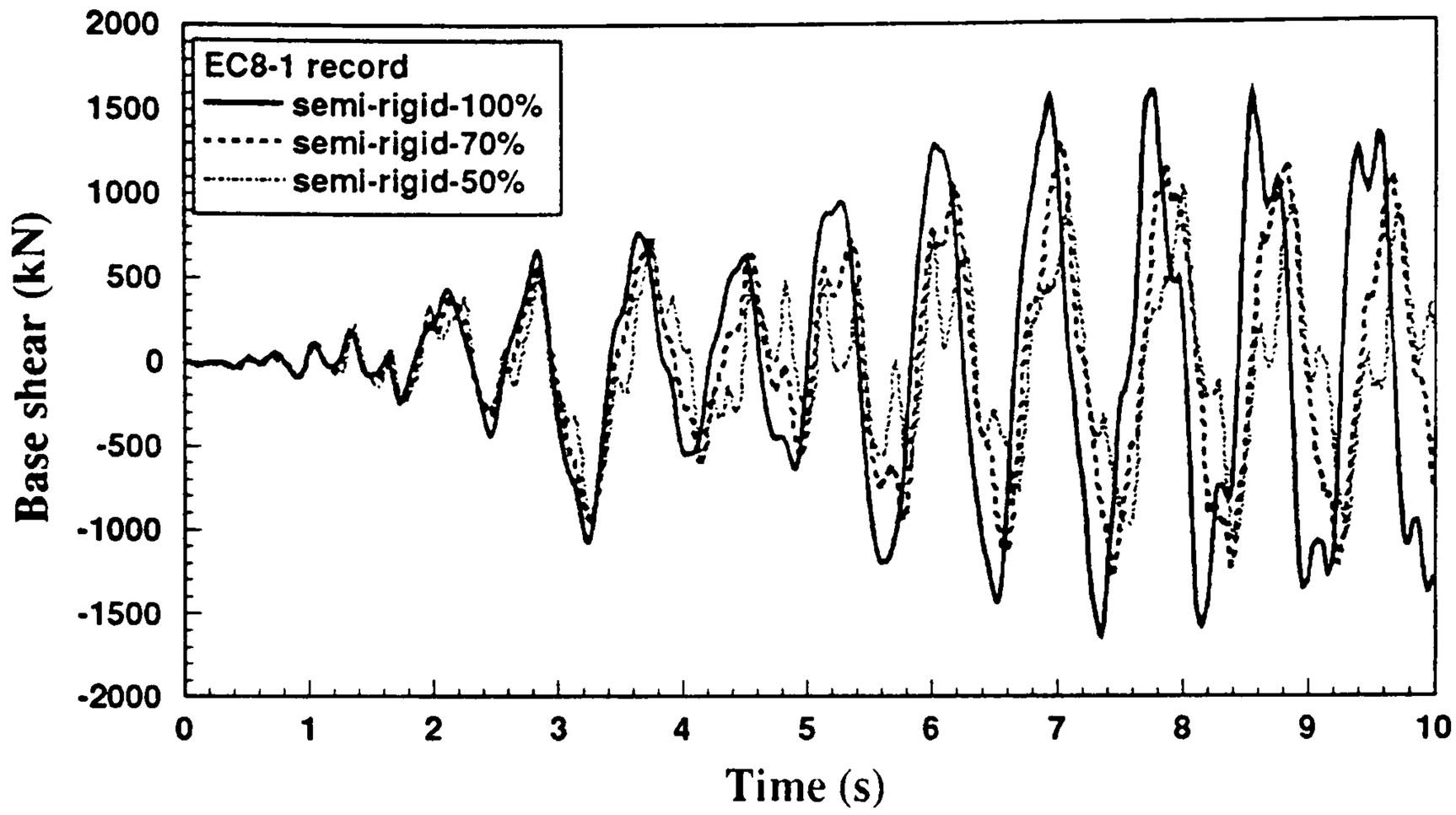

a) Base shear

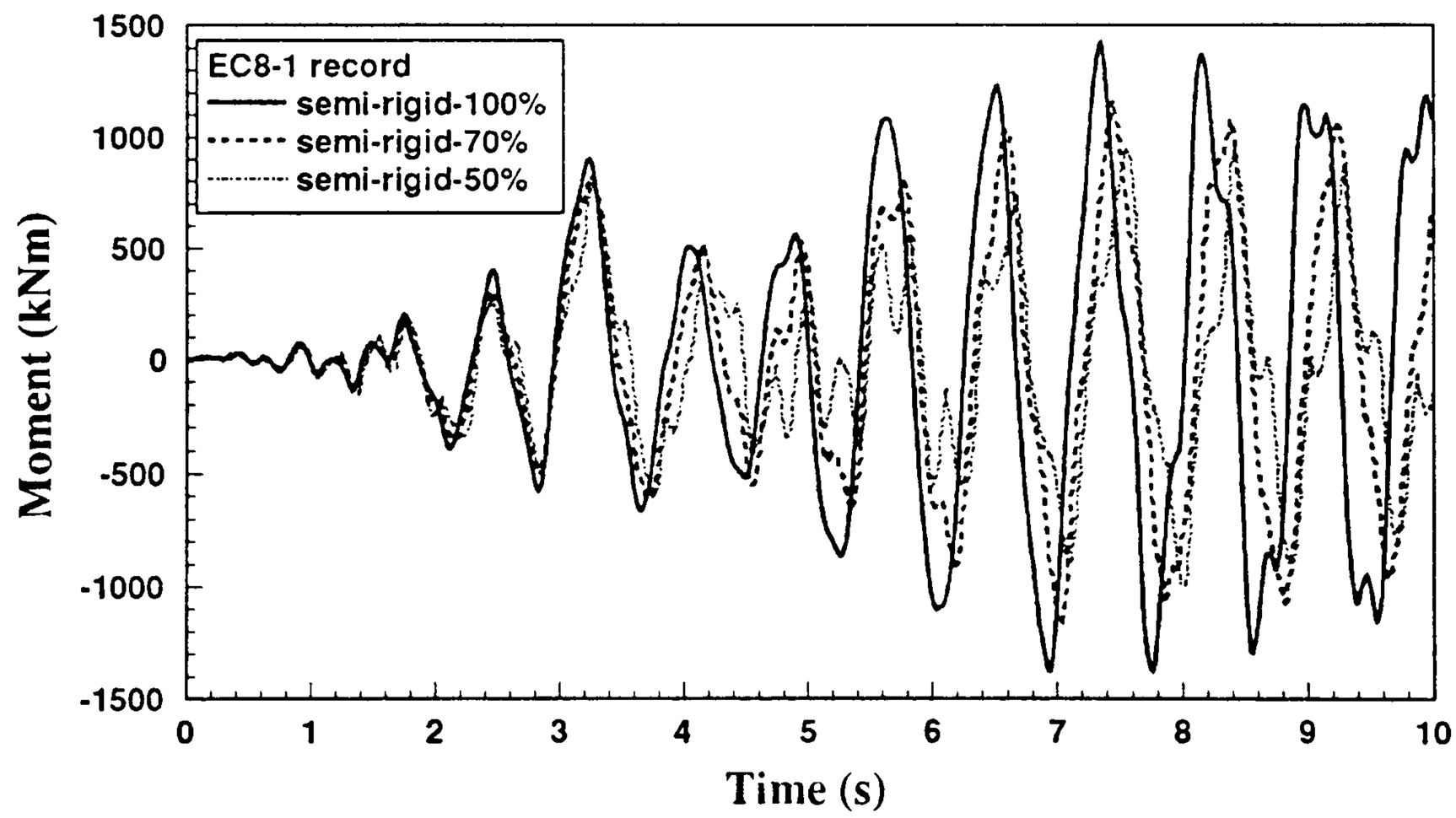

b) Moment at the base of the column in the first storey

Figure 6.16 Comparison of the response of six storey semi-rigid frames

CHAPTER 7

7. CLOSURE

7.1 Summary and Conclusion

In this thesis, the behaviour of semi-rigid steel frames subjected to cyclic and transient dynamic loading was studied. Published research work and code provisions were reviewed. A bilinear model for predicting the moment-rotation of top and seat angles with double web angles connection was proposed. Analytical studies were undertaken using advanced non-linear analysis methods. The main observations from the experimental and analytical investigations, and their implications on the design of semi-rigid steel frames, were presented.

Specific conclusions were given in each chapter. Hereafter, the main observations and their seismic design implications are re-iterated.

- The present state of codification in the application of semi-rigid connections in structures indicates that only Eurocode 3 provides guidance for the analysis of this type of connection. However, the code does not give guidance for the seismic design of semi-rigid steel frames.

- In order to improve the bilinear model given in EC3, which does not provide adequately accurate results, the terms accounting for the bearing components (which arise in the inelastic range) should be neglected. On the other hand, the influence of strain hardening should be taken into account. In order to model the moment-rotation response of top and seat with double web angle connections, a simple bilinear model was proposed for use in the non-linear dynamic analysis program ADAPTIC. This model was validated using the results extracted from the experiments and very good agreement was observed. The stiffness, yield moment

and the post-elastic region of the moment-rotation curves were well-predicted by the analysis.

- The results of the experimental work show that steel frames with semi-rigid connections exhibit stable cyclic behaviour with substantial energy absorption capacity. It was observed that the connections undergo large deformations without instability and were therefore capable of sustaining high seismic forces in the event of an earthquake.

- The flexibility of the connection produced an increase in the length of the plastic hinge in the column in semi-rigid steel frames when compared with the fully-welded steel frame. This had a direct effect on the ductility of the frame.

- The flexibility of the connection influenced the location of points of contra-flexure in the column members. Therefore, in checking the stability of columns, the influence of this flexibility should be considered in calculating the effective length.

- Semi-rigid connections result in elongated vibration periods depending on connection flexibility. Expressions relating the connection characteristics to the fundamental vibration period of semi-rigid frames were given.

- Analytical simulations using ADAPTIC, including the proposed bilinear moment-rotation approach, were compared with the experimental results. It was observed that the analytical yield and the ultimate parameters in all the models were in good agreement with the results of the cyclic and dynamic tests. This lends weight to the use of ADAPTIC in a predictive mode.

- It was conclusively indicated that in partial strength semi-rigid steel frames, a large proportion of the input energy during earthquake loading is dissipated by the connection undergoing extensive deformations. The connection therefore behaves as a fuse to control the forces in the column members and restrict the concentration of stresses at these locations. Consequently, the maximum moment transferred

from the beams to the column is less than the moment capacity of the beams and is only related to the moment capacity of the connections.

- The behavioural pattern of partial strength semi-rigid frames leads naturally towards a modification of the capacity design approach hitherto employed. By ensuring that the dissipative zone is actually the connection, over-strength requirements conventially imposed on columns may be waived. This leads to a direct design approach for columns, thus improving the economy of steel frames.

- To ensure ductile behaviour of the connections in semi-rigid steel frames, the angles and panel zone (in this order) should be designed to yield prior to the connected beam, while other brittle failure modes (e.g. bolt fracture) should be avoided. In addition, the slippage load should be calculated such that angle yielding precedes bolt slippage. This is because when angles yield prior to bolt slippage the connection dissipates higher levels of energy.

- In partial strength semi-rigid steel frames, the beam-column panel zone should have sufficient shear strength in order to allow the connection to undergo some inelastic deformation prior to the commencement of yielding in the panel zone. In this regard, it is recommended that the shear strength of the panel zone should be calculated using a value of 80% of the moment capacity of the beam.

- Slippage of the bolts can be used to control forces and dissipate energy during an earthquake. Thus, by designing the bolts to slip under predefined force limits, control is attained of the forces transmitted through the bolts.

- A comparison between the time-history response of the two storey rigid frames and the partial strength semi-rigid frames indicated that in most cases the latter are capable of sustaining larger earthquake excitation than the former. The maximum interstorey drift for these frames is in some cases less than that of the rigid frame.

- Semi-rigid frame design is usually governed by drift which may not be the case for rigid frames. This results in the observation that beam sizes in the former is larger than the latter. On the other hand, due to the waiver of the column over-strength requirements, columns of semi-rigid frames are usually of smaller sections than their rigid equivalents. The resultant of the two aforementioned effects is that the total weight of the two types of frame are comparable (within 2%).

- The yield acceleration for rigid and full strength semi-rigid frames were significantly greater than those of partial strength semi-rigid frames. In the case of the collapse acceleration, the converse was true. This leads to larger behaviour factors for partial strength semi-rigid frames when compared to the two other configurations.

- Comparisons between the results of the two storey partial strength semi-rigid frames with different connection flexibilities confirmed that frames with more flexible connections were capable of sustaining higher ground accelerations when compared with frames with stiffer connections. This is due to the longer period of this type of structure as well as the energy dissipated in the connections.

- Partial strength semi-rigid steel frames, with connection capacities in the range of 30%-70% of the moment capacity of the beams, satisfied the code requirements for both serviceability and collapse limit states. However, when the number of storeys is increased, a connection strength of 50%-70% of the beams is required.

- In general, the combined experimental and analytical results on cyclic and dynamic response of a large range of steel frames with semi-rigid partial strength connections show conclusively that this type of construction is indeed a feasible solution to earthquake design problems in areas of medium to high seismicity. By virtue of the elongated period of vibration and energy dissipation in connections, the response of the frame as a whole is well below its rigid counterpart. And, by applying capacity design principles and allowing to connection to yield, savings in column sections is availed of.

- In this thesis, the experimental and analytical results are used to propose a comprehensive seismic design framework for connections, members framing into them and overall structure. This provides an attractive alternative to fully welded steel frames, where problems of brittle fracture have been recently identified.

7.2 Future Research

The objectives of the experimental programme described in the thesis were mainly to confirm the feasibility of semi-rigid frames as seismic resistance structural systems and to provide bench-marks for analytical model verification. The design guidance given, though, are by-and-large analytically derived. Therefore, the most urgent research need arising from this work is verification of the design guidance by experimental studies. These would cover verification of the following proposals:

- Vibration periods as a function of connection characteristics.
- Expressions for effective length of the members.
- Length of plastic hinge zones for assessment and detailing.
- Relationships between connection flexibility and drift limits.
- Behaviour factors q for different design concepts, connection-to-beam capacity ratio, number of stories and characteristics of input motion.

Such an extensive experimental programme is an ideal application of the on-line computer controlled (pseudo-dynamic) test method developed previously at Imperial College for SDOF system and extended in this thesis to multi-degrees of freedom.

Furthermore, studies to explore the possible role of eccentric and concentric bracing in conjunction with semi-rigid connections may be of interest, with regard to tighter control on drift. This may result in even more economical frames owing to possible reduction in beam sections.

References

AISC-LRFD, 1986, Load and Resistance Factor Design Specification for Structural Steel Building, American Institute of Steel Construction, Chicago, Illinois.

Altman, w., Azizinamini, A., Bradburn, J. and Radziminski, J., 1982, "Moment-rotation Characteristics of Semi-rigid Steel Beam-to-Column Connections", Technical Report, Dept. of Civil Engineering, University of South Carolina, Columbia.

Ang, K.M. and Morris, G.A., 1984, "Analysis of Three-dimentional Frames with Flexible Beam-Column Connections", Canadian Journal of Civil Engineering, vol. 11, No. 2, pp. 245-254.

Astaneh, A., Nader, M.N. and Malik, L., 1989, "Cyclic behaviour of double angle connections", ASCE, Journal of Structural Division, vol. 115, No. 5, pp. 1101-1118.

Astaneh, A. and Nader, N., 1991, "Cyclic behaviour of frames with semi-rigid connection", Proceedings of the Second International Workshop Connections in Steel Structures II (Behaviour, strength and design), Pittsburgh, Pennsylvania.

Astaneh, A., 1989, "Demand and Supply of Ductility in Steel Shear Connections", Journal of Constructional Steel Research, vol. 14, No. 1, pp. 1-19.

Astaneh, A., Call, S.M. and Mcmullin, K.M., 1989, "Design of Single Plate Shear Connections", AISC, Engineering Journal, vol. 26, No. 1, pp. 21-32.

Atamiaz Sibai, W. and Frey, F., 1988 "Numerical Simulation of the Behaviour up to Collapse of Two Welded Unstiffened One-sided Flange Connections", Connections in Steel Structures: Behaviour Strength and Design, Elsevier Applied Sience Publishers, London, pp. 85-92.

Azizinamini, A. and Radziminski, J., 1985, "Prediction of Moment-Rotation behaviour of Semi-Rigid Beam-To-Column Connections", Connections in Steel Structures: Behaviour, Strength and Design, Elsevier Applied Science Publishers, London, pp. 33-40.

Bailey, J.R., 1970, "Strength and Rigidity of Bolted Beam-to-Column Connections", Conference on Joints in Structures, University of Sheffield, U.K., vol. 1, paper 4.

Baker, J.F., 1934, "A Note on the Effective Length of a Pillar Forming Part of a Continuous Member in a Building Frame", 2nd Report, Steel Structures Research Committee, Department of Scientific and Industrial Research of Great Britain, HMSO, London, pp. 13-34.

Ballio, G., Calado, L., De Martino, A., Faella, C. and Mazzolani, F.M., 1986, "Cyclic Behaviour of Steel Beam-to-Column Joints", Experimental Research, Estratto dalla Rivista Costruzioni Metalliche, vol. 2, pp. 3-24.

Batho, C., and Lash, S.D., 1936, "Further Investigations on Beam and Stanchion Connections Encased in Concrete", Steel Structures Research Committee, Department of Scientific and Industrial Research, HMSO, London, pp. 276-363.

Batho, C., 1931, "Investigations on Beam and Stanchion Connections", Steel Structures Research Committee, Department of Scientific and Industrial Research, HMSO, London, vol. 1-2, pp. 61-137.

Bernuzzi, C., Zandonini, R. and Zanon, P., 1992, "Semi-Rigid Steel Connections under Cyclic Loads", Proceeding of the First World Conference on Constructional Steel Design, Acapulco, Mexico, pp. 375-384.

Bathe, K.J., 1982, "Finite Element Procedures in Engineering Analysis", Prentice Hall Inc., New Jersey.

Bernuzzi, C., Zandonini, R. and Zanon, P., 1991, "Rotational Behaviour of End Plate Connections", Costruzioni Metalliche, No. 2, pp. 74-103.

Bertero, V.V., Anderson, J.C. and Krawinkler, H., 1994, "Performance of Steel Building Structures During the Northridge Earthquake", Report No. UCB/EERC-94/04, EERC, University of California, Berkeley.

Beaulieu, D., and Picard, A., 1988, "Finite Element Modelling of Connections", Connections in Steel Structures: Behaviour Strength and Design, Elsevier Applied Sience Publishers, London, pp. 96-103.

Bjorhovde, R., Brozzetti, J. and Colson, A., 1990, "A Classification System for Beam-to-Column Connections", ASCE, Journal of Structural Division, vol. 116, No. 11, pp. 3059-3076.

Bose, S.K., Mcneice, G.M. and Sherbourne, A.N., 1972, "Column Webs in Steel Beam-to-Column Connections", Part 1: Formulation and Verification, Computers and Structures, vol. 2, Feb., pp. 253-272.

Broderick, B.M., 1994, "Seismic Testing, Analysis and Design of Composite Frames", PhD Thesis, ESEE Section, Imperial College, University of London.

Calado, L. and Azevedo, J., 1994, "Hysteretic Behaviour of Steel Members: Analytical Models and Experimental Tests", Journal of Constructional Steel Research, vol. 29, Nos. 1-3, pp. 71-94.

Chen, W.F. and Lui, E.M., "Beam-to-Column Moment Resisting Connections", Steel Frame Structures: Stability and Strength, R. Narayanan Ed., Elsevier Applied Science Publishers, London, p. 153.

Colson, A. and Louveau, J.M., 1983, "Connections Incidence on the Inelastic Behaviour of Steel Structures", Euromech Colloquium, October, paper 174.

Davison, J.B., Kirby, P.A. and Nethercot, D.A., 1987, "Rotational Stiffness Characteristics of Steel Beam-to-Column Connections", Journal of Constructional Steel Research, vol. 8, No. 1, pp. 17-54.

Dews, R.J., 1979, "Experimental Test Results on Experimental End-plate Moment Connections", MSc. Thesis, Vanderbilt University, Nashville, Tennessee.

Drucker, D.C., 1956, "The Effect of Shear on the Plastic Bending of Beams", Journal of Applied Mechanics, vol. 3, pp. 509-514.

Dubina, D., Grecea, D. and R. Zaharia, 1995, "Numerical Simulation Concerning the Response of Steel Frames with Semi-rigid Joints under Static and Seismic Loads", Behaviour of Steel Structures in Seismic Areas, E & FN Spon Publishers, London, pp. 580-589.

Elnashai, A.S. and Elghazouli, A.Y., 1994, "Seismic Behaviour of Semi-rigid Steel Frames", Journal of Constructional Steel Research, vol. 29, Nos. 1-3, pp. 149-174.

Elnashai, A.S., Izzuddin, B.A. and Dowling, P.J., 1989, "Efficient Large Displacement Elasto-plastic Dynamic Analysis of Structures", Journal of European Earthquake Engineering, vol. 3, No. 3, pp.32-41.

Elnashai, A.S., Elghazouli, A.Y. and Dowling P.J., 1990, "Verification of Pseudo-Dynamic Testing of Steel Members", Journal of Constructional Steel Research, vol. 16, No.2, pp. 153-161.

Elnashai, A.S. and Chryssanthopoulos, M.K., 1991, "Effect of Random Material Variability on Seismic Design Parameters of Steel Frames", Earthquake Engineering and Structural Dynamic, vol. 20, No. 3, pp. 101-114.

Elghazouli, A.Y., 1991, "Earthquake Resistance of Composite Beam-Columns", PhD Thesis, ESEE Section, Imperial College, University of London, London, U.K.

European Convention for Constructional Steelwork, ECCS, 1992, "Analysis and Design of Steel Frames with Semi-rigid Joints", First Edition, TC8/TWG 8.1/8.2, Report No. 67/1992.

European Convention for Constructional Steelwork, ECCS, 1993, "Design of Steel Structures in Seismic Zones, Document No. TC 13 01/93.

European Convention for Constructional Steelwork, ECCS, 1986, Recommended Testing Procedure for Assessing the Behaviour of Structural Steel Elements Under Cyclic Loading", Technical Working Group 1.3-Seismic Design, First Edition.

Frye, M.J. and Morris, G.A., 1975, "Analysis of Flexibly Connected Steel Frames", Canadian Journal of Civil Engineering, vol. 2, No. 3, pp. 280-291.

Guerra, C.A., Mazzolani, F.M. and Piluso, V., 1990, "Overal Stability Effects in Steel Structures under Seismic Loads", Proceedings of Ninth the ECEE, Moscow, vol. 6, pp. 3-12.

Harper, Jr, W.L., Bradburn, J.H., Dickerson, J.R. and Radziminski, J.B., 1990, "Static and Cyclic Behaviour of Semi-rigid Bolted and Welded Beam-Column Connections", A Report Conducted by the Department of Civil Engineering, University of South Carolina, Columbia.

Hormby, D.E., Richard, R.M. and Kriegh, J.D., 1984, "Single-plate Framing Connections with Grade-50 Steel and Composite Construction, AISC, Engineering Journal, vol. 21, No. 3, pp.125-138.

Housner, G.W., 1952, "Spectrum Intensities of Strong Motion Earthquakes, Proceeding of Symposium on Earthquake and Blast Effects on Structures, EERI, University of California, Los Angeles, June, pp. 20-36.

Ioannides, S.A., 1978, "Flange Behaviour in Bolted End-plate Moment Connections", PhD Thesis, Vanderbilt University, Nashville, Tennessee.

Izzuddin, B.A. and Elnashai, A.S., 1989, "ADAPTIC, A Programme for Adaptive Large Displacement Elasto-plastic Dynamic Analysis of Steel, Concrete and Composite Frames", Research report No. ESEE 89/7, ESEE Section, Imperial College, London, U.K.

Izzuddin, B.A., 1990, "Nonlinear Dynamic Analysis of Framed Structures", PhD Thesis, ESEE Section, Imperial College, University of London, December.

Johnstone, N.D. and Walpole, W.R., 1981, "Bolted End-plate Beam to Column Connections under Earthquake Type Loading", Research Report 81-7, Department of Civil Engineering, University of Canterbury, Christchurch, New Zealand, September.

Kato, B., 1989, "Rotation Capacity of H-Section Members as Determined by Local Buckling", Journal of Constructional Steel Research, vol.13, Nos. 2&3, pp. 95-109.

Kato, B., 1990, "Deformation Capacity of Steel Structures", Journal of Constructional Steel Research, vol. 17, Nos. 1&2, pp. 33-94.

Kennedy, D.J.L. and Hafez, M., 1984, "A Study of End-plate Connections for Steel Beams", Canadian Journal of Civil Engineering, vol. 11, No. 2, pp. 139-149.

Kishi, N. and Chen, W.F., 1987, "Moment-Rotation of Semi-rigid Connections", Structural Engineering Report No. CE-STR-87-29, School of Civil Engineering, Purdue University, West Lafayette, September.

Kishi, N., Chen, W.F., Goto, Y. and Matsuoka, K.G., 1991, "Applicability of Three-Parameter Power Model to Structural Analysis of Flexibly Jointed Frames", Proceeding of Mechanics Computing in 1990's and Beyond, Columbus, OH, May 20-22, pp. 233-237.

Kishi, N. and Chen, W.F., 1986a, "Steel Connection Data Bank Programme", Structural Engineering Report No. CE-STR-86-11, School of Civil Engineering, Purdue University, West Lafayette, May.

Kishi, N., and Chen, W.F., 1986b, "Data Base of Steel Beam-to-Column Connections", Structural Engineering Report No. CE-STR-86-26, School of Civil Engineering, Purdue University, West Lafayette, August.

Krishnamurthy, N., Huang, H.T., Jeffrey, P.K. and Avery, L.K., 1979, "Analytical M-θ Curves for End-plate Connections", ASCE, Journal of Structural Division, vol. 105, No. 1, pp. 133-145.

Kuwamura, H. and Suzuki, T., 1992, "Low Cyclic Fatigue Resistance of Welded Joints of High-strength Steel under Earthquake Loading", Proceedings of the Tenth WCEE, Madrid, vol. 5, pp. 2851-2856.

Kuwamura, H. and Kato, B., 1989, "Effect of Randomness in Structural Members Yield Strength on the Structural Systems Ductility", Journal of Constructional Steel Research, vol. 13, Nos. 2&3, pp. 79-93.

Lightfoot, E. and Lemessurier, A.P., 1974, "Elastic Analysis of Frameworks with Elastic Connections", ASCE, Journal of Structural Division, vol. 100, No. 6, pp. 1297-1309.

Lionberger, S.R., 1967, "Static and Dynamic of Building Frames with Non-rigid Connections", PhD Thesis, Stanford University, Stanford, Calif.

Lionberger, S.R. and Weaver, W., 1969, "Dynamic Response of Frames with Non-rigid Connections", ASCE, Journal of Structural Division, vol. 95, No. 1, pp. 95-114.

Lipson, S.L., 1968, "Single Angle and Single Plate Beam Framing Connections", Canadian Structural Engineering Conference, Toronto, Ontario, pp. 141-162.

Lipson, S.L. and Antonio, M., 1980, "Single Angle Welded-Bolted Beam Connections", Canadian Journal of Civil Engineering, vol. 7, No. 2, pp. 315-324.

Lipson, S.L., 1977, "Single Angle Welded-Bolted Connections", ASCE, Journal of Structural Division, vol. 193, No. 3, pp.559-571.

Lui, E.M. and Chen, W.F., 1983, "Strength of H-columns with Small End Restraints", Journal of the Institution of Structural Engineers, London, vol. 61B, No. 1, March, pp.17-26.

Lui, E.M. and Chen, W.F., 1986, "Analysis and Behaviour of Flexibly-Joined Frames", Engineering Structures, vol. 8, April, pp. 107-118.

Melchers, R.E. and Kaur, D., 1982, "Behaviour of Frames with Flexible Joints", Proceedings of the 8th Australian Conference on Mechanics of Structural Materials, Newcastle, Australia, pp. 27.1-27.5.

Maxwell, S., Howlett, J., Jenkins, W. and Bose, B., 1981, "A Realistic Approach to the Performance and Application of Semi-rigid Jointed Structures" Joints In Structural

Steelwork, Howlett, J.H., Jenkins, W.M. and Stainsby, R., Eds., Pentech Press, U.K., pp. 2.71-2.98.

Madas, P.J., and Elnashai, A.S., 1992, "A Component-Based Model for the Response of Beam-Column Connections", Proceedings of the Tenth WCEE, Madrid, Spain, vol. 8, pp. 4495-4499.

Madas, P. and Elnashai, A.S., 1989, "A Theoretical Model for Composite Beam-Columns under Cyclic Loading", ESEE Research No. 89/10, ESEE Section, Imperial College, London, U.K.

Mahin, S.A., Shing, P.B., Thewalt, C.R. and Hanson, R.D., 1989, "Pseudo-Dynamic Test Method: Current Status and Future Directions", ASCE, Journal of Structural Division, vol. 115, No. 8., pp. 2113-128.

Mahin, S.A. and Shing, P.B., 1984, "Pseudo-Dynamic Method for Seismic Testing", ASCE, Journal of Structural Division, vol. 111, No. 7, pp. 1482-1503.

Marley, M.J. and Gerstle, K.H., 1982,"Analysis and Tests of Flexibly-Connected Steel Frames", Report to AISC under Project 199, American Institute of Steel Construction, Chicago, Illinois.

Monforton, A.R. and Wu, T.S., 1963, "Matrix Analysis of Semi-rigid Connected Frames", ASCE, Journal of Structural Division, , vol. 89, No. 6, pp. 13-42.

Nakashima, K. and Kato, H., 1988, "Experimental Error Growth Behaviour and Error Growth Control in Pseudo-Dynamic Test", Proceedings of the Ninth WCEE, Tokyo, Japan, Vol. 4, pp. 53-58.

Nader, M.N. and Astaneh, A., 1988, "Behaviour and Design of Steel Tee-Framing Connections, Report No. UCB/SEMM-88/11, SEMM, University of California, Berkeley.

Nader, M.N. and Astaneh, A., 1992, "Seismic Behaviour and Design of Semi-Rigid Steel Frames", Report No. UCB/EERC-92/06, EERC, University of California, Berkeley.

Ostrander, J.R., 1970, "An Experimental Investigation of End-plate Connections", MSc. Thesis, University of Saskatchewan, Canada, July.

Patel, K.V. and Chen, W.F., 1984, "Non-linear Analysis of Steel Moment Connections", ASCE, Journal of Structural Division, vol. 110, No. 8, pp. 1861-1875.

Popov, E.P. and Petersson, H., 1978, "Cyclic Metal Plasticity : Experiments and Theory", ASCE, Journal of Engineering Mechanics Division, vol. 104, No. 6, pp. 1371-1388.

Popov, E.P., Tsai, K.C. and Engelhardt, M.D., 1989, "On Seismic Steel Joints and Connections", Engineering Structures Journal, Vol.11, No. 3, pp. 148-162.

Landolfo R., and Mazzolani, F.M., 1990, "The Consequences of the Design Criteria on the Seismic Behaviour of Steel Frames", Proceedings of the Ninth ECEE, Moscow, September, vol. 2, pp. 11-19.

Ramberg, W. and Osgood, W.R., 1943, "Description of Stress-Strain Curves by Three Parameters", Technical Note No. 902, National Advisory Committee for Aeronautics, Washington, D.C.

Rathbun, J.C., 1936, "Elastic Properties of Riveted Connections", Transactions ASCE, Paper No. 1933, vol. 101, pp. 524-563.

Razzaq, Z., 1983, "End Restraint Effect on Steel Column Strength", ASCE, Journal of the Structural Division, vol. 109, No. 1, pp. 314-334.

Richard, R.M., Gillett, P.E., Kriegh, J.D. and Lewis, B.A., 1980, "The Analysis and Design of Single Plate Framing Connections", AISC, Engineering. Journal, vol. 17, No. 2, pp. 38-52.

Richard, R.M., Kriegh, J.D. and Hormby, D.F., 1982, "Design of Single Plate Framing Connections with A307 Bolts", AISC, Engineering Journal, vol. 19, No. 4, pp. 209-213.

Rosales. J.G.P., 1991, "Seismic Resistance of Steel Frames with Semi-rigid Connections", MSc. Thesis, ESEE Section, Imperial College, University of London, London, U.K.

Romstad, K.M. and Subramanian, C.V., 1970, "Analysis of Frames with Partial Connection Rigidity", ASCE, Journal of Structural Division, vol. 100, No 6, pp. 2283-2300.

Sawada, T., Hirao, K., Yamamoto, H. and Tsujihara, O.,1992, "Relation Between Maximum Amplitude Ratio (a/v, ad/v^2) and Spectral Parameters of Earhtquake Ground Motion", Proceedings of the Tenth WCEE, Madrid, Spain, vol. 4, pp. 617-622.

Sedlacek, G and Ballio, G., 1984, "The Response of Steel Structures with Semi-rigid Connections to Seismic Actions", Proceedings of the Workshop on Connections in Steel Structures, Cachan, France.

Shing, P.B. and Mahin, S.A., 1983, "Experimental Error Propagation in Pseudo-Dynamic Testing", Report No. UCB/EERC-83/12, EERC, University of California, Berkeley.

Summer, W.H., 1969, "Behaviour of Welded Header Plate Connections", MSc. Thesis, University of Toronto, Ontario, Canada.

Surtees, J.O. and Mann, A.P., 1970, "End-plate Connections in Plastically Designed Structures", Conference on Joints in Structures, University of Sheffield, Sheffield, U.K., vol 1, paper 5.

Takanashi, K., Udagawa, K. and Tanaka, H., 1980, "Pseudo-Dynamic Tests on a 2-Storey Steel Frame by a Computer-load Test Apparatus Hybrid System", Proceedings of the Seventh WCEE, Istanbul, Turkey, vol. 7, pp. 225-232.

Vinnakota, S., 1982, "Planar Strength of Restrained Beam-Columns", ASCE, Journal of Structural Division, vol. 108, No. 11, pp. 2496-2515.

Wales, M. W. and Rossow, E.C., 1983, "Coupled Moment-Axial Force Behaviour in Bolted Joints", ASCE, Journal of Structural Division, vol. 109, No 4, pp. 1250-1266.

Zhu, T.J., Heidebrecht, A.C. and Tso, W.K., 1988, "Effect of Peak Ground Acceleration to Velocity Ratio on Ductility Demand of Inelastic System", Earthquake Engineering and Structural Dynamic, vol. 16, pp. 63-79.

APPENDIX A

Strain Gauge Results

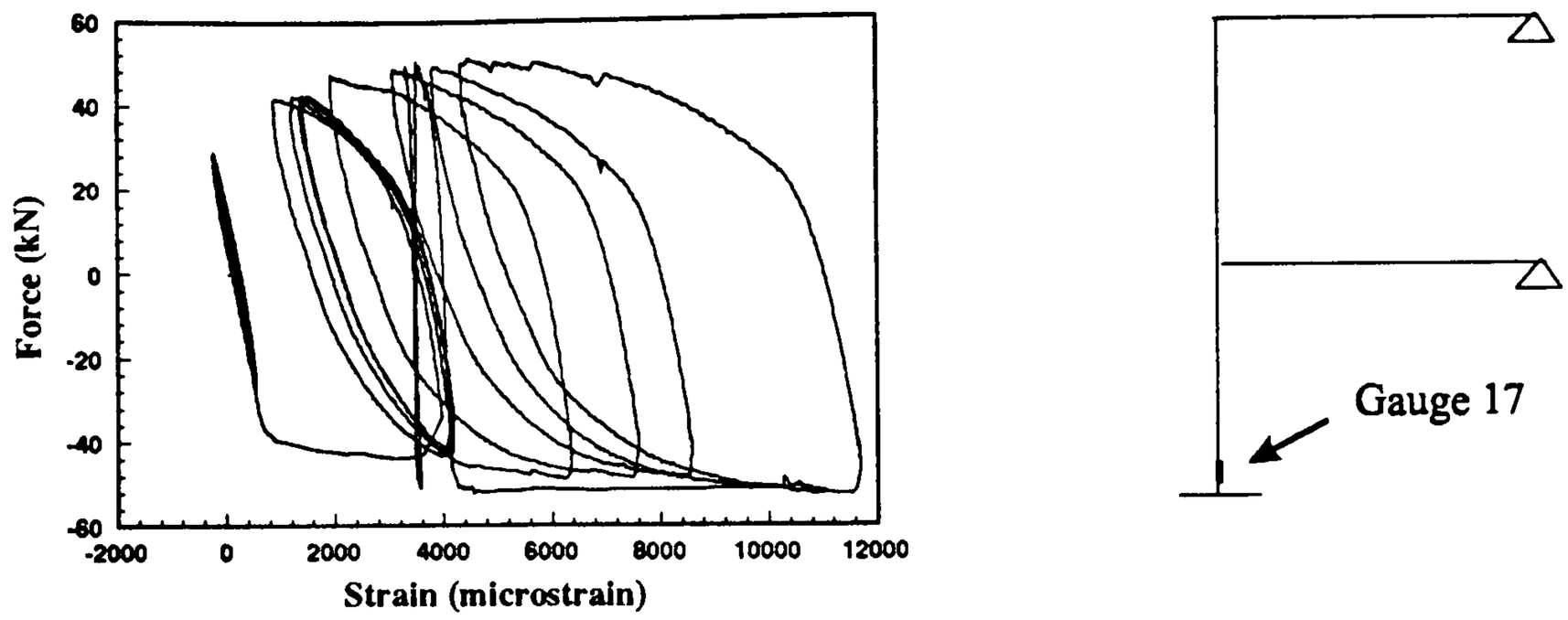

Figure A.1 Force at the second floor vs. strain (model CS1)

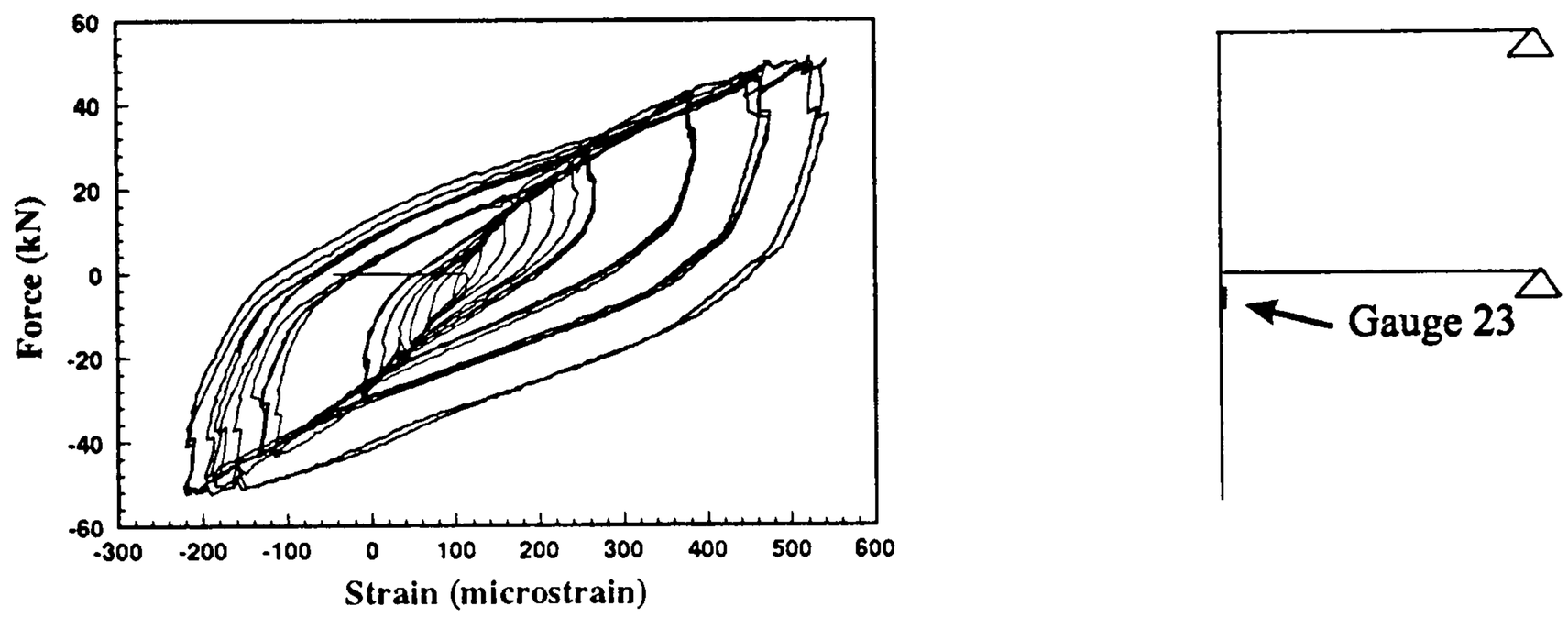

Figure A.2 Force at the second floor vs strain (model CS1)

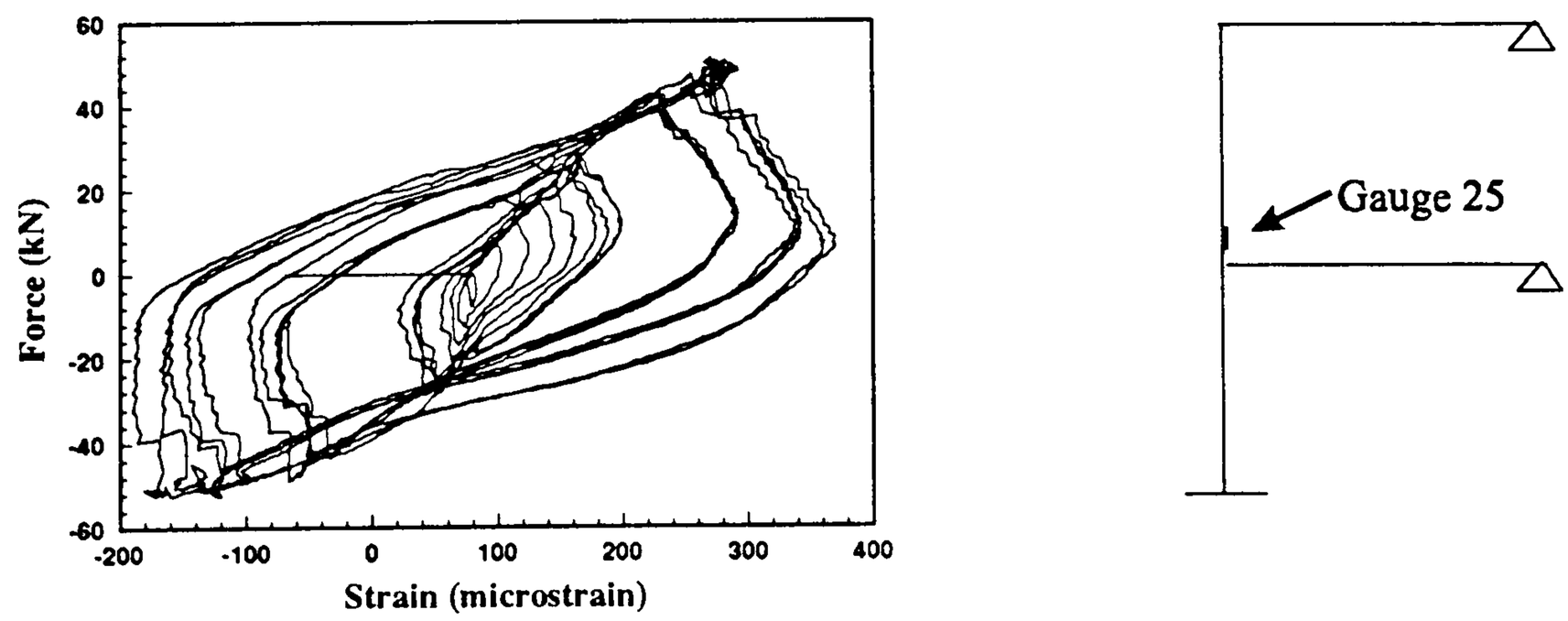

Figure A.3 Force at the second floor vs. strain (model CS1)

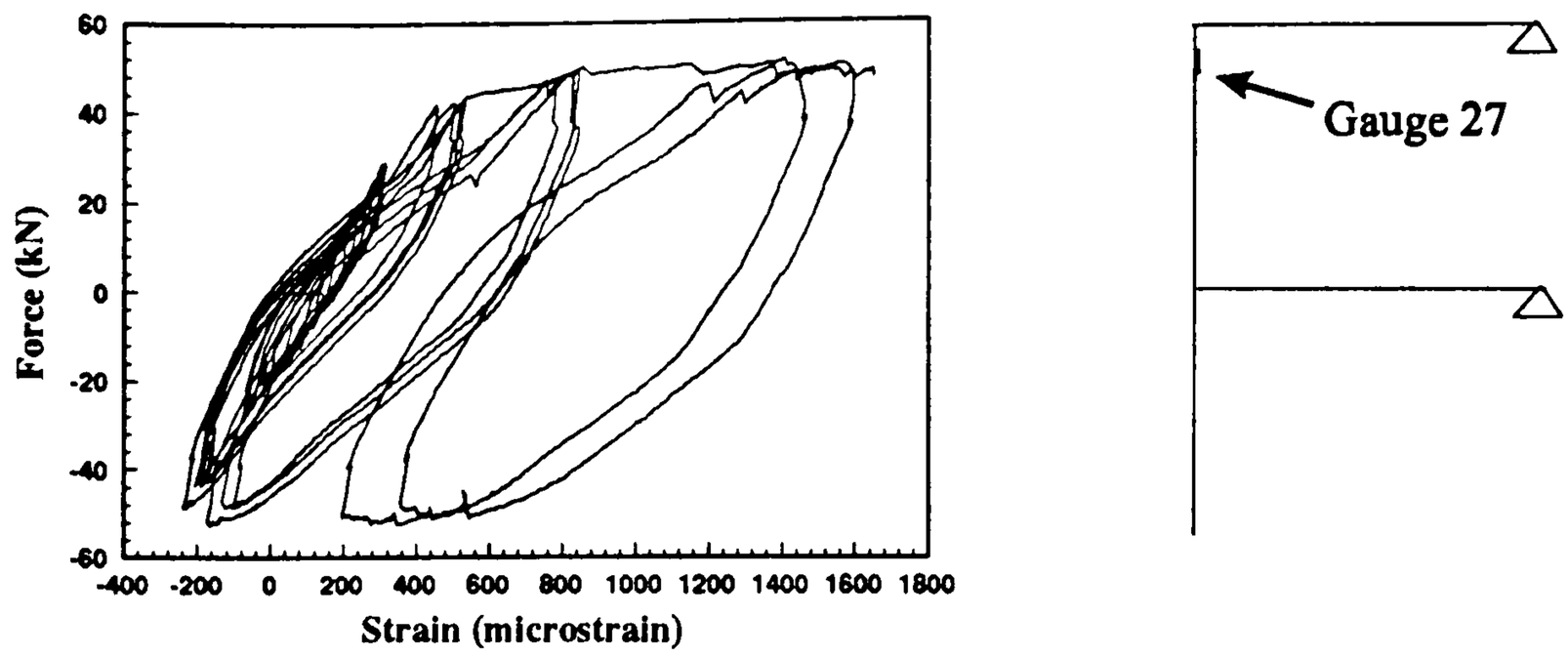

Figure A.4 Force at the second floor vs. strain (model CS1)

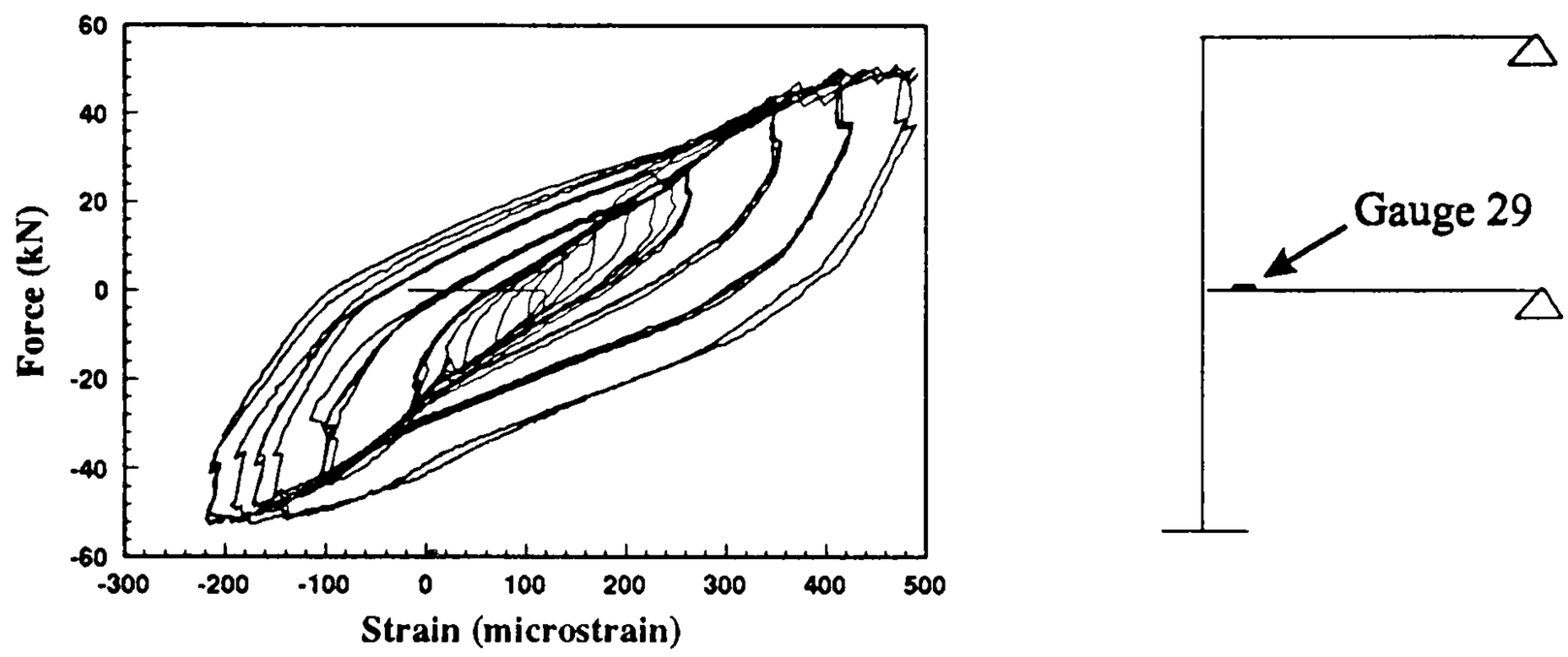

Figure A.5 Force at the second floor vs. strain (model CS1)

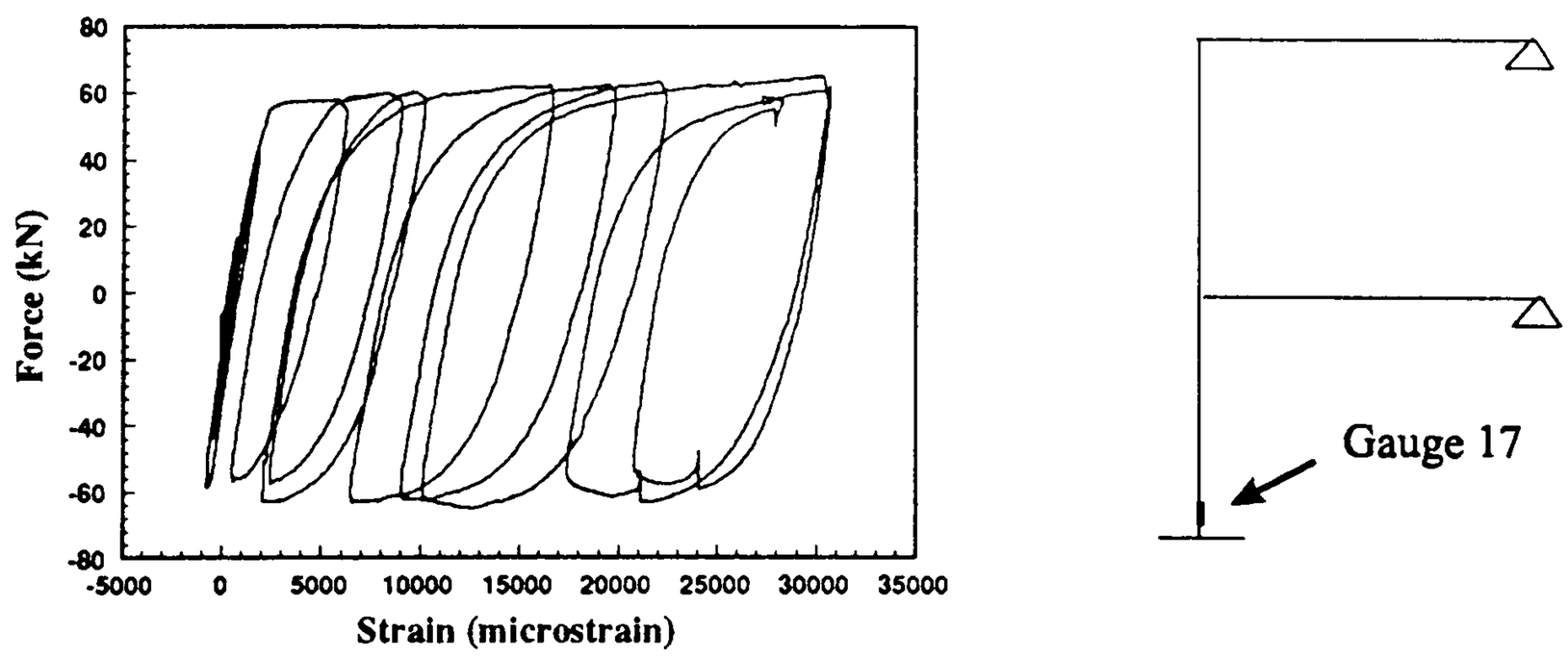

Figure A.6 Force at the second floor vs. strain (model CS2)

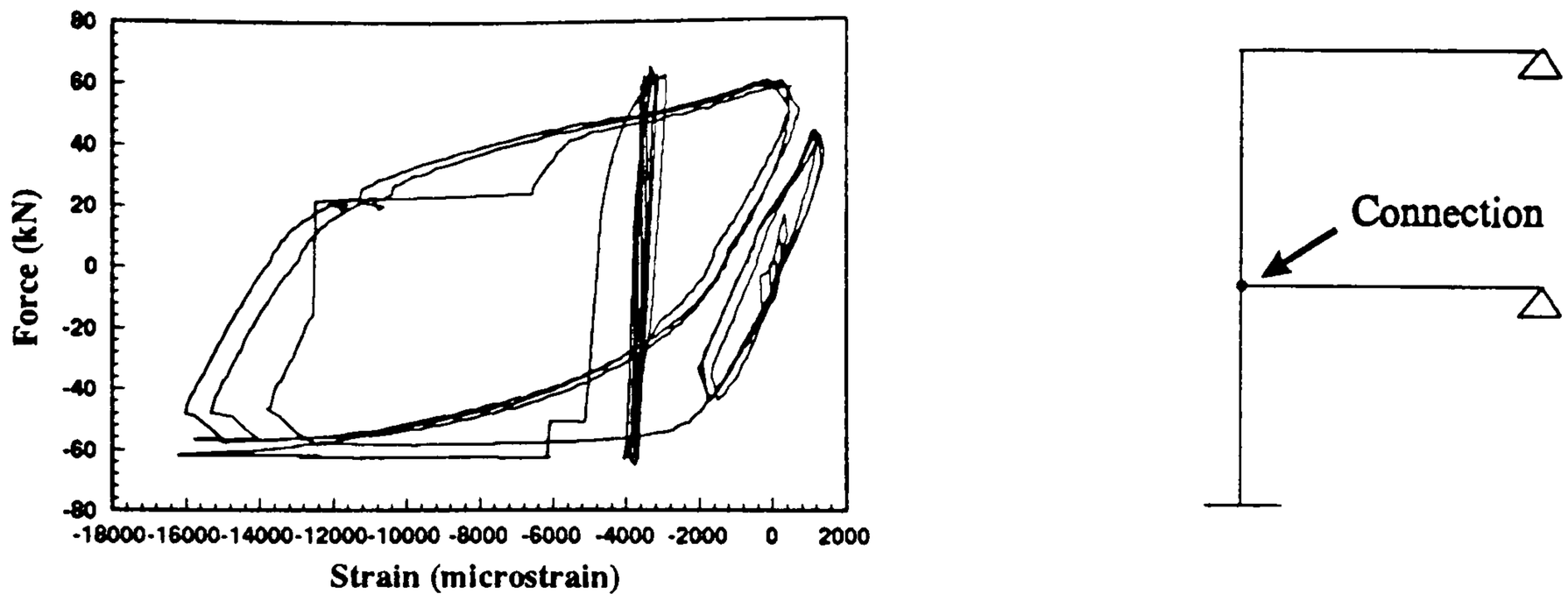

Figure A.7 Force at the second floor vs. strain in the top angle (model CS2)

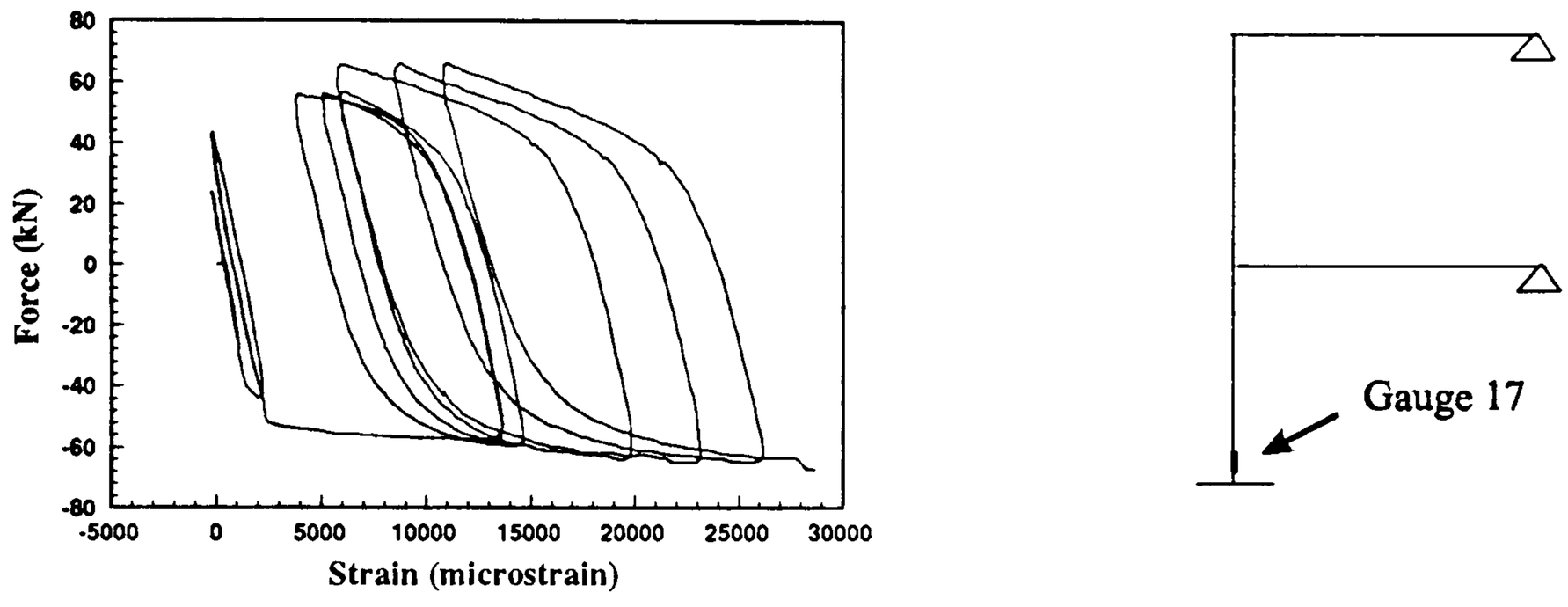

Figure A.8 Force at the second floor vs. strain (model CS3)

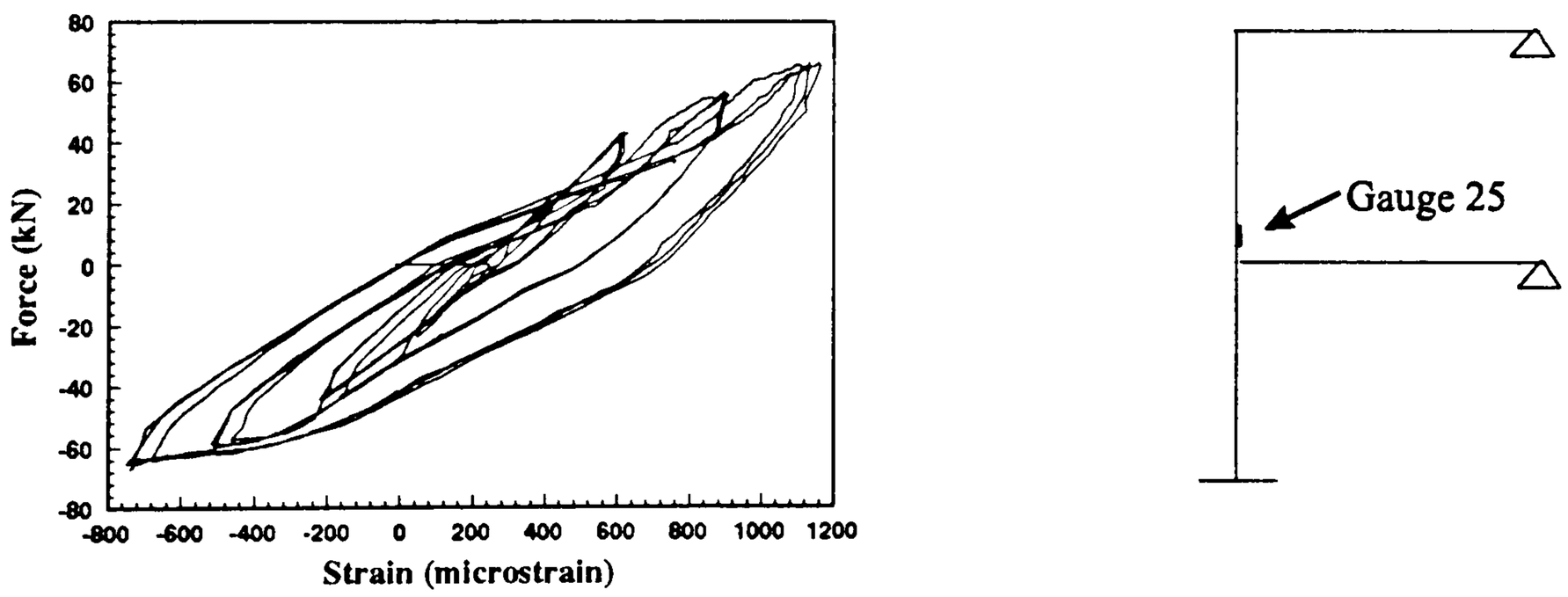

Figure A.9 Force at the second floor vs strain (model CS3)

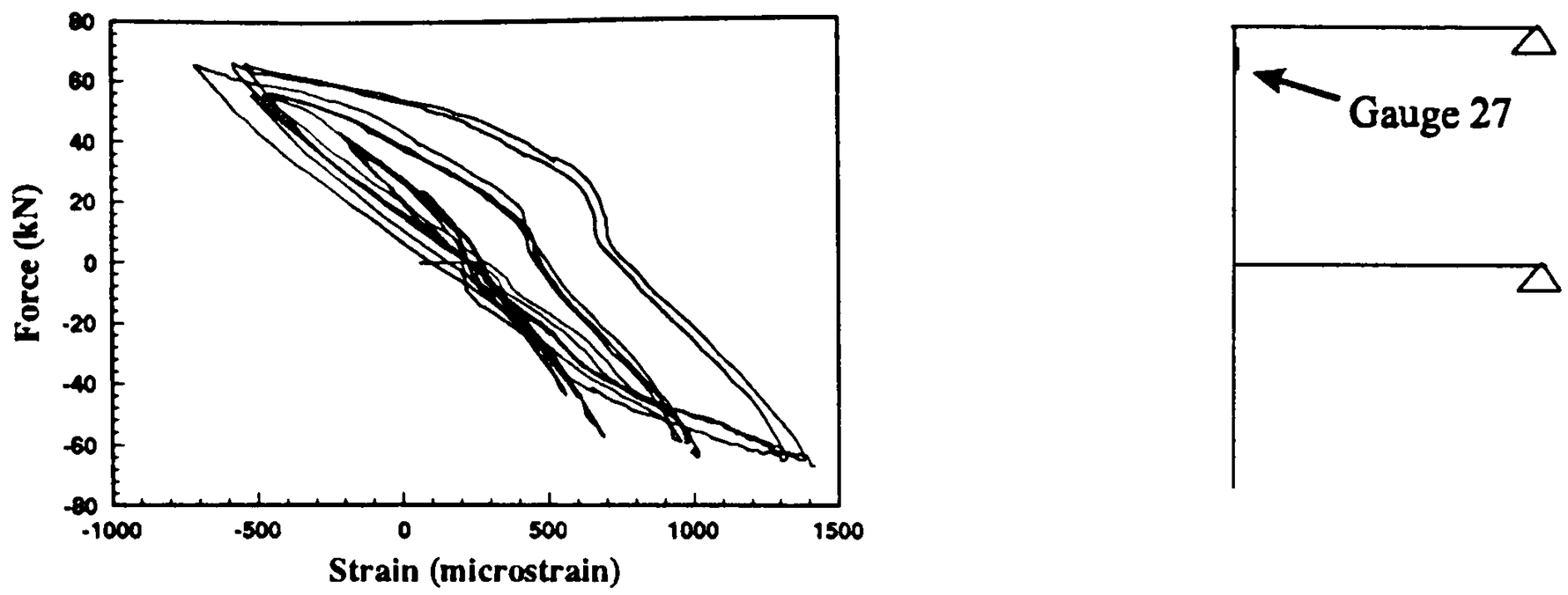

Figure A.10 Force at the second floor vs. strain (model CS3)

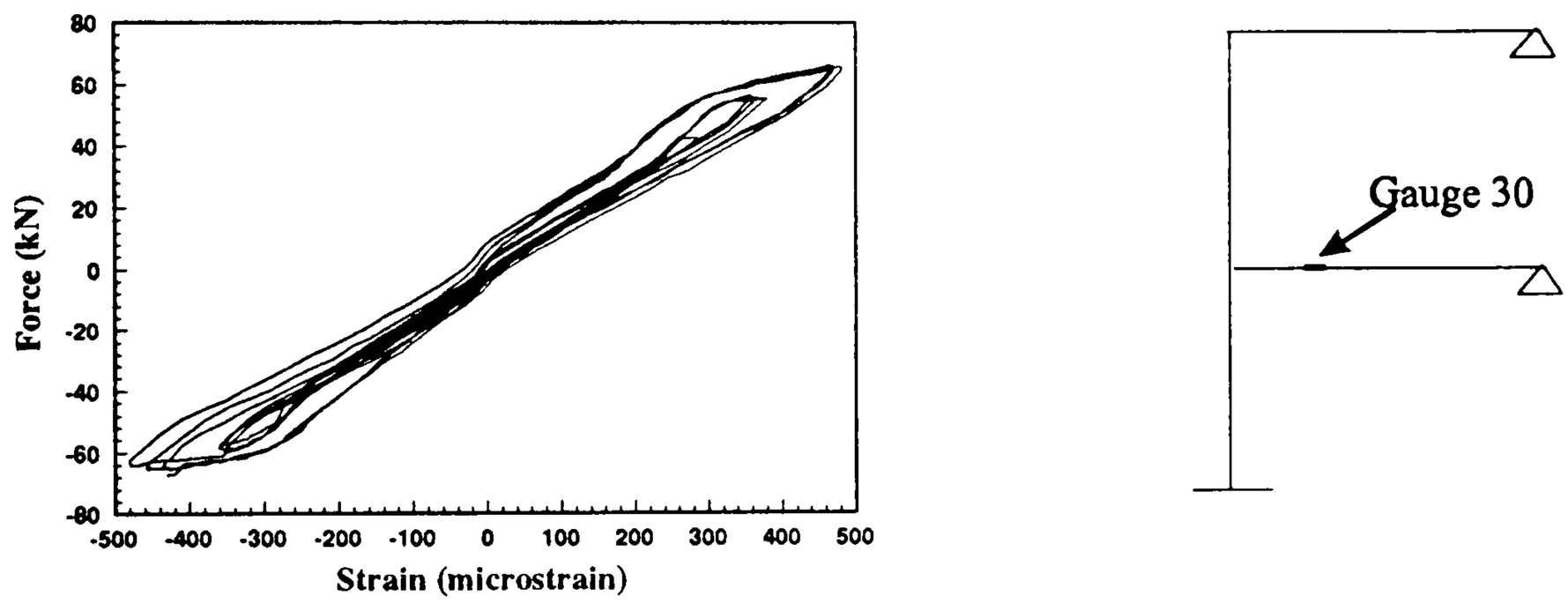

Figure A.11 Force at the second floor vs. strain (model CS3)

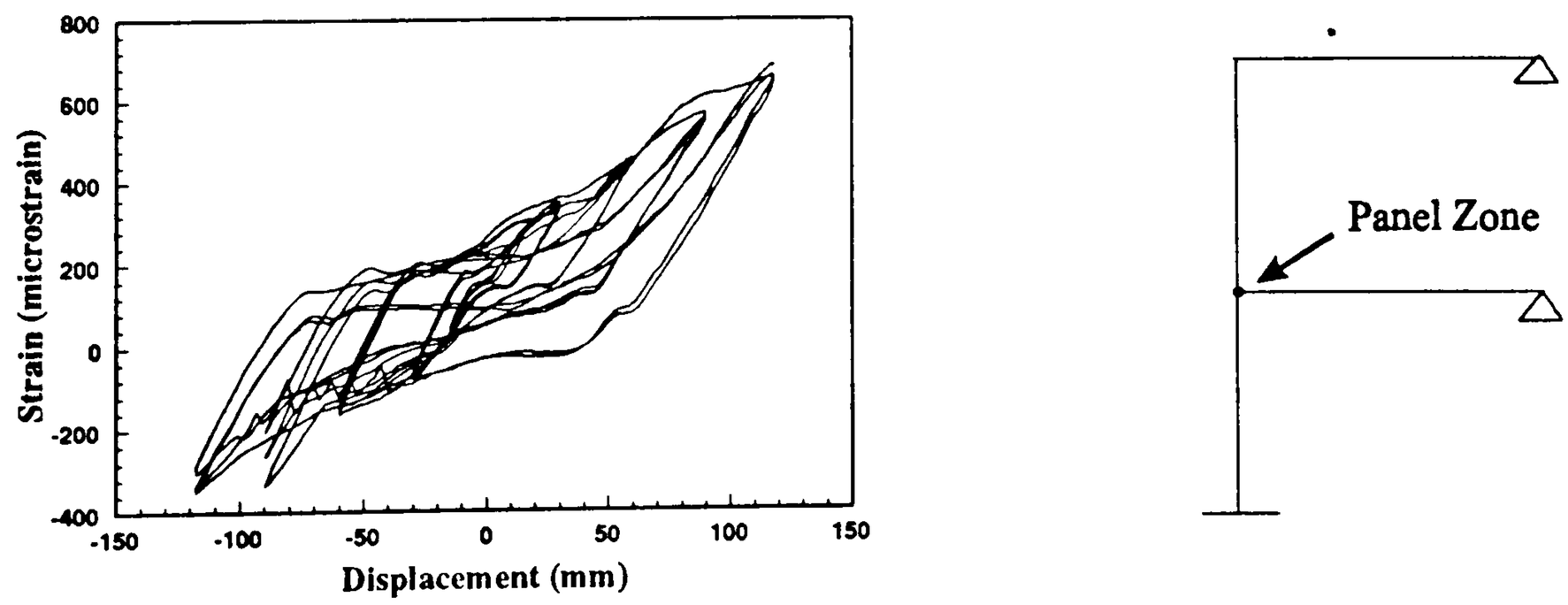

Figure A.12 Strain in the panel zone vs second floor displacement (model CS3)

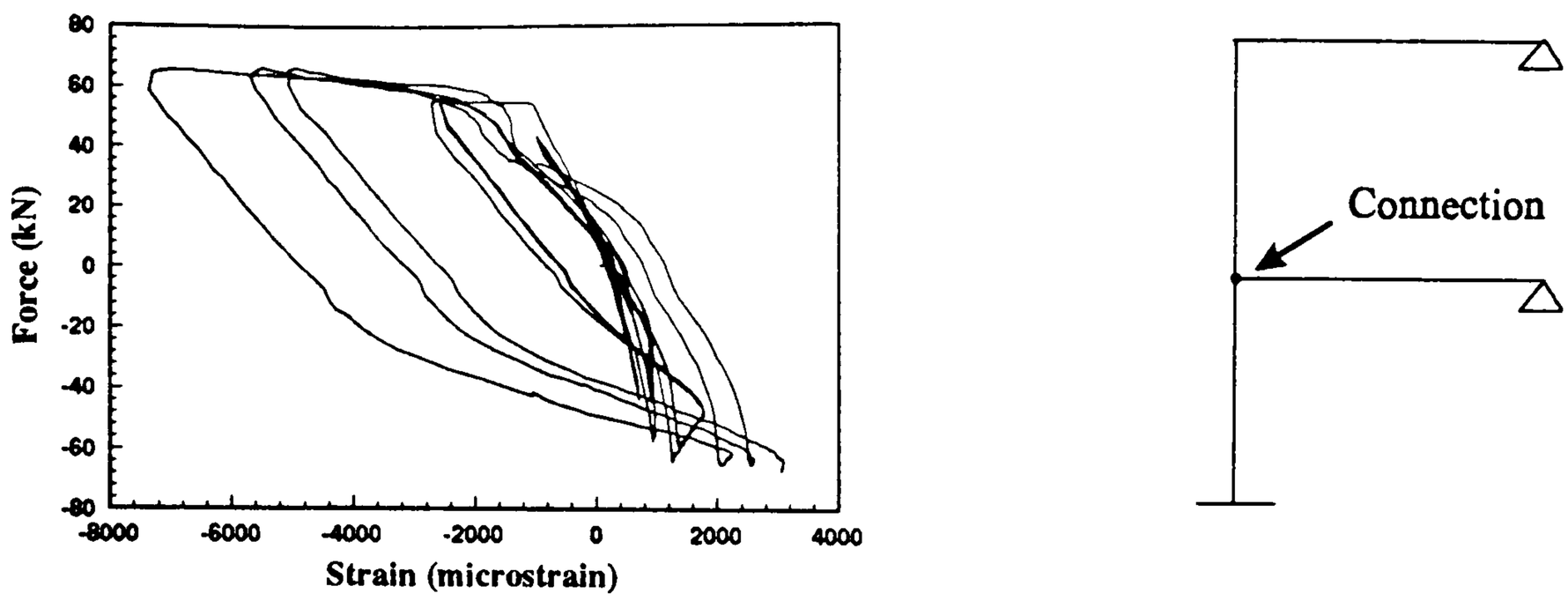

Figure A.13 Force at the second floor vs. strain in the top angle (model CS3)

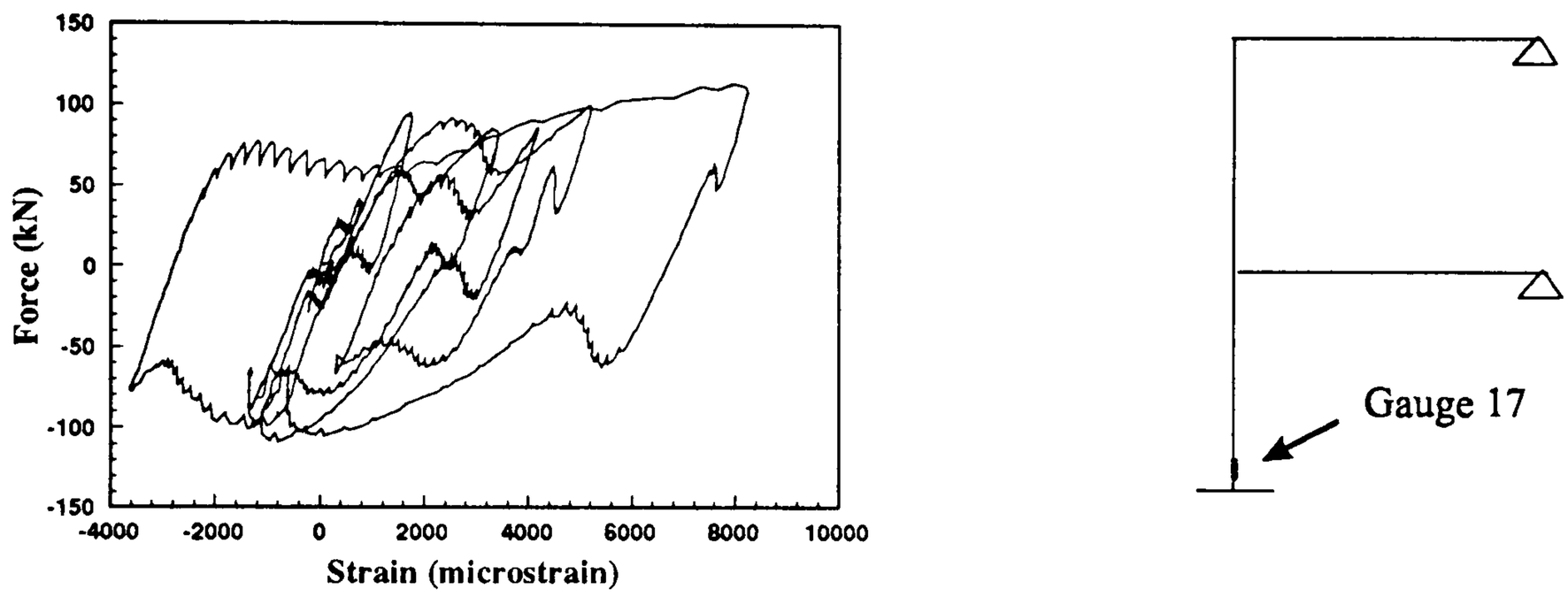

Figure A.14 Base shear vs. strain (model DS1)

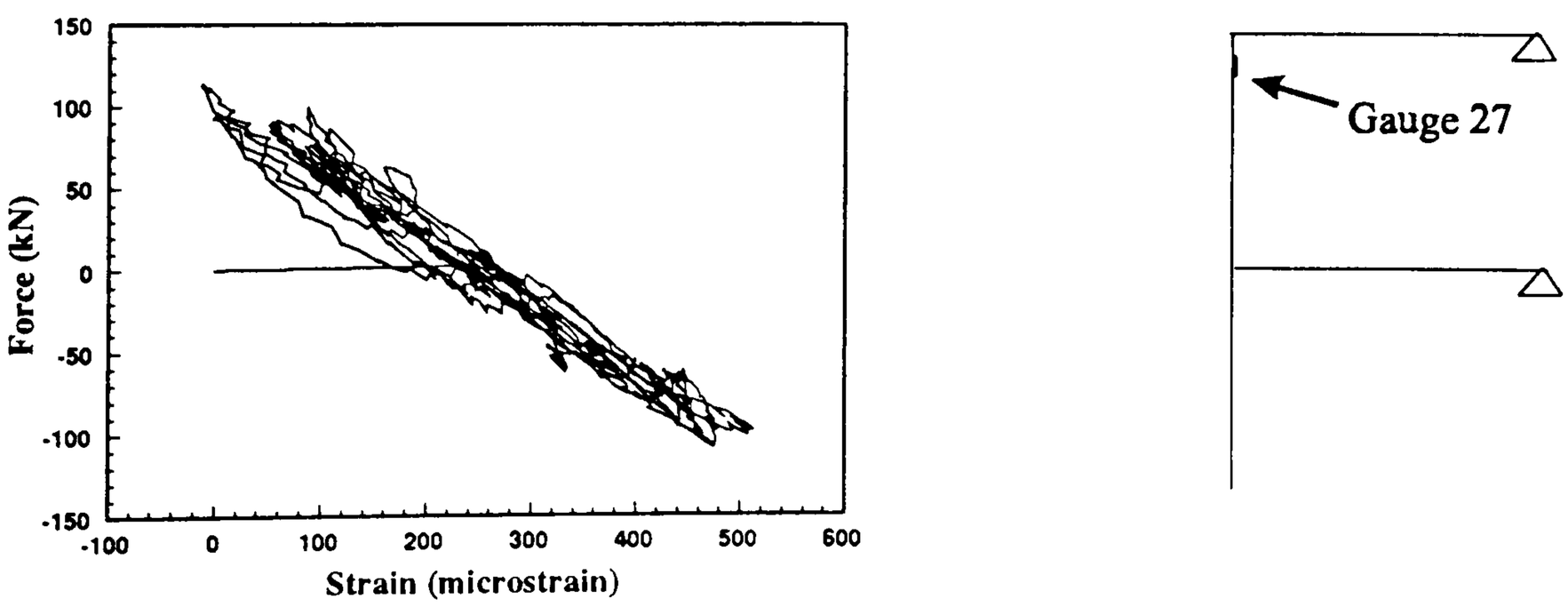

Figure A.15 Base shear vs. strain (model DS1)

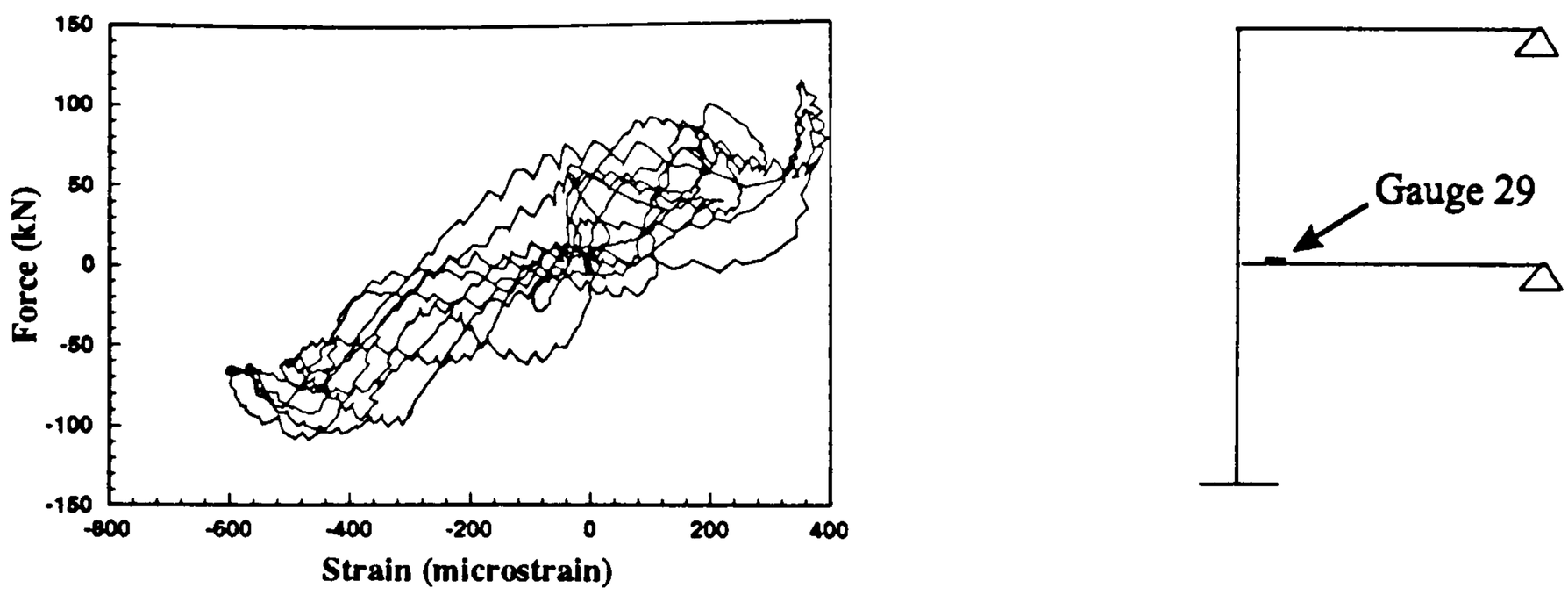

Figure A.16 Base shear vs. strain (model DS1)

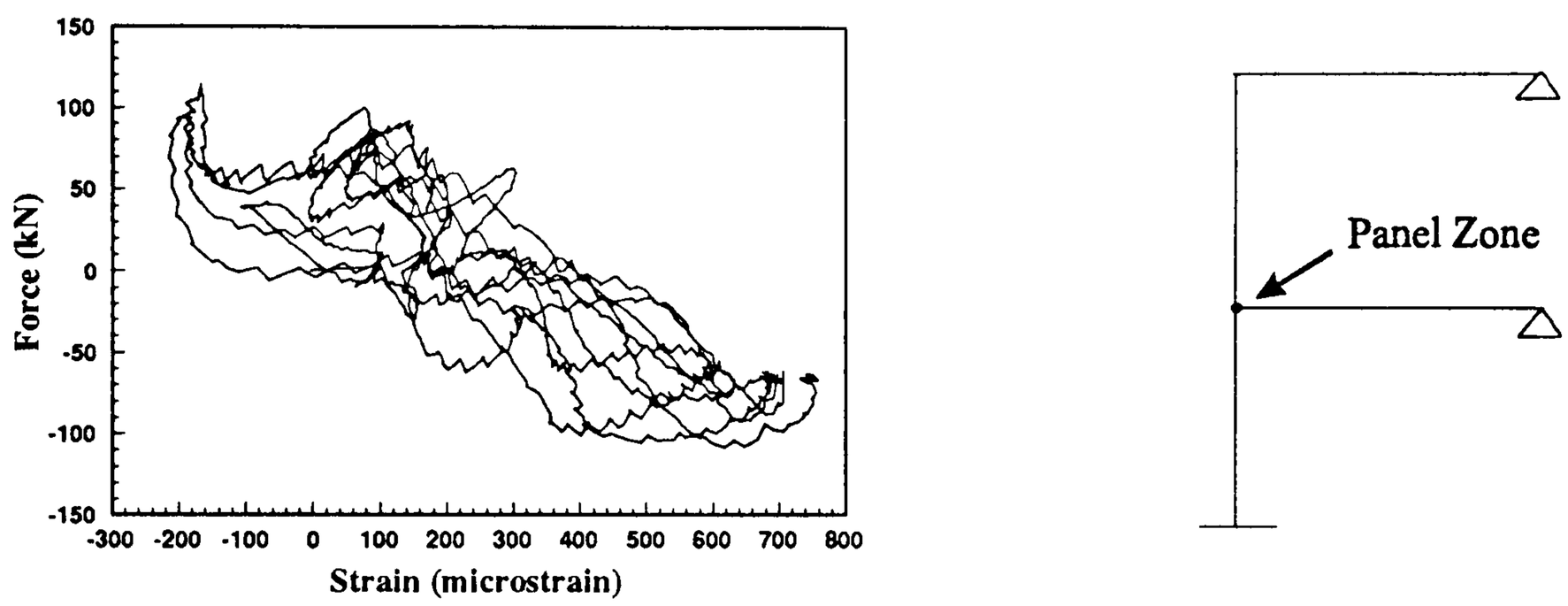

Figure A.17 Base shear vs. strain in the panel zone (model DS1)

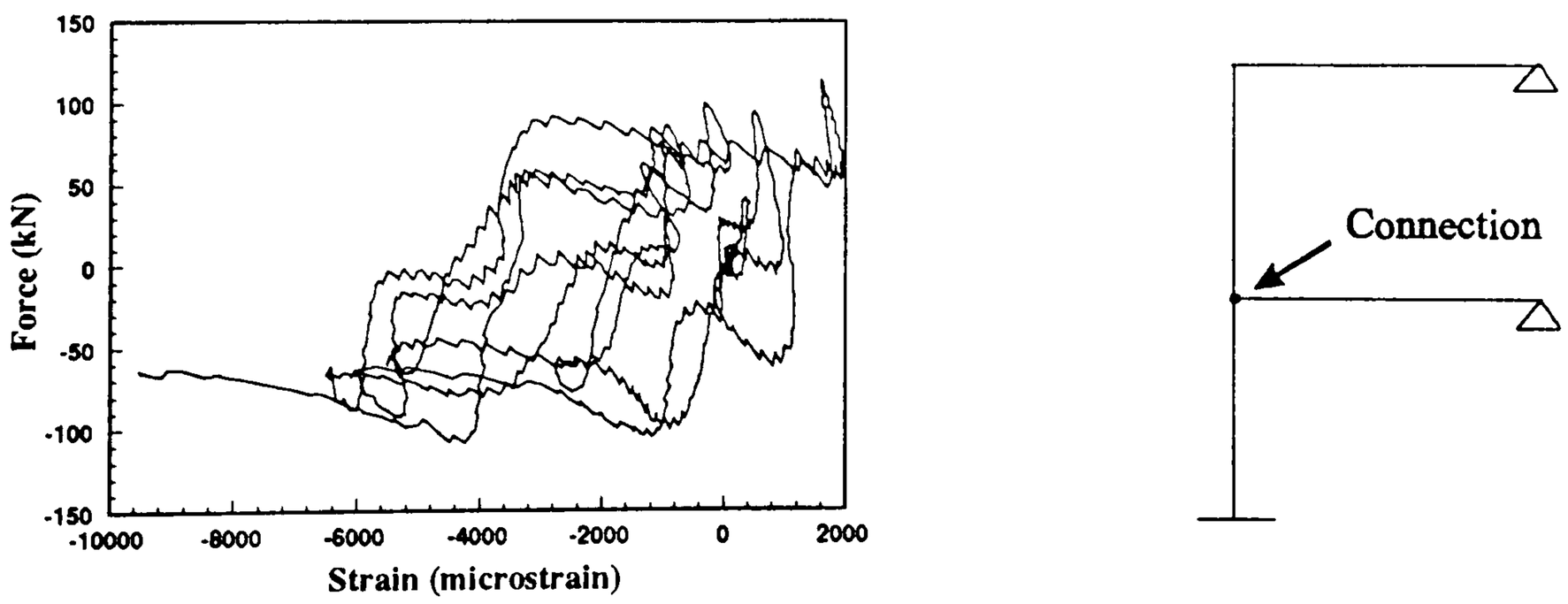

Figure A.18 Base shear vs. strain in the top angle (model DS1)

APPENDIX B

Frame Member Dimensions

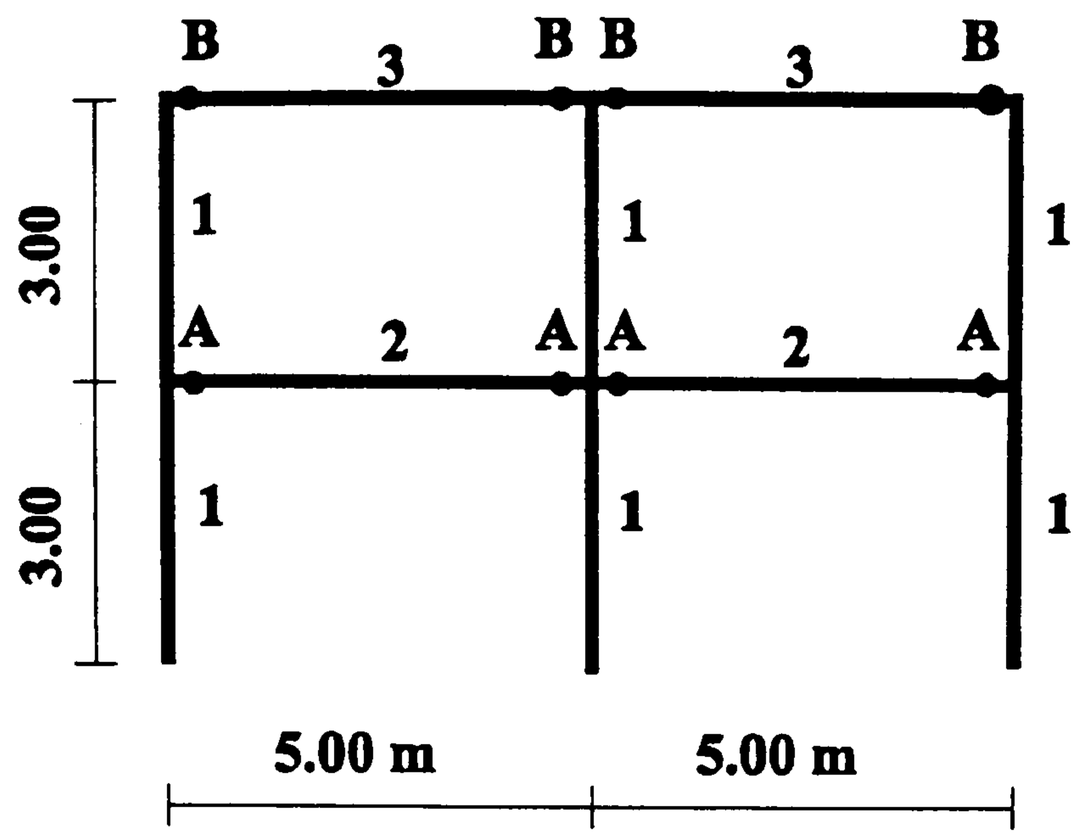

Two storey frame

Frame Member Dimensions (group A)

Type of Element	Frame S22D	Frame S22C	Frame R22C
1	UC152x152x30	UC203x203x52	UC203x203x52
2	UB305x127x37	UB305x127x37	UB305x127x37
3	UB305x102x25	UB305x102x25	UB305x102x25

Connection Properties

Type of Connection	K_1 (kNm/rad.)	K_2 (kNm/rad.)	θ_y (rad.)
A (Frame S22D30)	9680	968	0.0046
A (Frame S22D70)	22580	2258	0.0046
B (Frame S22D30)	6180	618	0.0054
B (Frame S22D70)	14160	1416	0.0054

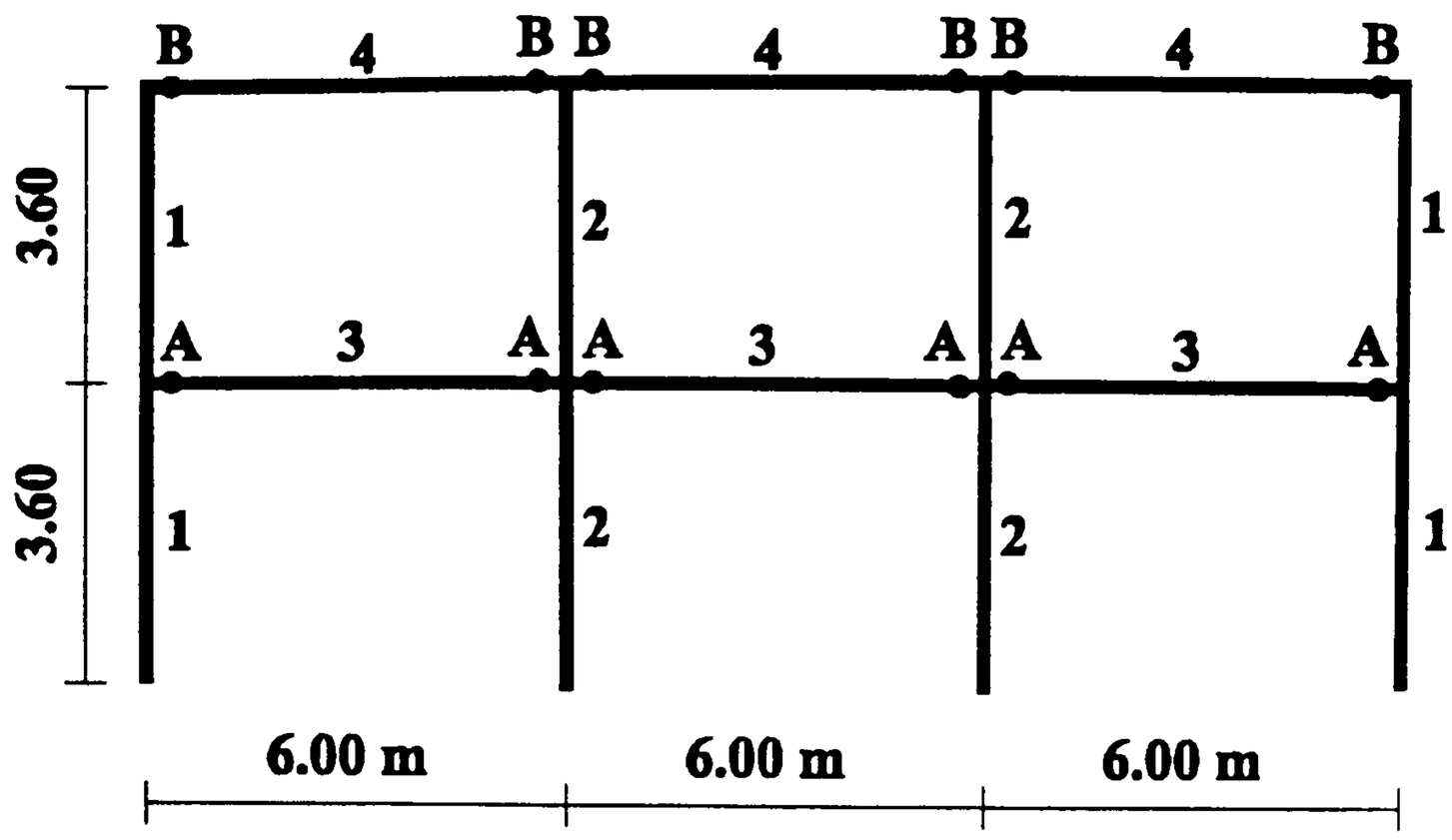

Two storey three bay frame

Frame Member Dimensions (group A)

Type of Element	Frame S23D30	Frame S23D70	Frame R23C
1	UC203x203x52	UC203x203x71	UC203x203x52
2	UC203x203x52	UC203x203c71	UC254x254x89
3	UB356x171x57	UB356x171x57	UB356x171x57
4	UB305x127x37	UB305x127x37	UB305x127x37

Frame Member Dimensions (group B)

Type of Element	Frame S23D30	Frame S23D50	Frame S23D70
1	UC254x254x107	UC254x254x89	UC254x254x71
2	UC254x254x107	UC254x254x89	UC254x254x71
3	UB356x171x57	UB356x171x57	UB356x171x57
4	UB305x127x37	UB305x127x37	UB305x127x37

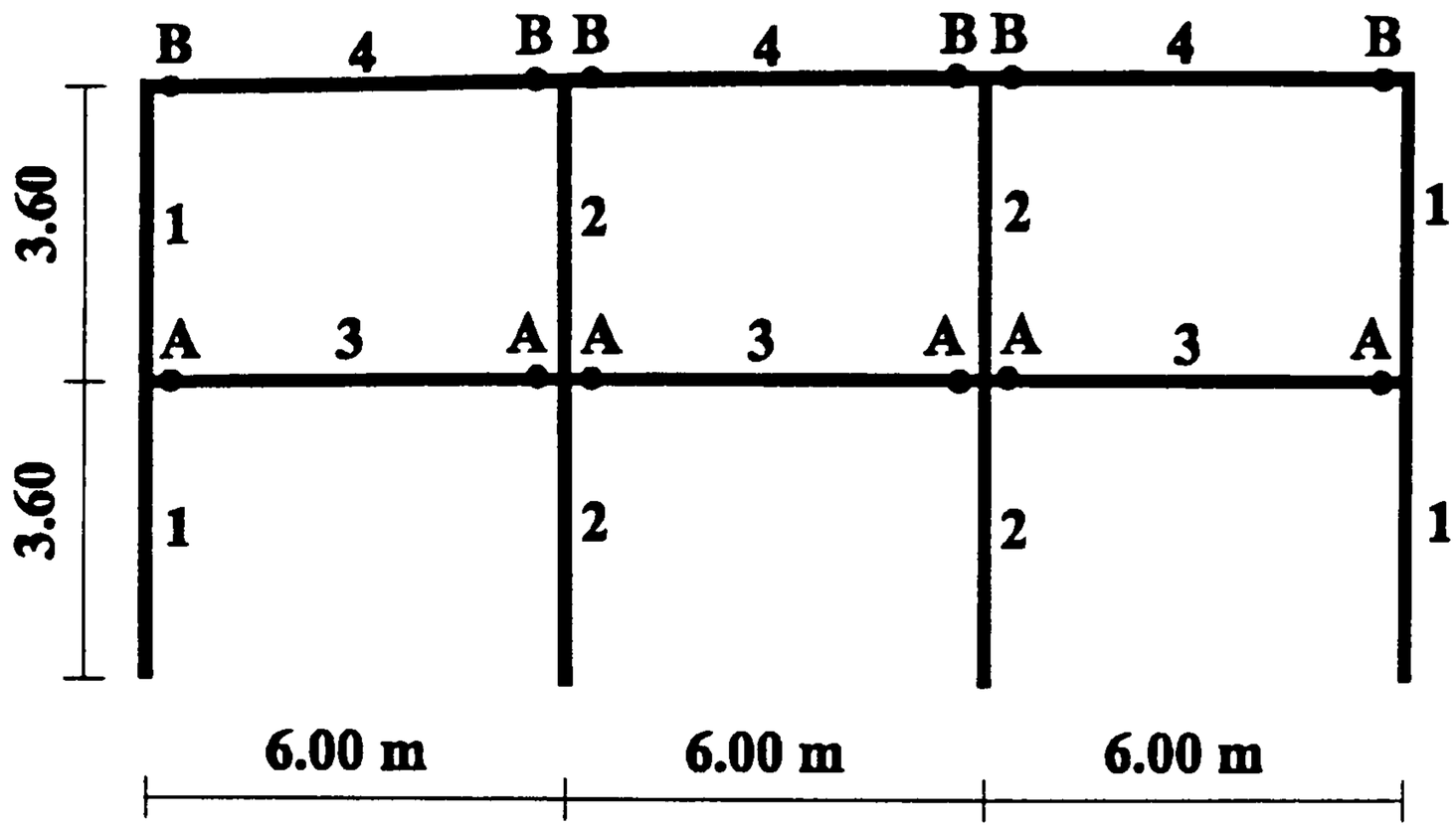

Two storey three bay frame

Frame Member Dimensions (group B)

Type of Elements	Frame S23C70	Frame S23C100	Frame R23C
1	UC203x203x60	UC203x203x60	UC203x203x60
2	UC254x254x89	UC254x254x89	UC254x254x89
3	UB356x171x57	UB356x171x57	UB356x171x57
4	UB305x127x37	UB305x127x37	UB305x127x37

Connection Properties

Type of Connection	K_1 (kNm/rad)	K_2 (kNm/rad)	θ_y (rad.)
A (Frame S23D30)	21400	2140	0.0039
A (Frame S23D50)	35520	3552	0.0039
A (Frame S23D70)	49740	4974	0.0039
A (Frame S23C70)	49740	4974	0.0039
A (Frame S23C100)	71057	7106	0.0039
B (Frame S23D30)	9680	968	0.0046
B (Frame S23D50)	16120	1612	0.0046
B (Frame S23D70)	22580	2258	0.0046
B (Frame S23C70)	22580	2258	0.0046
B (Frame S23C100)	32257	3226	0.0046

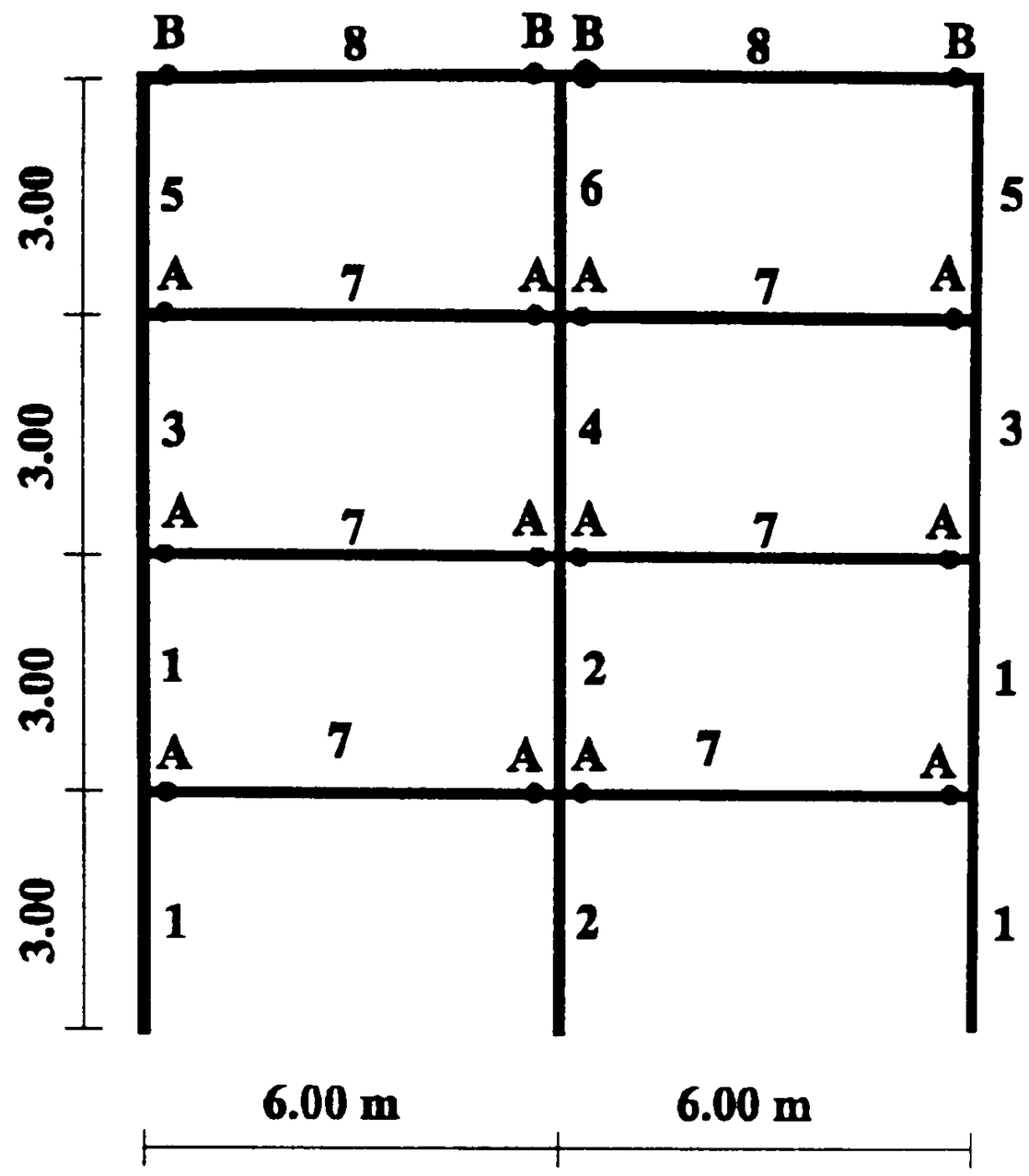

Four storey frame

Frame Member Dimensions (group A)

Type of Element	Frame S42D30	Frame S42D50	Frame S42D70
1	UC254x254x73	UC254x254x73	UC254x254x73
2	UC254x254x73	UC254x254x73	UC254x254x73
3	UC152x152x30	UC254x254x52	UC254x254x52
4	UC254x254x52	UC254x254x52	UC254x254x52
5	UC254x254x30	UC254x254x52	UC254x254x52
6	UC203x203x52	UC254x254x52	UC254x254x52
7	UB356x171x57	UB356x171x57	UB356x171x57
8	UB305x127x37	UB305x127x37	UB305x127x37

Frame Member Dimensions (group A)

Type of Element	Frame S42C30	Frame S42C50	Frame S42C70
1	UC254x254x73	UC254x254x73	UC254x254x73
2	UC254x254x89	UC254x254x89	UC254x254x89
3	UC152x152x52	UC254x254x52	UC254x254x52
4	UC254x254x52	UC254x254x52	UC254x254x52
5	UC254x254x52	UC254x254x52	UC254x254x52
6	UC203x203x52	UC254x254x52	UC254x254x52
7	UB356x171x57	UB356x171x57	UB356x171x57
8	UB305x127x37	UB305x127x37	UB305x127x37

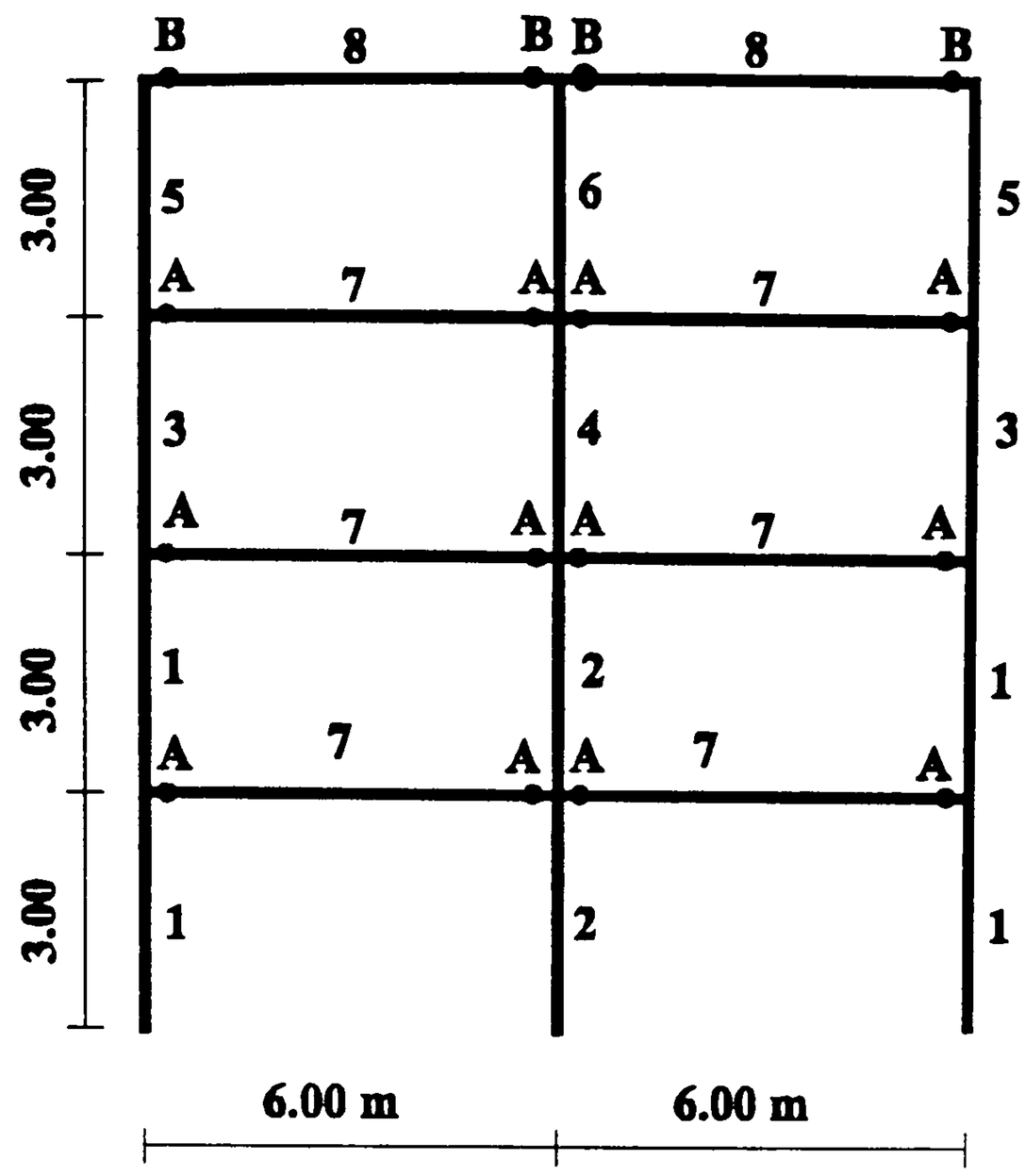

Four storey frame

Frame Member Dimensions (group B)

Type of Element	Frame S42D50	Frame S42D70 & S42C100	Frame R42C
1	UC305x305x137	UC305x305x137	UC305x305x137
2	UC305x305x137	UC305x305x137	UC305x305x137
3	UC203x203x52	UC203x203x52	UC203x203x52
4	UC203x203x52	UC203x203x52	UC305x305x137
5	UC203x203x52	UC203x203x52	UC203x203x52
6	UC203x203x52	UC203x203x52	UC203x203x71
7	UB356x171x67	UB356x171x67	UB356x171x57
8	UB305x127x57	UB305x127x57	UB305x127x37

Connection Properties

Type of Connection (group A)	K_1 (kNm/rad)	K_2 (kNm/rad)	θ_y (rad.)
A (Frame S42D30)	21400	2140	0.0039
A (Frame S42D50)	35520	3552	0.0039
A (Frame S42D70)	49740	4974	0.0039
A (Frame S42C100)	71057	7106	0.0039
B (Frame S42D30)	9680	968	0.0046
B (Frame S42D50)	16120	1612	0.0046
B (Frame S42D70)	22580	2258	0.0046
B (Frame S42C100)	32257	3226	0.0046
Type of Connection (group B)	K_1 (kNm/rad)	K_2 (kNm/rad)	θ_y (rad.)
A (Frame S42D50)	43330	4333	0.0038
A (Frame S42D70)	60660	6066	0.0038
A (Frame S42C100)	86660	8666	0.0038
B (Frame S42D50)	35520	3552	0.0039
B (Frame S42D70)	49730	4973	0.0039
B (Frame S42C100)	71900	7190	0.0039

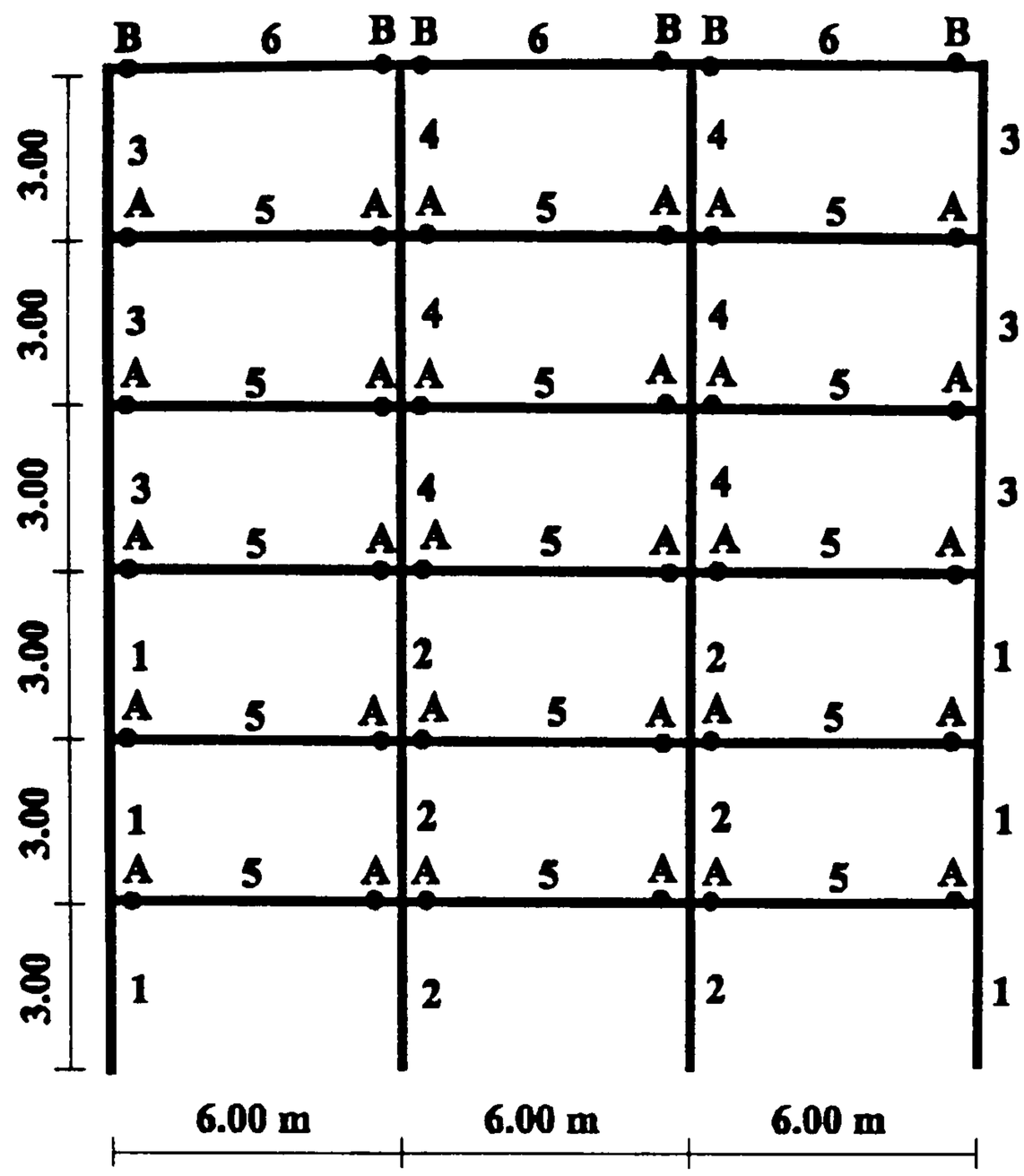

Six storey three bay frame

Frame Member Dimensions (group B)

Type of Element	Frame S63D50	Frame S63D70	Frame S63C100	Frame R63C
1	UC356x406x287	UC356x406x287	UC356x406x287	UC356x406x340
2	UC356x406x287	UC356x406x287	UC356x406x287	UC356x406x340
3	UC305x305x118	UC305x305x118	UC305x305x118	UC254x254x89
4	UC305x305x118	UC305x305x118	UC305x305x118	UC254x254x132
5	UB457x152x82	UB457x152x82	UB457x152x82	UB406x178x67
6	UB457x178x67	UB457x178x67	UB457x178x67	UB305x127x37

Connection Properties

Type of Connection	K_1 (kNm/rad)	K_2 (kNm/rad)	θ_y (rad.)
A (Frame S63D50)	82220	8222	0.0038
A (Frame S63D70)	115110	11511	0.0038
A (Frame S63C100)	164440	16444	0.0038
B (Frame S63D50)	54120	5412	0.0034
B (Frame S63D70)	75770	7577	0.0034
B (Frame S63C100)	108240	10824	0.0034

APPENDIX C

Calculation of moment capacity and rotational stiffness

The following example illustrates the procedure described in Section 5.4 of Chapter 5, for calculating the moment, rotation and rotational stiffness for top and seat angle connection with double web angles.

The details of the connection and the connected beam and column in the first floor of the frame S23D50 are:

Beam section:	UB356x171x57 (d_b = 358.6 mm)
Column section	UC254x254x107
Size of angles	100x200x20 mm (d1 =50 mm)
Diameter of bolts	20 mm (D =30 mm)
Length of angles	160 mm

Calculation the yield moment of the connection

The parameters defined in Section 5.4 for use in determining the moment of the connection are expressed as :

$L = d_1\text{-}k\text{-}D/2 = 50\text{-}18\text{-}15 = 17$ mm

$L/t_t = 17/20 = 0.85$

By substituting the value of L/t_t in equation (5.5), and using equations (5.1) to (5.6), the moment capacity of the top angle is evaluated as below:

$F_{pt}/F_o = 0.78$

$$F_o = \frac{\sigma_y\, l_t\, t_t}{2} = \frac{275\text{x}160\text{x}20}{2\text{x}10^6} = 440.00 \text{ kN}$$

$F_{pt} = 0.78\text{x}\ F_o = 0.78\text{x}440.0 = 343.20$ kN

$$M_{pt} = \frac{F_{pt}\ L}{2} = \frac{343.20\text{x}17}{2\text{x}10^3} = 2.92 \text{ kNm}$$

$d_2 = d_b + t_t = 358.6 + 20 = 378.60$ mm

$M_{ut} = M_{pt} + F_{pt}\, d_2 = 2.92 + 343.20\text{x}378.60/1000 = 132.67$ kNm

The moment capacity of the seat angle M_{us} is evaluated from equation (5.7) as :

$$M_{us} = \frac{\sigma_y l_t (t_t)^2}{4} = \frac{275x160x(20)^2}{4x10^6} = 4.40 \text{ kNm}$$

Then, the maximum moment of the connection is determined from equation (5.8);

$M_{yc} = M_{ut} + M_{us} = 132.67 + 4.40 = 137.10$ kNm

$M_{pb} = 275x1009x1000 = 277475000$ Nmm $= 277.475$ kNm

$M_{yc}/M_{pb} = 137.10/277.475 = 0.49$ then, $M_{yc} = 50\% \ M_{pb}$ O.K.

Calculation of rotational stiffness

As described in Section 5.4 of Chapter 5, the yield rotation of the connection is evaluated from equation (5.9) and given as :

$$\theta_y = \frac{1.4}{d_b} = \frac{1.4}{358.60} = 0.0039 \text{ rad.}$$

The rotational stiffnesses of the connection K_1 and K_2 are then expressed as :

$$K_1 = \frac{M_{yc}}{\theta_y} = \frac{137.10}{0.0039} = 35153.85 \text{ kNm / rad.}$$

$K_2 = 0.10 \ K_1 = 0.1x35153.85 = 3515.38$ kNm/rad.

BIBL. LAVORI. PUBB.